Nanogels à base d'acide hyaluronique fonctionnalisé, application à la séquestration et la libération controlée de composés hydrophobes

Huu Van Le

Normandie Université

UNIVERSITÉ DE ROUEN NORMANDIE

THÈSE

Pour obtenir le diplôme de doctorat

Spécialité **CHIMIE**

Préparée au sein de l'**Université de Rouen Normandie**

Nanogels à base d'acide hyaluronique fonctionnalisé, application à la séquestration et la libération controlée de composés hydrophobes

Présentée et soutenue par

HUU VAN LE

Thèse soutenue le 30/11/2022

devant le jury composé de :

M. DIDIER LE CERF	Professeur des Universités - Université de Rouen Normandie	Directeur de thèse
M. LAURENT DAVID	Professeur des Universités - Université Claude Bernard - Lyon 1	Président du jury
MME ANNE-CLAIRE GROO	Maître de Conférences - Université de Caen Normandie	Membre du jury
MME FLORENCE AGNELY	Professeur des Universités - Comue Universites Paris-Saclay	Rapporteur du jury
M. JACQUES DESBRIERES	Professeur des Universités - Université de Pau et des Pays de l'Adour	Rapporteur du jury

Thèse dirigée par **DIDIER LE CERF**

ED 508 NC Normande de Chimie

PBS Polymères Biopolymères Surfaces UMR 6270

REMERCIEMENTS

J'adresse mes remerciements les plus sincères,

A mon directeur de thèse, Professeur Didier LE CERF, qui m'a fait confiance en me confiant ce projet et qui m'a aidé à mener ce travail à bon port, surtout avec ses conseils précieux, ses encouragements et ses critiques pertinentes lors de nos discussions pour améliorer la qualité de cette thèse.

Au Professeur Luc PICTON et au Docteur Virginie DULONG pour leur implication dans ce projet et pour nos échanges scientifiques fructueux qui m'ont exposé des points de vue critiques très importants pour faire progresser nos recherches.

Au Professeur Florence AGNELY, pour ses soutiens pendant ma recherche de thèse, les connaissances scientifiques lors des cours de Master qui m'étaient très utiles pour la réalisation de ce travail, et pour l'intérêt qu'elle a bien voulu apporter à cette thèse en tant que rapporteur.

Au Professeur Laurent DAVID, au Professeur Jacques DESBRIERES et au Docteur Anne-Claire GROO pour l'attention qu'ils ont bien voulu m'accorder en jugeant ce travail.

Au Docteur Hung LE, qui m'a prodigué des conseils et des idées intéressantes pour la conception des expériences, au Docteur Mathieu MADAU pour ses instructions très détaillées concernant le protocole de greffage et les analyses de RMN, et au Docteur Christophe RIHOUEY pour la réalisation de la SEC.

Aux autres membres de l'équipe SCC et du laboratoire PBS, particulièrement Corinne, Morgane, Olive, Koceila, Guillaume, Laura et Alex, pour nos bons moments de convivialité et de détente, surtout les goûters où nous avons partagé des gâteaux vraiment délicieux.

Enfin, je remercie également toute ma famille, mes parents, mon frère et ma belle-sœur, pour leur confiance et leur soutien à distance pendant mes séjours en France, et leurs appels vraiment encourageants pour que je puisse bien travailler lors de ma thèse.

ABREVIATIONS ET SYMBOLES

BSA : albumine de sérum bovin

CDX : cyclodextrine

C_P : concentration totale en polymère

C_{TRE} : concentration en tréhalose

CTS : chitosane

CUR ou Cur : curcumine

DDS : système de délivrance de médicaments

DEAE-D : diéthylaminoéthyl dextrane

D_h : diamètre hydrodynamique

DLS : diffusion dynamique de la lumière

DNIC : complexes dinitrosyles de fer

DOP : dopamine

DOX : doxorubicine

DS : degré de substitution

Đ : dispersité du polymère

EE : efficacité d'encapsulation

EGCG : gallate d'épigallocatéchine

GSH : glutathion

HA : acide hyaluronique

HA-M2005 : HA fonctionnalisé de Jeffamine® M-2005

HIS : histidine

HIV : virus d'immunodéficience humaine

LC : taux d'encapsulation

LCST : température de solution critique inférieure (*lower critical solution temperature*)

LF : lactoferrine

M2005 : Jeffamine® M-2005

miRNA : microARN

M_n : masse molaire moyenne en nombre

MRI : imagerie par résonance magnétique

MW : masse molaire

M_W : masse molaire moyenne en masse

n-/n+ : ratio molaire entre les charges négatives et positives

NA : acide nucléique

NG : nanogel

NP : nanoparticule

ODN : oligodésoxynucléotide

PAR : polyarginine

PBAE : poly(β-aminoesters)

PBS : tampon phosphate saline

pDNA : acide désoxyribonucléique plasmidique

PDI : indice de polydispersité

PEC : complexe polyélectrolyte

PEG : polyéthylène glycol

PEI : polyéthylèneimine

PEO-PPO : poly(oxyde d'éthylène)-*co*-poly(oxyde de propylène)

PLGA : poly(D,L-lactide-*co*-glycolide)

PLL : poly-L-lysine

PROT : protamine

Py : pyrène

ROS : espèce réactive de l'oxygène

SA : substance active

sCT : calcitonine de saumon

SEC : chromatographie à exclusion stérique

siRNA : petit ARN interférent

TCA : acide taurocholique

TEM : microscopie électronique à transmission

TPC : concentration totale en particule

TPP : tripolyphosphate

UVB : ultraviolet B

ζ : potentiel zêta

SOMMAIRE

Introduction générale

Depuis la dernière décennie, les nanogels à base de complexes polyélectrolytes (PEC-NGs) de l'acide hyaluronique (HA), un polyanion naturel, émergent comme des nanomatériaux prometteurs dans le domaine biomédical, notamment pour la délivrance des substances actives (SAs) pour le traitement des cancers [1-3]. En effet, les principaux obstacles actuels dans la chimiothérapie contre les cancers sont la faible hydrosolubilité des agents anticancéreux, qui entraine souvent des problèmes concernant leur posologie ainsi que leur faible biodisponibilité, et leur toxicité systémique à cause de leur délivrance peu ciblée et peu contrôlée [4]. Les PEC-NGs à base de HA peuvent être un outil efficace pour surmonter ces problèmes avec des avantages très particuliers provenant d'une combinaison de trois aspects : (i) la chimie verte, soit une fabrication très simple sans solvant organique ni agent de réticulation [5], (ii) la nanomédecine, qui permet l'amélioration de l'hydrosolubilité apparente des SAs hydrophobes [4] et (iii) la nature du HA qui amène sa biocompatibilité excellente, sa capacité de ciblage des tumeurs et une structure chimiquement modifiable pour l'introduction de fonctions biologiquement ou physico-chimiquement actives [6].

C'est dans ce contexte que s'inscrit ce travail dont l'objectif est d'élaborer un prototype innovant de PEC-NGs à partir de HA pour l'encapsulation et la libération contrôlée de SAs peu hydrosolubles. Pour cela, nous avons préparé, évalué et optimisé des systèmes de PEC-NGs obtenues par la complexation entre différents polycations et le HA natif ou modifié (**Figure 1**). Les polycations étudiés sont le diéthylaminoéthyl dextrane (DEAE-D) et la poly-L-lysine (PLL), soient deux polycations biocompatibles couramment utilisés dans le domaine biomédical [7, 8]. Du HA a été fonctionnalisé par de la Jeffamine® M-2005 (M2005), dont le protocole a été développé par M. MADAU dans le cadre de sa thèse au sein de notre équipe [9, 10]. La Jeffamine® M-2005 est une polyétheramine commerciale thermosensible de type LCST (*lower critical*

solution temperature), signifiant qu'elle peut présenter une solubilité plus faible en milieu aqueux à cause d'une hydrophobicité plus importante lors d'une augmentation de température. Cette thèse porte ainsi une attention particulière aux PEC-NGs à base de HA-M2005 en raison de sa nouveauté et de ses propriétés intéressantes, notamment leurs comportements thermosensibles.

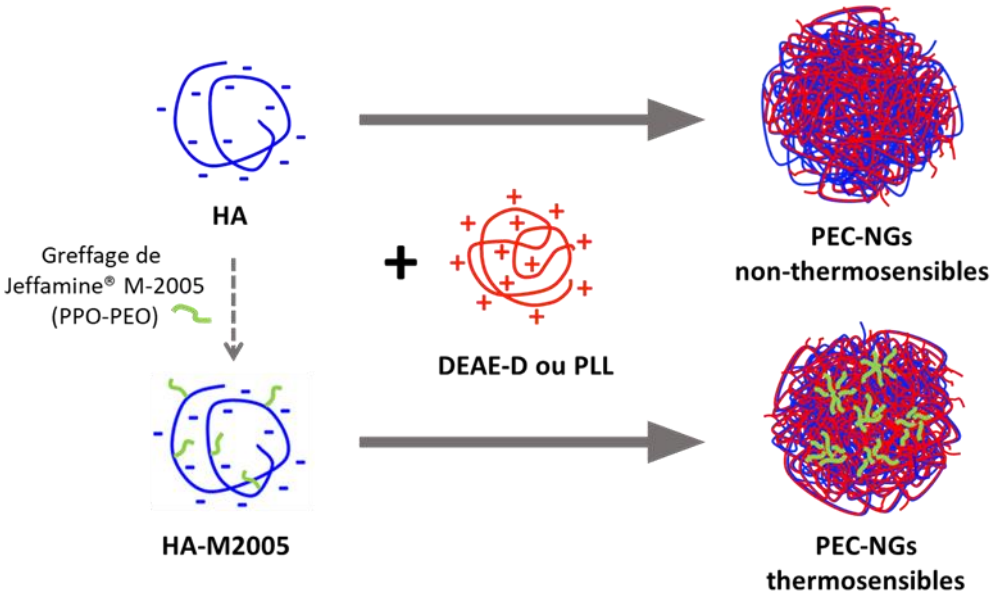

Figure 1. Formulations des PEC-NGs avec le HA ou le HA-M2005 comme polyanion et le DEAE-D ou la PLL comme polycation

Selon les objectifs ci-dessus, ce manuscrit intitulé «**Nanogels à base d'acide hyaluronique fonctionnalisé, application à la séquestration et la libération contrôlée de composés hydrophobes**» se compose de quatre chapitres :

(i) Le premier chapitre constitue une étude bibliographique sur les PECs colloïdaux à base de HA dans le contexte biomédical. Elle décrit en détail les avantages fondamentaux de ces systèmes, les principes de leur préparation en s'appuyant sur les rôles des différents facteurs impliqués dans la formation des PECs et les avancées récentes en termes d'applications biomédicales, notamment

pour la délivrance de principes actifs thérapeutiques ou pour la construction de matériaux multifonctionnels.

(ii) Le deuxième chapitre porte sur la préparation, la caractérisation et l'évaluation des PEC-NGs de HA/DEAE-D. Les effets de différents facteurs lors de l'élaboration des PECs sont étudiés pour comprendre les propriétés et les comportements colloïdaux des PECs préparé à partir de HA natif dans le but de trouver les conditions de préparation optimales en vue de futures applications.

(iii) Le troisième chapitre est consacré à l'élaboration et à la caractérisation des PEC-NGs thermosensibles obtenus par la complexation entre le HA-M2005 et deux polycations, le DEAE-D ou la PLL, avec plus particulièrement des études sur l'encapsulation et la libération de la curcumine comme SA hydrophobe modèle. L'évaluation comparative de ces PEC-NGs thermosensibles en référence à ceux obtenus avec du HA natif permet de comprendre les effets des greffons M2005 et du choix du polycation sur les structures des PEC-NGs. Ces études soulignent également les propriétés intéressantes des PEC-NGs de HA-M2005/PLL en termes de stabilité en milieu salin physiologique, de capacité d'encapsulation et de libération contrôlée de SAs peu hydrosolubles.

(iv) Le dernier chapitre s'intéresse à l'optimisation de la conservation, de la formulation et/ou de la stabilité des PEC-NGs en appliquant deux traitements physiques que sont la lyophilisation et le traitement autoclave. Pour la lyophilisation, les différents facteurs concernant la formulation pré-lyophilisation, notamment les caractéristiques des PEC-NGs et l'incorporation de cryoprotecteurs, sont évalués pour mettre en évidence leurs impacts sur la préservation de la structure colloïdale des PEC-NGs lors de la lyophilisation. Cela va nous permettre de trouver la stratégie la plus pertinente pour lyophiliser les PEC-NGs obtenus. Egalement, l'effet du traitement par autoclave sur les caractéristiques des PEC-NGs est évalué pour montrer le potentiel de ce

traitement comme un moyen simple et rapide pour fabriquer les nanoparticules à la fois stables et stériles à base de PECs thermosensibles.

Chacun des chapitres I, II et III dans ce manuscrit comprend une section d'introduction en français, suivie par les principaux résultats sous forme d'un article en anglais. De plus, pour les chapitres II et III, les sections avec des études complémentaires suivie d'une conclusion et des perspectives sont écrites en français. Les références citées sont ainsi présentées à la fin de chaque section. Pour le chapitre IV qui est rédigé entièrement en français, une liste complète des références est présentée à la fin du chapitre.

Enfin, une conclusion générale résume les principales avancées obtenues et décrites dans ce manuscrit de thèse. De nombreuses perspectives sont également proposées pour approfondir la compréhension des systèmes de PEC-NGs étudiés ainsi qu'élargir leurs applications.

Le financement des travaux de recherche dans le cadre de cette thèse a été assuré par la région Normandie et le Fonds Européen de Développement Régional. Ces travaux ont été dirigés par Pr Didier LE CERF et réalisés au sein de l'équipe Systèmes Colloïdaux Complexes (SCC) du Laboratoire Polymères, Biopolymères, Surfaces (PBS, UMR CNRS 6270, Université de Rouen Normandie, INSA de Rouen Normandie).

Références

[1] D. Xia, F. Wang, S. Pan, S. Yuan, Y. Liu, Y. Xu, Redox/pH-Responsive Biodegradable Thiol-Hyaluronic Acid/Chitosan Charge-Reversal Nanocarriers for Triggered Drug Release, Polymers, 13 (2021) 3785. https://doi.org/10.3390/polym13213785.

[2] M. Shariati, G. Lollo, K. Matha, B. Descamps, C. Vanhove, L. Van de Sande, W. Willaert, L. Balcaen, F. Vanhaecke, J.-P. Benoit, Synergy between intraperitoneal aerosolization

(PIPAC) and cancer nanomedicine: cisplatin-loaded polyarginine-hyaluronic acid nanocarriers efficiently eradicate peritoneal metastasis of advanced human ovarian cancer, ACS Applied Materials & Interfaces, 12 (2020) 29024-29036. https://doi.org/10.1021/acsami.0c05554.

[3] H. Zhang, M. Pei, P. Liu, pH-Activated surface charge-reversal double-crosslinked hyaluronic acid nanogels with feather keratin as multifunctional crosslinker for tumor-targeting DOX delivery, International Journal of Biological Macromolecules, 150 (2020) 1104-1112. https://doi.org/10.1016/j.ijbiomac.2019.10.116.

[4] Z. Edis, J. Wang, M.K. Waqas, M. Ijaz, M. Ijaz, Nanocarriers-mediated drug delivery systems for anticancer agents: an overview and perspectives, International Journal of Nanomedicine, 16 (2021) 1313. https://doi.org/10.2147/ijn.s289443.

[5] D. Wu, L. Zhu, Y. Li, X. Zhang, S. Xu, G. Yang, T. Delair, Chitosan-based colloidal polyelectrolyte complexes for drug delivery: a review, Carbohydrate Polymers, 238 (2020) 116126. https://doi.org/10.1016/j.carbpol.2020.116126.

[6] G. Huang, H. Huang, Hyaluronic acid-based biopharmaceutical delivery and tumor-targeted drug delivery system, Journal of Controlled Release, 278 (2018) 122-126. https://doi.org/10.1016/j.jconrel.2018.04.015.

[7] Q. Hu, Y. Lu, Y. Luo, Recent advances in dextran-based drug delivery systems: From fabrication strategies to applications, Carbohydrate Polymers, 264 (2021) 117999. https://doi.org/10.1016/j.carbpol.2021.117999.

[8] S. Manouchehri, P. Zarrintaj, M.R. Saeb, J.D. Ramsey, Advanced Delivery Systems Based on Lysine or Lysine Polymers, Molecular Pharmaceutics, 18 (2021) 3652-3670. https://doi.org/10.1021/acs.molpharmaceut.1c00474.

[9] M. Madau, D. Le Cerf, V. Dulong, L. Picton, Hyaluronic Acid Functionalization with Jeffamine® M2005: A Comparison of the Thermo-Responsiveness Properties of the Hydrogel Obtained through Two Different Synthesis Routes, Gels, 7 (2021) 88. https://doi.org/10.3390/gels7030088.

[10] M. Madau, Hydrogels adaptatifs stimuli-sensibles (temperature et lumière) à base d'acide hyaluronique (HA), Thèse de doctorat, Normandie Université (2021).

Chapitre I

Etude bibliographique

I.1. Introduction

L'objectif principal de cette partie bibliographique est de mettre en évidence les intérêts des nanogels de complexes polyélectrolytes (PEC-NGs) à base de HA pour les applications biomédicales afin de justifier l'utilisation de ce polysaccharide comme matériel de base dans notre projet. En vue d'élaborer les PEC-NGs les plus pertinents à base de HA pour les applications visées, il est primordial d'aborder et de comprendre préalablement les aspects fondamentaux de ce type de système, notamment son mécanisme de formation et les paramètres qui peuvent influencer les caractéristiques finales. En général, ces facteurs comprennent les paramètres intrinsèques des polymères de départ (e.g. masse molaire, rigidité, nature de la charge et distribution de charges), les paramètres de formulation (e.g. proportion des polymères, concentration en polymères, pH et contre-ions) et les paramètres de procédé (e.g. ordre et vitesse d'ajout, vitesse et temps d'agitation). De plus, en fonction des finalités recherchées, il est possible de conceptualiser différemment les PEC-NGs en utilisant un large éventail de polycations de nature chimique différente et en modifiant le HA par des groupes fonctionnels ayant des propriétés chimiques, physicochimiques ou/et biologiques spécifiques. Cela est illustré au travers de nombreux travaux de recherche sur ces systèmes pour la délivrance de principes actifs à structures variables, comme les petites molécules thérapeutiques, les acides nucléiques, les peptides et les agents de contraste, ou pour la fabrication de matériaux hybrides multifonctionnels. Tous ces aspects sont présentés dans la revue scientifique suivante, qui a été publiée dans le journal ***Small***.

I.2. Publication : Colloidal Polyelectrolyte Complexes from Hyaluronic Acid: Preparation and Biomedical Applications

Le, H. V. & Le Cerf, D. (2022). Small, 2204283.

Colloidal Polyelectrolyte Complexes from Hyaluronic Acid: Preparation and Biomedical Applications

Huu Van LE & Didier LE CERF *

Normandie Univ, UNIROUEN, INSA Rouen, CNRS, PBS UMR 6270, 76000 Rouen, France

*Corresponding author: E-mail address: didier.lecerf@univ-rouen.fr

Tel: 00 33 02 35 14 65 43; Fax: 00 33 02 35 14 67 04

Abstract: Hyaluronic acid (HA) is a natural occurring polysaccharide which has been extensively exploited in biomedical fields owing to its outstanding biocompatibility. Self-assembly of HA and polycations through electrostatic interactions can generate colloidal polyelectrolyte complexes (PECs), which can offer a wide range of applications while being relatively simple to prepare with rapid and "green" processes. The advantages of colloidal HA-based PECs stem from the combined benefits of nanomedicine, green chemistry and the inherent properties of HA, namely high biocompatibility, biodegradability and biological targeting capability. Accordingly, colloidal PECs from HA have received increasing attention in the recent years as high-performance materials for biomedical applications. Considering their potential, this review is aimed to provide a comprehensive understanding of colloidal PECs from HA in complex with polycations, from the most fundamental aspects of the preparation process to their various biomedical applications, notably as nanocarriers for delivering small molecule drugs, nucleic acids, peptides, proteins and bioimaging agents or construction of multifunctional platforms.

Keywords: Polyelectrolyte complexes, Colloids, Hyaluronic acid, Nanomedicine, Drug delivery

Graphical abstract:

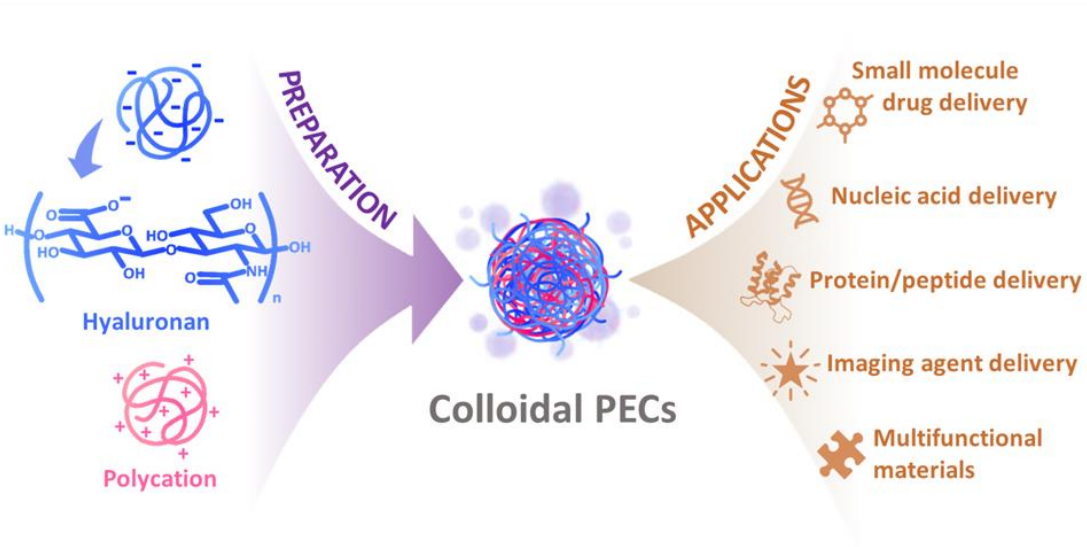

Abbreviations: BSA: bovine serum albumin; CDX: cyclodextrin; C_P: polymer concentration; CTS: chitosan; CUR: curcumin; DEAE-D: diethylaminoethyl dextran; DLS: dynamic light scattering; DNIC: dinitrosyl iron complex; DOP: dopamine; DOX: doxorubicin; EGCG: epigallocatechin gallate; GSH: glutathione; HA: hyaluronic acid; HIS: histidine; HIV: human immunodeficiency virus; LF: lactoferrin; miRNA: micro ribonucleic acid; MRI: Magnetic Resonance Imaging; MW: molecular weight; n-/n+: negative to positive charges molar ratio; NA: nucleic acid; NG: nanogel; NP: nanoparticle; ODN: oligodeoxynucleotide; PAR: polyarginine; PBAE: poly(β-amino esters); pDNA: plasmid deoxyribonucleic acid; PEC: polyelectrolyte complex; PEG: polyethylene glycol; PEI: polyethylenimine; PEO-PPO: poly(ethylene oxide)-*co*-poly(propylene oxide); PLGA: poly(D,L-lactide-*co*-glycolide); PLL: poly-L-lysine; PROT: protamine; ROS: reactive oxygen species; sCT: salmon calcitonin; siRNA: small interfering ribonucleic acid; TCA: taurocholic acid; TPP: tripolyphosphate; UVB: ultraviolet B; WPI: whey protein isolate

1. Introduction

Polyelectrolyte complexes (PECs), sometimes referred to as polyion complexes, can be spontaneously formed by electrostatic interactions between oppositely charged polyelectrolytes in aqueous media [1]. Under appropriate preparing conditions and depending on polyelectrolyte natures, such complexes can be elaborated as colloidal particles having submicronic size [2, 3]. Although colloidal PECs are technically comparable to nanogels (NGs) owing to the three-dimensional networks of physically bonded polyelectrolytes in their structures [2, 4, 5], they have also been described with several other terms depending on personal perceptions of researchers, most commonly as nanoparticles (NPs) [6, 7], nanocomplexes [8, 9], nanocomposites [10, 11], nanoassemblies [12] and coacervates [13, 14]. Such colloidal systems, especially when prepared from biopolymers, have been extensively investigated due to their promising properties for numerous applications in biomedical fields [1]. Their merits come from the combination of three aspects: nanomedicine, biomaterials and green chemistry. With the emergence of nanomedicine, the use of nanocarriers can offer tremendous advantages in drug encapsulation and delivery, namely enhancing chemical stability of drugs and improving drug solubility and bioavailability [15]. Due to their small size and the possibility of surface modification with biological ligands or molecular imprinting, nanocarriers can easily cross biological barriers, which have limited pore sizes (fenestrations) under 1 micron in most cases, then target and enter the tissues or cells of interest [16, 17]. Due to these aspects and the possibility of controlling drug distribution and release through particle engineering, nanocarriers can thus reduce systemic side effects and enhance therapeutic efficacy of drugs [15]. Nanosystems can also offer unique advantages for biomedical imaging with their ability of sensing, image enhancement and incorporating concomitantly therapeutic agents for theranostics, i.e. simultaneous therapeutic and

diagnostic applications [18-20]. When constructed from biomaterials, especially naturally occurring polysaccharides or proteins, PECs can become significantly biocompatible and biodegradable with much less immunogenicity and toxicity [21]. Beside such biorelevant aspects, the elaboration of biopolymer-based PECs is also in accordance with green chemistry principles since their preparation process usually requires only gentle mixing of polyelectrolyte solutions at room temperature, which is a simple and rapid procedure without the need for chemical agents, surfactants, organic solvents or high mechanical or thermal energy [1, 5].

Beyond the above-mentioned basic advantages, the potential of colloidal PEC systems is increased by the inherent biological and chemical properties of individual constituent polymers. Hyaluronic acid (HA), also called hyaluronan to generally mention both its acid and salt forms, has been one of the most common polyanions among several biopolymers reported so far for the elaboration of colloidal PECs. The significant attention dedicated to HA in biomedical fields is associated with its unique advantages, stemming from not only its outstanding biocompatibility but also interesting biological activities [22]. Consequently, HA has been widely used for elaboration of colloidal PECs with various cationic polymers of different natures: chitosan (CTS) and diethylaminoethyl dextran (DEAE-D) as polysaccharides; poly-L-lysine (PLL) and polyarginine (PAR) as homopolypeptides; zein, protamine (PROT), lactoferrin (LF), whey protein isolate (WPI), feather keratin and bovine serum albumin (BSA) as proteins; polyethylenimine (PEI) and poly(β-amino esters) (PBAE) as synthetic cationic polymers as well as their derivatives. Although the concept of colloidal PECs from HA has been described in the literature for more than a decade, it was not until five years ago did these systems start to be extensively investigated for drug delivery (see **Section 4**: **Table 2** and **Table 3**), while there has been so far no comprehensive review on such specific materials. In this context, the aim of the

current review is to summarize the advantages of HA-based colloidal PECs and offer a consolidated overview on the conception and fabrication principles of these systems. Their exploitation with the most recent advancements for biomedical application, mostly in drug delivery (**Figure 1**), as well as current challenges and perspectives for improving their utility will also be addressed.

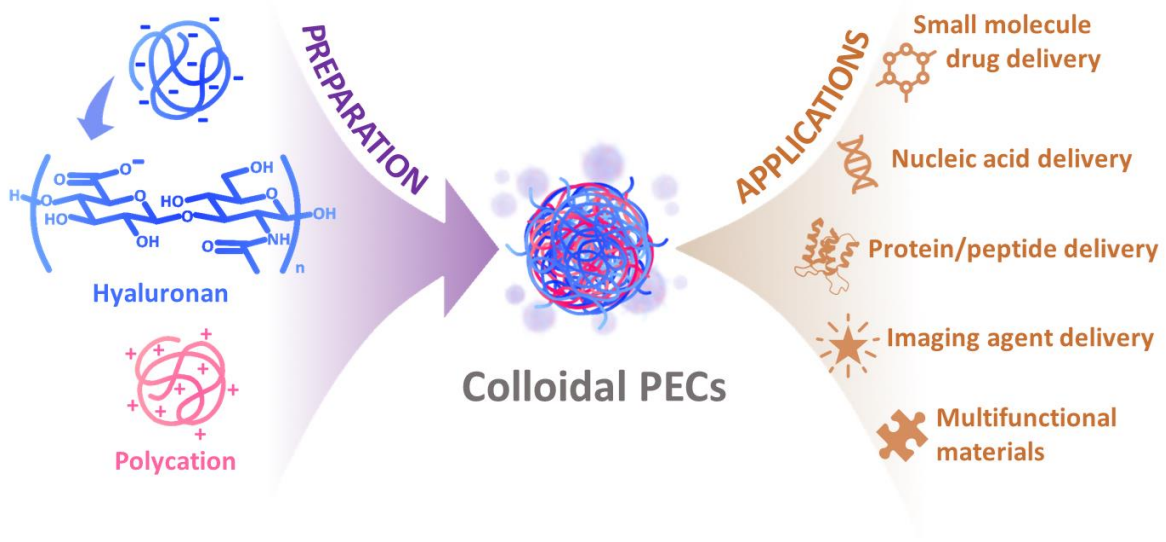

Figure 1. Applications of colloidal PECs prepared from HA and polycations

2. Advantages of hyaluronic acid as material for colloidal polyelectrolyte complexes

HA is a linear polysaccharide in the form of non-sulfated glycosaminoglycan which comprises repeating two-glycoside units of N-acetyl-D-glucosamine and D-glucuronic acid in its structure (**Figure 1**). It is naturally present in the extracellular matrix of epithelial, neural and connective tissues of the human body as well as other vertebrates, especially in umbilical cord, vitreous humor and synovial fluid [23]. Given its omnipresence in the human body, HA is extremely biocompatible, biodegradable and non-immunogenic, rendering it ideal as a material or excipient in biomedical and pharmaceutical domains [22]. In particular, HA is widely indicated in rheumatology, ophthalmology or dermatology due to its important biological functions, including

tissue moisturizing, angiogenesis, supporting cell migration and wound healing [24]. HA has also been known to react with reactive oxygen species (ROS) through the carbons in its glycosidic bonds or the nitrogen atom in its N-acetyl groups [25], leading to its potency as a ROS scavenger [14, 25, 26]. The protective effects of HA against oxidation stress have also been recently further emphasized with much more complicated mechanisms, which involve numerous cellular signaling pathways [27]. Commercial HA used to be mostly produced through extraction from animal tissues, mostly from rooster combs [23]. However, with the current production mainly based on microbial fermentation (e.g. *Streptococcus zooepidemicus*, *Bacillus subtilis* and *Escherichia coli*) as well as great advancements in extraction and purification methods, HA can be produced on larger scale, with larger range of molecular weight, higher purity, lower manufacturing cost and less environmental pollution [28-30].

Containing carboxyl groups (**Figure 1**) with a pKa of around 3, HA can display negative charges in aqueous media and therefore can spontaneously form PECs with positively charged macromolecules [31, 32]. For colloidal PECs with HA in excess, uncomplexed HA should be present on the particle surface to form an outer shell with a protective effect, which may offer the particles superior properties. For example, due to the cryoprotective effect of HA, such HA shell can improve the stability of PEC particles during lyophilization and reconstitution [33-35]. Indeed, during lyophilization of PEC particles as well as other nanosystems from biomacromolecules, water molecules are transferred from the liquid phase to the solid phase of ice during the freezing step and then removed by sublimation during the desiccation step, leading to a loss of hydrogen bonds between on the surface of these nanoobjects and thus destabilize their structure [36]. However, these hydrogen bonds may be preserved by a HA shell on the particle surface as HA is known for its extensive engagement in hydrogen bonding and can form intra- and intermolecular

hydrogen bonds on its own [37]. In addition, the remarkable water binding capacity of HA, its vitrification effect and its high intrinsic viscosity (i.e. large hydrodynamic volume) allow the HA shell to absorb a great amount of water and maintain them at molecular state in and around the particles to avoid their freezing, constituting thus a thick glassy layer to protect the particles from external mechanical stress of ice crystals and avoid particle aggregation during cryoconcentration [38, 39].

Furthermore, HA on the particle surface can significantly enhance PEC biocompatibility, which can be beneficial when polycations are included in their structure. Various polycations (e.g. PEI, PLL, DEAE-D or CTS) are known to be potentially cytotoxic, which usually depends on exposure time, polymer concentration and molecular weight [40-42]. Such toxicity has been reported to be caused by their interactions with anionic biological structures like cell membranes and their functional proteins, which lead to membrane disruption [41]. Combining polycations with HA may prevent those adverse interactions and counteract such toxicity due to the exceptional biocompatibility and negative charges of HA. More particularly, HA can enhance the stability of PEC particles in serum as well as reduce their immunogenicity by preventing the adsorption of serum proteins on the particle surface, as known as “protein corona” or opsonization [10, 12, 43, 44]. Opsonization is one of the most problematic factors which leads to the uptake of nanoparticulate drug delivery systems by the mononuclear phagocytic systems (e.g. macrophages and monocytes) and causes their early elimination from blood circulation before reaching their target sites *in vivo* [45]. As these proteins are more likely to bind to highly cationic and/or hydrophobic nanocarriers [16, 45], the presence of the hydrophilic and negative charged HA on their surfaces would probably prevent such interactions. Moreover, for the fabrication of nanocarriers from cationic proteins, e.g. zein or lactoferrin, although they can readily form

nanosized particles in water through their inherent hydrophobic interactions, further complexation with HA can result in more compact particles, which can improve drug encapsulation and stability as well as the properties of the complexed proteins [6, 46-50]. Likewise, although HA can also spontaneously form nanocomplexes with cationic drugs like doxorubicin (DOX) or pentamidine for their delivery, further complexation with a polycation should generate better-defined NPs with more useful properties [51, 52].

The tremendous interest in HA for biomedical applications is also associated with its unique biological behaviors, such as its capacity to recognize CD44 receptors and its specific cleavage by hyaluronidase (HAase) [53]. CD44, the principal cell surface receptor for HA, is overexpressed in various types of cancer cells, namely breast cancer, lung cancer, brain cancer, prostate cancer, pancreatic cancer and colon cancer [54]. Likewise, HAase is a family of enzymes catalyzing HA hydrolysis and also highly expressed at tumor sites, especially in intracellular vesicles of tumor cells [55]. Such particular distribution of CD44 and HAase can offer a possibility of drug targeting for oncotherapy, since HA on the particle surface can facilitate their specific uptake by tumor cells through CD44-mediated endocytosis and subsequent particle degradation by HAase for intracellular drug release, which can ultimately enhance drug performance at a local site (**Figure 2**) [12, 53, 56-62]. In the same manner, the CD44 targeting effect of HA also allows the fabrication of nanoplatform for cancer bioimaging for diagnosis or theranostics [19, 20]. Furthermore, HA can act synergistically with other biopolymers, namely CTS, in order to improve PEC mucoadhesiveness and offer more advantages for oral or nasal administration [63-65].

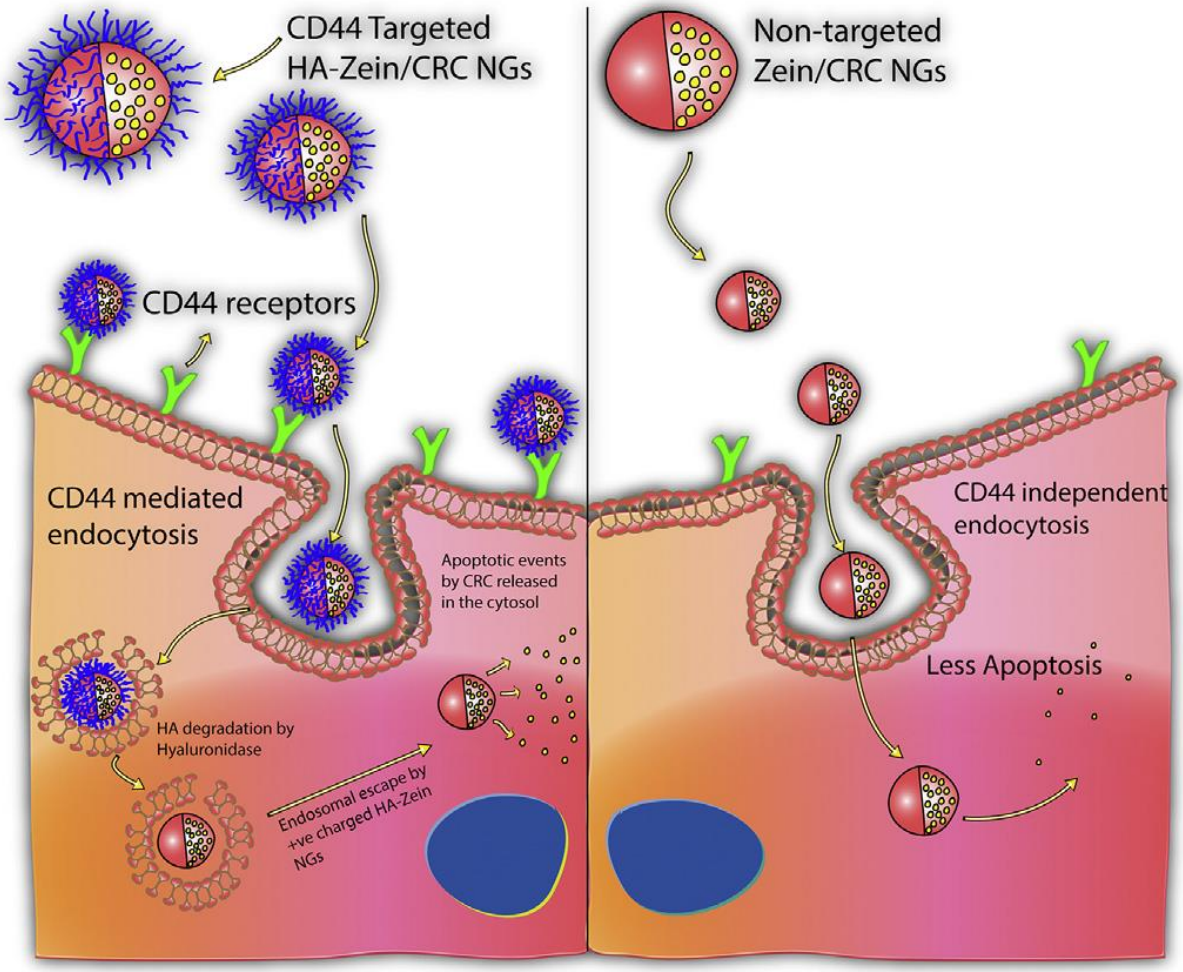

Figure 2. Specific cellular uptake through CD44-mediated endocytosis of the anticancer curcumin (CRC)-loaded HA/zein PEC NGs before their degradation by intracellular HAase for drug release in tumor cells (*left*) *vs.* non-specific cellular uptake of NGs without HA in normal cells (*right*). Reproduced with permission [4]. Copyright 2018, Elsevier.

HA can also be chemically modified owing to the ubiquitous distribution of carboxyl, hydroxyl and acetamido groups across the chain structure (**Figure 1**), leading to the perspectives of elaborating PECs with more interesting physicochemical and biological properties from HA derivatives [66]. For instance, introduction of hydrophobic groups like phospholipids [67] or alkyl chains [68] can generate amphiphilic HA derivatives for better encapsulation of hydrophobic

molecules. HA functionalization with short chains of amphiphilic and thermoresponsive copolymers can also allow fabricating colloidal PECs with thermo-dependent characteristics and better stability [69]. PECs prepared from thiolated HA (HA-SH) can be further stabilized by self-crosslinking upon disulfide bond formation to generate redox-responsive systems [70], while histidine (HIS) grafted on both HA and the associating polycations can result in PECs with pH-sensitive behaviors [71]. Bioactive ingredients, including chemotherapeutic agents [72, 73], nucleic acids [74] and peptide antigens [75], can also be directly grafted on HA in PECs in order to improve their therapeutic or biological performance. PECs from HA grafted with functional moieties like bile acids [60], dopamine (DOP) [76] or epigallocatechin gallate (EGCG) [3] can also offer better stability of macromolecule cargos during their delivery. These examples will be further described in their applications (**Section 4**). Collectively, the advantages of HA-based colloidal PECs lie from the material and methodological aspects to their applications, which are summarized in **Figure 3**.

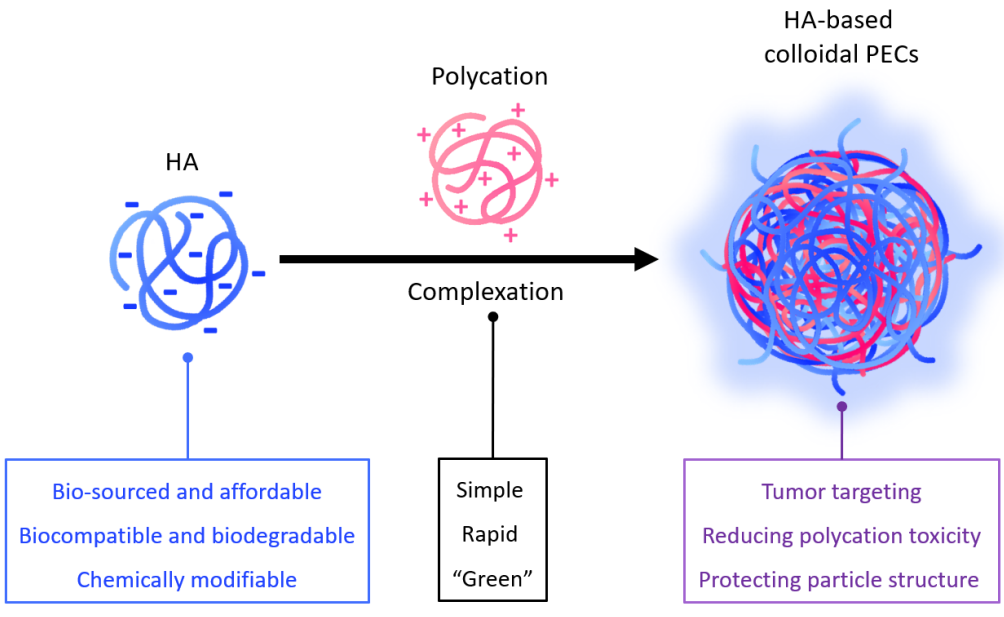

Figure 3. Main interests of colloidal PECs from HA in biomedical fields

3. Preparation of colloidal polyelectrolyte complexes from hyaluronic acid

From the above-mentioned advantages, HA should be among the most potential polyanions of choice to elaborate colloidal PECs for biomedical applications. Before the preparation, the properties of PEC particles should be understood in order to fabricate PEC systems with specifically pertinent properties for intended applications. To that end, the following sections will explain the formation mechanism of colloidal PECs, how their final characteristics should be anticipated for intended applications and the effects of various parameters during PEC elaboration on their characteristics.

3.1. Formation mechanism of colloidal PECs

The general mechanism of PEC formation from two soluble polyelectrolytes is illustrated in **Figure 4**. Complexation between oppositely charged polyelectrolytes can take place autonomously in aqueous media with an increase in entropy upon the release of counterions and water molecules as the main driving force [77]. The interactions involved in the formation of PECs are mainly electrostatic interactions (Coulomb force). The primary structure of PECs, which are formed at the first step of electrostatic association, can be classified as “scrambled egg” model or “ladder-like” model according to relative arrangement of polymer chains (**Figure 4**) [78]. However, PEC structures in practice may not strictly follow either of such models but rather a combination of both, with the former being closer to the reality [79, 80]. Double strain segments in these primary PECs are electrostatically neutralized, thus relatively less hydrophilic and can segregate to form secondary PECs, involving a combination of hydrophobic interactions, electrostatic interactions, hydrogen bonding and van der Waals force [78, 79, 81, 82].

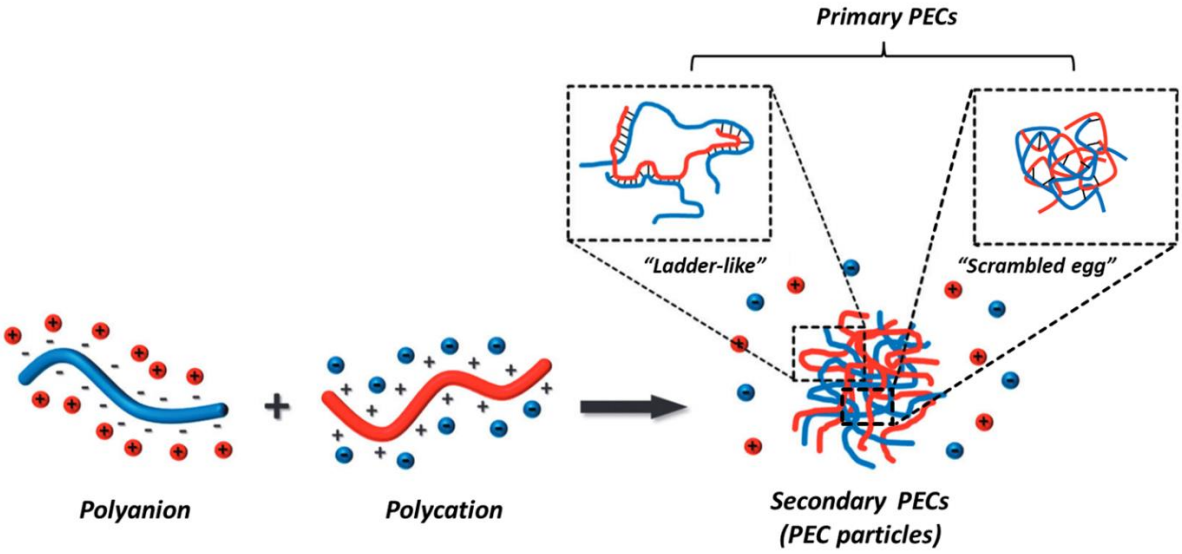

Figure 4. Mechanism of PEC formation from two soluble polyelectrolytes (modified from [83]): primary PECs can display "ladder-like" structures (orderly ion-paring) and/or "scrambled egg" structures (random ion-pairing). Segregation of neutralized segments in primary PECs can lead to secondary PECs in the form of PEC particles. Counterions are liberated from PECs as the electrostatic complexation occurs.

As long as the complexation parameters are appropriately controlled, which will be discussed in **Section 3.3**, final PECs can be formed as colloidal particles with a core-shell structure, i.e. a neutral PEC core surrounded by a highly charged and more hydrophilic shell of uncomplexed polyelectrolyte segments [84, 85]. More specifically, for colloidal PECs from HA and positively charged proteins with strong intramolecular hydrophobic interactions, e.g. in HA/zein PECs, the final particles should have a highly hydrophobic innermost core composed of mainly proteins, followed by a layer of HA/zein PECs in the strict sense and an outermost layer of mainly uncomplexed HA (**Figure 5**) [49, 86].

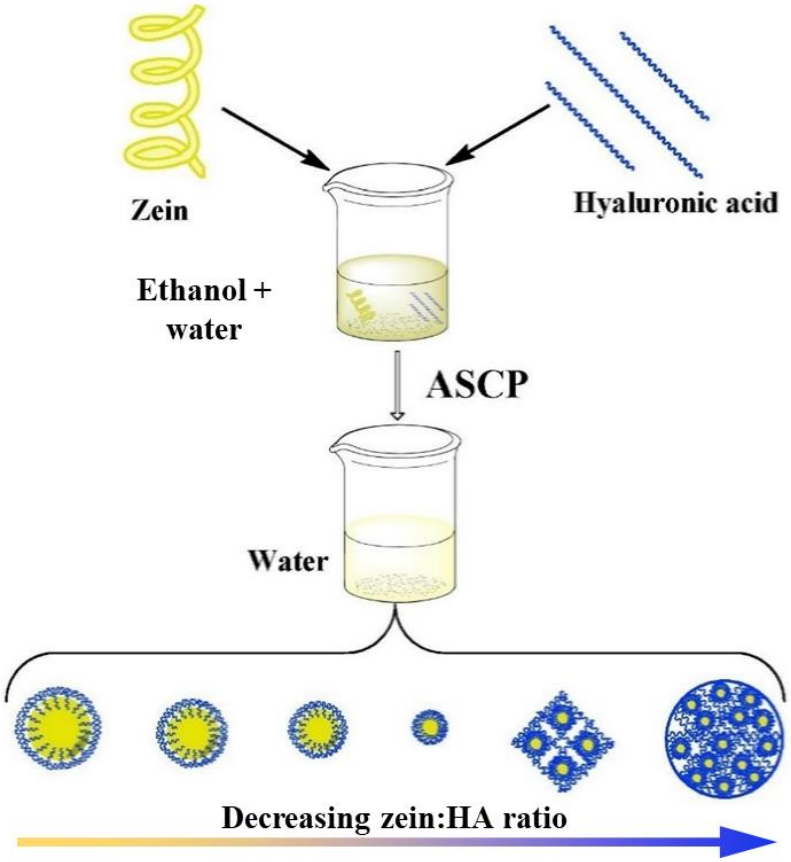

Figure 5. Schematic illustration of colloidal HA/zein PECs prepared by antisolvent coprecipitation (ASCP) method and their final structures in line with decreasing zein:HA ratio. Adapted with permission [49]. Copyright 2019, Elsevier.

3.2. Conception of colloidal PECs from HA

Final characteristics of biomedical nanocarriers should be envisaged depending on intended applications. Among the physicochemical characteristics of colloidal systems, particle size is of utmost importance for their performance *in vivo*. The particle size should be small enough to (i) be transported through biological barriers since they usually have limited opening or pore sizes (fenestrations), which can largely vary between 1 and 1000 nm depending on tissue type and pathological condition [87], (ii) avoid being recognized and cleared by monocytes and macrophages and (iii) be uptaken by target cells if intracellular drug delivery is necessary [16]. A

particle size of 100-200 nm may facilitate particle transport through the gastrointestinal tract or the blood-brain barrier [88]. For nanocarriers targeting tumor cells, which have been the most common subject of research in nanomedicine, the ideal particle size is reported to be around 70-200 nm to ensure tumor penetration and cellular uptake [87, 89]. A too large size (e.g. > 500 nm) may facilitate particle clearance by monocytes and macrophages and/or prevent the uptake of these particles by the target tumor cells [89, 90]. Meanwhile, particles with a too small size (e.g. under 20 nm) are more prone to rapid renal clearance [16, 87], or cannot offer enough energy to bend cell membranes and enter the target cells [45, 88]. In addition, reduced particle size leads to a larger total surface area, which may cause faster and less controlled drug release [91]. In terms of *in vitro* stability, for colloidal systems in general, a highly large particle size are prone to sedimentation while smaller particles are more prone to flocculation or agglomeration due to high total surface energy [92]. In the specific case of HA-based PECs, there has been so far no thorough study on the effects of their particle size on their *in vitro* stability and *in vivo* behaviors. In general, most of the colloidal PECs from HA studied for biomedical applications in the literature have their average particle size in the range of 100-400 nm with a polydispersity index (PDI) under 0.3 to ensure its relative homogeneity [2, 4, 7, 52, 93-96]. These characteristics are most commonly evaluated by dynamic light scattering (DLS) and can be further confirmed by transmission (TEM) or scanning (SEM) electron microscopy [31, 81].

Surface charge is also an important characteristic of nanocarriers for *in vivo* applications. As mentioned in the **Section 2** above, particles having a negative net surface charge are more biocompatible than positively charged particles as they are less likely to electrostatically interact with the negatively charged cell membranes [97-99]. The presence of the negatively charged HA on PEC surface can therefore enhance their biocompatibility. Umerska *et al.* found a three-fold

higher IC_{50} of CTS in cationic HA/CTS PEC NPs (zeta potential of +20 mV) compared to free CTS (IC_{50} = 84 µg.mL^{-1} *vs*. 26 µg.mL^{-1}), whereas anionic HA/CTS PEC NPs (zeta potential of -19 mV) showed no cytotoxicity on the whole range of CTS concentration studied [97]. However, due to electrostatic repulsion, anionic nanocarriers may be less ready to cross biological barriers (e.g. mucous membranes) and be internalized by targeted cells as compared to their cationic counterparts [45]. Meanwhile, highly cationic nanoparticles have been known to be more rapidly cleared from *in vivo* circulation by monocytes and macrophages than highly anionic nanoparticles, while nanoparticles with neutral or slight negative charges would show a more prolonged circulation [16]. The net charge on the particle surface is represented by zeta potential, which can be measured by electrophoretic light scattering (ELS) [100]. Technically, nanocarriers with zeta potentials between -10 and +10 mV are regarded as approximatively neutral, while a zeta potential less than -30 mV or higher than +30 mV indicates a highly anionic or cationic surface, respectively [100]. In terms of colloidal stability *in vitro*, it is a matter of common consensus that an absolute value of zeta potential should be greater than 30 mV to ensure sufficient electrostatic stabilization and avoid phase separation, unless steric stabilization is applied [101]. Due to the advantages of HA as discussed in **Section 2**, most of the HA-based colloidal PECs reported in the literature have HA in excess on the particle surface, thus a negative zeta potential with a common range between -10 and -50 mV [2, 4, 7, 52, 93-96].

Hydrophobicity is another important aspect. Stiff and hydrophobic nanoparticles are more prone to opsonization and elimination by the mononuclear phagocytic system [16, 45]. The most classical approach to overcome this problem is coating the particle surface with a hydrophilic polymer like polyethylene glycol (PEG) [45], but this may not be necessary for PECs having HA on the surfaces since HA can offer the same advantage with a high hydrophilicity as discussed

in **Section 2**. The common problem of HA-based PECs is a too hydrophilic structure, as they are formed mainly through electrostatic interactions and hydrogen bonding of hydrophilic polymers. Highly hydrophilic nanocarriers may show low encapsulation and fast release of drugs due to large pore size [102], as well as poor tissue penetration and cellular uptake as many biological barriers are basically hydrophobic [103]. This explains the emergence of using HA derivatives with amphiphilic or hydrophobic grafts for improving the performance of PECs as earlier described (**Section 2**).

Particle geometry can also affect the *in vivo* behaviors of nanocarriers. Discoidal particles are known to have unique tumbling and margination dynamics in blood circulation, which favor more vessel wall interaction than spherical particles, as well as improved particle binding and endothelium adhesion [16, 104, 105]. Particles with greater curvature are more likely to be uptake by macrophages [16]. Filamentous particles may also show long-circulating lifetimes compared with spherical counterparts [106]. The morphology of HA-based colloidal PECs in the literature are commonly verified by TEM or SEM and present mostly spherical or poorly defined shapes [93, 96, 107], with no attempt so far to control this parameter or study its effects.

Taken together, depending on the intended applications, especially the administration route and the targeted tissues or cells, the desired properties of final colloidal PECs should be anticipated before their fabrication. In particular, a target range should be set for quantifiable characteristics like particle size and zeta potential to ensure both PEC stability and performance. In order to obtain such desired characteristics, it is imperative to understand their structure and investigate the impact of different parameters on their properties during the preparation process, which are described in the next sections.

3.3. Parameters impacting the formation of colloidal PECs

The sections below give a detailed description of parameters having influence on PEC characteristics, including material parameters (molecular weight and charge density of polyelectrolytes), formulation parameters (total polyelectrolyte concentration, charge ratio, pH, ionic strength and adjuvant ions) and technical parameters (addition mode, addition order, stirring time and complexation temperature). It should be remembered that all of these parameters act interdependently, either synergistically or contradictorily to govern PEC properties. The resulting system is therefore a compromise between these factors and in no case should they be considered separately.

3.3.1. Polyelectrolyte molecular weight

HA used for fabricating colloidal PECs has a common MW between 20-1000 kDa (**Table 1**). As a general trend, an increase in molecular weight (MW) of either HA or the complexing polycations can foster electrostatic complexation and thus reinforce the stability of PECs [108]. Kayitmazer *et al.* found an enhancement of coacervation between CTS (260 kDa) and HA when the MW of HA is increased from 50 to 750 kDa, which was evidenced by a decrease in pH_ϕ (critical pH above which PEC particles are formed) from 2.7 to 2.2 (**Figure 6**B) [31]. Such results were attributed to less entropy loss when HA of higher MW is transferred from diluted to concentrated regime [31]. Logically, HA with a too low MW may be unable to form stable PECs with polycations, as shown with HA of 29 kDa in HA/PAR PECs reported by Oyarzun-Ampuero *et al.* (ref. [109] – **Table 1**).

Table 1. Notable results on HA-based PEC characteristics with different polymer ratios, concentrations and molecular weights.

System	–/+	C_P (g.L^{-1})	MW_{HA} (kDa)	MW_{PC} (kDa)	Average D (nm)	PDI	ζ (mV)	Ref.
HA/PAR	5:6 m/m	0.5	29	5-15	not formed			[109]
			165		128 ± 8	0.15 ± 0.05	+31.3 ± 1.0	
HA/PLL	2:3 n/n	1.25	200	4.7	200 ± 5	0.16 ± 0.02	-38.8 ± 0.1	[2]
			700		207 ± 9	0.21 ± 0.02	-40.9 ± 2.5	
			1200		278 ± 6	0.27 ± 0.18	-44.2 ± 2.2	
		1.8	200		255 ± 28	0.47 ± 0.06	-51.1 ± 2.6	
			700		244 ± 16	0.43 ± 0.05	1.2 ± 0.1	
			1200		aggregation			
	5:6 n/n	2	200		245 ± 4	0.09 ± 0.02	-38.8 ± 0.5	
			700		280 ± 9	0.26 ± 0.01	-55.4 ± 2.8	
			1200		aggregation			
HA/zein	1:5 m/m	4	100	22	180-190	ns	-32 to -38	[110]
			1000		235-245	ns	-30 to -36	
			2000		285-295	ns	-30 to -34	
HA/DEAE-D	0.1 n/n	0.5	270	700	300-350	0.19-0.23	+45 to +55	[81]
	0.8 n/n				160-200	0.06-0.1	+30 to +33	
	1 n/n				aggregation			
	1.25 n/n				160-170	0.11-0.14	-29 to -35	
	10 n/n				300-320	0.33-0.44	-46 to -50	
	0.1 n/n	1			770-830	0.75-0.87	ns	
	0.8 n/n				190-240	0.09-0.14	ns	
	1.25 n/n				200-220	0.14-0.15	ns	
	10 n/n				570-650	0.41-0.53	ns	
	0.1 n/n	0.5	830		aggregation			
	0.8 n/n				aggregation			
	1.25 n/n				aggregation			
	10 n/n				aggregation			

Table 1 (*continued*)

System	–/+	C_P (g.L^{-1})	MW_{HA} (kDa)	MW_{PC} (kDa)	Average D (nm)	PDI	ζ (mV)	Ref.
HA/PROT	3:1 m/m	1	176	5.1	70-130	0.10-0.13	-35 to -45	[111]
			257		70-130	0.16-0.19	-55 to -65	
			590		60-90	0.25-0.30	-85 to -105	
			2900		aggregation			
		2	257		110-170	0.1-0.2	-70 to -80	
HA/CTS DA 14 %	1:2 m/m	2	10	100	280-320	ns	+27 to +33	[96]
			50		250-300	ns	+30 to +35	
			120		400-450	ns	+30 to +35	
			500		450-550	ns	+20 to +37	
	2:1 m/m		10		300-350	ns	-15 to -25	
			50		380-320	ns	-10 to -30	
			120		200-220	ns	-18 to -20	
			500		950-1050	ns	-35 to -45	
HA/CTS DA 28%	1:3 n/n	2	39	90	450-470	ns	ns	[108]
	1:2.5 n/n				400-420	ns	ns	
	1:2 n/n				320-340	ns	ns	
	1:1.5 n/n				240-260	ns	ns	
HA/CTS DA 10%	0.05 n/n	1	120	50		not formed		[107]
	0.12 n/n					not formed		
	0.2 n/n				166 ± 1	ns	24.7 ± 0.3	
	0.31 n/n				113 ± 4	ns	26.4 ± 1.3	
	0.47 n/n				130 ± 2	ns	23.2 ± 0.7	
	0.71 n/n				220 ± 3	ns	20.2 ± 0.9	
	1.1 n/n				>1000	ns	-7.9 ± 1.6	
	1.89 n/n				>1000	ns	-11.6 ± 3.0	
	4.25 n/n				358 ± 11	ns	-18.7 ± 2.4	
	6.61 n/n				264 ± 7	ns	-21.1 ± 0.9	
	13.69 n/n				238 ± 4	ns	-21.8 ± 0.3	

Table 1 (*continued*)

System	–/+	C_P (g.L^{-1})	MW_{HA} (kDa)	MW_{PC} (kDa)	Average D (nm)	PDI	ζ (mV)	Ref.
HA/CTS DA 63%	1:2 m/m	0.7	90	90	200-250	0.16-0.20	+25 to +30	[112]
				170	200-250	0.14-0.18	+18 to +22	
				310	400-650	0.17-0.35	+22 to +30	

-/+: polyanion/polycation ratio, in weight (m/m) or in mol of charges (n/n); C_P: total polymer concentration; CTS: chitosan; D: diameter; DA: degree of acetylation of CTS; DEAE-D: diethylaminoethyl dextran; HA: hyaluronic acid; MW: molecular weight; ns: not specified; PAR: polyarginine; PC: polycation; PDI: polydispersity index; PLL: poly-L-lysine; PROT: protamine; ζ: zeta potential.

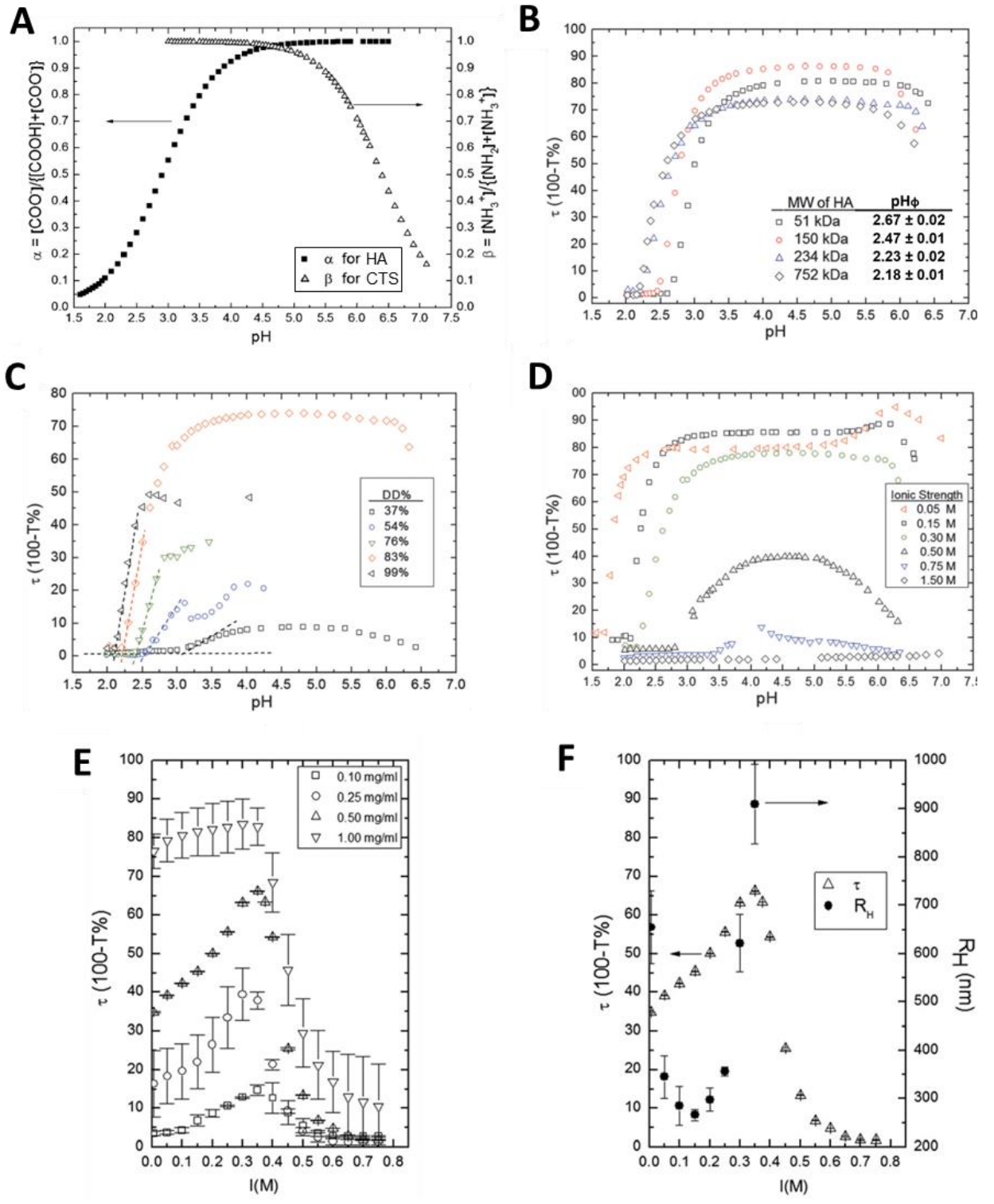

Figure 6. Characterization of colloidal HA/CTS PECs in varying conditions (adapted from [31] with permission from Royal Society of Chemistry, 2015): **A**: ionization rate of HA (α) and CTS (β) as a function of pH. B-D: Turbidity, i.e. τ(100-T%), as a function of pH with variation of MW of

HA (**B**), degrees of deacetylation (DD) of CTS (**C**) and ionic strength represented as NaCl concentration (**D**). E-H: Turbidity and radius of hydration (R_H) as a function of ionic strength (I) at different polymer concentrations (C_P) (**E**) or C_P fixed at 0.5 $g.L^{-1}$ (**F**). Standard parameters are MW_{HA} = 234 kDa, MW_{CTS} = 260 kDa with DD = 83 %, C_P = 0.5 $g.L^{-1}$, HA:CTS ratio of 1:1 m/m, I = 0.3 M and pH = 3. pH_ϕ denotes the pH above which the turbidity is abruptly increased, which translates the formation of PEC particles as HA is sufficiently ionized.

Increasing polymer MW can lead to larger particle size of PECs with larger distribution, or even aggregation at macroscopic level (precipitation or macrogelation) if their MW is too high (i.e. above 1000 kDa), as shown in **Table 1** (ref. [2], [110], [111], [96], [112]). However, a MW slightly under 1000 kDa is still susceptible to cause macro-aggregation if the MWs of both the complexing polymers are comparable, e.g. HA of 830 kDa in complex with DEAE-D of 700 kDa (ref. [81] - **Table 1**). Likewise, a MW higher than 1000 kDa can still form homogenous colloidal PECs when the partner polyelectrolyte has a much smaller MW, e.g. HA/zein PECs with HA MW of 2000 kDa and zein MW of 22 kDa showing a particle size of nearly 300 nm (ref. [110] - **Table 1**).

Specifically, the effect of HA MW should be more obvious when HA is the main polyelectrolyte in PECs [78]. For instance, an increase in MW of HA from 270 to 830 kDa can cause an important increase in particle size (1.6-fold) and polydispersity index (PDI) (2-fold) of HA/DEAE-D PECs having negative to positive charge ratio (n-/n+) of 10, while only small increases by around 1.2-fold are observed with n-/n+ = 0.1, i.e. with HA being the minor polymer [81]. Similar observation was also reported when comparing HA/CTS PECs having HA:CTS ratio of 1:2 m/m and 2:1 m/m (ref. [96] - **Table 1**). **Figure 7** depicts the general effects of polyelectrolyte MW on PEC structure, as well as those of charge density, polymer concentration, charge ratio and ionic strength, which are described in the next sections.

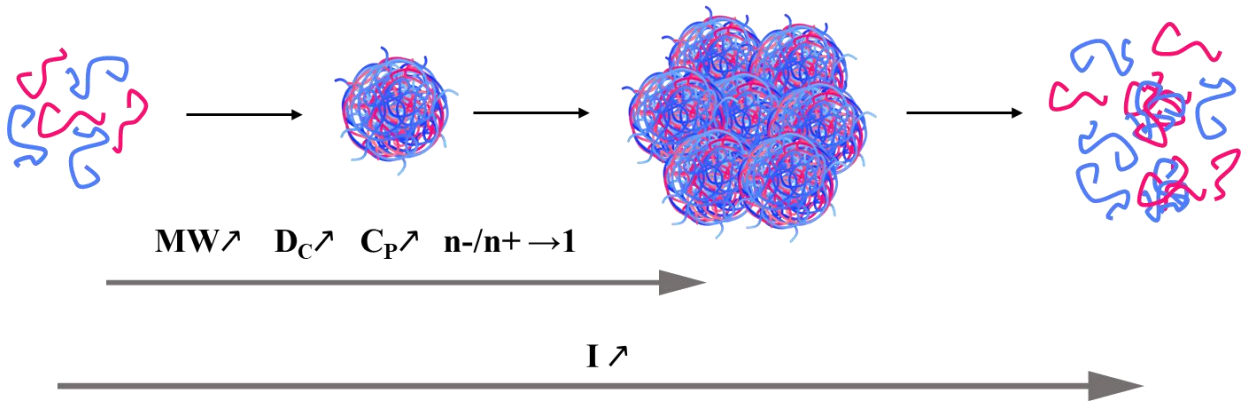

Figure 7. Effects of polymer molecular weight (MW), charge density (D_C), total polymer concentration (C_P), charge ratio (n-/n+) and ionic strength (I) on PECs from polyanions (blue) and polycations (red). (↗: increase, →: towards)

Regarding surface charges, higher MW of HA may cause more steric hindrance for their compaction in the PEC core and thus more exposure of their charges on PEC surface, leading to a lower zeta potential [9, 96, 109, 113]. This can be observed from the decreasing trend of zeta potential when HA MW is increased in HA/PLL, HA/zein, HA/PROT and HA/CTS PECs (ref. [2], [110], [111], [96] in **Table 1**, respectively). As a result, for negative particles, such decrease in zeta potential may lead to better colloidal stability due to stronger electrostatic stabilization. In an experiment regarding lyophilization of pDNA-loaded HA/CTS PEC NPs, Sato *et al.* observed large increases in particle size after freeze-drying and rehydrating PEC NPs with a HA MW of 400 kDa (from 340 to 1200 nm) or 600 kDa (from 320 to 710 nm), while a HA MW of 1300 kDa resulted in less particle size increase (from 470 to 670 nm) [34]. In this work, the high exposure of the high MW HA on the PEC surface may also explain the increase of 4 to 5-fold in cellular uptake efficiency when the HA MW is increased from 400 kDa to1300 kDa, probably due to better interaction between HA and CD44 receptors.

3.3.2. Charge density

The effect of charge density on HA-based colloidal PECs is ascribed for both the absolute charge density on each polyelectrolyte and the relative arrangement between their charges. In principle, when the charge densities of polyelectrolytes in PECs increase and/or become comparable to each other, their electrostatic attraction should be stronger and subsequently increase phase separation, from microscopic (increased PEC particle yield or particle size) to macroscopic level (precipitation) (**Figure 7**) [31, 80, 114]. For PECs from HA, the effects of charge density are usually studied in the case of HA/CTS PECs. Unlike the natural HA which has a fixed distribution of carboxyl groups, amine groups on CTS result from the deacetylation of natural chitins, which leads to CTS of different grades in terms of degree of deacetylation (DD) [108]. CTS with a high DD has therefore a high number of amine groups. As a results, an increase in DD, or a decrease in degree of acetylation (DA) in other words, can lead to a higher charge density and allow better coacervation between CTS and HA, thus foster phase separation as well as aggregation rate during PEC formation [31, 108]. This can be seen from the enlargement in the pH range for effective PEC formation and the increase in suspension turbidity when DD of CTS is increased from 37 % to 99% in the work of Kayitmazer *et al.*(**Figure 6**C) [31]. Concerning the relative arrangement between two complexing polyelectrolytes, Le *et al.* reported that HA forms more stable PECs with PLL than with DEAE-D, as both HA and PLL have their charges distributed evenly on the polymer chains which may allow more optimal ion-pairing than in the case of HA/DEAE-D PECs, where DEAE-D has random charge distribution [69]. It should be noted that since biopolymers usually have weak charges, their ionization rate also depends on media pH. A change in pH may lead to an increase in ionization rate, thus higher charge density as well as enhance the rigidity of polymer chains and increase thus the yield or particle size of

resulting PECs, or *vice versa* [115]. The effects of pH on PECs are further described in **Section 3.3.5**.

3.3.3. Total polyelectrolyte concentration

The most common range of total polymer concentration (C_P) for obtaining colloidal PECs from HA is 0.5-2 $g.L^{-1}$ (**Table 1**). Generally, with a fixed polyanion/polycation ratio, an increase in C_P would enhance PEC formation, i.e. larger size and higher yield of PEC particles or macro-aggregation due to involvement of more polymer chains (**Figure 7**). Kayitmazer *et al*. observed higher turbidity of HA/CTS PEC suspensions when C_P is increased from 0.1 to 1 $g.L^{-1}$ (**Figure 6**E) [31]. Umerska *et al.* reported an increase in particle size and turbidity for PECs from HA/PROT [111] (**Table 1**) and HA/CTS [97] when C_P is increased from 1 to 2 $g.L^{-1}$. Greater particle size and PDI are also observed when C_P becomes higher in the systems of HA/PLL and HA/DEAE-D PECs (ref. [2] and [81] in **Table 1**, respectively), or other HA/CTS PECs [107, 108]. Logically, an increase in C_P can also facilitate macro-aggregation if the polyelectrolyte MW is relatively high, e.g. when C_P is increased from 1.25 to 1.8 $g.L^{-1}$ in HA/PLL PECs with HA MW of 1200 kDa (ref. [2] in **Table 1**), or even lead to a macrogel at extremely high C_P, e.g. HA/CTS PECs at C_P of 40 $g.L^{-1}$ [116]. In general, acceptable characteristics of polysaccharide-based PECs can be guaranteed by using dilute polymer solutions, usually corresponding to a C_P under 1 $g.L^{-1}$ [115, 117].

3.3.4. Charge ratio

In aqueous media with a given ionic strength, the molar ratio between negative and positive charges (n-/n+) of two complexing polyelectrolytes decides the sign and strongly affects the magnitude of the net surface charge of PECs, thus influences their structure and stability. A n-/n+ which is far from the stoichiometric ratio (n-/n+ = 1) can lead to a great mismatch in ion-pairing

and generate particles with more unpaired charges, thus a greater net charge. This would result in looser, more expanded and more polydisperse structures of PEC particles, with a more pronounced and highly charged shell from uncomplexed polyelectrolyte segments [81, 95, 97]. The presence of such uncomplexed segments on particle shell can be evidenced through zeta potential: a negative zeta potential indicates uncomplexed polyanion chains on PEC surface, while a positive value indicates an excess of polycations [52]. When n-/n+ is closer to 1, more effective charge compensation would generate more compact and hydrophobic PEC particles with a lower net charge. This can be seen from the decrease in particle size, PDI and absolute zeta potential as n-/n+ is varied from 0.1 to 0.8 or from 10 to 1.25 in HA/DEAE PECs (ref. [81] - **Table 1**), and from 1:3 to 1:1.25 (ref. [108] - **Table 1**) or from 0.2 to 0.31 (ref. [107] - **Table 1**) in HA/CTS PECs.

However, when n-/n+ is sufficiently close to 1, their low net surface charge may not allow enough electrostatic stabilization, thus can facilitate their agglomeration to form larger particles as illustrated in **Figure 7** and eventually precipitation [6, 97, 118-120]. This can be seen at n-/n+ = 1 for HA/DEAE-D PECs (ref. [81] - **Table 1**) and n-/n+ between 0.47 and 6.6 for HA/CTS PECs (ref. [107] - **Table 1**). Meanwhile, if n-/n+ is extremely far from 1, PECs may not be formed due to the insignificant amount of either polycation or polyanion, as reported at n-/n+ under 0.12 for HA/CTS PEC in ref. [107] in **Table 1**. This effect can be compensated by increasing C_P or MW [81, 109]. It is thus necessary to set an upper and lower limit for n-/n+ in order to ensure sufficient polyanion and polycation for PEC formation depending on polymer nature and preparation condition [31]. The critical n-/n+ values for effective formation of PEC particles can be determined with an abrupt change in transmittance or viscosity of PEC suspensions upon n-/n+ evolution: when the microscopic phase separation corresponding to particle formation occurs, the transmittance would be reduced due to the increase in size and number of particles while the

viscosity would also be decreased because there are less free polymer chains in the continuous phase [31, 84]. In some cases, the effect of n-/n+ can be important enough to outweigh the other factors, e.g. for HA/zein PECs where an increase in the concentration of HA with unchanged concentration of zein can result in PEC particles with a smaller shape despite an increase in the overall C_P, probably because of the strong ability of HA in crosslinking zein to generate more compact particles [4].

Taken together, for obtaining colloidal PECs with good colloidal stability, n-/n+ should be optimized to be far enough from 1 to ensure a sufficient electrostatic stabilization (namely zeta potential over ± 30 mV [6, 97]) and avoid large aggregates but not too far from 1 to avoid poorly defined particles with large size or ineffective PEC formation. It should also be remembered that n-/n+ can change as a function of polyelectrolyte ionization rate and thus affected by media pH (see **Section 3.3.5**).

3.3.5. pH

Since charges in HA as well as other biopolyelectrolytes are mostly constituted by weakly charged groups (i.e. carboxyl and amine groups), pH can govern their ionization rate and subsequently the complexation efficiency and thus phase behaviors of PEC systems [31, 121]. Generally, pH should remain between the pKa values of HA (pKa = 3) and polycations to ensure their adequate charges for complexation [31]. A pH higher than 4.5 is ideal to ensure the complete deprotonation of HA (**Figure 6**A) in order to form stable PEC particles [84]. In most cases, both HA and polycations are readily dissolved in deionized water and sufficiently ionized to generate PECs without further pH adjustment [81, 93, 95, 109], except for CTS which requires a starting pH under 5.5 to ensure its dissolution [122]. After PEC formation, a gradual change from acidic to alkaline conditions will increase the deprotonation rate of polyelectrolytes, thus increase n-/n+

and reduce the zeta potential, and *vice versa* [47]. This can lead to the transformation in PEC morphology according to the effects of n-/n+ as described above in the **Section 3.3.4**. In other words, an extremely low or high pH can render the charge density of respectively HA or polycations inadequate for an effective charge compensation, which can lead to more expanded structures (i.e. larger particle size) or even disintegration of PECs, while either more compact particles or macroscopic aggregates can be observed when the actual n-/n+ approaches the stoichiometric ratio with a net surface charge closer to zero [47, 123, 124]. Particularly, a pH under 2 would deionize HA nearly completely and cause disintegration of PECs, which is proven by the change from turbid suspension to transparent solution of HA/CTS PECs when pH is decreased below 2 in the work of Kayitmazer *et al.* (**Figure 6**A-D) [31]. These results also show that the favorable pH range for efficient PEC formation depends also on other parameters, namely a wider range if polyelectrolytes with higher MWs are used (**Figure 6**B). The effect of pH is critical to consider when colloidal PECs are formulated for biomedical applications since particle stability should be maintained in the strict pH ranges corresponding to physiological conditions [26, 108], e.g. 7.35-7.45 in extracellular fluid (including blood plasma) [125], 4.1-5.8 on skin surface [126], 1.0-2.5 in gastric fluid and 6.5-7.5 in the intestines [127].

3.3.6. Counterions

Also due to the weak nature of ionic interactions in PECs, the presence of salts, typically NaCl, can lead to charge screening of the polyelectrolytes by counterions and thus profoundly affect the formation and stability of PECs. For colloidal PECs, an increase in ionic strength can cause higher charge screening on particle surface, which can be seen through a reduction in the absolute value of zeta potential and lead to higher PEC yield due to particle aggregation or even macroscopic precipitation due to weakened interparticle electrostatic repulsion (weaker long-range

repulsive force) [31, 82]. Such effects were observed in the work of Kayitmazer *et al.*, where the increase of NaCl concentration from 5 mM to 0.3 M led to a higher turbidity and a larger particle size of HA/CTS PECs, while the decrease in turbidity at NaCl concentration beyond 0.3 M was attributed to the sedimentation of macroaggregates (**Figure 6**E-F) [31]. In case of HA being complexed with proteins, a salting-out effect may also enhance hydrophobic interactions as a supplementary stabilization to favor the formation of PEC particles. This is suggested by Zhong *et al*. after remarking a larger particle size of PECs from HA and whey protein isolate (WPI) with more hydrophobic interactions within PECs when NaCl concentration is increased from 0 to 30 mM [128]. However, an extremely high ionic strength can prevent PEC formation or cause PEC disintegration because the electrostatic attraction between oppositely charged polyelectrolytes (short-range attractive force) is also reduced as charge screening takes place at molecular level [48, 129]. Changes in phase behaviour as well as average particle size of colloidal PEC systems are thus the net result of the two contradictory effects of charge screening at particle and molecular levels. Therefore, particle size evolution can be non-monotonic during the increase of salt concentration. For instance, in the above-mentioned work regarding HA/WPI, when NaCl increases beyond 40 mM, PEC hydrophobicity and particle size start to decrease since WPI is more likely to dissociate from PECs [128]. Similarly, the particle size of HA/DEAE-D PECs was reported to go up when NaCl concentration increases from 1 mM to 0.1 M but then decrease abruptly when the salt concentration reach 1 M [81]. Such effects of ionic strength are also illustrated in **Figure 7**. As with pH, ionic strength is also an important parameter for evaluation when PEC systems are designed for *in vivo* applications since the physiological ionic strength (i.e. NaCl 0.9 % or 0.15 M) is usually sufficiently high to destabilize HA-based colloidal PECs [81, 108].

The effects of counterions on PECs can also depend on counterion nature and some of them can even stabilize PECs against physiological ionic strength. For HA/CTS PECs, compared to Na^+, Ca^{2+} may have no different effect on complexation rate but can result in a more porous and swelling structure of PEC particles with higher water content, since the chaotropic property and larger hydration number of Ca^{2+} would not only increase the solubility and thus the hydrophilicity of polyelectrolytes but also make itself as well as its neighboring water molecules preferably remain in PECs rather than be expelled during the complexation [13]. Meanwhile, Zn(II) has been shown to stabilize HA/CTS PECs against physiological ionic strength [108, 130]. Wu *et al.* found that the addition of $ZnCl_2$ or $ZnSO_4$ at 1.5 mM before HA/CTS PEC formation (pre-stabilization) results in PEC NPs with good stability regrading particle size and zeta potential in PBS at both 4 °C and 37 °C for at least one month, while NPs without Zn(II) are disintegrated immediately upon submersion in PBS [108]. The stabilizing effect of Zn(II) in such case is supposed to stem from its chelation with CTS as ligands, in which Zn(II) adopts a tetracoordinate mode with primary amines and hydroxyl groups of CTS [131]. Nevertheless, the coordination between Zn(II) and the oxygen-containing donor groups of HA can also be considered as another mechanism [132]. The order of Zn(II) addition also affected the stability of these PECs, since NPs with Zn(II) added after the complexation (post-stabilized NPs) were stable in PBS at 4 °C but unstable at 37 °C. However, the work did not clarify the reason behind such difference between post-stabilized and pre-stabilized NPs, as well as between the two storage temperatures. Indeed, in the case of post-stabilization, the penetration of Zn(II) cations into the NP core may be limited by positive charges of the NP surface, as well as the increased hydrophobicity of these NPs at 37 °C since many CTS-based complexes can show thermoresponsiveness due to the thermo-dependent hydrophobic interactions between CTS chains [133, 134]. The salt form of Zn(II) had also a certain impact, as $ZnCl_2$ showed better

stabilizing efficiency than $ZnSO_4$ [108]. However, the work did not clearly describe the mechanism behind such results. This might be explained by the participation of sulfate in PECs as divalent crosslinking ions through electrostatic interactions with cationic charges of CTS, which can limit the exposure of these charges on particle surface and reduce their electrostatic stabilization [135].

Beside Zn(II), tripolyphosphate (TPP) can also be used as an adjuvant ion to stabilize HA/CTS PEC NPs in physiological salines [112, 136-141]. The stabilizing effect of TPP stems from the crosslinking of CTS through electrostatic interactions between anionic charges of phosphate groups in TPP and amine groups in CTS [142]. The effects of glutamate as a counter-anion on HA/CTS PECs have also been described. The chaotropic nature with dispersed charges of glutamate can increase considerably the solubility of CTS and renders glutamate less likely to screen the positive charges of CTS than chloride ions, allowing therefore a wider n-/n+ range for effective colloidal PECs formation [13]. It was also reported that glutamate would remain in PECs rather than be released and thus reduce the zeta potential of PEC particles through its negative charges [97].

3.3.7. Mixing method

When PECs are produced by simply mixing two polymer solutions, addition mode (rapid one-shot or slow dropwise addition) and addition order (HA in polycations or *vice versa*) can influence the properties of the resulting PECs [107, 143]. Dropping slowly the major polyelectrolyte into the other can result in large aggregates or macroscopic phase separation in the system, because at a certain point during such a gradual addition, the actual n-/n+ can reach the unity and the aggregation of neutral particles may take place at a much greater speed compared to that of n-/n+ evolution and thus leading to aggregation, which may be merely irreversible even

with a final n-/n+ far from the stoichiometric value if there is no further external interference [81, 113]. Accordingly, slow addition of the minor polymer in the major polymer can generate finer and more homogeneous PEC particles, which would give the same particle structure as that of one-shot dropping. Yang *et al*. reported a high turbidity (absorbance largely varied between 0.3-1.2) for PEC suspension of HA/CTS with HA:CTS ratio under 1:1 prepared by adding dropwise CTS to HA solution, indicating the formation of large aggregates, while the opposite order resulted in either absence of PEC particles or colloidal PECs having relatively small size (130-170 nm), making up transparent suspensions with a low absorbance which stays under 0.05 [107]. Concerning the one-shot method, the effect of addition order should be insignificant since the target n-/n+ can be immediately reached without sufficient time for particle aggregation to occur [81]. For instance, HA/DEAE-D PECs at n-/n+ of 0.8 have relatively small and similar particle size (150-200 nm) upon one-shot mixing regardless of addition order and dropwise addition of HA in DEAE-D solution, while dropwise addition of DEAE-D to HA leads to large particle size over 400 nm [81].

Despite being of minor importance, stirring rate, stirring time and complexation temperature might also have certain effects on physicochemical properties of colloidal PECs between HA and polycations. In an experimental design study, formation of smaller and more monodisperse particle size of HA/CTS PECs was reported to be favored by a middle stirring rate, as homogeneous distribution of both polyelectrolytes in the reaction media might not be guaranteed with either a low stirring rate (e.g. under 300 rpm) due to insufficient kinetic energy or a too high stirring rate (e.g. above 1300 rpm) which may cause bubbles and solution splashing [72]. Another experimental design study concerning HA/CTS PECs prepared with three different stirring times (10, 95 and 180 min) suggests that a longer stirring time can result in more

monodisperse PEC particles as shear can be offered during a sufficient time to generate rigid and stable particles [123]. In case of PECs from thermosensitive polymers, e.g. PECs between HA and elastin-like polypeptide, temperature should be sufficiently high (e.g. above 30-40 °C) to render their coacervation effective to generate particles [144]. Otherwise, temperature variation on a common range (4 to 60 °C) usually has little effect on the formation and/or the stability of colloidal PECs [72, 81, 107].

Beside the classical mixing method which requires adequate stirring, colloidal PECs can also be produced using electrospray ionization technique. This was applied in a work of Simonson and co-workers, where HA solution was propelled as nanosized droplets from the outlet of an electrically-charged capillary into a bath containing PLL solution without agitation, followed by centrifugation of the resulting dispersion to obtain HA/PLL PEC NGs (**Figure 8**A) [93]. Such colloidal PECs could thus be produced rapidly by electrospray method with relatively small and monodisperse particle size as well as good colloidal stability (**Figure 8**B-C).

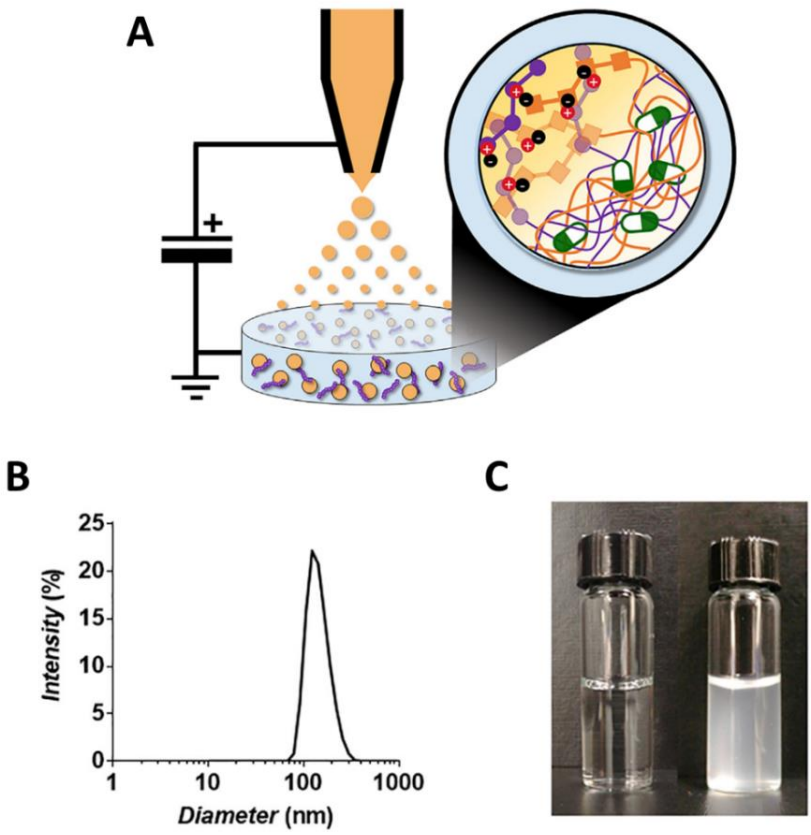

Figure 8. (**A**) Schematic illustration of using electrospray for preparing colloidal PECs from HA (yellow) and PLL (purple): drugs can be incorporated in either starting solution for their encapsulation in PEC particles. The obtained HA/PLL PEC suspension shows relatively monodisperse particle size (**B**) and good colloidal stability with homogeneous turbidity (**C**, *right*) as compared with the transparent aspect of the starting PLL solution (**C**, *left*). Reproduced with permission [93]. Copyright 2019, Elsevier.

4. Applications of colloidal polyelectrolyte complexes from hyaluronic acid

The following sections will provide a global view on various applications reported so far of HA-based colloidal PECs with a focus on recent advances within the last five years. These systems have been widely developed to deliver small molecule drugs (**Section 4.1**), nucleic acids (**Section 4.2**) and peptides or proteins (**Section 4.3**) for therapeutic purposes. Imaging agents can

also be delivered by colloidal HA-based PECs for bioimaging and diagnosis, possibly in combination with the above-mentioned therapeutic agents for theranostics (**Section 4.4**). Some nanoparticulate HA-based PECs which are not necessarily loaded with other bioactive or bioimaging cargo can also be employed as multifunctional platforms, e.g. carriers for HA delivery, emulsion stabilizers or building blocks for biomedical micro- or macro-materials (**Section 4.5**). Notably, a large number among those studies concern oncologic applications due to the rising need for cancer diagnosis and treatment, for which colloidal HA-based PECs can offer tremendous advantages as mentioned in **Section 1** and **Section 2**.

4.1. Small molecule drug delivery

Colloidal HA-based PECs have been described as nanocarriers for delivering small molecule drugs in numerous works, which are listed in **Table 2**. Many of them show positive results *in vitro* and/or *in vivo* regarding improvement in therapeutic efficacy of the drugs of interest, most of which are anticancer agents since their delivery is usually problematic due to poor aqueous solubility, poor stability, low bioavailability and high systemic toxicity owing to lack of cellular selectivity and thus needs more improvement [145]. Some works did not include *in vitro* or *in vivo* studies on therapeutic performance but still reported good drug encapsulation and/or controlled release with satisfactory physicochemical stability, showing thus their potential as promising nanocarriers for drug delivery. It should also be mentioned that among the presented works, drug-loaded colloidal PECs of Hsu *et al.* [146] and Freitas *et al.* [94] were further incorporated in secondary carriers as multifunctional platforms rather than employed directly in their colloidal form for their applications, for which a more detailed description will be provided in **Section 4.5**.

Table 2. Research on colloidal PECs from HA for small molecule drug delivery (references sorted in order of recentness)

Polyanion	Polycation	Drugs	Additives	Studied applications	Publication year	Ref.
PEO-PPO-grafted HA	DEAE-D or PLL	Curcumin	-	Drug encapsulation	2022	[69]
HA	Zein	Tetrahydrocurcumin	-	UVB-induced skin photoaging treatment *in vitro*	2022	[26]
HA	BSA	Ibuprofen or picolinic acid	-	Drug encapsulation and controlled release	2021	[84]
HA + pectin	CTS	Lidocaine	-	Drug encapsulation and controlled release	2021	[63]
Thiolated HA	CTS	Doxorubicin	-	pH/redox-responsive drug delivery, breast cancer treatment *in vitro*	2021	[70]
HA	CTS	DNICs	-	Cardiovascular disease treatment *in vitro*	2020	[147]
HA	PLL	Berberine	-	Wound healing *in vitro*	2020	[2]
HA	Zein	Quercetin	PEI-coated PLGA NPs	Implantable multiparticle gel assemblies; anti-inflammatory therapy *in vitro*	2020	[94]
HA	PAR	Cisplatin	-	Ovarian cancer treatment *in vitro* and *in vivo* through intraperitoneal aerosolization	2020	[148]

Table 2 (*continued*)

Polyanion	Polycation	Drugs	Additives	Studied applications	Publication year	Ref.
HA	CTS	Tocopherol or cholecalciferol	TPP (optional)	Drug encapsulation	2020	[137]
HA	Feather keratin	Doxorubicin	-	pH/redox-responsive drug delivery, colorectal carcinoma treatment *in vitro*	2020	[121]
HA	Zein	Honokiol	-	Breast cancer treatment *in vitro* and *in vivo*	2020	[6]
HA	Deoxycholic acid-grafted CTS	Doxorubicin	TPP	Cancer treatment *in vitro*	2019	[139]
HA	LF	EGCG	-	Encapsulation and antioxidant activity enhancement of EGCG	2019	[47]
HA	PAR	Pentamidine isethionate	-	Lung cancer and breast cancer *in vitro*	2019	[52]
HA	PLL	Doxorubicin or vancomycin	-	Doxorubicin: lung cancer and multidrug resistant ovarian cancer treatment *in vitro*; vancomycin: antimicrobial activity *in vitro*	2019	[93]
HA	Zein	Quercetagetin	-	Drug encapsulation for oral delivery	2018-2019	[49, 50]

Table 2 (*continued*)

Polyanion	Polycation	Drugs	Additives	Studied applications	Publication year	Ref.
HA	Zein	Curcumin	-	Drug encapsulation for oral delivery	2018	[110]
HIS-grafted HA	HIS-grafted PEI	Doxorubicin	Gellan gum	Chemoembolization	2018	[146]
HA	Zein	Curcumin	-	Colorectal carcinoma treatment *in vitro* and *in vivo*	2018	[4]
HA	Thiolated PLL	Chlorin e6	-	pH/redox-responsive drug delivery, breast cancer treatment *in vitro*	2018	[149]
HA	Lactose-modified CTS	Dexamethasone or fluoresceinamine	-	Drug encapsulation and controlled release, ROS scavenging	2018	[14]
HA	CTS	Mitoxantrone	Methoxy PEG	Improving particle stability and pharmacokinetics *in vivo*	2018	[7]
HA	CTS	Butyrate	TPP	ROS scavenging	2017	[141]
HA	CTS	Mitoxantrone + verapamil	-	Multidrug resistant breast cancer treatment *in vitro*	2017	[96]
HA	CTS	Curcumin	PEG	Glioma treatment *in vitro* and *in vivo*	2017	[150]
HA	CTS	Curcumin	PEG + LF	Glioma treatment *in vitro* and *in vivo*	2017	[151]

Table 2 (*continued*)

Polyanion	Polycation	Drugs	Additives	Studied applications	Publication year	Ref.
Gemcitabine-grafted HA	Pt(IV)-grafted CTS	Gemcitabine + Pt(IV)	-	Lung cancer treatment *in vitro* and *in vivo*	2017	[73]
Docetaxel-grafted HA	CTS	Docetaxel	-	Breast cancer treatment *in vitro*	2016	[72]
HA	CTS	Tenofovir	Zn(II)	HIV treatment *in vitro*	2016	[130]
HIS-grafted HA	HIS-grafted PEI	Doxorubicin	-	pH-responsive drug delivery, melanoma treatment *in vitro*	2015	[71]
HA	CTS	Curcumin	-	Glioma treatment *in vitro*	2015	[107]
HA	Galactosylated CTS	Doxorubicin	-	pH-responsive drug delivery, liver cancer treatment *in vitro*	2015	[152]

BSA: bovine serum albumin, CTS: chitosan; CUR: curcumin; DEAE-D: diethylaminoethyl dextran; DNIC: dinitrosyl iron complex; EGCG: epigallocatechin gallate; HA: hyaluronic acid; HIS: histidine; HIV: human immunodeficiency virus; LF: lactoferrin; PAR: polyarginine; PEG: polyethylene glycol; PEI: polyethylenimine; PEO-PPO: poly(ethylene oxide)-*co*-poly(propylene oxide); PLGA: poly(D,L-lactide-*co*-glycolide); PLL: poly-L-lysine; ROS: reactive oxygen species; TPP: tripolyphosphate; UVB: ultraviolet B

During the formulation and preparation steps of colloidal PECs, different factors (e.g. polymer concentration, mixing ratio, ionic strength, starting drug amount, addition order of drugs, stirring time and dialysis time) should be studied and optimized as they can affect drug encapsulation and release rate [96, 107, 128]. The effective encapsulation of drugs in PECs, i.e. in molecular or amorphous state, can be verified though differential scanning calorimetry (DSC) or X-ray diffraction (XRD) techniques [7, 96, 107]. For encapsulation of a positively charged drug like DOX, a high n-/n+ ratio which leads to negatively charged particles should allow a better encapsulation rate due to electrostatic attraction between particles and drug molecules [70]. For hydrophobic drugs, adding drugs before the complexation can offer better drug encapsulation when compared to incubating the fully formed particles with the drugs since the highly charged and hydrophilic shell around a PEC particle can inhibit the adsorption of hydrophobic molecules, as proven in the case of pyrene encapsulation in HA/DEAE-D PECs [81]. However, being also a hydrophobic drug, DOX was reported to be better encapsulated in HA/PLL PEC particles after their formation, since including DOX in the starting polymer solution can cause precipitation [93]. Yang *et al.* also found that adding curcumin (CUR) before the complexation between HA and CTS can lead to micro-scaled rather than nanosized PECs [107]. In order to limit the precipitation of such hydrophobic drugs and maintain their molecular state in a sufficient time during the complexation or the co-incubation for an effective inclusion of drug molecules in PEC particles, organic cosolvents like ethanol or acetone can be used, which should be thereafter removed by evaporation or dialysis [69, 107]. Specifically, to encapsulate hydrophobic bioactive polyphenols like CUR and quercetagetin in HA/zein PECs, the complexation should take place in an ethanol-water mixture due to the low aqueous solubility of both zein and the active compounds, followed by ethanol evaporation in order to obtain the final drug-loaded PECs (antisolvent coprecipitation

method, **Figure 5**) [49, 50, 86, 110]. For PECs from HA and proteins, encapsulation of a hydrophobic drug like CUR can also be improved with an adequate NaCl concentration due to enhanced hydrophobic force with "salting-out" effect, as reported for colloidal PECs from HA and whey protein isolate [128]. Physical coating of PECs with polyethylene glycol (PEG) might also reduce the leakage of hydrophobic drugs and therefore enhance their encapsulation, as suggested by Xu *et al.* in their work regarding CUR encapsulation in HA/CTS PECs [150]. By using HA functionalized with thermosensitive amphiphilic polyethers, i.e. poly(ethylene oxide)-*co*-poly(propylene oxide) (PEO-PPO), Le *et al.* also found that the encapsulation of CUR in PECs can be improved by controlling complexation temperature [69]. Covalent conjugation of drug molecules on parent polymers of PECs as prodrugs instead of physical entrapment method can also improve drug solubility and encapsulation, pharmacokinetic properties and therapeutic efficacy while reducing their systemic side effects, for example HA/CTS PECs with covalently bonded gemcitabine and platinum (IV) on HA and CTS respectively [73] or with docetaxel grafted on HA [72]. Another finding worth mentioning is that for HA/CTS PECs loaded with tocopherol (also known as vitamin E), which is a lipophilic compound, using TPP for further particle stabilization as mentioned in **Section 3.3.6** can lead to particles having a better controlled structure but may reduce the encapsulation rate of tocopherol [137].

The stability of colloidal PECs in biological fluids, as for other nanoparticulate systems, is greatly affected by the high ionic strength and proteins in these fluids since the former can lead to PEC aggregation or disintegration as described in **Section 3.3.6,** while the latter can form a "protein corona" (opsonization) on the particle surface that would possibly modify their stability with undesirable effects, such as aggregation or phagocytosis by immune cells [148, 153, 154]. Evaluating the particle size in biological fluid can allow verifying their stability in such conditions.

Considering some inconveniences of DLS in observing particle stability in undiluted biofluids, Shariati *et al.* reported the use of fluorescent single-particle tracking as an alternative but more pertinent method to ascertain the stability of HA/PAR PEC particles in undiluted ascetic fluid [148]. Such good stability of HA-based colloidal PECs can be attributed to the protecting effect of HA against protein adsorption [10]. PEGylation, one of the most common method to produce "stealth" NPs in nanomedicine, can also be applied to protect colloidal PECs from opsonization, therefore improve their circulation time *in vivo* and bioavailability of the loaded drugs, as evidenced with PEGylated HA/CTS PECs for mitoxantrone delivery [7]. In addition, complementary counterions have been employed to stabilize drug-loaded PEC particles against physiological salines as mentioned in **Section 3.3.6**, e.g. Zn(II) ions for stabilizing tenofovir-loaded HA/CTS PECs [130] or TPP for HA/CTS PECs encapsulating DOX [139]. The amphiphilic PEO-PPO grafts on constituent polymers can also stabilize PEC particles against physiological ionic strength through supplementary intraparticle hydrophobic interactions [69]. Moreover, when prepared from thiol-disposing polymers, e.g. HA-SH, PLL-SH or feather keratin, PEC particles can be further stabilized by self-crosslinking though the formation of the cleavable disulfide bonds as a result of redox reaction between thiol groups, either spontaneously with oxygen readily present in the media or more favorably upon adding an oxidizing agent like hydroxy peroxide, which may ultimately enhance drug encapsulation and PEC stability against high ionic strength [70, 121, 149].

Regarding drug release, PECs can offer a controlled release which follows an initial burst release phase and might depend on the studied pH [4, 107]. In case of DOX, which becomes more positively charged and thus more hydrophilic at lower pH, a mild acidic condition as in tumor microenvironment (pH between 6-7) or intracellular vesicles (pH between 4.5-6.5) can trigger drug release from PECs, since the protonation of both polyanions and polycations can favor PEC

swelling for drug diffusion and the increase in positive charges can extrude drug molecules from PECs through electrostatic repulsion, allowing thus a pH-responsive behavior for controlling drug release [26, 152]. Conjugation of HIS on parent polymers was also reported to enhance PEC stability and encapsulation rate of DOX through hydrophobic interactions and favor drug release in acidic conditions owing to the pH-dependent hydrophilic-hydrophobic balance of HIS, where the protonation of HIS moieties at low pH can reduce their hydrophobic interaction with more positive charges and lead to the expulsion of DOX from the particles [71]. Moreover, self-crosslinking though disulfide bonds in HA-based PECs can result in not only better PEC stability as previously mentioned but also a dual-responsive behavior for triggering drug release in tumor intracellular microenvironment, since the extremely high concentrations of both HAase and glutathione (GSH) at these locations can cause respectively HA degradation and disulfide bond cleavage to destabilize PECs and release the loaded drugs [70, 121, 149].

In terms of drug targeting, beside the CD44-targeting effect of HA, further addition of other ligands can improve the tumor targeting effect, e.g. LF attachment on PEC particle surface through electrostatic interactions with HA can offer these particles with better permeation through the blood-brain barrier, leading to a dual-targeting effect for treating brain tumors [151], whereas grafting with galactose moieties can further improve hepatoma-targeting capacity through the recognition of galactose receptors on hepatocytes [152]. Co-delivery of anticancer drugs with other therapeutic agents can also be applied for additional benefits, e.g. HA/CTS PEC NPs for attacking multidrug resistant breast tumor cells by co-delivering mitoxantrone, a nonspecific anticancer drug, and verapamil, a calcium antagonist which can effectively reverse drug resistance in order to enhance the cytotoxic effect of mitoxantrone [96]. Administration route can also affect the therapeutic efficacy of drug loaded PECs, e.g. delivering cisplatin-loaded HA/PAR PEC

nanocarriers intraperitoneally by pressurized local aerosolization demonstrated a more homogeneous distribution of particles with a deeper drug penetration at targeted tumor sites and thus better antitumor efficacy compared to the classical intravenous (IV) injection [148].

HA-based colloidal PECs have also been developed to deliver small molecule drugs for non-oncologic therapy. Simonson *et al.* suggested that HA/PLL PEC NGs are promising for improving the antibiotic potency of vancomycin against both Gram-negative and Gram-positive bacteria, as the minimum inhibitory concentration (MIC) of vancomycin delivered by such NGs in treating *E. coli* and *S. aureus* was respectively 4-fold and 15-fold lower when compared to free vancomycin [93]. The mechanism proposed by the authors for this effect is that HA can preferentially recruit the bacteria pathogens to the NG surface since this polysaccharide is a carbon source for their essential activities, while the subsequent electrostatic interactions between PLL and bacterial cell wall can permeabilize the latter and therefore bacterial cells are more exposed to the drug. Encapsulation of berberine in HA/PLL PEC NGs for wound healing with satisfactory *in vitro* results was also described by Amato *et al.* [2]. Meanwhile, Wu *et al.* reported the delivery of tenofovir, a HIV-1 reverse transcriptase inhibitor, by colloidal HA/CTS PECs stabilized with Zn(II) ions and decorated with anti-α4β7 immunoglobulin as a ligand for targeting HIV-infected cells [130]. The work showed good biocompatibility of such PECs and their ability to improve the inhibitory effect of tenofovir on HIV-1 infection, in which the contributing roles of Zn(II) ions and the targeting ligand were evident. HA/CTS PEC NPs were also elaborated by Akentieva *et al.* to deliver dinitrosyl iron complexes (DNICs) as a nitric oxide (NO) donor for treating cardiovascular diseases [147]. Their studies demonstrated the capability of HA/CTS PEC NPs to incorporate and stabilize DNICs, then increase and prolong NO generation from such complexes and subsequently improve the viability of cardiomyocytes *in vitro*. In another work, HA/zein PEC NPs were reported

for topical delivery of tetrahydrocurcumin (THC) to alleviate Ultraviolet B (UVB)-induced skin photoaging, since the particles can be uptaken by UVB-exposed keratinocytes through CD44-mediated endocytosis, where the ROS produced in UVB-induced inflammation can promote the degradation of HA to liberate both THC and low MW HA, which can act synergistically in turn as scavengers of ROS to reduce oxidative damage and cell apoptosis [26]. Indeed, the protective effects of HA against radiation damage may stem from not only its chemical reactions with ROS but also a biological mechanism involving a complexity of cellular signaling pathways [27].

4.2. Nucleic acid delivery

Nucleic acid (NA) delivery has been applied in gene therapy technologies as emerging approaches for treating genetic diseases, especially cancers [155, 156]. Classical gene therapy involves transporting coding DNAs into diseased cells in order that their expression can correct defective genes, replace absent genes or provoke antitumor reactions [155]. Gene silencing, which is a more recent technology for gene therapy, is done by introducing specific non-coding RNAs like small interfering RNAs (siRNAs) or microRNAs (miRNAs) into targeted cells so as to suppress the translation and thus the expression of targeted genes [156]. Numerous cationic polymers (e.g. PROT, CTS, PEI, PLL and PAR) have long been known as cellular transfection agents due to the capability to form electrostatic complexes with NAs, which can neutralize their strong negative charges and thus facilitate their intracellular delivery [157]. However, such binary complexes can exhibit insufficient compaction and low stability as well as nonspecific interactions with biological molecules due to extensive positive charges and high toxicity [41, 158, 159], leading to the need of further complexation with a biocompatible polyanion like HA to form ternary complexes disposing better properties [160]. As for small drugs-loaded PECs, HA can also contribute to the physicochemical stability of NA-loaded PECs in serum [43, 161]. Furthermore,

the presence of HA as a protecting shell can prevent aggregation of NA-loaded PEC particles and the inactivation of NAs after lyophilization and rehydration in order to ensure an unimpaired transfection efficiency [33]. Accordingly, high transfection efficiency was reported in multiple studies regarding colloidal PECs from HA for delivering different types of NAs, including siRNA, miRNAs, oligoRNAs and linear or plasmid DNAs (pDNAs) (**Table 3**).

Table 3. Research on colloidal PECs from HA for delivering nucleic acids (references sorted in order of recentness)

Polyanion	Polycation	Cargo	Additives	Studied applications	Publication year	Ref.
DOP-grafted HA	PBAE	DNA	-	Cell transfection	2021	[76]
HA	PROT	siRNA + Pt(IV)	Polyglutamic acid	Pt-resistant lung cancer treatment *in vitro* and *in vivo*	2021	[160]
HA	Imidazole-grafted PLL	miRNA	-	Triple-negative breast cancer treatment *in vitro*	2020	[98]
HA	Trimethyl CTS	siRNA	-	Breast cancer, colon cancer and melanoma treatment *in vitro* and *in vivo*	2020	[162]
TCA-grafted HA	PROT	siRNA	-	Colorectal liver metastasis treatment *in vitro* and *in vivo*	2019	[60]
HA	PROT	siRNA + EGCG	Cell-penetrating peptide	Drug-resistant triple-negative breast cancer treatment *in vitro* and *in vivo*	2018	[53]
HA	PEI-grafted CTS	pDNA	-	Cell transfection	2018	[43]
HA	CTS	pDNA	-	Liver cancer treatment *in vitro* and *in vivo*	2017	[34]
HA	CDX-grafted PLL	oligoRNA + doxorubicin	-	Hepatocellular carcinoma treatment *in vitro* and *in vivo*	2017	[62]

Table 3 (*continued*)

Polyanion	Polycation	Cargo	Additives	Studied applications	Publication year	Ref.
HA	CTS	miRNA + doxorubicin	TPP	Triple-negative breast cancer treatment *in vitro* and *in vivo*	2014	[140]
HA	PEI	pDNA	-	Melanoma treatment *in vitro* and *in vivo*	2010	[33]
HA	CTS	pDNA	-	Cell transfection	2009	[120]
HA	PAR	siRNA	-	Melanoma treatment *in vitro* and *in vivo*	2009	[56]
HA	PEI	pDNA	-	Cell transfection	2009	[10]
HA	CTS	pDNA	TPP	Cell transfection	2008	[117]
ODN-grafted HA	PROT	ODN	-	Cell transfection	2007	[74]

CDX: cyclodextrin; CTS: chitosan; DOP: dopamine; EGCG: epigallocatechin gallate; HA: hyaluronic acid; miRNA: micro ribonucleic acid; ODN: oligodeoxynucleotide; PAR: polyarginine; PBAE: poly(β-amino esters); pDNA: plasmid deoxyribonucleic acid; PEI: polyethylenimine; PLL: poly-L-lysine; PROT: protamine; siRNA: small interfering ribonucleic acid; TCA: taurocholic acid; TPP: tripolyphosphate

During PEC formulation, the proportion of every component, i.e. HA, polycations and NAs, are highly important as they can affect the affinity of NAs to PECs and thus both their loading and release rate. A too low proportion of polycations or a too high proportion of HA might prevent efficient incorporation of NAs in PECs due to insufficient positive charges to form complexes with NAs. Accordingly, evaluating the amount of free NAs remaining in the formulation through gel electrophoresis can be realized to find the optimal proportion of these components [160, 161]. For example, Ma *et al.* reported that the amount of HA/PROT PECs with HA:PROT ratio of 1:1 m/m should be at least 20 times higher than that of siRNA in order to include all siRNA in the complexes [160]. Meanwhile, Kim *et al.* found that the optimal PEC:siRNA mass ratio is at least 12:5 when using PECs of HA/PAR (1:10 m/m) but this should be increased to at least 24:5 when HA:PAR ratio is increased to 1:1 m/m [56]. However, an excessively high proportion of polycation may result in large aggregates, e.g. HA/PLL/miRNA PECs with N/P ratio (molar ratio of amine groups on PLL to phosphate groups on miRNA) of 20 were reported to show a high particle size of 450 nm, which is much greater than the particle size of 120 nm obtained with N/P of 10 and 5 [98]. The MW and the proportion of HA are also important and can have various impacts on gene delivery efficacy. Sato *et al.* reported that HA has a protective effect on NA-loaded PEC NPs during lyophilization and rehydration, where a higher MW of HA can strengthen such effect to improve the transfection efficiency due to a better exposure of HA on the particle surface as mentioned in **Section 3.3.1** and thus better interaction with CD44 receptors [34]. Meanwhile, although HA can improve cell targeting through CD44 receptors, a too high proportion of HA in PECs may increase excessively negative charges in the complexes and therefore limit NA loading or cellular uptake due to stronger electrostatic repulsion between PECs and NAs or cell membranes respectively [56, 98, 99]. In return, once uptaken by cells, HA can accelerate the expression of the

transported genes by enhancing transcriptional activity in the transfected cells through certain cellular signaling pathways [34, 163].

In order to improve the stability of NAs in colloidal HA-based PECs, further modifications on PEC particles can be applied. Similar to small drug molecules, oligodeoxynucleotides (ODNs) can also be conjugated to HA in PECs through the cleavable disulfide bonds, which might allow better incorporation and stabilization of ODNs while still ensuring their intracellular release in the presence of GSH [74, 164]. Functional additives can also be introduced through either physical attachment or chemical grafting. For oral delivery, e.g. in targeting colorectal liver metastasis, the low oral stability of NAs can be a great challenge and might be overcome by using HA grafted with bile acids like taurocholic acid (TCA) in PEC nanocarriers. In a work of Hyun *et al.* regarding siRNA oral delivery for treating liver tumor, it was shown that inclusion in HA-TCA/PROT PECs can better protect the siRNA from gastrointestinal pH and nuclease than complexing with PROT alone [60]. Furthermore, these PECs were also shown to enhance intestinal absorption as well as increase and prolong liver biodistribution of siRNA. Such advantages may stem from the enterohepatic circulation of TCA as a bile acid: TCA in the gastrointestinal tract can bind to apical sodium bile acid transporters (ASBT) proteins in the small intestine for intestinal absorption of TCA, then be transported to the liver for recycling and reintroduced back into intestines with minimal clearance in the whole process (around only 5 %) [165]. However, the contribution of TCA in such improvement was not convincingly proven as these studies did not include HA/PROT PECs as a referent sample [60]. Another example is DOP grafted on HA for complexation with the biodegradable synthetic polycation PBAE and DNA to form DNA-loaded nanocomplexes in a work of Guo and co-workers [76], who took advantage of the bioadhesive abilities of DOP through

interactions with cell membrane and the high expression of DOP receptors on tumor cell surfaces in order to favor the tumor cellular uptake of such nanocomplexes.

Colloidal HA-based PECs were also studied for co-delivery of NAs and chemotherapeutic small molecules, which may offer synergistic effects. Ma *et al.* developed HA/PROT PEC nanocarriers for co-delivery of Pt(IV) as a platinum prodrug with survivin siRNA, which can reduce survivin overexpression and reverse Pt resistance to improve its cytotoxic effect in drug-resistant lung cancer cells [160]. In this work, Pt(IV) was used as a prodrug instead of Pt(II) (i.e. cisplatin) in order to avoid their interactions with siRNA, whereas polyglutamic acid was used not only as an additional anionic coating agent to increase the biocompatibility of the system but also as a layer of drug reservoir with covalently bonded Pt(IV), which offers a slower release of Pt(IV) compared to siRNA, allowing the reversal of drug resistance by siRNA to take place before the cytotoxic Pt(II) is produced and exerts its function. HA/PROT NGs were also described for the co-delivery of EGCG and siRNA [53]. EGCG is a natural compound exhibiting anticancer activity and NA stabilizing effect due to their noncovalent interactions, while siRNA can be useful for downregulation of drug resistance-related factors to allow better response to EGCG. The decoration of PEC NGs with tumor-homing cell-penetrating peptides was also employed in this work in order to improve particle accumulation in the tumors (**Figure 9**). In another work, coadministration of miRNA with DOX by TPP-stabilized HA/CTS PECs was also demonstrated by Deng et al [140]. Grafting cyclodextrin (CDX) on polycations in complex with HA is another approach which may allow not only a concurrent delivery of both NAs and hydrophobic chemotherapeutic compounds owing to the inclusion of the latter in CDX moieties, as reported for co-delivering oligoRNA and DOX with PECs from HA and CDX-grafted PLL [62], but also a

better biocompatibility and higher transfection rate when compared to non-modified polycations, for which the mechanism remains undiscovered [161, 166].

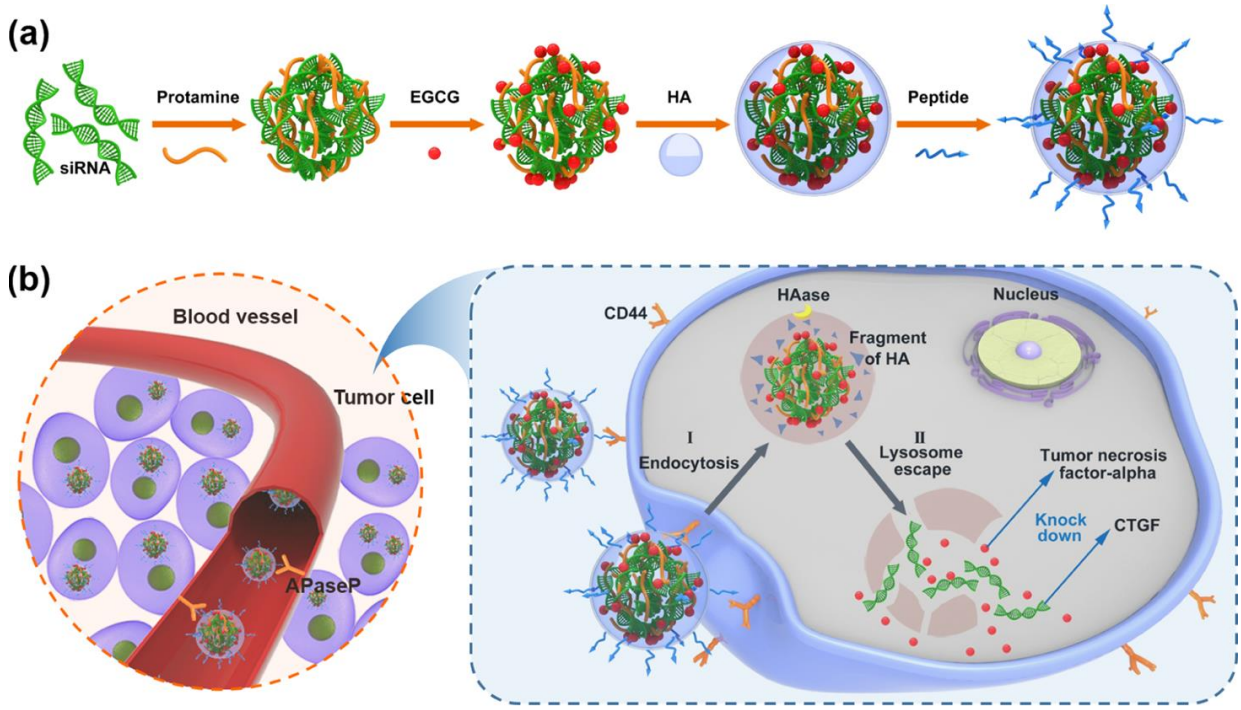

Figure 9. NGs from self-assembly of siRNA, PROT, EGCG, HA and tumor-homing cell-penetrating peptides. (**a**) Fabrication scheme and (**b**) Antitumor mechanism: NGs are accumulated in blood vessels of tumors through specific recognition of peptide ligands on the NG surface by aminopeptidase P (APaseP) on tumor blood vessel wall. The NGs are then bound to CD44 receptors on tumor cells before cell internalization, which is followed by NG degradation by HAase in lysosomes to liberate EGCG and siRNAs in order that EGCG can reduce the generation tumor necrosis factor-alpha to exert its antitumor functions while siRNA can downregulate the expression of connective tissue growth factor (CTGF) to reduce chemoresistance against EGCG. Reproduced with permission [53]. Copyright 2018, American Chemical Society.

Compared with oncotherapy, non-oncologic therapy has been less described for applications of NA delivered with colloidal HA-based PECs. An example is PEC NPs from HA and PEI-grafted CTS oligosaccharide (CSO) loaded with siRNA for the treatment of endometriosis [167]. In this work, HA/CSO-PEI/siRNA particles showed better selectivity to endometriosis lesion when compared to CSO-PEI/siRNA complexes, probably due to the targeting effect of HA through CD44 receptors on these cells. The former also exhibited no toxicity on reproductive organs while favoring both reduction in endometriosis lesion size and degeneration of ectopic endometrium in rat models. Colloidal PECs from HA and oleoyl-carboxymethyl-chitosan were also developed to deliver pDNA as oral vaccine for fish [168], where the incorporation of HA was reported to enhance the cellular uptake of the nanocomplexes by Caco-2 cells and improve the immune response in carps immunized with the DNA-loaded PECs through oral route, which was evidenced with a higher antigen-specific antibody titer.

4.3. Peptide and protein delivery

As for NAs, proteins as well as peptides are also biomacromolecules which can be delivered by HA-based PECs with improved stability. In contrast to NAs, which dispose strong negative charges, proteins can be either negatively or positively charged depending on pH and thus their associations in HA/polycations PECs would be mainly based on their electrostatic interactions with polycations or HA respectively, which can dictate the structure and properties of protein-loaded PECs. Umerska *et al.* reported that the effective inclusion of salmon calcitonin (sCT) in HA/PROT nanoplexes is due to electrostatic interactions between HA and positive charges of sCT [111]. Therefore, a higher proportion of HA can improve the loading rate of sCT and ultimately result in negatively charged PECs with sCT located nearer to the particle surface rather than the core, as the latter is rich in highly cationic PROT which may propel the protein

toward the particle surface. It should be noticed from this study that even though HA and sCT can readily form electrostatic complexes, the use of PROT as a polycation is still necessary since the relatively weak complexation between HA and the protein alone is not sufficient to form well-defined and stable particles, but an excessive presence of PROT might prevent sCT loading due to electrostatic repulsion and destabilize the system. In coherence with its relative emplacement near the particle surface, sCT showed great effects of on both particle size and surface charges as well as a release pattern starting with an initial burst followed by a prolonged release. Similar findings on protein displacement and release pattern were also described for positively charged HA/CTS PEC NPs loaded with the negatively charged insulin [138]. On the contrary, proteins with the same charge sign as that of PEC shells are more likely to be compacted in the innermost core rather than near the surface of PEC particles, which can be evidenced through the negligible effects of protein loading on particle size and net surface charge in the case of insulin loaded in negative HA/CTS PECs [115] and green fluorescent protein (GFP) loaded in negative HA/PLL PECs [93]. This may lead to a very different release pattern of proteins from PECs compared to that of small molecule drugs, as Simonson *et al.* reported that the release pattern of GFP from their negative HA/PLL PEC NGs started with an initial slow-release phase before the rapid release in the second phase corresponding to the degradation of the PEC core, while it is the opposite for the release of DOX from the same PEC particles [93]. Despite such a difference in release manner between the two types of cargo, both of them were effectively delivered into the studied cancer cells by CD44 targeting and exerted the desired effects, as evidenced by the cytotoxic assay in the case of DOX and intracellular fluorescence evaluation in the case of GFP. In another work, Liang *et al.* reported PEC NGs from PEI and EGCG-grafted HA loaded with lysozyme as a model protein or granzyme B as a cytotoxic protein with anticancer effect [3], where the role of EGCG grafting is

to facilitate the binding of protein cargos in PEC NGs through physical interactions and result in NGs with smaller size, better homogeneity and higher stability. The optimized systems showed promising results with a targeted cellular uptake and significant cytotoxic effect on CD44-overexpressing colon cancer cells. Nevertheless, as lysozyme disposes positive charges and was thus included in PECs through its association with HA [169], an excessively high proportion of HA-EGCG can reduce protein release and lower the therapeutic efficacy [3]. Collectively, the distribution of loaded proteins inside PEC particles and also their release pattern can be different case by case in function of protein nature and particle design.

Colloidal PECs from HA were also investigated in several works for oral delivery of proteins, which is usually challenging due to the low stability of proteins in the gastrointestinal tract as well as their low permeation through the mucous layer and enterocytes. Logically, most of these works focused on PECs from HA and CTS due to their synergistic effects in enhancing the mucoadhesive property of drug delivery systems [64]. In a work of Cui *et al.* regarding insulin oral delivery with HA/biotin-grafted CTS/insulin ternary nanocomplexes, HA can enhance the permeation of the studied systems in the mucous layer while the grafted biotin can enhance the uptake of insulin-loaded nanocomplexes in enterocyte though their biotin receptors, leading to an improvement in hypoglycemic effect *in vivo*, which can be optimized with a medium MW of HA and the highest substitution degree of biotin within the studied range [9]. Oral delivery of insulin with HA/CTS nanocomplexes was also reported by Sladek *et al.* but with a slightly different delivery mechanism, where the role of PECs was to protect insulin in digestive media and facilitate its passage through mucus but not through the epithelial wall due to scarce epithelial uptake of these nanocomplexes. Therefore, insulin should be released in the mucus and penetrate in its free form through epithelium, which can be assisted by sucrose laureate as a permeation

enhancer [115]. The group also found that insulin in plain HA/CTS/insulin PECs is indeed more prone to degradation by digestive enzymes than free insulin despite the compact inclusion of insulin within the PEC core. Such a lower stability of insulin in PECs was attributed to insulin restructuring upon complexation in PECs and can be avoided by coating PECs with a specific commercial enteric coating polymer [115]. On the contrary, Umerska *et al.* reported that HA/PROT nanocomplexes can limit the digestive degradation of sCT even though the protein was found to be located near the PEC surface [111].

HA-based nanoparticulate PECs have also been investigated for delivering antigenic peptides or proteins as a vaccine. Specifically, intranasal delivery of ovalbumin was reported in some research regarding PECs from HA/poly-L-lysine-*co*-polylactide [170] and HA-SH/trimethyl CTS-SH [65]. In the former work, the PECs of interest could effectively deliver ovalbumin into dendritic cells to upregulate cytokine production *in vitro* and enhance the production of IgG antibody *in vivo* upon intranasal administration in mouse models, which was attributed to the mucosal adhesion property of HA as well as its ability to enhance specific uptake of PECs through CD44 receptors on mucosal epithelium and immune cells. Regarding ovalbumin-loaded HA-SH/trimethyl CTS-SH PECs, Verheul *et al.* reported that the presence of thiol groups allowed the self-crosslinking of PECs with two main advantages: (i) better physicochemical stability of PECs during post-particle chemical modification (PEGylation) or under physiological saline condition and (ii) enhancing the adjuvant effects of PECs to improve ovalbumin-induced immunological response [65]. However, the work also showed that PEGylation offers no additional benefit or even abolishes the positive effect of PEC crosslinking on immunogenicity when the particles are delivered intranasally, which was contradictory to many previous works and could be attributed to the change in particle surface charge after the PEG-grafting reaction.

HA/CTS as well as chondroitin sulfate/CTS PEC particles were also described in the work of Dacoba *et al.* on delivering the peptide antigen PCS5 as an anti-HIV vaccine [75], where it was found that the covalent conjugation of the antigen on material polymers and their coadministration with polyinosinic:polycytidylic acid as an immunostimulant can both improve the immunological response, i.e. activation of antigen-presenting cells *in vitro*.

4.4. Imaging agent delivery

Imaging agent delivery has also been reported among the applications of colloidal PECs from HA and polycations, especially HA/PROT PECs. Xu *et al.* developed PECs from PROT in complex with HA and HA-SYL3C aptamer conjugation for delivering fluorescent catalytic hairpin assemblies (CHAs) as a novel type of nanoprobe for *in situ* detection of living circulating tumor cells (CTCs) in undiluted blood [171]. The mechanism of this approach is that once the catalytic hairpins are uptaken and released within CTCs, miRNA-21 readily present in these cells will activate the amplification of CHAs, which will restore and intensify their fluorescence. As HA and SYL3C aptamers on the PEC surface can bind respectively to CD44 receptors and epithelial cell adhesion factors on CTCs, they would provide the nanoprobes with dual targeting capability in order to efficiently deliver the CHA systems into these cells. HA/PROT PECs were also employed by Xia *et al.* for delivering GSH-coated gold nanoclusters (AuNCs) as a theranostic agent into tumor cells [11]. Their results showed that the stable complexes were formed based on electrostatic interactions between carboxyl groups of both HA and GSH on AuNC surface and amine groups of PROT as well as their hydrophobic interactions. The cytotoxic activity of AuNCs is based on the concept of photodynamic therapy, in which AuNCs are photosensitizing agents which can be transformed to excited state by irradiation and then react with intracellular triplet oxygen ($^3O_2$), i.e. ground state oxygen, to produce cytotoxic singlet oxygen ($^1O_2$) [172, 173]. In parallel, the

return of AuNCs to their lower energy state can also emit fluorescence. Due to the above-mentioned interactions among HA, PROT and GSH, the nanocomposites demonstrated enhanced fluorescence emission and better singlet oxygen generation when compared to plain AuNCs, respectively leading to better imaging results and greater cytotoxic effect on tumor cells *in vitro* after the selective cellular uptake which was favored by specific binding of HA to CD44 receptors. In another work, Sim *et al.* reported the delivery of ferumoxytol-loaded HA/PROT nanocomplexes (HAPF) to natural killer cells (NK cells) in order to obtained HAPF-labelled NK cells, which can be subsequently administered to solid tumors for adoptive cell transfer therapy (**Figure 10**) [8]. Labeling NK cells with HAPF has two advantages: (i) the possibility of exploiting magnetic resonance imaging (MRI) for guiding the transcatheter delivery of NK cells to tumors and (ii) magneto-activation of NK cells [174], which means that applying an alternating magnetic field can lead to mechanical movements of HAPF in NK cells and subsequently activate their cytolytic function through a mechanical-sensing mechanism to attack tumor cells. The efficient attachment of HAPF to NK cells was ascribed to the presence of both HA and PROT in HAPF, leading therefore to the high labelling efficiency of NK cells as observed in the study. For proof-of-concept, the authors reported the successful transcatheter intra-arterial local delivery of HAPF-labelled NK cells in a hepatocellular carcinoma rat model with good accumulation of NK cells at the tumor site and significant suppression of tumor growth.

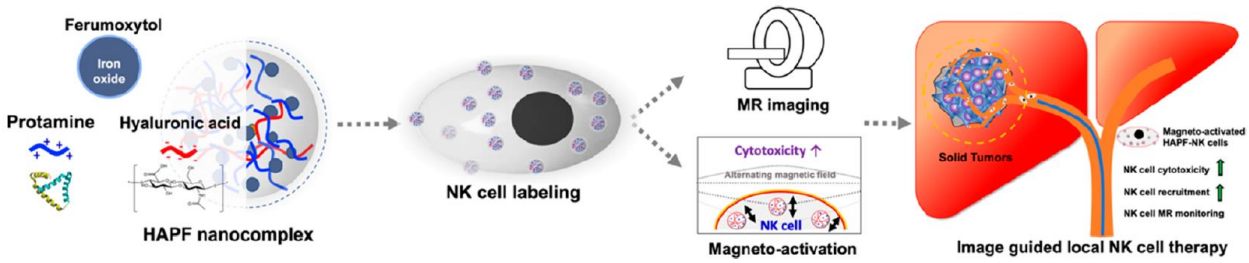

Figure 10. Schematic illustration of NK cell labeling with ferumoxytol-loaded HA/PROT PECs for MRI-guided local transcatheter delivery of NK cells in liver tumors and NK cell magneto-activation for antitumor effects. Reproduced with permission [8]. Copyright 2021, American Chemical Society.

PECs between HA and disulfide crosslinked PEI were also utilized for theranostic purposes, e.g. the delivery of hausmannite (Mn_3O_4) and hematite (Fe_3O_4) NPs as MRI contrast agents in combination with DOX and pDNA encoding Bcl-2 shRNA as therapeutic agents [12]. The obtained nanoassemblies showed excellent MRI contrast by reducing artifact signals and significant toxicity on cancer cells by the synergistic effect of both pDNA and DOX, while the CD44-targeting effect of HA was necessary for the selective tumor cellular uptake of such nanocomplexes. In another work, near-infrared (NIR) fluorescent indocyanine green (ICG) as a fluorescent probe was delivered to tumor cells by using HA/PBAE PEC NGs, which could be effectively internalized within these cells through CD44-mediated cellular uptake and thereafter disassembled under the highly acidic condition of intracellular vesicles in order to liberate ICG from its quenched state and strongly recover its NIR fluorescence [175].

4.5. Multifunctional platforms

With respect to dermatologic application of HA, the research group of Tokudome reported the use of nanoparticulate HA-based PECs as a novel approach for effective HA delivery into the

skin [95, 176]. In a first approach, HA/PROT PEC NPs were investigated and showed the capability to effectively penetrate into the dermis layer of the skin both *in vitro* and *in vivo* while free HA could only reach the stratum corneum, i.e. the outermost layer of the epidermis. Such studies further showed that after the penetration of HA/PROT PECs into the dermis, HA could be liberated in its free form and diminish the transepidermal water loss caused by UV irradiation [95]. Following this work, the group continued the research with HA/PLL PECs in simulated skin environment in order to elucidate the skin penetration pathway of HA-based PEC NPs [176], where the obtained results suggested that the better skin penetration of such NPs compared to free HA is due to the less hydrophilic characteristics of the particles as compared to free HA, which facilitates their penetration through intercellular lipids rather than transcellular pathway, while the subsequent release of free HA from these particles may be the result of PEC disintegration due to the high ionic strength under physiological conditions. It could be seen that for such topical administration, the disassembly of PECs under physiological salinity was indeed beneficial and necessary for HA release, in contrast with many works previously mentioned where it is a problem to overcome.

In regard to HA/CTS PECs, HA/CTS coacervates were shown to be promising scaffolds for cartilage tissue engineering since bone marrow stem cells can be encapsulated in such systems with long-term cell viability and well-spread cell morphology [13]. In addition to drug delivery capability, coacervates from HA and lactose-modified CTS can also scavenge ROS produced by neutrophils during inflammatory processes since both HA and CTS have been shown to possess ROS scavenging effect [14]. All of those results have highlighted the interest of HA/CTS coacervates for treating joint inflammation [14]. HA/CTS PEC NPs were also reported for the fabrication of polysaccharide composite films by particle casting in a work of

Yamazaki *et al.* [177], where the obtained films showed satisfactory mechanical properties with good adhesion to CD44-overexpressing cells and revealed therefore great potential as a material for biomedical and drug delivery applications.

Some nanocomplexes from HA and cationic proteins have also been described as emulsion stabilizers with more interesting properties than the proteins alone, for example in studies regarding HA/LF PECs [46, 178]. Such complexation was reported to enhance the thermal stability and antioxidant property of LF, while the emulsifying capability can only be improved upon covalent crosslinking between HA and LF [46]. In a work of Freitas *et al.*, anionic HA/zein PEC NGs were exploited as building blocks for fabricating colloidal gel assemblies though the electrostatic interactions between the former and cationic PEI-coated PLGA NPs (**Figure 11**) [94]. This concept was developed based on the usefulness of such a multiparticle assembly, including (i) moldability to generate solid implants with desired shapes and (ii) autonomous multiparticle shedding, i.e. spontaneous and gradual release of the constituent NPs and NGs into the adjacent microenvironment to exert specific functions on neighboring cells. For proof-of-concept, HA/zein NGs encapsulating quercetin as a model drug were used to obtain the quercetin-loaded multicomponent gels for delivering this drug to macrophages *in vitro*, which showed thereafter high drug loading with significant improvement in anti-inflammatory activity of macrophages. Hsu *et al.* also described the inclusion of DOX-loaded nanoparticulate PECs from HIS-grafted HA and HIS-grafted PEI in Gellan gum microspheres for chemoembolization [146]. Chemoembolization is a process widely used for treating liver tumors, in which anticancer agents at a high concentration are delivered into the tumors through a small catheter along an artery, which is then blocked off (embolized) by an embolizing agent (e.g. microparticles) in order to deprive the tumors from blood supply and keep a long-term high concentration of the drugs in the

tumors [179]. The above-mentioned studies showed that the unitary PEC NPs can facilitate DOX delivery into liver cancer cells, while the microspheres can serve at the same time as an effective embolic agent and a reservoir for releasing the PEC NPs to cause necrosis in the embolized regions *in vivo*, showing thus the potential of this system for application in transcatheter arterial chemoembolization to treat liver tumors.

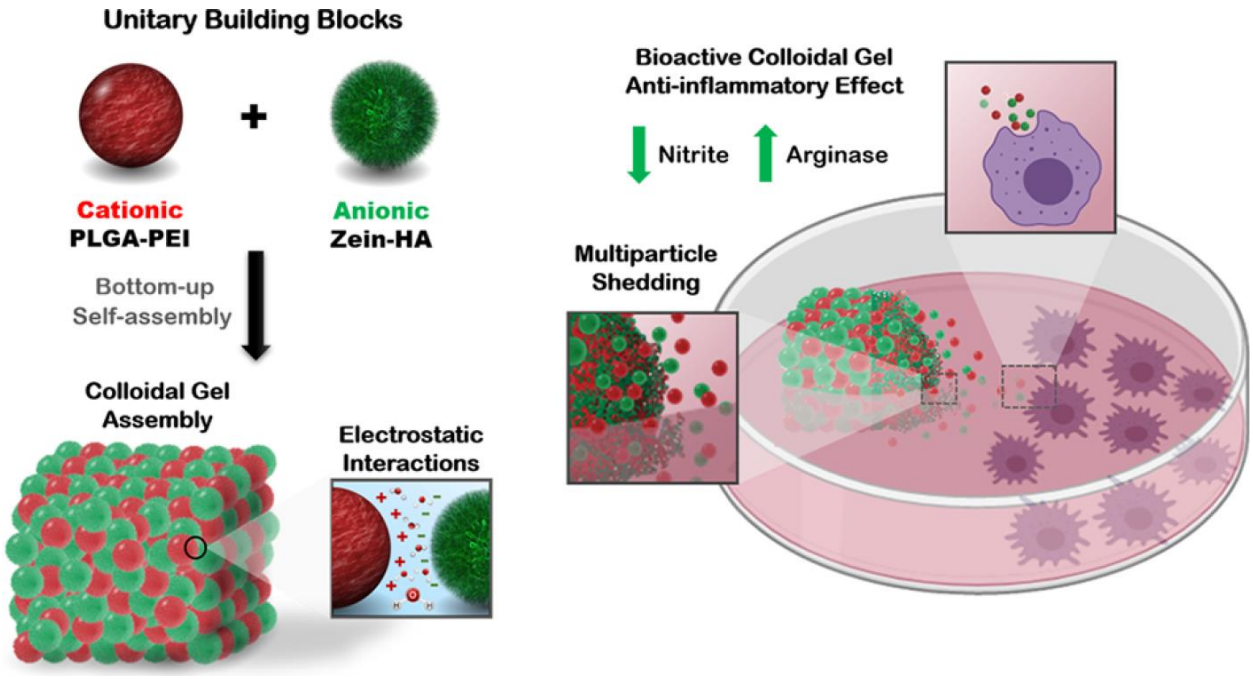

Figure 11. Bottom-up self-assembly of nanostructured colloidal gels through electrostatic interactions between PEI-coated PLGA NPs and HA/zein PEC NGs. Quercetin-loaded particles can be thereafter shed from the gel assembly and uptaken by neighboring macrophages to reduce their production of nitrite as a proinflammatory biomarker and increase the expression of arginase as an anti-inflammatory biomarker. Reproduced with permission [94]. Copyright 2020, American Chemical Society.

5. Current limitations and future perspectives

Despite the huge biomedical potential revealed through tremendous advancements in research, HA-based colloidal PECs are regarded as relative new systems and receive less attention than their counterparts from other polysaccharides, e.g. CTS or alginate. PubMed database (PubMed.gov) shows only 185 articles related to HA-based PECs, while 915 and 354 articles are found for CTS-based and alginate-based PECs, respectively. In terms of clinical trials, according to ClinicalTrials.gov, there has been so far no clinical trial of HA-based colloidal PECs or even HA-based NPs in general, while there are at least 8 and 1 clinical trials regarding CTS-based and alginate-based NPs, respectively. Needless to say, due to the lack of clinical evidence, no HA-based nanoformulation has reached the healthcare market, while commercialized HA-based products approved by FDA (US Food and Drug Administration) regard only HA concentrated solutions (e.g. Healon® and Triluron®) or HA-based films (e.g. Seprafilm®) according to FDA Medical Device Database. These observations show that many critical aspects regarding HA-based colloidal PECs remain to be thoroughly understood before they can be recognized as safe and efficacious for human application. One big gap in the literature for HA-based colloidal PECs concerns their behaviors *in vivo*, in terms of both therapeutic efficacy and toxicity. Namely, very few works on HA-based colloidal PECs for small molecule drug delivery in **Table 2** (**Section 4.1**) include *in vivo* results, rendering their therapeutic potential less convincing since the *in vitro* data may not reflect exactly the *in vivo* pathological conditions. The pharmacokinetic profile and therapeutic efficacy *in vivo* of the carried drugs should be therefore assessed. Nanotoxicology is another important issue receiving inadequate attention, which may prevent future clinical applications of HA-based colloidal PECs as well as all nanoformulations in general [180]. Most of the biocompatibility studies for HA-based colloidal PECs have been realized through cytotoxic

assay on healthy cells *in vitro* without considering their interactions with biological barriers and biomacromolecules during *in vivo* circulation. In this context, as mentioned in the **Section 3.2**, the transport through biological fenestrations *in vivo*, the possibility of opsonization, the uptake by the mononuclear phagocytic systems and the *in vivo* circulation time of HA-based PEC particles as well as the effects of particle characteristics (namely size, surface charge and hydrophobicity) on these aspects are of pivotal importance and should thus be evaluated in order to verify the biocompatibility and optimize the *in vivo* stability of these nanocarriers.

Although both CD44-targeting effect and HAase-induced degradation of HA can improve tumor-targeting drug delivery as mentioned in the advantages of HA-based colloidal PECs (**Section 2**), the latter effect seems to receive much less attention. HA-based colloidal PECs are often implied to be degradable by HAase without supporting empirical results [7, 53, 149]. Indeed, the degradation of HA by HAase is not always the case for HA in complex state. Le *et al.* reported that HA/PLL PEC particles with PLL in excess ($n_-/n_+ < 1$) are stable against HAase, which is attributed to the protective effect of PLL on the particle surface [69]. More interestingly, HA-based nanostructures may not only be stable against HAase but also inhibit this enzyme from degrading free HA, as reported by Duan *et al.* with micelles from HA grafted with poly(γ-benzyl-l-glutamate) as a potential HAase inhibitor for biomedical applications [181]. Therefore, HAase-induced degradation should not be generalized for all HA-based colloidal PECs and needs to be evaluated case by case, which can verify their potential as a HAase-responsive system for tumor targeting or a HAase-inhibiting agent. Furthermore, when HA-based colloidal PECs are degradable by HAase, one may doubt whether such a degradation can be catalyzed by extracellular HAase in tumors and liberate free HA fragments that compete with PECs for interactions with CD44 receptors [182]. This question is highly relevant as it can reduce the cell targeting effect of

PECs and should be therefore verified. Additionally, free HA has been known for its low stability in the presence of multiple factors, including high temperature [183], extremely acidic or alkaline conditions [184], UV irradiation and oxidizing species [25, 185] or ultrasound [186]. Electrostatic complexation with polycations may alter the stability of HA against these factors, which should be an essential topic of investigation and potentially leads to unprecedented applications of HA-based PECs.

From several works regarding HA-based colloidal PECs mentioned in **Section 4**, it is undeniable that their most prominent potential concerns cancer treatment. However, anticancer applications of HA-based colloidal PECs have been mostly limited to the delivery of chemotherapeutic agents and nucleic acids, while depending on CD44-receptor binding and responsiveness to tumor microenvironment factors like acidic pH, HAase and glutathione for enhancing targeting effects. With the flexible utility of HA-based colloidal PECs, they should be applied for more advanced concepts of anticancer therapy. As can be seen in **Section 4.4**, the work of Xia *et al*. with intracellular delivery of gold nanoclusters (AuNCs) is seemingly the only one using HA-based colloidal PECs for cancer treatment through ROS generation [11]. Intracellular delivery of Fe_3O_4 [8, 12] or Mn_3O_4 NPs [12] by means of HA-based colloidal PECs was also reported but only for bioimaging. It would be therefore interesting to verify their potential to treat tumor through ROS production, since Fe_3O_4 and Mn_3O_4 NPs have also been known for applications in chemodynamic therapy based on Fenton reactions, i.e. interactions between metal-based nanomaterials and H_2O_2 abundantly present in cancer cells to generate cytotoxic hydroxyl radicals (·OH) [172, 173, 187]. Furthermore, the recent emergence of photoresponsive [188, 189] and thermoresponsive [190-192] HA derivatives may allow the elaboration of much more intriguing HA-based colloidal PECs with multi-stimuli-responsiveness, which can be applied for

photo-triggered and/or thermo-triggered drug release and allow thus spatiotemporal control of drug delivery to target tumors [182].

Compared with oncologic applications, vaccine delivery and bacterial infection treatment are also topical and prominent subjects but have been much less investigated for HA-based colloidal PECs. From little but encouraging results reported in the **Section 4.3** on the immunologic adjuvant properties of colloidal PECs from HA/poly-L-lysine-*co*-polylactide [170], HA-SH/trimethyl CTS-SH [65] and HA/CTS [75], more studies should be dedicated to HA-based colloidal PECs as a potential vaccine adjuvant. Particularly, while the works above concern only peptide or protein vaccine delivery, HA-based colloidal PECs have also demonstrated their capacity to deliver different types of RNA and therefore can be studied for RNA-based vaccines, which are emerging as a new vaccine generation [193]. Those studies would not only shed more light on the immunological effects of HA-based colloidal PECs, which remain barely understood, but also be highly practical in the race to find the most safe, efficacious and economic vaccines against newly emerging human viruses, like SARS-CoV-2 and new Monkeypox virus variants. Likewise, HA-based colloidal PECs have not been widely studied for antibiotic delivery. From the bacterial targeting effect of HA suggested by Simonson *et al.* after their studies on HA/PLL colloidal PECs for treating *E. coli* and *S. aureus* [93] (**Section 4.1**) and several recent works which reveal remarkable interest in HA-based nanoformulations for infection treatment [194, 195], antimicrobial applications of HA-based colloidal PECs should be considered for more serious investigation, especially in the current era where more powerful therapeutic platforms are needed to cope with increasing antibiotic resistance.

6. Conclusion

HA-based colloidal PECs can be fabricated with a simple, rapid and "green" process based on self-assembly of HA and polycations through electrostatic attraction. These systems combine several advantages from green chemistry, nanotechnology and the exceptional characteristics of HA, namely excellent biocompatibility, flexibility in chemical modification and specific biological properties including the CD44-binding capability and HAase-induced degradation. Despite a technically simple process of preparation, designing the structures of colloidal PECs to fit their intended applications and accordingly choosing the right parameters to achieve such desired characteristics are not straightforward. The performance of colloidal PECs should be dictated by their size, surface charge and hydrophobicity, while these characteristics are governed by a complexity of interdependent parameters, including polyelectrolyte characteristics (MW and charge density), formulation composition (polymer concentration, mixing ratio, pH and counterions) and preparation technique (addition order and addition speed). It is therefore necessary to optimize these parameters and find the best compromise in order to obtain PEC particles with satisfactory properties. Through numerous research works, colloidal HA-based PECs have been proven as potential materials for biomedical platforms and drug carriers with continuous advancements in drug and nanocarrier stabilization as well as biological selectivity. Nevertheless, some fundamental aspects of these structures remain to be deciphered, namely their *in vivo* fate and toxicity, as well as the stability of HA in complex state. In addition, novel HA derivatives with stimuli-responsive characteristics can be applied in the future to elaborate more high-performing PECs for targeted drug delivery. Last but not least, many potential applications of HA-based colloidal PECs remained insufficiently exploited and should be therefore studied

more closely, especially for applications in chemodynamic therapy, vaccine delivery and bacterial infection treatment.

Acknowledgements

The authors from Normandie Université thank the Graduate School of Research XL-Chem (ANR-18-EURE-0020 XL-Chem), the Normandy region and the European Union for financial support.

References

[1] Kulkarni, A. D.; Vanjari, Y. H.; Sancheti, K. H.; Patel, H. M.; Belgamwar, V. S.; Surana, S. J.; Pardeshi, C. V., *Artif. Cells, Nanomed., Biotechnol.* **2016,** *44* (7), 1615-1625. DOI https://doi.org/10.3109/21691401.2015.1129624.

[2] Amato, G.; Grimaudo, M. A.; Alvarez-Lorenzo, C.; Concheiro, A.; Carbone, C.; Bonaccorso, A.; Puglisi, G.; Musumeci, T., *Pharmaceutics* **2020,** *13* (1), 34. DOI https://doi.org/10.3390/pharmaceutics13010034.

[3] Liang, K.; Ng, S.; Lee, F.; Lim, J.; Chung, J. E.; Lee, S. S.; Kurisawa, M., *Acta Biomater.* **2016,** *33*, 142-152. DOI https://doi.org/10.1016/j.actbio.2016.01.011.

[4] Seok, H.-Y.; Rejinold, N. S.; Lekshmi, K. M.; Cherukula, K.; Park, I.-K.; Kim, Y.-C., *J. Controlled Release* **2018,** *280*, 20-30. DOI https://doi.org/10.1016/j.jconrel.2018.04.050.

[5] Xu, Y.; Zhu, H.; Denduluri, A.; Ou, Y.; Erkamp, N. A.; Qi, R.; Shen, Y.; Knowles, T. P., *Small* **2022**, 2200180. DOI https://doi.org/10.1002/smll.202200180.

[6] Zhang, Q.; Wang, J.; Liu, D.; Zhu, W.; Guan, S.; Fan, L.; Cai, D., *Carbohydr. Polym.* **2020,** *240*, 116325. DOI https://doi.org/10.1016/j.carbpol.2020.116325.

[7] Wang, J.; Asghar, S.; Yang, L.; Gao, S.; Chen, Z.; Huang, L.; Zong, L.; Ping, Q.; Xiao, Y., *Int. J. Biol. Macromol.* **2018,** *113*, 345-353. DOI https://doi.org/10.1016/j.ijbiomac.2018.02.128.

[8] Sim, T.; Choi, B.; Kwon, S. W.; Kim, K.-S.; Choi, H.; Ross, A.; Kim, D.-H., *ACS Nano* **2021,** *15* (8), 12780-12793. DOI https://doi.org/10.1021/acsnano.1c01889.

[9] Cui, Z.; Qin, L.; Guo, S.; Cheng, H.; Zhang, X.; Guan, J.; Mao, S., *Carbohydr. Polym.* **2021,** *261*, 117873. DOI https://doi.org/10.1016/j.carbpol.2021.117873.

[10] Pathak, A.; Swami, A.; Patnaik, S.; Jain, S.; Chuttani, K.; Mishra, A. K.; Vyas, S. P.; Kumar, P.; Gupta, K. C., *J. Biomed. Nanotechnol.* **2009,** *5* (3), 264-277. DOI https://doi.org/10.1166/jbn.2009.1031.

[11] Xia, J.; Wang, X.; Zhu, S.; Liu, L.; Li, L., *ACS Appl. Mater. Interfaces* **2019,** *11* (7), 7369-7378. DOI https://doi.org/10.1021/acsami.8b19679.

[12] Rajendrakumar, S. K.; Venu, A.; Revuri, V.; George Thomas, R.; Thirunavukkarasu, G. K.; Zhang, J.; Vijayan, V.; Choi, S.-Y.; Lee, J. Y.; Lee, Y.-K., *Mol. Pharmaceutics* **2019,** *16* (5), 2226-2234. DOI https://doi.org/10.1021/acs.molpharmaceut.9b00189.

[13] Karabiyik Acar, O.; Kayitmazer, A. B.; Torun Kose, G., *Biomacromolecules* **2018,** *19* (4), 1198-1211. DOI https://doi.org/10.1021/acs.biomac.8b00047.

[14] Vecchies, F.; Sacco, P.; Decleva, E.; Menegazzi, R.; Porrelli, D.; Donati, I.; Turco, G.; Paoletti, S.; Marsich, E., *Biomacromolecules* **2018,** *19* (10), 3936-3944. DOI https://doi.org/10.1021/acs.biomac.8b00863.

[15] Patra, J. K.; Das, G.; Fraceto, L. F.; Campos, E. V. R.; Rodriguez-Torres, M. d. P.; Acosta-Torres, L. S.; Diaz-Torres, L. A.; Grillo, R.; Swamy, M. K.; Sharma, S., *J. Nanobiotechnol.* **2018,** *16* (1), 1-33. DOI https://doi.org/10.1186/s12951-018-0392-8.

[16] Blanco, E.; Shen, H.; Ferrari, M., *Nat. Biotechnol.* **2015,** *33* (9), 941-951. DOI https://doi.org/10.1038/nbt.3330.

[17] Tse Sum Bui, B.; Haupt, K., *ChemBioChem* **2022,** *23* (8), e202100598. DOI https://doi.org/10.1002/cbic.202100598.

[18] Rafique, R.; Kailasa, S. K.; Park, T. J., *TrAC, Trends Anal. Chem.* **2019,** *120*, 115646. DOI https://doi.org/10.1016/j.trac.2019.115646.

[19] Kazemi, Y.; Dehghani, S.; Nosrati, R.; Taghdisi, S. M.; Abnous, K.; Alibolandi, M.; Ramezani, M., *Life Sci.* **2022**, 120593. DOI https://doi.org/10.1016/j.lfs.2022.120593.

[20] Dennahy, I. S.; Han, Z.; MacCuaig, W. M.; Chalfant, H. M.; Condacse, A.; Hagood, J. M.; Claros-Sorto, J. C.; Razaq, W.; Holter-Chakrabarty, J.; Squires, R., *Pharmaceutics* **2022,** *14* (5), 917. DOI https://doi.org/10.3390/pharmaceutics14050917.

[21] Zhao, L.; Skwarczynski, M.; Toth, I., *ACS Biomater. Sci. Eng.* **2019,** *5* (10), 4937-4950. DOI https://doi.org/10.1021/acsbiomaterials.9b01135.

[22] Huang, G.; Huang, H., *J. Controlled Release* **2018,** *278*, 122-126. DOI https://doi.org/10.1016/j.jconrel.2018.04.015.

[23] Necas, J.; Bartosikova, L.; Brauner, P.; Kolar, J., *Vet. Med.* **2008,** *53* (8), 397-411. DOI https://doi.org/10.17221/1930-vetmed.

[24] Fallacara, A.; Baldini, E.; Manfredini, S.; Vertuani, S., *Polymers* **2018,** *10* (7), 701. DOI https://doi.org/10.3390/polym10070701.

[25] Šoltés, L.; Mendichi, R.; Kogan, G.; Schiller, J.; Stankovska, M.; Arnhold, J., *Biomacromolecules* **2006,** *7* (3), 659-668. DOI https://doi.org/10.1021/bm050867v.

[26] Zhu, J.-J.; Huang, X.-N.; Yang, T.; Tang, C.-H.; Yin, S.-W.; Jia, X.-J.; Yang, X.-Q., *Ind. Crops Prod.* **2022,** *177*, 114521. DOI https://doi.org/10.1016/j.indcrop.2022.114521.

[27] Lierova, A.; Kasparova, J.; Filipova, A.; Cizkova, J.; Pekarova, L.; Korecka, L.; Mannova, N.; Bilkova, Z.; Sinkorova, Z., *Pharmaceutics* **2022,** *14* (4), 838. DOI https://doi.org/10.3390/pharmaceutics14040838.

[28] Liu, L.; Liu, Y.; Li, J.; Du, G.; Chen, J., *Microb. Cell Fact.* **2011,** *10* (1), 1-9. DOI https://doi.org/10.1186/1475-2859-10-99.

[29] Rigo, D.; da Silva, L. M.; Fischer, B.; Colet, R.; Dallago, R. M.; Zeni, J., *Biointerface Res. Appl. Chem.* **2022**. DOI https://doi.org/10.33263/BRIAC133.211.

[30] Rodriguez-Marquez, C. D.; Arteaga-Marin, S.; Rivas-Sánchez, A.; Autrique-Hernández, R.; Castro-Muñoz, R., *Int. J. Mol. Sci.* **2022,** *23* (11), 6038. DOI https://doi.org/10.3390/ijms23116038.

[31] Kayitmazer, A.; Koksal, A.; Iyilik, E. K., *Soft Matter* **2015,** *11* (44), 8605-8612. DOI https://doi.org/10.1039/c5sm01829c.

[32] Vandamme, M.; Moss, J.; Murphy, W.; Preston, B., *Arch. Biochem. Biophys.* **1994,** *310* (1), 16-24. DOI https://doi.org/10.1006/abbi.1994.1134.

[33] Ito, T.; Yoshihara, C.; Hamada, K.; Koyama, Y., *Biomaterials* **2010,** *31* (10), 2912-2918. DOI https://doi.org/10.1016/j.biomaterials.2009.12.032.

[34] Sato, T.; Nakata, M.; Yang, Z.; Torizuka, Y.; Kishimoto, S.; Ishihara, M., *J. Gene Med.* **2017,** *19* (8), e2968. DOI https://doi.org/10.1002/jgm.2968.

[35] Fukushige, K.; Tagami, T.; Naito, M.; Goto, E.; Hirai, S.; Hatayama, N.; Yokota, H.; Yasui, T.; Baba, Y.; Ozeki, T., *Int. J. Pharm.* **2020,** *583*, 119338. DOI https://doi.org/10.1016/j.ijpharm.2020.119338.

[36] Trenkenschuh, E.; Friess, W., *Eur. J. Pharm. Biopharm.* **2021,** *165*, 345-360. DOI https://doi.org/10.1016/j.ejpb.2021.05.024.

[37] Peer, D.; Florentin, A.; Margalit, R., *Biochimica et Biophysica Acta (BBA)-Biomembranes* **2003,** *1612* (1), 76-82. DOI https://doi.org/10.1016/s0005-2736(03)00106-8.

[38] Almalik, A.; Alradwan, I.; Kalam, M. A.; Alshamsan, A., *Saudi Pharm. J.* **2017,** *25* (6), 861-867. DOI https://doi.org/10.1016/j.jsps.2016.12.008.

[39] Liu, X.; Hu, Y.; Pan, Y.; Fang, M.; Tong, Z.; Sun, Y.; Tan, S., *Mater. Today Bio* **2021,** *12*, 100156. DOI https://doi.org/10.1016/j.mtbio.2021.100156.

[40] Monnery, B. D.; Wright, M.; Cavill, R.; Hoogenboom, R.; Shaunak, S.; Steinke, J. H.; Thanou, M., *Int. J. Pharm.* **2017,** *521* (1-2), 249-258. DOI https://doi.org/10.1016/j.ijpharm.2017.02.048.

[41] Fischer, D.; Li, Y.; Ahlemeyer, B.; Krieglstein, J.; Kissel, T., *Biomaterials* **2003,** *24* (7), 1121-1131. DOI https://doi.org/10.1016/s0142-9612(02)00445-3.

[42] Wei, X.; Shao, B.; He, Z.; Ye, T.; Luo, M.; Sang, Y.; Liang, X.; Wang, W.; Luo, S.; Yang, S., *Cell Res.* **2015,** *25* (2), 237-253. DOI https://doi.org/10.1038/cr.2015.9.

[43] Hong, W.-G.; Jeong, G.-W.; Nah, J.-W., *Int. J. Biol. Macromol.* **2018,** *115*, 459-468. DOI https://doi.org/10.1016/j.ijbiomac.2018.04.053.

[44] Almalik, A.; Benabdelkamel, H.; Masood, A.; Alanazi, I. O.; Alradwan, I.; Majrashi, M. A.; Alfadda, A. A.; Alghamdi, W. M.; Alrabiah, H.; Tirelli, N., *Sci. Rep.* **2017,** *7* (1), 1-9. DOI https://doi.org/10.1038/s41598-017-10836-7.

[45] Mitchell, M. J.; Billingsley, M. M.; Haley, R. M.; Wechsler, M. E.; Peppas, N. A.; Langer, R., *Nat. Rev. Drug Discovery* **2021,** *20* (2), 101-124. DOI https://doi.org/10.1038/s41573-020-0090-8.

[46] Li, M.; Li, X.; McClements, D. J.; Shi, M.; Shang, Q.; Liu, X.; Liu, F., *LWT* **2021,** *151*, 112121. DOI https://doi.org/10.1016/j.lwt.2021.112121.

[47] Liu, R.; Yan, X.; Liu, Z.; McClements, D. J.; Liu, F.; Liu, X., *Food Funct.* **2019,** *10* (2), 1098-1108. DOI https://doi.org/10.1039/c8fo02146e.

[48] Water, J. J.; Schack, M. M.; Velazquez-Campoy, A.; Maltesen, M. J.; van de Weert, M.; Jorgensen, L., *Eur. J. Pharm. Biopharm.* **2014,** *88* (2), 325-331. DOI https://doi.org/10.1016/j.ejpb.2014.09.001.

[49] Chen, S.; Han, Y.; Wang, Y.; Yang, X.; Sun, C.; Mao, L.; Gao, Y., *Food Chem.* **2019,** *276*, 322-332. DOI https://doi.org/10.1016/j.foodchem.2018.10.034.

[50] Chen, S.; Sun, C.; Wang, Y.; Han, Y.; Dai, L.; Abliz, A. l.; Gao, Y., *J. Agric. Food Chem.* **2018,** *66* (28), 7441-7450. DOI https://doi.org/10.1021/acs.jafc.8b01046.

[51] Battistini, F.; Flores-Martin, J.; Olivera, M.; Genti-Raimondi, S.; Manzo, R., *Eur. J. Pharm. Sci.* **2014,** *65*, 122-129. DOI https://doi.org/10.1016/j.ejps.2014.09.008.

[52] Carton, F.; Chevalier, Y.; Nicoletti, L.; Tarnowska, M.; Stella, B.; Arpicco, S.; Malatesta, M.; Jordheim, L. P.; Briançon, S.; Lollo, G., *Int. J. Pharm.* **2019,** *568*, 118526. DOI https://doi.org/10.1016/j.ijpharm.2019.118526.

[53] Ding, J.; Liang, T.; Min, Q.; Jiang, L.; Zhu, J.-J., *ACS Appl. Mater. Interfaces* **2018,** *10* (12), 9938-9948. DOI https://doi.org/10.1021/acsami.7b19577.

[54] Chen, C.; Zhao, S.; Karnad, A.; Freeman, J. W., *J. Hematol. Oncol.* **2018,** *11* (1), 1-23. DOI https://doi.org/10.1186/s13045-018-0605-5.

[55] Stern, R., Hyaluronidases in Cancer Biology. In *Hyaluronan in Cancer Biology*, Stern, R., Ed. Academic Press: San Diego, 2008; pp 207-220. DOI https://doi.org/10.1016/B978-012374178-3.10012-2.

[56] Kim, E. J.; Shim, G.; Kim, K.; Kwon, I. C.; Oh, Y. K.; Shim, C. K., *J. Gene Med.* **2009,** *11* (9), 791-803. DOI https://doi.org/10.1002/jgm.1352.

[57] Ke, Z.; Yang, L.; Wu, H.; Li, Z.; Jia, X.; Zhang, Z., *Int. J. Pharm.* **2018,** *545* (1-2), 306-317. DOI https://doi.org/10.1016/j.ijpharm.2018.04.016.

[58] Wang, T.; Yu, X.; Han, L.; Liu, T.; Liu, Y.; Zhang, N., *Int. J. Nanomed.* **2017,** *12*, 4773. DOI https://doi.org/10.2147/ijn.s134378.

[59] An, T.; Zhang, C.; Han, X.; Wan, G.; Wang, D.; Yang, Z.; Wang, Y.; Zhang, L.; Wang, Y., *RSC Adv.* **2016,** *6* (45), 38624-38636. DOI https://doi.org/10.1039/c6ra03997a.

[60] Hyun, E.-J.; Hasan, M. N.; Kang, S. H.; Cho, S.; Lee, Y.-K., *Int. J. Pharm.* **2019,** *555*, 250-258. DOI https://doi.org/10.1016/j.ijpharm.2018.11.009.

[61] Liu, L.; Xu, Y.; Zhang, P.; You, J.; Li, W.; Chen, Y.; Li, R.; Rui, B.; Dou, H., *Langmuir* **2020,** *36* (29), 8580-8588. DOI https://doi.org/10.1021/acs.langmuir.0c01458.

[62] Xiong, Q.; Cui, M.; Bai, Y.; Liu, Y.; Liu, D.; Song, T., *Colloids Surf., B* **2017,** *155*, 93-103. DOI https://doi.org/10.1016/j.colsurfb.2017.04.008.

[63] Supachawaroj, N.; Damrongrungruang, T.; Limsitthichaikoon, S., *Saudi Pharm. J.* **2021,** *29* (9), 1070-1081. DOI https://doi.org/10.1016/j.jsps.2021.07.007.

[64] Wadhwa, S.; Paliwal, R.; Paliwal, S. R.; Vyas, S., *J. Drug Targeting* **2010,** *18* (4), 292-302. DOI https://doi.org/10.3109/10611860903450023.

[65] Verheul, R. J.; Slütter, B.; Bal, S. M.; Bouwstra, J. A.; Jiskoot, W.; Hennink, W. E., *J. Controlled Release* **2011,** *156* (1), 46-52. DOI https://doi.org/10.1016/j.jconrel.2011.07.014.

[66] Schanté, C. E.; Zuber, G.; Herlin, C.; Vandamme, T. F., *Carbohydr. Polym.* **2011,** *85* (3), 469-489. DOI https://doi.org/10.1016/j.carbpol.2011.03.019.

[67] Surace, C.; Arpicco, S.; Dufaÿ-Wojcicki, A.; Marsaud, V.; Bouclier, C.; Clay, D.; Cattel, L.; Renoir, J.-M.; Fattal, E., *Mol. Pharmaceutics* **2009,** *6* (4), 1062-1073. DOI https://doi.org/10.1021/mp800215d.

[68] Ondreas, F.; Dusankova, M.; Sita, J.; Cepa, M.; Stepan, J.; Belsky, P.; Velebny, V., *Appl. Surf. Sci.* **2021,** *546*, 149161. DOI https://doi.org/10.1016/j.apsusc.2021.149161.

[69] Le, H. V.; Dulong, V.; Picton, L.; Le Cerf, D., *Carbohydr. Polym.* **2022**, 119711. DOI https://doi.org/10.1016/j.carbpol.2022.119711.

[70] Xia, D.; Wang, F.; Pan, S.; Yuan, S.; Liu, Y.; Xu, Y., *Polymers* **2021,** *13* (21), 3785. DOI https://doi.org/10.3390/polym13213785.

[71] Chen, J.-X.; Wang, M.; Tian, H.-H.; Chen, J.-H., *Colloids Surf., B* **2015,** *134*, 81-87. DOI https://doi.org/10.1016/j.colsurfb.2015.06.039.

[72] Shabani Ravari, N.; Goodarzi, N.; Alvandifar, F.; Amini, M.; Souri, E.; Khoshayand, M. R.; Hadavand Mirzaie, Z.; Atyabi, F.; Dinarvand, R., *Daru, J. Pharm. Sci.* **2016,** *24* (1), 1-12. DOI https://doi.org/10.1186/s40199-016-0160-y.

[73] Zhang, R.; Ru, Y.; Gao, Y.; Li, J.; Mao, S., *Drug Des., Dev. Ther.* **2017,** *11*, 2631. DOI https://doi.org/10.2147/dddt.s143047.

[74] Mok, H.; Park, J. W.; Park, T. G., *Bioconjugate Chem.* **2007,** *18* (5), 1483-1489. DOI https://doi.org/10.1021/bc070111o.

[75] Dacoba, T. G.; Omange, R. W.; Li, H.; Crecente-Campo, J.; Luo, M.; Alonso, M. J., *ACS Nano* **2019,** *13* (5), 4947-4959. DOI https://doi.org/10.1021/acsnano.8b07662.

[76] Guo, M.; Meng, Y.; Qin, X.; Zhou, W., *Crystals* **2021,** *11* (4), 347. DOI https://doi.org/10.3390/cryst11040347.

[77] Bucur, C. B.; Sui, Z.; Schlenoff, J. B., *J. Am. Chem. Soc.* **2006,** *128* (42), 13690-13691. DOI https://doi.org/10.1021/ja064532c.

[78] Koetz, J.; Kosmella, S., *Polyelectrolytes and nanoparticles*. Springer Science & Business Media: Berlin, **2007**. DOI https://doi.org/10.1007/978-3-540-46382-5.

[79] Yamazaki, M.; Yabe, M.; Iijima, K., *Polym. J.* **2022**, 1-10. DOI https://doi.org/10.1038/s41428-021-00602-y.

[80] Philipp, B.; Dautzenberg, H.; Linow, K.-J.; Kötz, J.; Dawydoff, W., *Prog. Polym. Sci.* **1989,** *14* (1), 91-172. DOI https://doi.org/10.1016/0079-6700(89)90018-x.

[81] Le, H. V.; Dulong, V.; Picton, L.; Le Cerf, D., *Colloids Surf., A* **2021,** *629*, 127485. DOI https://doi.org/10.1016/j.colsurfa.2021.127485.

[82] Luo, D.; Yan, C.; Wang, T., *Small* **2015,** *11* (45), 5984-6008. DOI https://doi.org/10.1002/smll.201501783.

[83] Pergushov, D. V.; Müller, A. H.; Schacher, F. H., *Chem. Soc. Rev.* **2012,** *41* (21), 6888-6901. DOI https://doi.org/10.1039/c2cs35135h.

[84] Kovács, A. N.; Varga, N.; Juhász, Á.; Csapó, E., *Carbohydr. Polym.* **2021,** *251*, 117047. DOI https://doi.org/10.1016/j.carbpol.2020.117047.

[85] Pan, W.; Yin, D.-X.; Jing, H.-R.; Chang, H.-J.; Wen, H.; Liang, D.-H., *Chin. J. Polym. Sci.* **2019,** *37* (1), 36-42. DOI https://doi.org/10.1007/s10118-018-2166-z.

[86] Chen, S.; McClements, D. J.; Jian, L.; Han, Y.; Dai, L.; Mao, L.; Gao, Y., *ACS Appl. Mater. Interfaces* **2019,** *11* (41), 38103-38115. DOI https://doi.org/10.1021/acsami.9b11782.

[87] Gaumet, M.; Vargas, A.; Gurny, R.; Delie, F., *Eur. J. Pharm. Biopharm.* **2008,** *69* (1), 1-9. DOI https://doi.org/10.1016/j.ejpb.2007.08.001.

[88] Kulkarni, S. A.; Feng, S.-S., *Pharm. Res.* **2013,** *30* (10), 2512-2522. DOI https://doi.org/10.1007/s11095-012-0958-3.

[89] He, C.; Hu, Y.; Yin, L.; Tang, C.; Yin, C., *Biomaterials* **2010,** *31* (13), 3657-3666. DOI https://doi.org/10.1016/j.biomaterials.2010.01.065.

[90] Alqahtani, M. S.; Syed, R.; Alshehri, M., *Polymers* **2020,** *12* (11), 2576. DOI https://doi.org/10.3390/polym12112576.

[91] Sandri, G.; Bonferoni, M. C.; Ferrari, F.; Rossi, S.; Caramella, C. M., The role of particle size in drug release and absorption. In *Particulate Products*, Springer International Publishing: **2013**; pp 323-341. DOI https://doi.org/10.1007/978-3-319-00714-4_11.

[92] Wiese, G.; Healy, T. W., *Trans. Faraday Soc.* **1970,** *66*, 490-499. DOI https://doi.org/10.1039/tf9706600490.

[93] Simonson, A. W.; Lawanprasert, A.; Goralski, T. D.; Keiler, K. C.; Medina, S. H., *Nanomedicine* **2019,** *17*, 391-400. DOI https://doi.org/10.1016/j.nano.2018.10.008.

[94] Freitas, B.; Lavrador, P.; Almeida, R. J.; Gaspar, V. M.; Mano, J. o. F., *ACS Appl. Mater. Interfaces* **2020,** *12* (28), 31282-31291. DOI https://doi.org/10.1021/acsami.0c09270.

[95] Tokudome, Y.; Komi, T.; Omata, A.; Sekita, M., *Sci. Rep.* **2018,** *8* (1), 1-9. DOI https://doi.org/10.1038/s41598-018-20805-3.

[96] Xu, Y.; Asghar, S.; Gao, S.; Chen, Z.; Huang, L.; Yin, L.; Ping, Q.; Xiao, Y., *Int. J. Nanomed.* **2017,** *12*, 7337. DOI https://doi.org/10.2147/ijn.s145620.

[97] Umerska, A.; Paluch, K. J.; Inkielewicz-Stępniak, I.; Santos-Martinez, M. J.; Corrigan, O. I.; Medina, C.; Tajber, L., *Int. J. Pharm.* **2012,** *436* (1-2), 75-87. DOI https://doi.org/10.1016/j.ijpharm.2012.07.011.

[98] Djafari, J.; Fernández-Lodeiro, J.; Santos, H. M.; Lorenzo, J.; Rodriguez-Calado, S.; Bértolo, E.; Capelo-Martínez, J. L.; Lodeiro, C., *Materials* **2020,** *13* (23), 5309. DOI https://doi.org/10.3390/ma13235309.

[99] Zaki, N. M.; Nasti, A.; Tirelli, N., *Macromol. Biosci.* **2011,** *11* (12), 1747-1760. DOI https://doi.org/10.1002/mabi.201100156.

[100] Clogston, J. D.; Patri, A. K., Zeta potential measurement. In *Characterization of nanoparticles intended for drug delivery*, McNeil, S., Ed. Humana Press: **2010**; Vol. 697, pp 63-70. DOI https://doi.org/10.1007/978-1-60327-198-1_6.

[101] Joseph, E.; Singhvi, G., Multifunctional nanocrystals for cancer therapy: a potential nanocarrier. In *Nanomaterials for drug delivery and therapy*, **2019**; pp 91-116. DOI https://doi.org/10.1016/b978-0-12-816505-8.00007-2.

[102] Mauri, E.; Giannitelli, S. M.; Trombetta, M.; Rainer, A., *Gels* **2021,** *7* (2), 36. DOI https://doi.org/10.3390/gels7020036.

[103] Cuggino, J. C.; Blanco, E. R. O.; Gugliotta, L. M.; Igarzabal, C. I. A.; Calderon, M., *J. Controlled Release* **2019,** *307*, 221-246. DOI https://doi.org/10.1016/j.jconrel.2019.06.005.

[104] Gentile, F.; Chiappini, C.; Fine, D.; Bhavane, R.; Peluccio, M.; Cheng, M. M.-C.; Liu, X.; Ferrari, M.; Decuzzi, P., *J. Biomech.* **2008,** *41* (10), 2312-2318. DOI https://doi.org/10.1016/j.jbiomech.2008.03.021.

[105] Decuzzi, P.; Lee, S.; Bhushan, B.; Ferrari, M., *Ann. Biomed. Eng.* **2005,** *33* (2), 179-190. DOI https://doi.org/10.1007/s10439-005-8976-5.

[106] Geng, Y.; Dalhaimer, P.; Cai, S.; Tsai, R.; Tewari, M.; Minko, T.; Discher, D. E., *Nat. Nanotechnol.* **2007,** *2* (4), 249-255. DOI https://doi.org/10.1115/sbc2008-192418.

[107] Yang, L.; Gao, S.; Asghar, S.; Liu, G.; Song, J.; Wang, X.; Ping, Q.; Zhang, C.; Xiao, Y., *Int. J. Biol. Macromol.* **2015,** *72*, 1391-1401. DOI https://doi.org/10.1016/j.ijbiomac.2014.10.039.

[108] Wu, D.; Delair, T., *Carbohydr. Polym.* **2015,** *119*, 149-158. DOI https://doi.org/10.1016/j.carbpol.2014.11.042.

[109] Oyarzun-Ampuero, F. A.; Goycoolea, F. M.; Torres, D.; Alonso, M. J., *Eur. J. Pharm. Biopharm.* **2011,** *79* (1), 54-57. DOI https://doi.org/10.1016/j.ejpb.2011.04.008.

[110] Chen, S.; Han, Y.; Sun, C.; Dai, L.; Yang, S.; Wei, Y.; Mao, L.; Yuan, F.; Gao, Y., *Carbohydr. Polym.* **2018,** *201*, 599-607. DOI https://doi.org/10.1016/j.carbpol.2018.08.116.

[111] Umerska, A.; Paluch, K. J.; Martinez, M.-J. S.; Corrigan, O. I.; Medina, C.; Tajber, L., *J. Biomed. Nanotechnol.* **2014,** *10* (12), 3658-3673. DOI https://doi.org/10.1166/jbn.2014.1878.

[112] Furlani, F.; Donati, I.; Marsich, E.; Sacco, P., *Colloids Interfaces* **2020,** *4* (1), 12. DOI https://doi.org/10.3390/colloids4010012.

[113] Raik, S. V.; Gasilova, E. R.; Dubashynskaya, N. V.; Dobrodumov, A. V.; Skorik, Y. A., *Int. J. Biol. Macromol.* **2020,** *146*, 1161-1168. DOI https://doi.org/10.1016/j.ijbiomac.2019.10.054.

[114] Dautzenberg, H.; Hartmann, J.; Grunewald, S.; Brand, F., *Ber. Bunsenges. Physik. Chem.* **1996,** *100* (6), 1024-1032. DOI https://doi.org/10.1002/bbpc.19961000654.

[115] Sladek, S.; McCartney, F.; Eskander, M.; Dunne, D. J.; Santos-Martinez, M. J.; Benetti, F.; Tajber, L.; Brayden, D. J., *Pharmaceutics* **2020,** *12* (3), 259. DOI https://doi.org/10.3390/pharmaceutics12030259.

[116] Lu, K.-Y.; Lin, Y.-C.; Lu, H.-T.; Ho, Y.-C.; Weng, S.-C.; Tsai, M.-L.; Mi, F.-L., *Carbohydr. Polym.* **2019,** *206*, 664-673. DOI https://doi.org/10.1016/j.carbpol.2018.11.050.

[117] De la Fuente, M.; Seijo, B.; Alonso, M. J., *Invest. Ophthalmol. Visual Sci.* **2008,** *49* (5), 2016-2024. DOI https://doi.org/10.1167/iovs.07-1077.

[118] Yang, J.; Zhao, R.; Feng, Q.; Zhuo, X.; Wang, R., *Invest. New Drugs* **2021,** *39* (1), 66-76. DOI https://doi.org/10.1007/s10637-020-00986-3.

[119] Kudo, S.; Nagasaki, Y., *Macromol. Rapid Commun.* **2015,** *36* (21), 1916-1922. DOI https://doi.org/10.1002/marc.201500224.

[120] Duceppe, N.; Tabrizian, M., *Biomaterials* **2009,** *30* (13), 2625-2631. DOI https://doi.org/10.1016/j.biomaterials.2009.01.017.

[121] Zhang, H.; Pei, M.; Liu, P., *Int. J. Biol. Macromol.* **2020,** *150*, 1104-1112. DOI https://doi.org/10.1016/j.ijbiomac.2019.10.116.

[122] Madera-Santana, T. J.; Herrera-Méndez, C. H.; Rodríguez-Núñez, J. R., *Green Mater.* **2018,** *6* (4), 131-142. DOI https://doi.org/10.1680/jgrma.18.00053.

[123] Nazeri, N.; Avadi, M. R.; Faramarzi, M. A.; Safarian, S.; Tavoosidana, G.; Khoshayand, M. R.; Amani, A., *Int. J. Biol. Macromol.* **2013,** *62*, 642-646. DOI https://doi.org/10.1016/j.ijbiomac.2013.09.041.

[124] Zhong, W.; Li, C.; Diao, M.; Yan, M.; Wang, C.; Zhang, T., *Colloids Surf., B* **2021,** *203*, 111758. DOI https://doi.org/10.1016/j.colsurfb.2021.111758.

[125] Doane, T.; Burda, C., *Adv. Drug Delivery Rev.* **2013,** *65* (5), 607-621. DOI https://doi.org/10.1016/j.addr.2012.05.012.

[126] Lukić, M.; Pantelić, I.; Savić, S. D., *Cosmetics* **2021,** *8* (3), 69. DOI https://doi.org/10.3390/cosmetics8030069.

[127] Evans, D.; Pye, G.; Bramley, R.; Clark, A.; Dyson, T.; Hardcastle, J., *Gut* **1988,** *29* (8), 1035-1041. DOI https://doi.org/10.1136/gut.29.8.1035.

[128] Zhong, W.; Zhang, T.; Dong, C.; Li, J.; Dai, J.; Wang, C., *Colloids Surf., A* **2022,** *632*, 127828. DOI https://doi.org/10.1016/j.colsurfa.2021.127828.

[129] Campbell, J.; Abnett, J.; Kastania, G.; Volodkin, D.; Vikulina, A. S., *ACS Appl. Mater. Interfaces* **2021,** *13* (2), 3259-3269. DOI https://doi.org/10.1021/acsami.0c21194.

[130] Wu, D.; Ensinas, A.; Verrier, B.; Primard, C.; Cuvillier, A.; Champier, G.; Paul, S.; Delair, T., *J. Mater. Chem. B* **2016,** *4* (32), 5455-5463. DOI https://doi.org/10.1039/c6tb00898d.

[131] Wang, X.; Du, Y.; Liu, H., *Carbohydr. Polym.* **2004,** *56* (1), 21-26. DOI https://doi.org/10.1016/j.carbpol.2003.11.007.

[132] Burger, K.; Illés, J.; Gyurcsik, B.; Gazdag, M.; Forrai, E.; Dékány, I.; Mihályfi, K., *Carbohydr. Res.* **2001,** *332* (2), 197-207. DOI https://doi.org/10.1016/s0008-6215(01)00065-9.

[133] Schuetz, Y. B.; Gurny, R.; Jordan, O., *Eur. J. Pharm. Biopharm.* **2008,** *68* (1), 19-25. DOI https://doi.org/10.1016/j.ejpb.2007.06.020.

[134] Ahsan, A.; Farooq, M. A.; Parveen, A., *ACS Omega* **2020,** *5* (32), 20450-20460. DOI https://doi.org/10.1021/acsomega.0c02548.

[135] Al-Remawi, M. M., *Am. J. Appl. Sci.* **2012**, *9* (7), 1091. DOI https://doi.org/10.3844/ajassp.2012.1091.1100.

[136] Turcsányi, Á.; Ungor, D.; Csapó, E., *Crystals* **2020,** *10* (12), 1113. DOI https://doi.org/10.3390/cryst10121113.

[137] Turcsányi, Á.; Varga, N.; Csapó, E., *Int. J. Biol. Macromol.* **2020,** *148*, 218-225. DOI https://doi.org/10.1016/j.ijbiomac.2020.01.118.

[138] Al-Qadi, S.; Alatorre-Meda, M.; Martin-Pastor, M.; Taboada, P.; Remuñán-López, C., *Colloids Surf., B* **2016,** *141*, 223-232. DOI https://doi.org/10.1016/j.colsurfb.2016.01.029.

[139] Chen, L.; Zheng, Y.; Feng, L.; Liu, Z.; Guo, R.; Zhang, Y., *Int. J. Biol. Macromol.* **2019,** *126*, 254-261. DOI https://doi.org/10.1016/j.ijbiomac.2018.12.215.

[140] Deng, X.; Cao, M.; Zhang, J.; Hu, K.; Yin, Z.; Zhou, Z.; Xiao, X.; Yang, Y.; Sheng, W.; Wu, Y., *Biomaterials* **2014,** *35* (14), 4333-4344. DOI https://doi.org/10.1016/j.biomaterials.2014.02.006.

[141] Sacco, P.; Decleva, E.; Tentor, F.; Menegazzi, R.; Borgogna, M.; Paoletti, S.; Kristiansen, K. A.; Vårum, K. M.; Marsich, E., *Macromol. Biosci.* **2017,** *17* (11), 1700214. DOI https://doi.org/10.1002/mabi.201700214.

[142] de Carvalho, F. G.; Magalhaes, T. C.; Teixeira, N. M.; Gondim, B. L. C.; Carlo, H. L.; Dos Santos, R. L.; de Oliveira, A. R.; Denadai, Â. M. L., *Mater. Sci. Eng., C* **2019,** *104,* 109885. DOI https://doi.org/10.1016/j.msec.2019.109885.

[143] Vecchies, F.; Sacco, P.; Marsich, E.; Cinelli, G.; Lopez, F.; Donati, I., *Polymers* **2020,** *12* (4), 897. DOI https://doi.org/10.3390/polym12040897.

[144] Tang, J. D.; Caliari, S. R.; Lampe, K. J., *Biomacromolecules* **2018,** *19* (10), 3925-3935. DOI https://doi.org/10.1021/acs.biomac.8b00837.

[145] Tran, P.; Pyo, Y.-C.; Kim, D.-H.; Lee, S.-E.; Kim, J.-K.; Park, J.-S., *Pharmaceutics* **2019,** *11* (3), 132. DOI https://doi.org/10.3390/pharmaceutics11030132.

[146] Hsu, M. F.; Tyan, Y. S.; Chien, Y. C.; Lee, M. W., *Sci. Rep.* **2018,** *8* (1), 1-10. DOI https://doi.org/10.1038/s41598-018-19191-7.

[147] Akentieva, N. P.; Gizatullin, Đ.; Sanina, N. A.; Dremova, N. N.; Torbov, V. I.; Shkondina, N. I.; Zhelev, N.; Aldoshin, S. M., *Nanomed. J.* **2020,** *7* (3), 199-210. DOI https://doi.org/10.22038/NMJ.2020.07.0004.

[148] Shariati, M.; Lollo, G.; Matha, K.; Descamps, B.; Vanhove, C.; Van de Sande, L.; Willaert, W.; Balcaen, L.; Vanhaecke, F.; Benoit, J.-P., *ACS Appl. Mater. Interfaces* **2020,** *12* (26), 29024-29036. DOI https://doi.org/10.1021/acsami.0c05554.

[149] Sun, H.; Li, S.; Qi, W.; Xing, R.; Zou, Q.; Yan, X., *Colloids Surf., A* **2018,** *538*, 795-801. DOI https://doi.org/10.1016/j.colsurfa.2017.11.072.

[150] Xu, Y.; Asghar, S.; Yang, L.; Chen, Z.; Li, H.; Shi, W.; Li, Y.; Shi, Q.; Ping, Q.; Xiao, Y., *Int. J. Biol. Macromol.* **2017,** *102*, 1083-1091. DOI https://doi.org/10.1016/j.ijbiomac.2017.04.105.

[151] Xu, Y.; Asghar, S.; Yang, L.; Li, H.; Wang, Z.; Ping, Q.; Xiao, Y., *Carbohydr. Polym.* **2017,** *157*, 419-428. DOI https://doi.org/10.1016/j.carbpol.2016.09.085.

[152] Zhao, X.; Liu, P.; Song, Q.; Gong, N.; Yang, L.; Wu, W. D., *J. Mater. Chem. B* **2015,** *3* (30), 6185-6193. DOI https://doi.org/10.1039/c5tb00600g.

[153] Monopoli, M. P.; Åberg, C.; Salvati, A.; Dawson, K. A., *Nat. Nanotechnol.* **2012,** *7* (12), 779-786. DOI https://doi.org/10.1201/9780429399039-7.

[154] Mahmoudi, M.; Lynch, I.; Ejtehadi, M. R.; Monopoli, M. P.; Bombelli, F. B.; Laurent, S., *Chem. Rev.* **2011,** *111* (9), 5610-5637. DOI https://doi.org/10.1021/cr100440g.

[155] Mulligan, R. C., *Science* **1993,** *260* (5110), 926-932. DOI https://doi.org/10.1126/science.8493530.

[156] Deng, Y.; Wang, C. C.; Choy, K. W.; Du, Q.; Chen, J.; Wang, Q.; Li, L.; Chung, T. K. H.; Tang, T., *Gene* **2014,** *538* (2), 217-227. DOI https://doi.org/10.1016/j.gene.2013.12.019.

[157] Franck, C. O.; Fanslau, L.; Bistrovic Popov, A.; Tyagi, P.; Fruk, L., *Angew. Chem., Int. Ed.* **2021,** *60* (24), 13225-13243. DOI https://doi.org/10.1002/ange.202010282.

[158] Lee, S. H.; Chung, B. H.; Park, T. G.; Nam, Y. S.; Mok, H., *Acc. Chem. Res.* **2012,** *45* (7), 1014-1025. DOI https://doi.org/10.1021/ar2002254.

[159] Goldshtein, M.; Forti, E.; Ruvinov, E.; Cohen, S., *Int. J. Pharm.* **2016,** *515* (1-2), 46-56. DOI https://doi.org/10.1016/j.ijpharm.2016.10.009.

[160] Ma, S.; Li, X.; Ran, M.; Ji, M.; Gou, J.; Yin, T.; He, H.; Wang, Y.; Zhang, Y.; Tang, X., *Int. J. Pharm.* **2021,** *601*, 120577. DOI https://doi.org/10.1016/j.ijpharm.2021.120577.

[161] Jain, S.; Kumar, S.; Agrawal, A.; Thanki, K.; Banerjee, U., *RSC Adv.* **2015,** *5* (51), 41144-41154. DOI https://doi.org/10.1039/c5ra03283k.

[162] Masjedi, A.; Ahmadi, A.; Atyabi, F.; Farhadi, S.; Irandoust, M.; Khazaei-Poul, Y.; Chaleshtari, M. G.; Fathabad, M. E.; Baghaei, M.; Haghnavaz, N., *Int. J. Biol. Macromol.* **2020,** *149*, 487-500. DOI https://doi.org/10.1016/j.ijbiomac.2020.01.273.

[163] Ito, T.; Iida-Tanaka, N.; Niidome, T.; Kawano, T.; Kubo, K.; Yoshikawa, K.; Sato, T.; Yang, Z.; Koyama, Y., *J. Controlled Release* **2006,** *112* (3), 382-388. DOI https://doi.org/10.1016/j.jconrel.2006.03.013.

[164] Li, G.; Sun, B.; Li, Y.; Luo, C.; He, Z.; Sun, J., *Small* **2021,** *17* (52), 2101460. DOI https://doi.org/10.1002/smll.202101460.

[165] Grüner, N.; Mattner, J., *Int. J. Mol. Sci.* **2021,** *22* (3), 1397. DOI https://doi.org/10.3390/ijms22031397.

[166] Yao, H.; Ng, S. S.; Tucker, W. O.; Man, K.; Wang, X.-m.; Chow, B. K.; Kung, H.-F.; Tang, G.-P.; Lin, M. C., *Biomaterials* **2009,** *30* (29), 5793-5803. DOI https://doi.org/10.1016/j.biomaterials.2009.06.051.

[167] Zhao, M.-D.; Cheng, J.-L.; Yan, J.-J.; Chen, F.-Y.; Sheng, J.-Z.; Sun, D.-L.; Chen, J.; Miao, J.; Zhang, R.-J.; Zheng, C.-H., *Int. J. Nanomed.* **2016,** *11*, 1323. DOI https://doi.org/10.2147/ijn.s99692.

[168] Liu, Y.; Wang, F.-Q.; Shah, Z.; Cheng, X.-J.; Kong, M.; Feng, C.; Chen, X.-G., *Colloids Surf., B* **2016,** *145*, 492-501. DOI https://doi.org/10.1016/j.colsurfb.2016.05.035.

[169] Han, S. K.; Lee, J. H.; Kim, D.; Cho, S. H.; Yuk, S. H., *Sci. Technol. Adv. Mater.* **2005,** *6* (5), 468. DOI https://doi.org/10.1016/j.stam.2005.03.017.

[170] Suzuki, K.; Yoshizaki, Y.; Horii, K.; Murase, N.; Kuzuya, A.; Ohya, Y., *Biomater. Sci.* **2022,** *10* (8), 1920-1928. DOI https://doi.org/10.1039/d1bm01985f.

[171] Xu, C.; He, X.-Y.; Ren, X.-H.; Cheng, S.-X., *Biosens. Bioelectron.* **2021,** *190*, 113401. DOI https://doi.org/10.1016/j.bios.2021.113401.

[172] Tang, Z.; Zhao, P.; Wang, H.; Liu, Y.; Bu, W., *Chem. Rev.* **2021,** *121* (4), 1981-2019. DOI https://doi.org/10.1021/acs.chemrev.0c00977.

[173] Yang, B.; Chen, Y.; Shi, J., *Chem. Rev.* **2019,** *119* (8), 4881-4985. DOI https://doi.org/10.1021/acs.chemrev.8b00626.

[174] Kalita, M.; Payne, M. M.; Bossmann, S. H., *Nanomedicine* **2022,** *42*, 102542. DOI https://doi.org/10.1016/j.nano.2022.102542.

[175] Park, H. S.; Lee, J. E.; Cho, M. Y.; Hong, J. H.; Cho, S. H.; Lim, Y. T., *Macromol. Rapid Commun.* **2012,** *33* (18), 1549-1555. DOI https://doi.org/10.1002/marc.201200246.

[176] Shigefuji, M.; Tokudome, Y., *Materialia* **2020,** *14*, 100879. DOI https://doi.org/10.1016/j.mtla.2020.100879.

[177] Yamazaki, M.; Iijima, K., *Polymers* **2020,** *12* (2), 435. DOI https://doi.org/10.3390/polym12020435.

[178] Liu, R.; Zhang, J.; Zhao, C.; Duan, X.; McClements, D. J.; Liu, X.; Liu, F., *Molecules* **2018,** *23* (12), 3291. DOI https://doi.org/10.3390/molecules23123291.

[179] Bruix, J.; Sala, M.; Llovet, J. M., *Gastroenterology* **2004,** *127* (5), S179-S188. DOI https://doi.org/10.1053/j.gastro.2004.09.032.

[180] Domingues, C.; Santos, A.; Alvarez-Lorenzo, C.; Concheiro, A.; Jarak, I.; Veiga, F.; Barbosa, I.; Dourado, M.; Figueiras, A., *ACS Nano* **2022,** *16* (7), 9994-10041. DOI https://doi.org/10.1021/acsnano.2c00128.

[181] Duan, H.; Donovan, M.; Hernandez, F.; Di Primo, C.; Garanger, E.; Schultze, X.; Lecommandoux, S., *Angew. Chem., Int. Ed.* **2020,** *59* (32), 13591-13596. DOI https://doi.org/10.1002/ange.202005212.

[182] Hou, X.; Zhong, D.; Chen, H.; Gu, Z.; Gong, Q.; Ma, X.; Zhang, H.; Zhu, H.; Luo, K., *Carbohydr. Polym.* **2022**, 119662. DOI https://doi.org/10.1016/j.carbpol.2022.119662.

[183] Mondek, J.; Kalina, M.; Simulescu, V.; Pekař, M., *Polym. Degrad. Stab.* **2015,** *120*, 107-113. DOI https://doi.org/10.1016/j.polymdegradstab.2015.06.012.

[184] Maleki, A.; Kjøniksen, A. L.; Nyström, B., *Macromolecular Symposia* **2008,** *274* (1), 131-140. DOI https://doi.org/10.1002/masy.200851418.

[185] Lapčík, L.; Schurz, J., *Colloid Polym. Sci.* **1991,** *269* (6), 633-635. DOI https://doi.org/10.1007/bf00659919.

[186] Miyazaki, T.; Yomota, C.; Okada, S., *Polym. Degrad. Stab.* **2001,** *74* (1), 77-85. DOI https://doi.org/10.1016/s0141-3910(01)00104-5.

[187] Li, H.; Cai, X.; Yi, T.; Zeng, Y.; Ma, J.; Li, L.; Pang, L.; Li, N.; Hu, H.; Zhan, Y., *J. Nanobiotechnol.* **2022,** *20* (1), 1-22. DOI https://doi.org/10.1186/s12951-022-01441-6.

[188] Zhao, W.; Li, Y.; Zhang, X.; Zhang, R.; Hu, Y.; Boyer, C.; Xu, F.-J., *J. Controlled Release* **2020,** *323*, 24-35. DOI https://doi.org/10.1016/j.jconrel.2020.04.014.

[189] Sun, F.; Zhang, P.; Liu, Y.; Lu, C.; Qiu, Y.; Mu, H.; Duan, J., *Carbohydr. Polym.* **2019,** *206*, 309-318. DOI https://doi.org/10.1016/j.carbpol.2018.11.005.

[190] Madau, M.; Morandi, G.; Rihouey, C.; Lapinte, V.; Oulyadi, H.; Cerf, D. L.; Dulong, V.; Picton, L., *Polymer* **2021,** *230*, 124059. DOI https://doi.org/10.1016/j.polymer.2021.124059.

[191] Madau, M.; Morandi, G.; Lapinte, V.; Le Cerf, D.; Dulong, V.; Picton, L., *Polymer* **2022,** *244*, 124643. DOI https://doi.org/10.1016/j.polymer.2022.124643.

[192] Xu, L.; Zhong, S.; Gao, Y.; Cui, X., *Int. J. Biol. Macromol.* **2022,** *194*, 811-818. DOI https://doi.org/10.1016/j.ijbiomac.2021.11.133.

[193] Facciolà, A.; Visalli, G.; Laganà, A.; Di Pietro, A., *Vaccines* **2022,** *10* (5), 819. DOI https://doi.org/10.3390/vaccines10050819.

[194] Alipoor, R.; Ayan, M.; Hamblin, M. R.; Ranjbar, R.; Rashki, S., *Front. Bioeng. Biotechnol.* **2022,** *10*. DOI https://doi.org/10.3389/fbioe.2022.913912.

[195] Mohammed, M.; Devnarain, N.; Elhassan, E.; Govender, T., *Wiley Interdiscip. Rev.: Nanomed. Nanobiotechnol.* **2022**, e1799. DOI https://doi.org/10.1002/wnan.1799.

Chapitre II

Préparation et caractérisation

des nanogels de l'acide hyaluronique en complexe avec

le diéthylaminoéthyl dextrane

II.1. Introduction

Ce chapitre présente les études exploratoires sur la formation et les caractéristiques des PECs formés entre le HA et le diéthylaminoéthyl dextrane (DEAE-D), systèmes qui nous servira de référence pour les études plus approfondies dans les chapitres suivants. Les PECs de HA/DEAE-D ont été caractérisés physico-chimiquement, notamment par la taille (la valeur moyenne et la distribution du diamètre hydrodynamique) ainsi que la charge nette de surface (potentiel zêta) par diffusion dynamique et électrophorétique de la lumière respectivement, et par détermination de l'hydrophobicité relative obtenue par spectroscopie de fluorescence en encapsulant du pyrène comme sonde fluorescente. En faisant varier des paramètres comme le ratio de charge, la concentration totale en polymères, la masse molaire du HA et la concentration en NaCl, ainsi que le mode et l'ordre de mélange, nous avons pu évaluer les impacts de ces facteurs sur les caractéristiques et la stabilité des PECs formés. Comme abordé dans notre revue bibliographique, ces paramètres sont des facteurs clés qui peuvent influer sur les structures des PECs mais il n'existe pas de conditions optimales universelles pour garantir la stabilité colloïdale pour tous les systèmes de PECs. Les résultats présentés dans ce chapitre nous ont ainsi permis de trouver les meilleures conditions pour obtenir les PECs à base de HA sous forme colloïdale (i.e. PEC-NGs). Pour cette étude exploratoire assez vaste qui a nécessité une grande quantité d'expériences, nous avons choisi le DEAE-D comme polycation dans un premier temps puisqu'il est déjà largement utilisé pour la transfection d'ADN dans la littérature [1], avec un prix abordable et nous avions déjà réalisé une étude précédente qui a montré la capacité du DEAE-D de former des PECs colloïdaux avec un autre polyanion (i.e. le carboxyméthylpullulane) [2], alors qu'il n'existe pas encore de recherche dans la littérature portant sur sa complexation avec le HA.

Les études sur les PECs de HA/DEAE-D dans cette partie ont ainsi fait l'objet d'une publication dans ***Colloids and Surfaces A: Physicochemical and Engineering Aspects*** *(2021), Vol. 629, p. 127485*, qui est présentée dans la section suivante. A la suite de cela, une étude complémentaire concernant la stabilité de ces PECs en fonction du pH sera également présentée pour montrer l'impact du pH sur ces systèmes.

Références

[1] Q. Hu, Y. Lu, Y. Luo, Recent advances in dextran-based drug delivery systems: From fabrication strategies to applications, Carbohydrate Polymers, 264 (2021) 117999. https://doi.org/10.1016/j.carbpol.2021.117999.

[2] D. Le Cerf, A.S. Pepin, P.M. Niang, M. Cristea, C. Karakasyan-Dia, L. Picton, Formation of polyelectrolyte complexes with diethylaminoethyl dextran: Charge ratio and molar mass effect, Carbohydrate Polymers, 113 (2014) 217-224. https://doi.org/10.1016/j.carbpol.2014.07.015.

II.2. Publication : Polyelectrolyte complexes of hyaluronic acid and diethylaminoethyl dextran: Formation, stability and hydrophobicity

Le, H. V., Dulong, V., Picton, L., & Le Cerf, D. (2021). Colloids and Surfaces A: Physicochemical and Engineering Aspects, Volume 629, 127485.

Polyelectrolyte complexes of hyaluronic acid and diethylaminoethyl dextran: formation, stability and hydrophobicity

Huu Van LE, Virginie DULONG, Luc PICTON, Didier LE CERF *

Normandie Univ, UNIROUEN, INSA Rouen, CNRS, PBS UMR 6270, 76000 Rouen, France

*Corresponding author: E-mail address: didier.lecerf@univ-rouen.fr

Tel: 00 33 02 35 14 65 43; Fax: 00 33 02 35 14 67 04

Abstract: Polyelectrolyte complexes (PECs) of hyaluronic acid (HA) and diethylaminoethyl dextran (DEAE-D), promising for biomedical applications, have been investigated with respect to physicochemical properties, mainly in terms of particle size and relative hydrophobicity as well as storage stability. Influences of charge ratio, polymer concentration, molar masses of HA, ionic strength and mixing methods have been particularly investigated. The complexation between HA and DEAED generally resulted in colloidal particles having mean hydrodynamic diameter of 150-350 nm, with larger particle size observed at negative to positive charge ratio (n-/n+) further from the unity. Higher polymer concentration or higher molar mass of HA also led to higher particle size of the PECs, whereas the increasing ionic strength led to a non-monotonic evolution in particle size. The effects of mixing mode and mixing order on particle size were interdependent and depended also on n-/n+. PECs at n-/n+ $\leq$ 0.4 showed lack of stability, which seemed not to be sensitive to storage temperature but significantly improved at higher salt concentration or lower polymer concentration. The relative hydrophobicity of such PECs was also confirmed by the fluorescence spectra of pyrene incorporated in PEC particles. Such results gave a better insight to polysaccharides-based PECs, especially as a potential system to encapsulate hydrophobic active molecules for drug delivery purposes.

Keywords: polyelectrolyte complexes; hyaluronic acid; diethylaminoethyl dextran, polysaccharide; pyrene fluorescence

Graphical abstract:

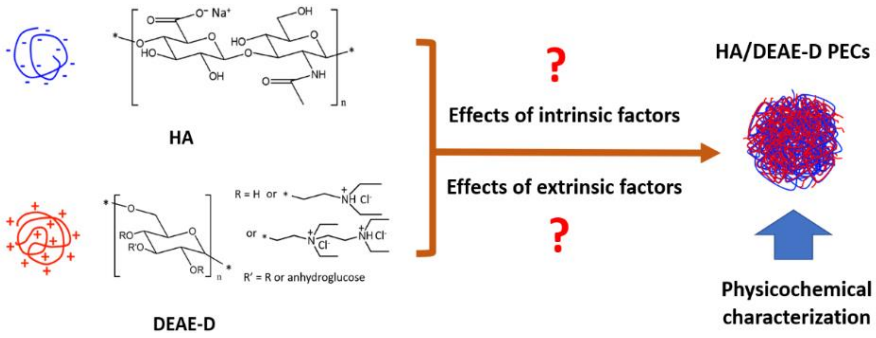

1. Introduction

Polyelectrolyte complexes (PECs), sometimes referred to as polyion complexes, are formed by self-assembly of oppositely charged polymers, i.e. polyanions and polycations. The formation of PECs in aqueous media is consensually regarded as an entropy-driven phenomenon, as the association between polyanions and polycations occurs by means of electrostatic interactions (Coulomb forces) with the main driving force being the increase in entropy due to the release of water molecules and counter-ions [1, 2]. Hydrogen bonding, hydrophobic interactions and van der Waals forces can also be involved in PEC formation [3, 4].

Different kinds of PECs can be elaborated with different possible morphologies, including water-soluble PECs, colloidal PECs, PEC coacervates and solid PECs or precipitates. These morphologies as well as their phase behaviours vary widely depending on the balance of the polyelectrolytes, salt ions and water within the complex, which is directly related to several factors: total polymer concentration (C_P) and polymer molar mass, salt concentration, electrostatic interaction strength, charge density and charge ratio, i.e. molar ratio between negative and positive charges (n-/n+), which is usually related to the pH of reaction media [4-8]. Complexation of low molar mass polyelectrolytes having weak ionic groups and a large difference in chain lengths at a non-stoichiometric mixing ratio would favourably generate soluble PECs which could be compared to chains of block copolymer with neutralized segments as hydrophobic blocks and unpaired segments as hydrophilic blocks, or colloidal stable PECs, usually described as particles with neutral and hydrophobic cores surrounded by hydrophilic and polar shells [4, 6, 9]. On the contrary, high and similar molar masses, strong charge-charge interactions and stoichiometric mixing of the complexing polyelectrolytes usually favour aggregation, phase separation and precipitation of PECs [4, 9]. Also, PEC morphology is possibly influenced by preparation

parameters such as mode of mixing (e.g. rapid one-shot or slow dropwise addition) and order of addition [6, 10]. A comprehensive and in-depth understanding of these factors as well as their intercorrelation may therefore allow the tunability of PECs in terms of physicochemical properties for a wide range of applications, e.g. biomedicine, pharmaceutics, nutraceuticals, cosmetics, food and paper industries [9, 11, 12].

For healthcare applications, PECs from biopolymers usually attract more interest compared with those of synthetic polyelectrolytes, since the formers are generally more biocompatible and biodegradable [13]. Accordingly, biomaterials-based PECs from polysaccharides, proteins or polypeptides have been extensively reported in the literature [14, 15]. Among several biopolymers employed so far for such applications, hyaluronic acid (HA) has attracted a great deal of attention due to its excellent biocompatibility, stemming from the fact that HA is naturally found in the human body [16]. HA has also been widely used as a ligand in drug delivery systems to target tumours *via* the relevant CD44 receptors on tumour cells [17]. Owing to the carboxylic groups of the D-glucuronic acid in its structure, HA would display negative charges in aqueous media at certain pH range and thus forms PECs upon mixing with positively charged polymers. Typically, PECs from HA and polycations, most commonly chitosan (CTS), have become a topic of great interest for clinical and biomedical applications. For instance, solid HA/CTS PECs were elaborated as nasal insert encapsulating vancomycin and insulin [18]. Coacervates of HA and lactose-modified CTS were also studied for radical-scavenging activities [19]. HA/CTS nanoparticles for curcuminoid delivery in glioma cells were also reported [20].

While such studies of PECs from HA and CTS are abundant, there has been less research focusing on the complexation between HA and other positively charged biopolymers. Specifically, to the best of our knowledge, no studies so far have focused on PECs prepared from HA and

diethylaminoethyl dextran (DEAE-D). DEAE-D is a polycationic derivative of dextran, a natural and more flexible polysaccharide than CTS. The most studied application of DEAE-D is its capacity to form complexes with negatively charged biomacromolecules like nucleic acids and proteins for nucleic acid transfection or to provide sustained-release protein delivery [21, 22]. DEAE-D can also be used as a coating agent for nano/microparticles in drug delivery systems due to its stabilizing effects [23, 24]. Furthermore, DEAE-D itself could exert therapeutic effects, namely inhibition of tumour growth [25, 26]. Like CTS, DEAE-D is also a low-cost polysaccharide with satisfactory biocompatibility and biodegradability. The advantage of DEAE-D over CTS lies in its good solubility in aqueous solutions at any pH which renders DEAE-D more favourable in certain cases, for example when a neutral or high pH is needed [23].

With their opposite charges in aqueous media, HA and DEAE-D must form PECs through ion-pairing (**Figure 1**). The aim of this study was to investigate the HA/DEAE-D complexation by evaluating the impacts of different parameters involved in the complexation process. The resulting systems were evaluated in terms of morphology through their visual aspect and the physicochemical characteristics of PEC nanoparticles, including particle size, particle concentration, particle net surface charge and the stability of particle size, as well as their potential hydrophobicity. This would allow a better insight into PEC structures and behaviours, which is associated with optimizing the relevant parameters for elaboration of nanocarriers encapsulating therapeutic agents.

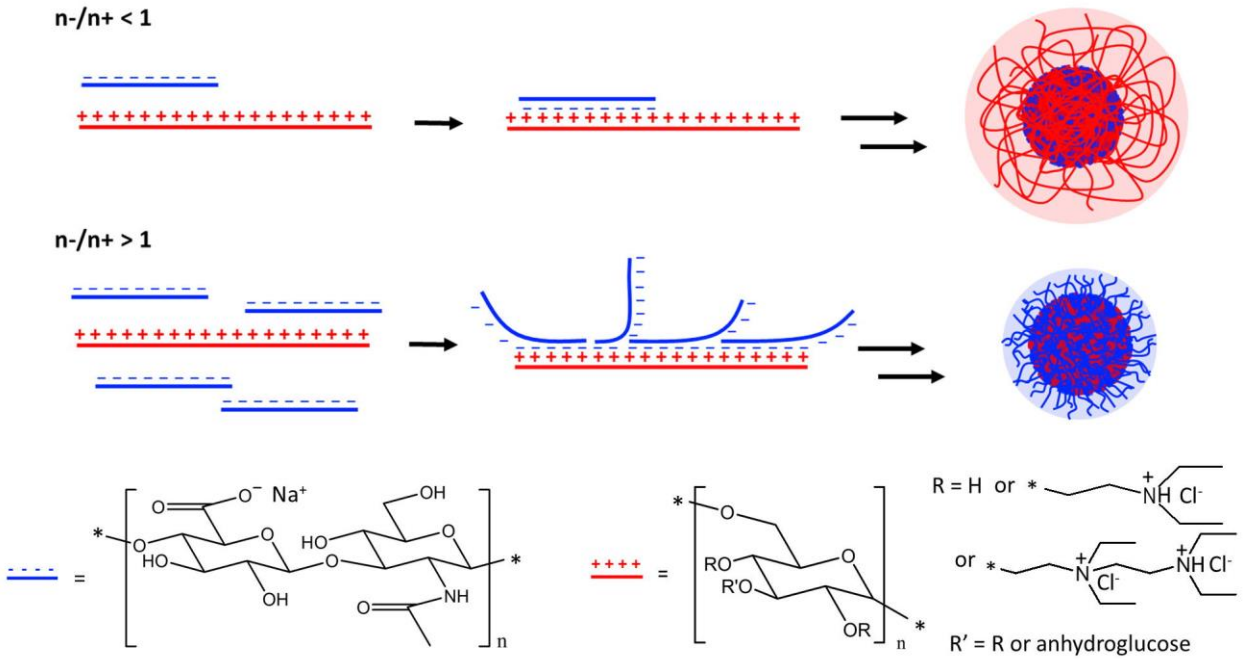

Figure 1. Schematic illustration of the complexation between HA as polyanion (blue) and DEAE-D of higher molar mass as polycation (red), in case of polycation in excess (n-/n+ < 1) or polyanion in excess (n-/n+ > 1). The double strain segments in the primary complexes formed by ion-pairing could be relatively hydrophobic. The aggregation of primary complexes through intercomplex interactions (including electrostatic and hydrophobic interactions, van der Waals forces and hydrogen bonding) could finally lead to particles with relatively hydrophobic cores and highly hydrophilic shells.

2. Materials and methods

2.1. Materials

Medium- and high-molar-mass sodium hyaluronates (HA_M and HA_H respectively) with purity over 95% were kindly provided by Givaudan (France). DEAE-D hydrochloride and polyethyleneimine (PEI) hydrochloride were purchased from Sigma-Aldrich (USA). The macromolecular characteristics of HAs and DEAE-D were obtained by size exclusion chromatography coupled with multi-angle light scattering, differential refractive index and

viscosity detectors (see **Appendix**). The ionization rate (α) of HA units (number of deprotonated carboxylic groups per D-glucuronic-N-acetylglucosamine unit) in function of pH was calculated from the modified Henderson-Hasselbalch (**Equation 1**):

$$pH = pKa + \log[\alpha/(1-\alpha)] \qquad \textbf{(Equation 1)}$$

with pKa of HA equal to 2.9, obtained from HA having comparable molar mass reported in the literature [27]. For DEAE-D, the degree of substitution per anhydroglucose unit of quaternary amino groups (0.26) and of tertiary amino groups (0.29) as well as the ionization rate of anhydroglucose units in function of pH were reported in our previous studies [28]. All data are summarized in **Table 1** and **Figure 2**. Pyrene with purity of 98% was purchased from Acros Organics (USA). Sodium chloride (NaCl), hydrochloric acid (HCl), sodium hydroxide (NaOH) and acetone were purchased from VWR (France). Water used for all experiments was purified with Milli-Q system (Millipore, USA).

Table 1. Macromolecular characteristics of polyelectrolytes

Samples	**M_n (g.mol^{-1})**	**M_w (g.mol^{-1})**	**Đ**	**Rg_w (nm)**
HA_M	210,000	270,000	1.3	53
HA_H	670,000	830,000	1.2	115
DEAE-D	270,000	700,000	2.6	29
PEI[(a)]	12,586	-	1.3	-

M_n: number average molar mass; M_w: weight average molar mass; Đ: dispersity; Rg_w: weight average gyration radius; [(a)] Supplier data

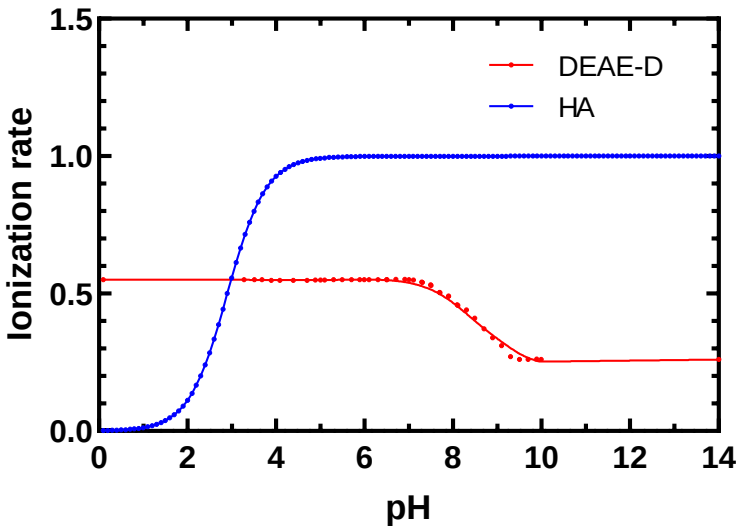

Figure 2. Ionization rate of HA units (D-glucuronic-N-acetylglucosamine) and DEAE-D units (anhydroglucose) as a function of pH

2.2. PEC preparation and storage

Polyelectrolyte solutions were prepared by dissolving polymers in the aqueous solvents of interest under stirring at 200 rpm for one night at room temperature before complexation experiments. Depending on each study, the aqueous solvents used were Milli-Q water, NaCl solutions at various concentrations or pyrene 4×10^{-7} mol.L^{-1}. C_P was varied from 0.25 to 1 g.L^{-1}. The pH of polymer solutions was measured using a pH meter equipped with a LE438 electrode (Mettler Toledo, Switzerland). All polyelectrolyte solutions were thereafter filtered through 0.45 µm regenerated cellulose membrane filter units (Sartorius, Germany). The complexation was performed by mixing the polyanion and polycation solutions of the same C_P and solvent under mild stirring (200 rpm) at room temperature. Unless otherwise stated, the usual mixing method was a rapid one-shot dropping of the polyanion in the polycation using a micropipette. The total stirring time from the beginning of mixing and the total volume of complexation were 30 min and

5 mL, respectively. The volume ratios between the two polymer solutions were varied and calculated from the target n-/n+ by using **Equation 2**:

$$n-/n+= (\alpha^{-}V^{-}C^{-}M_o^{+})/(\alpha^{+}V^{+}C^{+}M_o^{-}) \quad \textbf{(Equation 2)}$$

with α, V, C and M_o being respectively unit ionization rate, solution volume (mL), polymer solution concentration ($g.L^{-1}$) and unit average molar mass ($g.mol^{-1}$) of the polyanion (-) and the polycation (+). M_o for (D-glucuronic-N-acetylglucosamine) units of HA and anhydroglucose units of DEAE-D were 378 and 217 $g.mol^{-1}$, respectively. α values of HA and DEAE-D units at defined pH values were obtained from **Figure 2** and were at their maxima (1 and 0.55 respectively) in Milli-Q water (pH = 5-6). For stability studies, PECs were stored either at 4 °C or at 25 °C following their first characterization for evaluation of particle size stability after 1, 3, 7 and 30 days. All experiments were carried out at least three times.

2.3. Particle size, particle concentration and zeta potential measurement

Particle size, particle concentration and zeta potential (i.e. electrophoretic mobility) characterizations were carried out using Zetasizer Ultra instrument (Malvern Panalytical, UK) for visually homogeneous PEC samples without further dilution. Particle size as average hydrodynamic diameter (D_h), polydispersity index (PDI) and total particle concentration (TPC) were determined by dynamic light scattering (DLS) technique. For the measurements of D_h and PDI, at least 1 mL of samples was placed in a two-clear sided plastic cuvette (VWR, France) and back scatter was set as angle of detection. For the measurements of TPC, at least 1 mL of samples was placed in a four-clear sided plastic cuvette (Brand, Germany) as the process required back scatter, side scatter and forward scatter detections. Zeta potential (ζ) was measured by electrophoretic light scattering technique with samples placed in a plastic folded capillary cell (Malvern Panalytical, UK). For each sample, at least three measurements were performed at 25 °C

after 120 seconds of temperature stabilization. The measurement data were processed on ZS XPLORER v1.2.0.91 software.

2.4. Pyrene fluorescence studies

Sample preparation: A stock solution having pyrene concentration (C_{Py}) of 10^{-3} mol.L^{-1} in acetone was prepared and stored at 4 °C. In order to prepare pyrene 4×10^{-7} mol.L^{-1} and 8×10^{-7} mol.L^{-1} aqueous solutions, 10 µL and 20 µL aliquots of the stock solution were introduced to 50 mL volumetric flasks respectively, which were then filled with Milli-Q water after complete acetone evaporation and stirred for 24 h. Samples of HA_M/DEAE-D PECs containing pyrene (HA_M/DEAE-D/Py) at $C_{Py} = 4\times10^{-7}$ mol.L^{-1} were then prepared for $C_P = 0.25$ and 0.5 g.L^{-1} by either: (a) mixing the pyrene 8×10^{-7} mol.L^{-1} aqueous solution with the same volume of PEC suspensions with $C_P = 0.5$ and 1 g.L^{-1} respectively or (b) complexation upon mixing polyelectrolyte solutions with $C_P = 0.25$ and 0.5 g.L^{-1} readily prepared in pyrene 4×10^{-7} mol.L^{-1} aqueous solution. All samples were stirred at 200 rpm at room temperature overnight before fluorescence measurements. All samples were prepared in triplicate.

Fluorescence measurements: Fluorescence measurements were carried out at room temperature with a Fluoromax-4 spectrofluorometer (Horiba Jobin Yvon, France). The fluorescence emission spectra (λ_{em} = 350-450 nm) were obtained with the excitation wavelength λ_{ex} = 335 nm. The ratio I_I/I_{III} was calculated as the intensity ratio between the first and third vibronic bands recorded respectively at 373 nm and 383 nm in the emission spectra [29, 30]. The fluorescence excitation spectra (λ_{ex} = 300-360 nm) were also recorded at the emission wavelength λ_{em} = 373 nm. The ratio I_{335}/I_{338} was calculated as the intensity ratio between the bands recorded respectively at 335 nm and 338 nm in the excitation spectra [31, 32]. Polyelectrolyte solutions

containing pyrene at the same concentrations were also measured as references. All measurements were done at least three times for each sample.

3. Results and discussion

3.1. Influences of different factors on PEC formation

In this section, HA/DEAE-D PECs were evaluated in terms of suspension visual aspect, particle size (hydrodynamic diameter, D_h) and particle size distribution (polydispersity index, PDI), particle amount (total particle concentration, TPC) and net surface charge (zeta potential, ζ) after 30 minutes of complexation. The PECs were prepared with different varied intrinsic parameters including charge ratio, polymer concentration, polymer molar mass (i.e. HA molar mass), ionic strength and experimental parameters (i.e. mixing mode and mixing order) in order to study their influences on PECs.

3.1.1. Influence of charge ratio

The impact of n-/n+ ratio, from 0.1 to 10, was studied for HA_M/DEAE-D PECs with C_P = 0.5 $g.L^{-1}$ in Milli-Q water. Before the complexation, the pH values of HA and DEAE-D 0.5 $g.L^{-1}$ solutions were 5.7 ± 0.2 and 4.4 ± 0.2 respectively, implying their maximal ionization rate (1 and 0.55 respectively) as shown in **Figure 2**. At the beginning of the complexation (polyanion in polycation), a visible turbidity was observed immediately following the mixing of the two polyelectrolytes, indicating an instantaneous formation of PECs. This could be attributed to the maximal ionization of the polyelectrolytes in the mixture. After 30 minutes of complexation, macroscopic phase separation was observed only for stoichiometric complexation (n-/n+ = 1), characterized by a coexistence of small precipitates and a clear supernatant (**Figure 3**). Meanwhile, all other n-/n+ led to the formation of visually homogeneous systems, changing from clear to turbid dispersions as n-/n+ was closer to the stoichiometric value. Only such homogeneous samples were

subjected to particle size and zeta potential measurements. As shown in **Figure 4**A, the non-stoichiometric complexation between HA_M and DEAE-D formed nanoparticles with mean D_h in the range of 150-350 nm. As n-/n+ approached the unity, the particle sizes decreased, along with narrower size distributions and lower absolute values of zeta potential (**Figure 4**A-B).

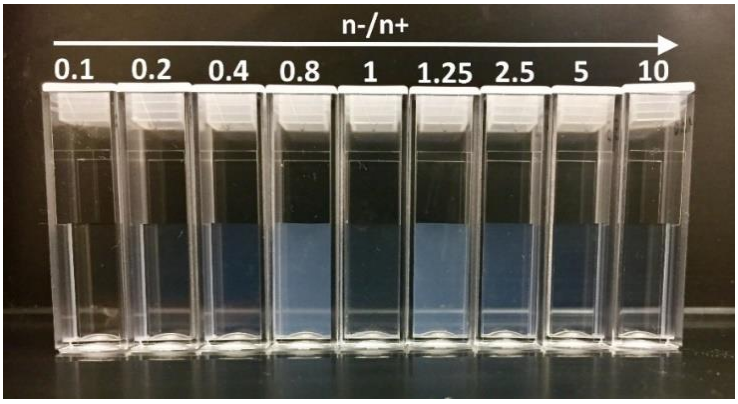

Figure 3. Visual aspect of HA_M/DEAE-D PEC suspension at C_P = 0.5 g.L^{-1} in Milli-Q water at different n-/n+ after 30 minutes of complexation under stirring.

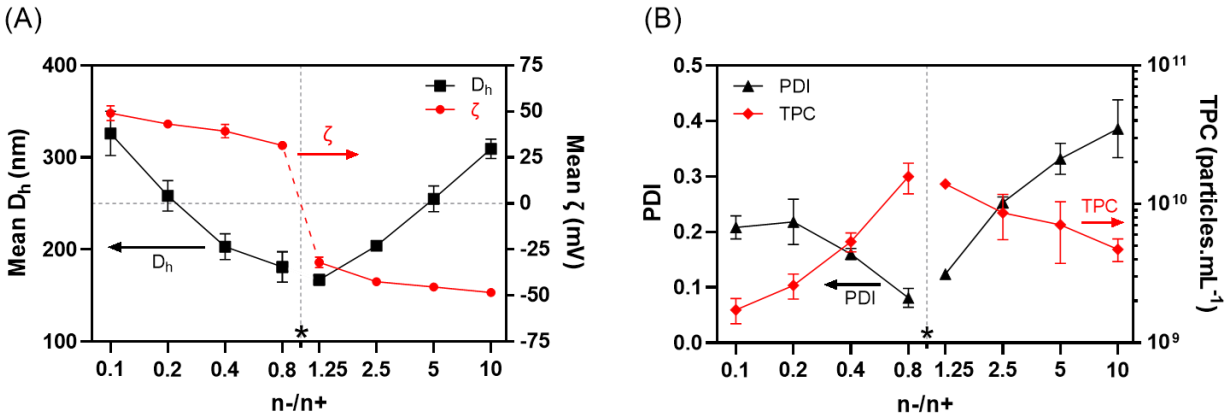

Figure 4. (**A**) Mean hydrodynamic diameter and mean zeta potential, (**B**) polydispersity index and total particle concentration (TPC) of HA_M/DEAE-D PECs at C_P = 0.5 g.L^{-1} in Milli-Q water at different n-/n+ after 30 minutes of complexation under stirring. Asterisks denote precipitation at n-/n+ = 1. Error bars represent mean ± standard deviation (n ≥ 3).

In the literature, relatively similar tendencies in particle size (i.e. lower particle size at charge ratio nearer to 1) were also observed for chitosan/dextran sulfate PECs by Schatz *et al.* [8] and poly[2-(dimethylamino)ethyl methacrylate]/polyphosphate PECs by Kabanov and Zezin [33]. Such tendencies might be explained based on the model of PEC particles as secondary complexes shown in **Figure 1** as followings. At non-stoichiometric mixing ratio, ion-pairing between polyanions and polycations would lead to the formation of primary complexes comprising neutral double-stranded complexed segments and polar single-stranded segments of uncomplexed polyelectrolytes [8, 33]. Hydrophobic interactions and self-assembly of neutralized complexed segments could occur due to their potential nonpolar characteristic and might be enhanced by the presence of ethyl groups in uncharged DEAE groups, which are also known to have a slightly hydrophobic property [34]. The segregation of such nonpolar segments *via* hydrophobic interactions with other interactions (i.e. van der Waals forces and hydrogen bonding) would form final PEC particles as secondary complexes comprising relatively hydrophobic cores surrounded by hydrophilic corona shells of polar uncomplexed polyelectrolyte segments [3, 4, 8, 35, 36]. Although the core-shell model has been widely used to describe PEC-based colloidal particles, the work of Raik *et al*. which studied PECs from HA and diethylaminoethyl chitosan by structure factor analysis suggested PEC particles not following this model [37]. Furthermore, Zhang and Shklovskii suggested other structural models for non-stoichiometric PECs, for example intercomplex disproportionation in which there is a coexistence of macroscopic neutral droplets and highly charged soluble PECs, and intracomplex disproportionation in which PECs are described as "tadpoles" having one end as neutral complex in the form of a condensed droplet and the other end as a highly charged tail [38]. However, in our work, the high zeta potential which decreases when n-/n+ is nearer to 1 (**Figure 4**) with accordingly decreased I_I/I_{III} in the pyrene

fluorescence spectra (see **Section 3.3**) seem to suggest the copresence of a highly charged and hydrophilic outer shell and a relatively more hydrophobic core respectively in HA/DEAE-D particles. Based on this presumption, a n-/n+ ratio closer to 1 probably generates particles having thinner and less polar shells with more hydrophobic cores due to more efficacious charge neutralization, leading to a more compact structure (i.e. smaller size) of the final particles. This trend was also observed at other polymer concentrations (i.e. C_P = 0.3 and 1 $g.L^{-1}$) as mentioned in **Section 3.1.2**.

At the stoichiometric charge ratio, the charge compensation was probably complete, as seen with the zeta potential (net surface charge) around zero (**Figure 4**A). This could favour aggregation and explained the observed precipitation. One should also notice that particle size of PECs can abruptly increase at n-/n+ very close to the unity due to particle aggregation when charge compensation is nearly complete [8]. However, this was not observed in the current work as n-/n+ at 0.8 and 1.25 might not be extremely close to 1 for such phenomenon to be visible. Despite the smaller particle size, the turbidity become more pronounced for these samples (**Figure 3**), which should be attributed to the increase in particle concentration (**Figure 4**B) as also described in the literature [8]. It should be noticed that high turbidity might lead to multiple light scattering which could affect particle size analysis [39]. However, for the systems in this work, the turbidity was not extremely high and the mass concentrations of the studied samples were rather low (0.3-1 $g.L^{-1}$, which means 0.03-0.1 % m/v) in comparison with the high concentrations at which multiple light scattering starts showing major effects as described in the literature, for example 8 $g.L^{-1}$ or 10 % m/v for some protein-based colloidal systems [39]. Furthermore, the Malvern Zetasizer Ultra in this work uses the Non-Invasive Backscatter technique allowing automatic optimization of measurement position to avoid the multiple light scattering effect and the attenuator index in the

particle size analysis results was not too low (5 to 7) with the resulting mean count rates of 200-500 kcps (kilo counts per second), which suggest acceptable concentrations for DLS [40]. For these reasons, the multiple light scattering is likely to have little effect on our particle size results.

3.1.2. Influence of total polymer concentration

To evaluate the impact of total polymer concentration (C_P), HA_M/DEAE-D PECs with n-/n+ from 0.1 to 10 were prepared and studied at C_P of 0.3, 0.5 (**Section 3.1.1**) and 1 $g.L^{-1}$ in Milli-Q water. As for C_P = 0.5 $g.L^{-1}$, the stoichiometric mixing at C_P of 0.3 and 1 $g.L^{-1}$ also led to visible precipitation. The DLS results of PECs at other n-/n+ showed that larger particles with larger size distributions were formed as C_P was increased from 0.3 to 1 $g.L^{-1}$ (**Figure 5**A-B). However, the general trends of D_h and PDI as a function of n-/n+ are the same for all the studied C_P, i.e. lower mean D_h and PDI at n-/n+ nearer to 1 as described in **Section 3.1.1**.

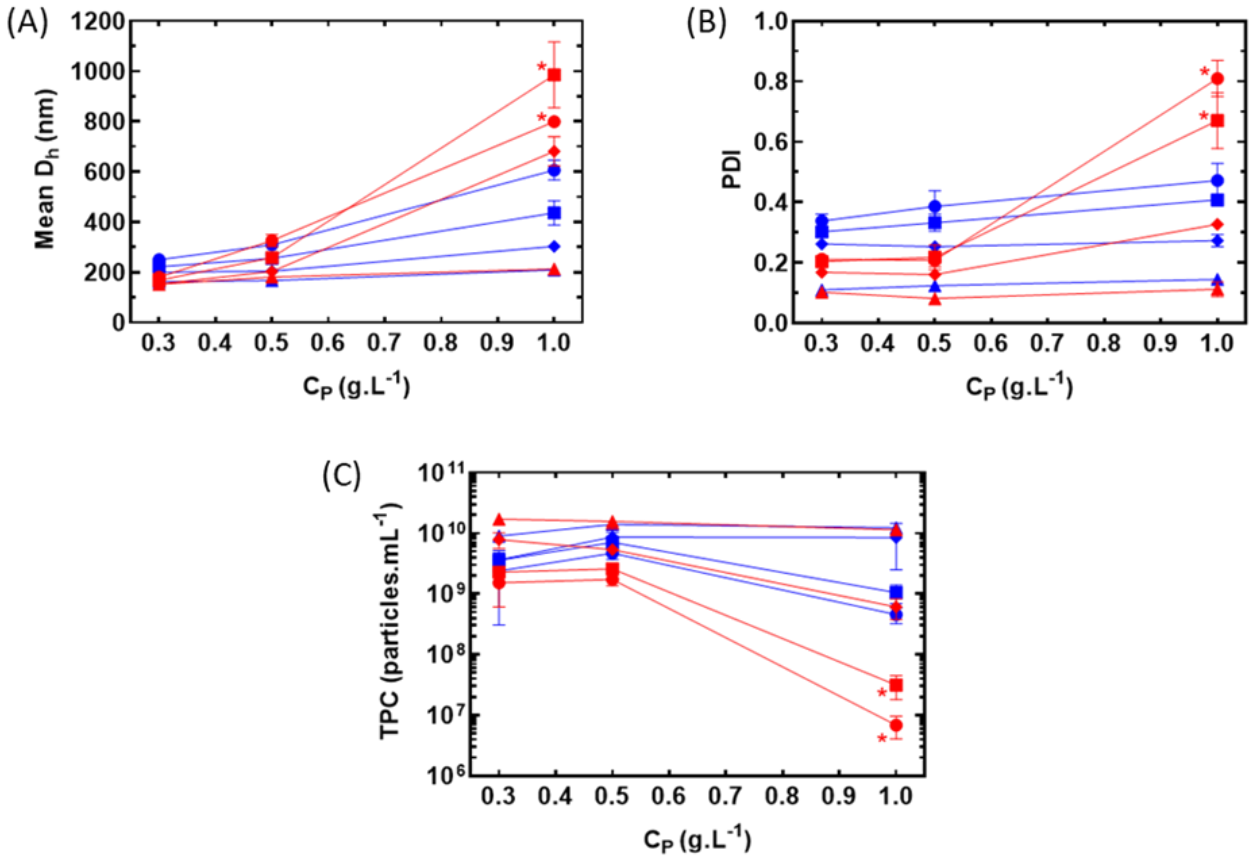

Figure 5. (**A**) Mean hydrodynamic diameter, (**B**) polydispersity index and (**C**) total particle concentration of HA_M/DEAE-D PECs in Milli-Q water as a function of total polymer concentration at different n-/n+ ratios: 0.1 (–●–), 0.2 (–■–), 0.4 (–◆–), 0.8 (–▲–), 1.25 (–▲–), 2.5 (–◆–), 5 (–■–), 10 (–●–). Asterisks denote samples having highly heterogeneous multimodal particle size distribution with poor repeatability. Error bars represent mean ± standard deviation ($n \geq 3$).

The larger PEC particles observed at higher C_P for all n-/n+ were probably due to a higher amount of polymer associated in the particles. According to Müller *et al.*, as final particles of PECs are secondary particles formed by the aggregation of primary PECs, the increase in C_P would reduce the Debye length of the system and in turn lead to a reduction in the repulsion between

primary PECs, which favours the formation of bigger secondary PECs [36]. The increase range in particle size was less important at n-/n+ near 1, presumably due to the more compact structure of PECs at such charge ratios. In accordance with the increasing particle size, we observed higher turbidity of PEC suspensions at higher C_P for the same n-/n+ (results not shown). Hence, the turbidity in this case seemed to be dependent on particle size, but not necessarily on particle number since the amounts of particles were not greatly changed (for n-/n+ $\geq$ 0.4) or even decreased (for n-/n+ of 0.1 and 0.2) with increased C_P (**Figure 5**C).

Furthermore, at $C_P = 1$ g.L^{-1}, the remarkably high mean D_h with multimodal size distribution and very high PDI (PDI > 0.5) at low values of n-/n+ (i.e. 0.1 and 0.2) coincided with significant low TPC. These results seem to indicate fewer but larger particles uncontrolled in size. This could be explained again from the model of PECs shown in **Figure 1**. In case of very low n-/n+, the neutral segments in primary PECs are much shorter than those at high n-/n+, which would consequently require a very high number of primary PECs involved to form sufficiently stable cores in secondary particles, leading to much fewer final particles with much larger size. Such large particle sizes can also be attributed to the loose structure of the core due to weaker hydrophobic interactions of shorter neutral complexed segments [6]. Beside the core, the particle size should also be greatly governed by the thickness of their shell, which is directly related to the chain length (contour length) of the polyelectrolyte in excess [6]. This assumption could also explain the larger particle size for HA_M/DEAE-D PECs at very low n-/n+ compared with high n-/n+ since the corona shell in the former case was formed by long segments of uncomplexed DEAE-D, which had a higher chain length than that of HA_M. Such difference in particle size between the two extremities of the n-/n+ range seemed to be only significant at $C_P = 1$ g.L^{-1}. In case of $C_P = 0.5$ g.L^{-1}, this was not observed after 30 minutes of complexation but became evident

after 24 h (see **Section 3.2.1**). This was possibly because lower C_P led to weaker interchain and intercomplex interactions within the PEC suspension, resulting in slower kinetics of the systems to reach their equilibrium state.

3.1.3. Influence of molar mass

In order to evaluate the impact of polyelectrolyte molar mass on PEC formation, HA_H/DEAE-D PECs were compared with HA_M/DEAE-D at the same n-/n+ and C_P (n-/n+ = 0.1-10 and C_P of 0.3 and 0.5 $g.L^{-1}$). At C_P = 0.5 $g.L^{-1}$, the complexation between HA_H and DEAE-D consistently led to precipitation in the whole studied range of n-/n+. Upon decreasing C_P to 0.3 $g.L^{-1}$, the precipitation was less intense and not observed at n-/n+ of 0.1 and 10. As can be seen from the particle size measurements of these samples (**Figure 6**), complexation between DEAE-D and HA of higher molar mass led to PECs with higher diameter and PDI but TPC not significantly changed.

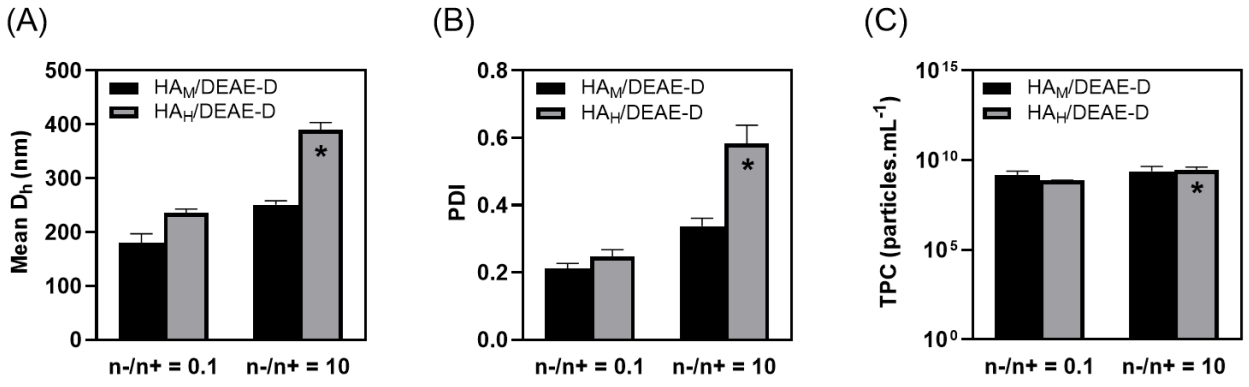

Figure 6. (**A**) Mean hydrodynamic diameter, (**B**) polydispersity index and (**C**) total particle concentration of HA_M/DEAE-D and HA_H/DEAE-D PECs at C_P = 0.3 $g.L^{-1}$ in Milli-Q water at n-/n+ of 0.1 and 10. Asterisks denote samples having highly heterogeneous multimodal particle size distributions with poor repeatability. Error bars represent mean ± standard deviation ($n \geq 3$).

A similar observation reported by Schatz *et al.* also showed an increase in PEC particle size after increasing the molar mass of chitosan (from 0.13 × 10^5 to 3.65 × 10^5 g.mol^{-1}) for complexation with dextran sulfate of fixed molar mass (5 × 10^5 g.mol^{-1}) [8]. Müller *et al.* also reported increasing particle size of PEI/polyacrylic acid PECs resulting from the increase in molar mass of the two associating polyelectrolytes [36]. In the current work, while DEAE-D is a flexible polysaccharide with mainly α(1→6) glycosidic linkages, HA is relatively stiffer with less flexible β(1→4) and β(1→3) glycosidic bonds [41, 42]. This can also be seen from the expanding coil structure of HA shown by its high Rg values in **Table 1**. As a result, a HA chain length which is higher and closer to that of DEAE-D would certainly lead to the formation of longer and more rigid neutralized segments in primary complexes compared with medium molar mass HA, which could favour the aggregation to form larger secondary particles and hence the macroscopic phase separation. In the case of n-/n+ > 1, the observed increase in particle size could also be attributed to the increased thickness of the particle shells due the presence of higher chain length and more expanding hydrodynamic coil structure of HA_H compared with HA_M. All these synergistic effects probably explain the more obvious increase in PEC size at n-/n+ = 10 than at n-/n+ = 0.1. Furthermore, at n-/n+ = 10, the D_h distribution of HA_H/DEAE-D PECs was multimodal and heterogeneous. This might result from the high viscosity of the bulk phase due to the excessive presence and the long chain length of HA_H, preventing the homogeneous distribution of DEAE-D to form same-sized particles.

3.1.4. Influence of ionic strength

The effect of ionic strength on PEC formation was studied by characterizing HA_M/DEAE-D PECs (C_P = 0.5 g.L^{-1}) and HA_H/DEAE-D PECs (C_P = 0.3 g.L^{-1}) at n-/n+ from 0.1

to 10 prepared at many NaCl concentrations ([NaCl] varying from 0 to 1 mol.L^{-1}). After the complexation, samples showing precipitation are reported in **Table 2**.

Table 2. Visual aspect of HA/DEAE-D PEC dispersions at various NaCl concentrations

	[NaCl] (mol.L^{-1})	n-/n+ 0.1	0.2	0.4	0.8	1	1.25	2.5	5	10
HA_M/DEAE-D C_P = 0.5 g.L^{-1}	0	-	-	-	-	+	-	-	-	-
	1×10^{-3}	-	-	-	-	+	-	-	-	-
	1×10^{-2}	-	-	-	+	+	+	-	-	-
	1×10^{-1}	-	-	+	+	+	+	+	-	-
	1	-	-	-	-	-	-	-	-	-
HA_H/DEAE-D C_P = 0.3 g.L^{-1}	0	-	+	+	+	+	+	+	+	-
	5×10^{-4}	-	-	-	+	+	-	-	-	-
	1×10^{-3}	-	-	-	-	+	-	-	-	-
	5×10^{-3}	-	-	-	-	+	+	-	-	-
	1×10^{-2}	-	-	-	+	+	+	-	-	-
	1×10^{-1}	-	-	+	+	+	+	-	-	-
	1	-	-	-	-	-	-	-	-	-

+ : precipitation; - : homogeneous samples

The presence of NaCl seemed to have a non-monotonic influence on PECs depending on its concentration: (i) reducing the formation of PECs at a low salt concentration (10^{-3} mol.L^{-1}), (ii) favouring PECs aggregation as well as macroscopic phase separation at intermediate salt concentrations (10^{-2} -10^{-1} mol.L^{-1}) and (iii) depress the complexation at a very high salt concentration (1 mol.L^{-1}). For HA_M/DEAE-D PECs (C_P = 0.5 g.L^{-1}), the initial n-/n+ range of precipitation might be too narrow for the reduction of precipitation at the low salt concentration to be visible. The last two effects of salt on the phase behaviour (i.e. increase followed by suppression of phase separation) were also described for other PEC systems [38, 43]. This may result from the fact that associative phase separation (caused by ion pairing) and segregative phase separation (caused by hydrogen bonding and hydrophobic interactions) are respectively reduced and

enhanced with added salt [44]. In order to clarify such effects of salt on our specific system, particle size characterization by DLS was conducted for the HA_M/DEAE-D PECs (C_P = 0.5 g.L^{-1}) samples at n-/n+ = 0.2 and 5 within the studied range of salt concentration (**Figure 7**).

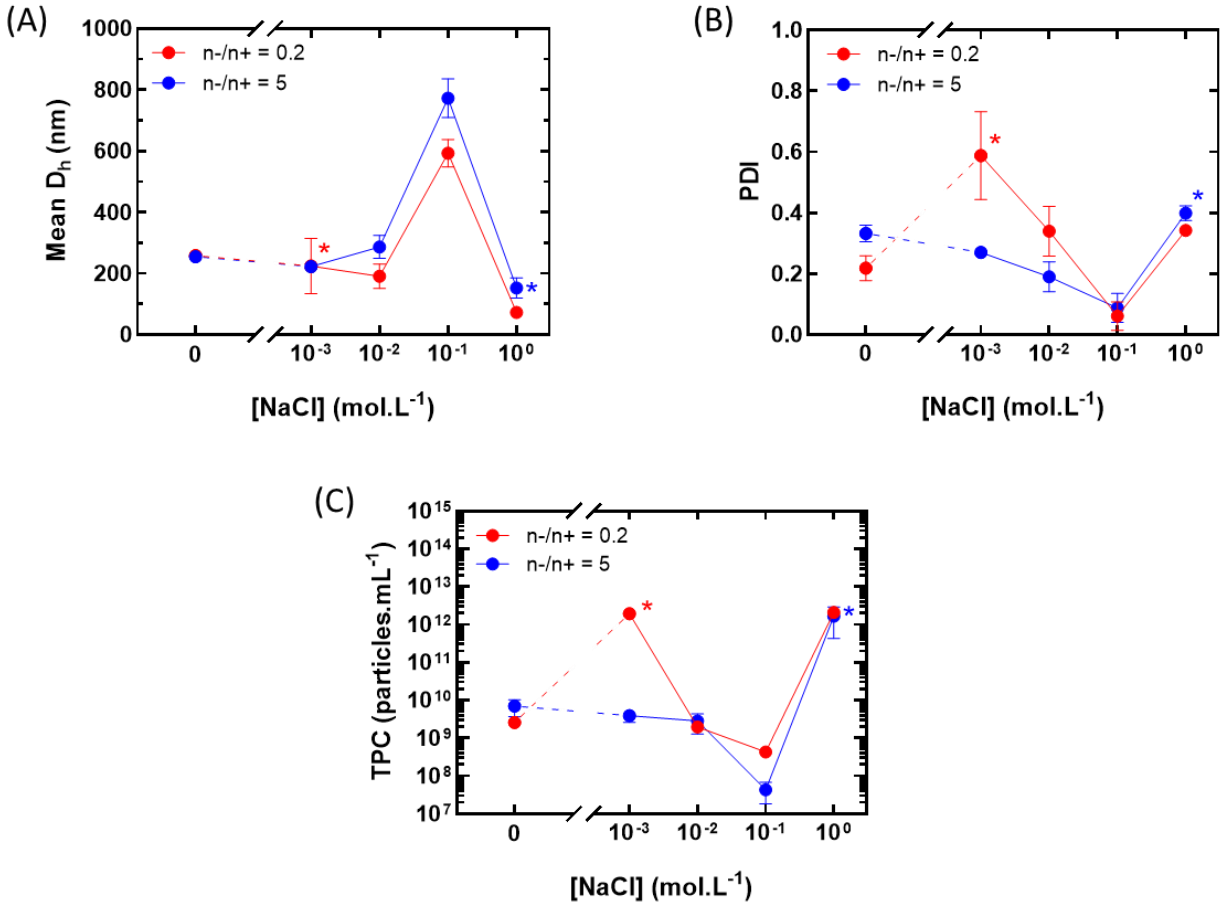

Figure 7. (**A**) Mean hydrodynamic diameter, (**B**) polydispersity index and (**C**) total particle concentration of HA_M/DEAE-D PECs (C_P = 0.5 g.L^{-1}) of n-/n+ = 0.2 and 5 prepared at different NaCl concentrations. Asterisks denote samples having highly heterogeneous multimodal particle size distributions with poor repeatability. Error bars represent mean ± standard deviation (n ≥ 3).

The suggested effects of ionic strength can be clearly seen from the results obtained with the samples having n-/n+ = 0.2. At [NaCl] = 10^{-3} mol.L^{-1}, the PEC particle size became poorly defined with its distribution being highly heterogeneous and remarkably high TPC, probably due

to the formation of loosely structured PECs with some small-sized particle populations, possibly because the primary complexation is rendered less effective by charge screening at macromolecular level. However, this effect seems to be hindered for PECs of n-/n+ = 5, possibly due to the more stable structure of these PECs (**Sections 3.1.2** and **3.2**). Anyway, when [NaCl] is higher than 10^{-3} mol.L^{-1}, effects of salt on PECs seem to be similar for both n-/n+ ratios: less particles were counted while the particle size distributions were narrower, but the mean D_h was increased to more than 500 nm as the salt concentration reached 10^{-1} mol.L^{-1}, indicating the formation of fewer but larger particles in accordance with the observed increase in precipitation at other n-/n+ between 0.2 and 5. This may be due to higher aggregation of PECs because of more efficacious hydrophobic interactions and weaker electrostatic repulsion caused by charge screening at complex and particle level. Specifically, the mean D_h at n-/n+ = 0.2 at [NaCl] $\geq 10^{-2}$ mol.L^{-1} was better defined with less variation than at [NaCl] = 10^{-3} mol.L^{-1} (**Figure 7**A). Therefore, an intermediate salt concentration seems to favour secondary complexation in compensation for the weakened primary complexation, leading to a stabilizing effect to form more close-packed and homogeneous PECs. These two opposing effects of salt on PEC particle size were also reported for sodium polystyrene sulfonate/poly(diallyldimethylammonium chloride) PECs by Dautzenberg *et al.* [45]. However, when salt concentration was extremely high (1 mol.L^{-1}), the charged groups of the two polyelectrolytes were almost completely screened from the beginning and the complexation was almost ineffective, leading to the clear aspect of all PEC suspensions even at n-/n+ = 1. This was also shown by the abrupt fall of particle sizes with very high particle concentration (**Figure 7**). It should be noticed that the critical salt concentration needed to completely suppress the complexation may vary depending on not only the type of polyelectrolytes but also their concentration and pH in the system [43, 44].

3.1.5. Influence of mixing order and mixing mode

To study the influence of mixing mode and mixing order, PECs of HA_M/DEAE-D in Milli-Q water at $C_P = 0.5$ g.L^{-1} and n-/n+ of 0.1, 0.8, 1.25 and 10 were prepared by either one-shot addition using a micropipette or dropwise addition (0.3 mL.min^{-1}) using a syringe pump in both addition orders. The impact of these two parameters on PEC formation was evaluated by comparing the mean particle sizes of PECs prepared by different methods (**Figure 8**).

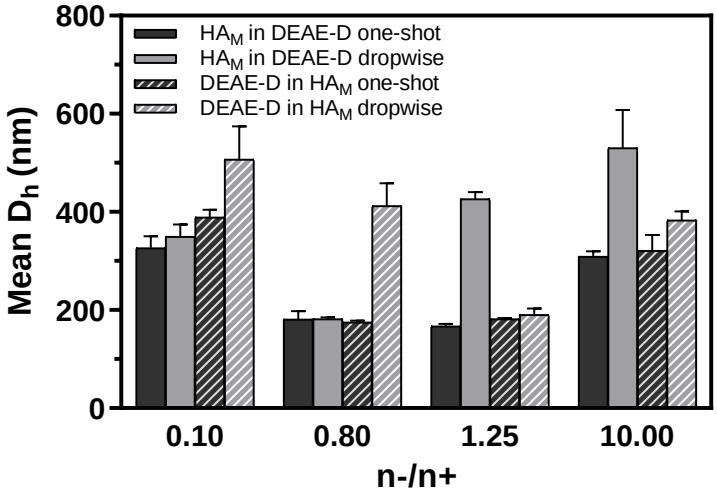

Figure 8. Mean hydrodynamic diameter of HA_M/DEAE-D PECs in Milli-Q water at $C_P = 0.5$ g.L^{-1} prepared with different mixing orders and mixing modes. Error bars represent mean ± standard deviation ($n \geq 3$).

As can be seen from the results, the effect of mixing order on mean particle size was negligible in one-shot mode but became considerable when PECs were prepared by dropwise mixing. At any n-/n+ ratio, remarkably large particle sizes were only observed when the polyelectrolyte in excess was added dropwise to the other polyelectrolyte, while the other three mixing methods resulted in lower and similar particle sizes. The distinct result in the former case could be explained based on the actual evolution of n-/n+ during the mixing, which was also

described by Schatz *et al.* [6] and Raik *et al.* [37]. In this case, on adding slowly excess HA to default DEAE-D or excess DEAE-D to default HA, the actual n-/n+ of the mixture would evolve from 0 to more than 1 or from +∞ to less than 1, respectively. Large aggregates could hence be formed due to complete charge neutralization as n-/n+ passed over 1, as the dropping speed was sufficiently low compared with the aggregation kinetics [37]. The large aggregates remained even at extreme final n-/n+ (0.1 and 10), meaning that such aggregation was apparently irreversible. In case of one-shot addition, such effect was hindered since the n-/n+ changed so rapidly that the aggregation did not have enough time to occur and hence the particle sizes were lower and did not show significant difference between the two orders of addition. In case of adding the default polyelectrolyte to the excess polyelectrolyte, the particle sizes were not considerably different between the two modes of mixing at whichever n-/n+, indicating the addition speed does not have great influence on PEC particle size in such cases.

3.2. Stability of PECs

3.2.1. Effect of charge ratio and storage temperature

In order to investigate the stability of HA/DEAE-D PECs, particle size of HA_M/DEAE-D PECs in Milli-Q water at C_P = 0.5 $g.L^{-1}$ and n-/n+ = 0.1-10 were revaluated after 1, 3, 7 and 30 days of conservation at 25 °C or 4 °C. PECs at n-/n+ = 1 were not studied due the macroscopic phase separation from the beginning. For the other PECs, stability monitoring was ceased when the samples started to show highly heterogeneous particle size distribution. As can be seen from the obtained results (**Figure 9**), PECs of low n-/n+ ratios (n-/n+ = 0.1-0.2) showed increasing particle size with larger and heterogeneous particle size distribution after one day regardless of storage temperature. PECs at n-/n+ = 0.4 showed a quite similar tendency but to a lesser extent, whereas PECs at n-/n+ ≥ 0.8 had mean particle size and PDI minorly changed after one month.

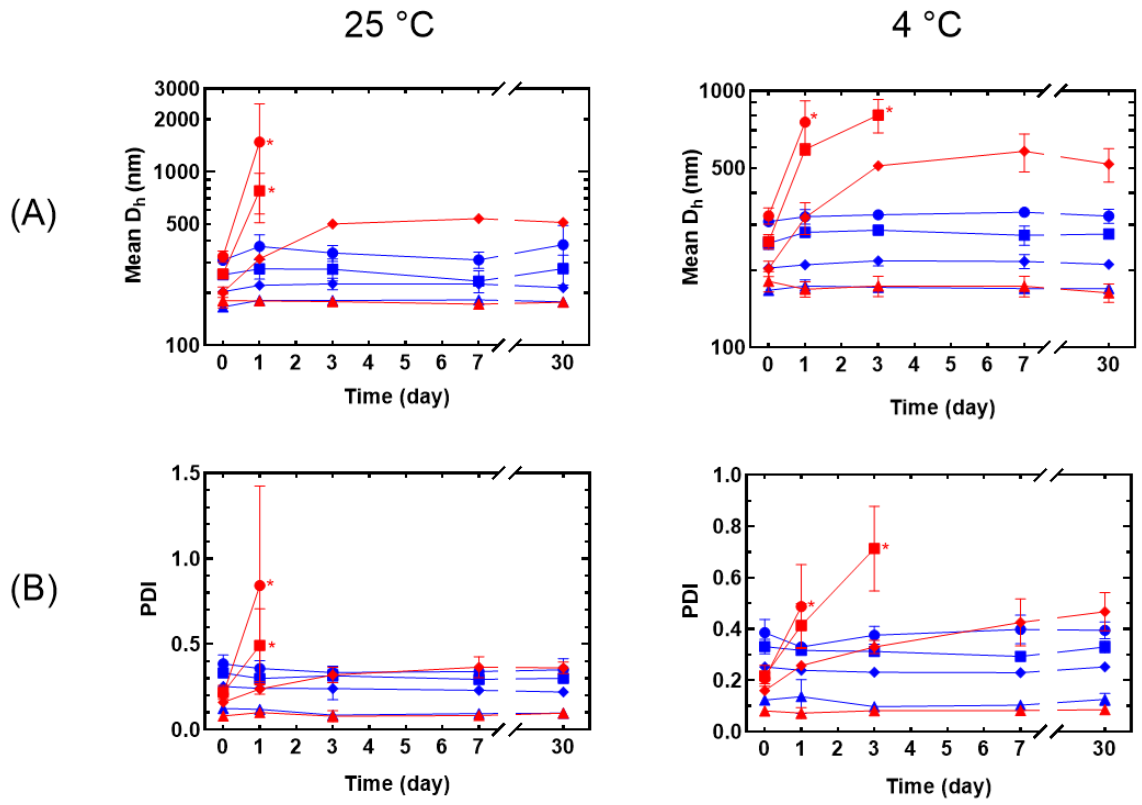

Figure 9. (**A**) Mean hydrodynamic diameter and (**B**) polydispersity index of HA_M/DEAE-D PECs (C_P = 0.5 g.L^{-1}) in Milli-Q water at different n-/n+ ratios: 0.1 (●), 0.2 (■), 0.4 (◆), 0.8 (▲), 1.25 (▲), 2.5 (◆), 5 (■), 10 (●) stored at 25 °C and 4 °C as a function of storage time. Asterisks denote samples having highly heterogeneous multimodal particle size distributions with poor repeatability. Error bars represent mean ± standard deviation (n ≥ 3).

The very high D_h and PDI of PECs at low n-/n+ after one day should not be taken as their precise characteristics because DLS measurements are less reliable when D_h approaches 1000 nm and beyond. However, such results evidenced that HA_M/DEAE-D PECs were totally instable at such low n-/n+ and storage temperature did not have significant effect on their stability. The observed lack of stability can be once again explained by the weaker hydrophobic interactions of neutral complexed blocks in primary PECs due to their lower length. To compensate this effect,

the final PECs should involve more primary PECs and optimize their conformation over time to reach their equilibrium state, which could be even practically unreachable after one day. Such aggregation was also confirmed by the decrease in particle concentration after one day as shown in **Figure 10**A.

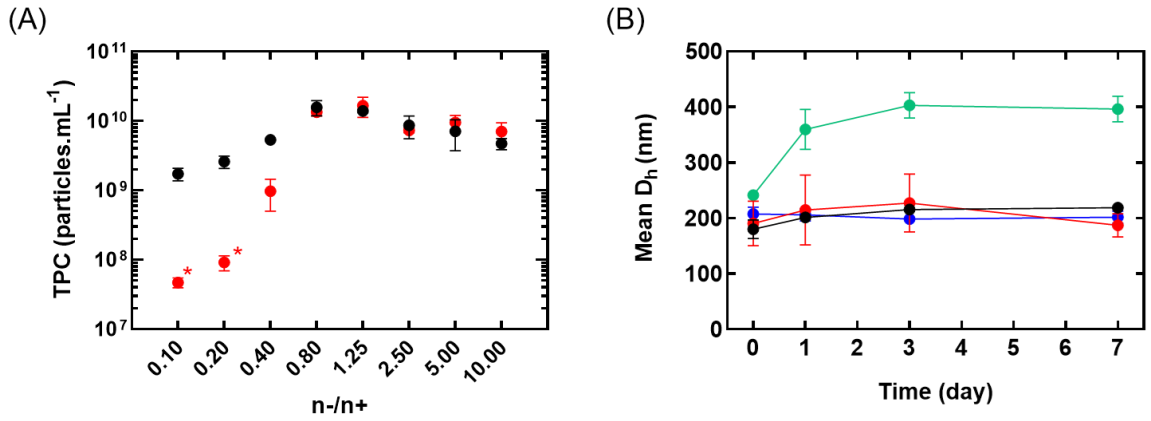

Figure 10. (**A**) Total particle concentration of HA_M/DEAE-D PECs (C_P = 0.5 g.L^{-1}) in Milli-Q water at different n-/n+ ratios after 30 min of complexation (●) and one day after storage at 4 °C (●). Asterisks denote samples having multimodal and heterogeneous particle size distribution. Otherwise size distributions are adequately homogeneous and unimodal. (**B**) Mean hydrodynamic diameter of HA_M/DEAE-D PECs at C_P = 0.5 g.L^{-1} and: n-/n+ = 0.1 – [NaCl] = 0.1 mol.L^{-1} (●), n-/n+ = 0.2 – [NaCl] = 0.01 mol.L^{-1} (●), n-/n+ = 0.4 – [NaCl] = 0.01 mol.L^{-1} (●); and C_P = 0.3 g.L^{-1}, n-/n+ = 0.1 in Milli-Q water (●) stored at 4 °C as a function of storage time. Error bars represent mean ± standard deviation (n ≥ 3).

3.2.2. Effect of ionic strength and total polymer concentration

In order to evaluate the effect of ionic strength on the stability of HA_M/DEAE-D PECs at low n-/n+, the stability studies were also done for samples of such PECs at C_P = 0.5 g.L^{-1} in the presence of salt that have homogeneous particle size and initial mean D_h < 400 nm, namely

samples having n-/n+ = 0.1 in NaCl 0.1 mol.L^{-1} and n-/n+ = 0.2-0.4 in NaCl 0.01 mol.L^{-1}. As shown in **Figure 10**B, the stability of HA_M/DEAE-D PECs at C_P = 0.5 g.L^{-1} was obviously improved in NaCl 0.01-0.1 mol.L^{-1}. Particularly, the particle size of PECs at n-/n+ = 0.1 in NaCl 0.1 mol.L^{-1} increased during the first three days but the range of increase was less considerable than the previous results obtained in the absence of salt and the particle size distribution was always homogeneous. For PECs at n-/n+ of 0.2 and 0.4 in NaCl 0.01 mol.L^{-1}, the particle sizes were relatively stable after 7 days. This improvement of stability could be attributed to the stabilizing effect of salt at intermediate concentration as described in **Section 3.1.4**. In order to assess the importance of C_P in PEC stability, HA_M/DEAE-D at a lower C_P (C_P = 0.3 g.L^{-1}) at n-/n+ = 0.1 in Milli-Q water were also studied. As shown in **Figure 10**B, the particle size of this sample seemed not to significantly change after 7 days of storage, indicating a higher physicochemical stability at lower C_P. The mechanism of this phenomenon, however, remains unclear. The only possible explanation should be the presence of fewer complexes leading to less intercomplex interactions and hence lower aggregation rate.

3.3. Pyrene fluorescence

In this work, the fluorescence of pyrene incorporated in HA_M/DEAE-D PECs was characterized in order to evaluate the relative hydrophobicity of these PECs since pyrene has its fluorescence spectra changed according to microenvironmental polarity: the presence of more hydrophobic or less hydrophilic nanodomains normally lead to a lower I_I/I_{III} ratio in its emission spectra and a higher I_{335}/I_{338} in its excitation spectra [29-32]. As presented in **Figure 11**A, pyrene in HA_M/DEAE-D samples at n-/n+ closer to the unity had lower I_I/I_{III} in the emission spectra and higher I_{335}/I_{338} in the excitation spectra, compared with reference values in Milli-Q water without PECs (I_I/I_{III} = 1.894 ± 0.017 and I_{335}/I_{338} = 0.370 ± 0.012).

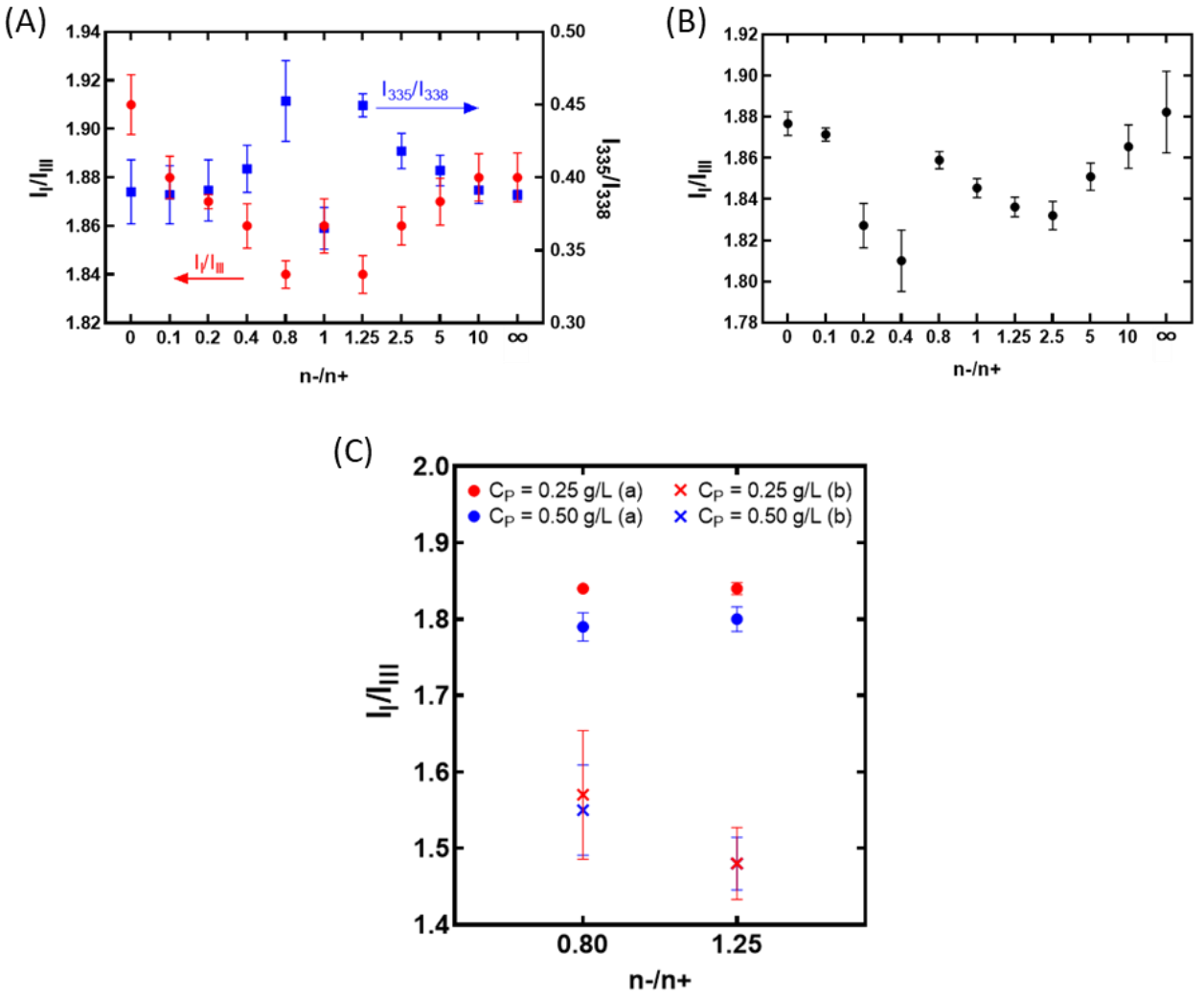

Figure 11. (**A**) I_I/I_{III} of the fluorescence emission spectra at λ_{ex} = 335 nm and I_{335}/I_{338} of the fluorescence excitation spectra at λ_{em} = 373 nm of HA_M/DEAE-D/Py in Milli-Q water at C_P = 0.25 g.L^{-1} and $C_{Py} = 4\times10^{-7}$ mol.L^{-1} prepared with method (a) at different n-/n+. (**B**) I_I/I_{III} of the fluorescence emission spectra at λ_{ex} = 335 nm of HA_M/PEI/Py in Milli-Q water at C_P = 0.25 g.L^{-1} and $C_{Py} = 4\times10^{-7}$ mol.L^{-1} prepared with method (a) at different n-/n+. The values 0 and ∞ of n-/n+ correspond respectively to the aqueous solutions of DEAE-D and HA_M containing pyrene. (**C**) I_I/I_{III} of the fluorescence emission spectra at λ_{ex} = 335 nm of HA_M/DEAE-D/Py in Milli-Q water at n-/n+ = 0.8 and 1.25, $C_{Py} = 4\times10^{-7}$ mol.L^{-1}, C_P = 0.25 and 0.5 g.L^{-1}, prepared with methods (a) or (b). Error bars represent mean ± standard deviation (n ≥ 3).

The exceptional values at n-/n+ = 1 were certainly caused by the precipitation which separated PECs from the bulk phase. These results suggest the formation of slightly less hydrophilic or more hydrophobic nanodomains in PECs following charge neutralization. However, the formation of such hydrophobic nanodomains might also be attributed to hydrophobic interactions of some DEAE groups possibly remaining deprotonated [34]. To verify this, the pyrene fluorescence characterization was also performed for PECs with the same C_P and C_{Py} from HA_M and PEI, a highly hydrophilic polycation without DEAE groups. For this experiment, the pH values of the reacting solutions were adjusted to 2.9 with HCl or NaOH 0.1-1 $mol.L^{-1}$ before their complexation because (i) the pH of freshly prepared PEI hydrochloride solution was readily around 2.9 and (ii) this pH could ensure the complete protonation of PEI, otherwise at any higher pH its ionization rate could not be straightforward estimated as for HA [46]. For n-/n+ calculation, the α values of HA and PEI at pH = 2.9 were 0.5 and 1 respectively and M_o of PEI was 43 $g.mol^{-1}$. As can be seen from **Figure 11**B, HA_M/PEI PECs also showed decreasing I_I/I_{III} when n-/n+ approached 1. During this experiment, precipitation was remarked in samples at n-/n+ from 0.8 to 1.25, which explained the unusually high I_I/I_{III} values at these charge ratios. These results confirmed the formation of hydrophobic core in PEC particles due to charge neutralization irrespective of polyelectrolyte chemical structure and that the DEAE groups did not significantly contribute to the hydrophobicity of HA/DEAE-D PECs.

To further investigate the importance of C_P and pyrene incorporation order, we also prepared HA_M/DEAE-D PECs (n-/n+ = 0.8 and 1.25) containing pyrene by alternating C_P (0.25 and 0.5 $g.L^{-1}$) and preparation methods: method (a) consisted in incorporating pyrene into PECs after their formation, while in method (b) pyrene was present during the complexation. As can be seen from **Figure 11**C, changing from method (a) to method (b) led to a considerable decrease in

I_I/I_{III} of pyrene fluorescence. Such results with method (b) could be attributed to the entrapment of pyrene in PECs during the complexation which resulted in a more effective incorporation of pyrene, while in method (a) the entrance of pyrene molecules into the PEC cores was disfavoured by the hydrophilic shells of PECs. Meanwhile, the increase from 0.25 to 0.5 $g.L^{-1}$ in C_P led to a slight decrease in I_I/I_{III} for method (a) and almost no difference in I_I/I_{III} for method (b), probably because the presence of numerous and large PEC particles at higher C_P allowed a more efficient incorporation of pyrene to PECs in method (a) while the entrapment of readily present pyrene in PECs in the case of method (b) did not depend on this effect. In case of elaboration of PECs as a means for drug delivery, such results with pyrene as a model molecule could contribute to the optimization of encapsulation method for hydrophobic active ingredients.

4. Conclusion

In this work, the influences of charge ratio, total polymer concentration, polymer molar mass, ionic strength, mixing order and mixing mode on the formation of HA/DEAE-D PECs were investigated. When the n-/n+ approached the unity, PECs had more compact and relatively more hydrophobic structure with lower particle size, while phase separation occurred following stoichiometric mixing due to optimum charge neutralization. Higher polymer concentrations generally led to larger PEC particles. The employment of HA having higher molar mass also resulted in higher particle sizes. Unlike these factors, the influence of ionic strength was non-monotonic as a compromise between limiting effect and enhancement effect on PEC formation, due to charge screening at macromolecular level and particle level respectively. The effects of mixing order and mixing mode were interdependent and depended also on n-/n+, with larger PECs being formed in case of adding dropwise the polyelectrolyte in excess to the other. Furthermore, the physicochemical stability of HA/DEAE-D PECs during storage was proved to

be strongly dependent on n-/n+ and can be improved by increasing ionic strength or decreasing polymer concentration. The pyrene fluorescence studies also confirmed the relatively hydrophobic core in PECs resulting from charge neutralization. The addition of pyrene prior to polyelectrolyte complexation also led to a more efficacious incorporation of pyrene in PECs. In the context of drug delivery, such results suggested a promising conception for efficient encapsulation and delivery of hydrophobic active molecules. To that end, further studies are also ongoing based on HA/DEAE-D as a low-cost model system to understand and optimize PEC systems for therapeutic applications.

Acknowledgments

We thank the Normandy region and the European Union for their financial support.

Appendix: Macromolecular characterization

Average molar masses, molar mass distributions and average gyration radii of hyaluronic acids (HAs) and diethylaminoethyl dextran (DEAE-D) were determined at 25 °C by size exclusion chromatography (SEC) coupled online with three detectors: multiangle light scattering (MALS) apparatus DAWN Heleos-II (Wyatt Technology, USA), differential refractive index (DRI) detector RID-10A (Shimadzu, Japan) and a viscometer detector ViscoStar II (Wyatt Technology, USA). The MALS detector was equipped with a Ga-As laser (λ = 690 nm), a K5 cell of 50 µL and 18 photodiodes (relatively normalized to the 90° detector using bovine serum albumin). The SEC line consisted of a degasser DGU-20A3 (Shimadzu, Japan), a pump LC10Ai (Shimadzu, Japan) for a flow rate of 0.5 $mL.min^{-1}$ and an automatic injector SIL-20A (Shimadzu, Japan) followed by analytical size-exclusion columns: OHpak SB 804 and 806 HQ columns (Shodex Showa Denko K.K., Japan) for HA or CATSEC 100 and 1000 columns (Eprogen, USA) for DEAE-D. The eluents for HA and DEAE-D were $LiNO_3$ 0.1 $mol.L^{-1}$ and acetate buffer 0.1 $mol.L^{-1}$ (pH = 5) respectively. The injected sample volume for each analysis was 100 µL. The samples for analysis were solutions of HAs of medium and high molar masses and DEAE-D at concentrations of 1 $g.L^{-1}$, 0.1 $g.L^{-1}$ and 0.5 $g.L^{-1}$ respectively, prepared in the corresponding eluents by stirring overnight at 200 rpm at room temperature and filtered through a 0.45 µm filter units (Sartorius, Germany). The results (**Figure A1**) were treated using Astra 6.1.7.16 ® software package via a data processing Zimm order 1 [47]. The refractive index increment (dn/dC) of 0.15 mL/g was applied for both HA and DEAE-D [28, 48]. For DEAE-D, molar mass distribution was fitted using 1^{st} order exponential model.

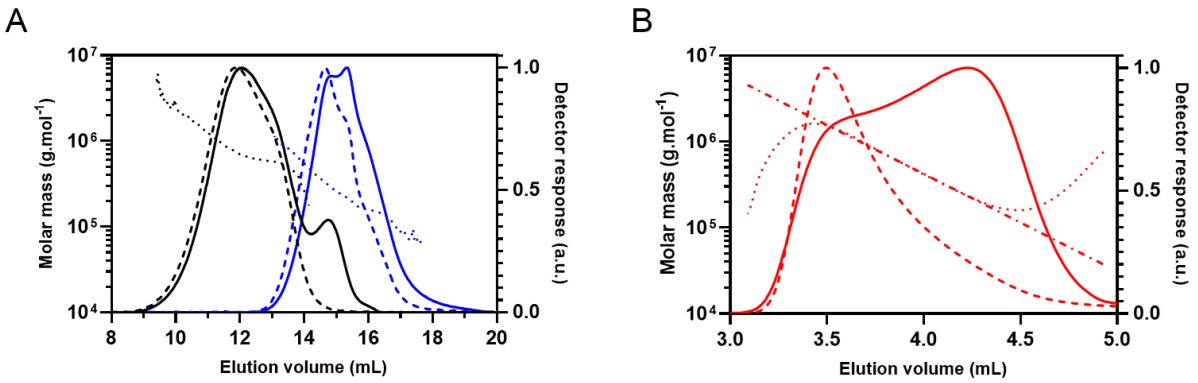

Figure A1. Elution profiles at 25 °C of (A) hyaluronic acids having medium (blue) and high (black) molar masses in $LiNO_3$ 0.1 $mol.L^{-1}$ and (B) DEAE-D in acetate buffer 0.1 $mol.L^{-1}$ at pH = 5. The full lines and dashed lines represent the responses of DRI and 90° light scattering detectors respectively. The dashdotted and dotted lines represent the molar mass distributions with and without 1^{st} order exponential fitting respectively.

References

[1] C.B. Bucur, Z. Sui, J.B. Schlenoff, Ideal mixing in polyelectrolyte complexes and multilayers: Entropy driven assembly, J. Am. Chem. Soc., 128 (2006) 13690-13691. https://doi.org/10.1021/ja064532c.

[2] B. Philipp, H. Dautzenberg, K.-J. Linow, J. Kötz, W. Dawydoff, Polyelectrolyte complexes - recent developments and open problems, Prog. Polym. Sci., 14 (1989) 91-172. https://doi.org/10.1016/0079-6700(89)90018-X.

[3] S.L. Perry, L. Leon, K.Q. Hoffmann, M.J. Kade, D. Priftis, K.A. Black, D. Wong, R.A. Klein, C.F. Pierce, K.O. Margossian, Chirality-selected phase behaviour in ionic polypeptide complexes, Nat. Commun., 6 (2015) 1-8. https://doi.org/10.1038/ncomms7052.

[4] J. Koetz, S. Kosmella, Polyelectrolytes and nanoparticles, Springer Science & Business Media, Berlin, 2007.

[5] Q. Wang, J.B. Schlenoff, The polyelectrolyte complex/coacervate continuum, Macromolecules, 47 (2014) 3108-3116. https://doi.org/10.1021/ma500500q.

[6] C. Schatz, A. Domard, C. Viton, C. Pichot, T. Delair, Versatile and efficient formation of colloids of biopolymer-based polyelectrolyte complexes, Biomacromolecules, 5 (2004) 1882-1892. https://doi.org/10.1021/bm049786.

[7] H. Fukuda, Y. Kikuchi, Polyelectrolyte complexes of sodium dextran sulfate with chitosan, 2, Makromol. Chem., 178 (1977) 2895-2899. https://doi.org/10.1002/macp.1977.021781012.

[8] C. Schatz, J.-M. Lucas, C. Viton, A. Domard, C. Pichot, T. Delair, Formation and properties of positively charged colloids based on polyelectrolyte complexes of biopolymers, Langmuir, 20 (2004) 7766-7778. https://doi.org/10.1021/la049460m.

[9] A.D. Kulkarni, Y.H. Vanjari, K.H. Sancheti, H.M. Patel, V.S. Belgamwar, S.J. Surana, C.V. Pardeshi, Polyelectrolyte complexes: mechanisms, critical experimental aspects, and applications, Artif. Cells, Nanomed., Biotechnol., 44 (2016) 1615-1625. https://doi.org/10.3109/21691401.2015.1129624.

[10] A. Drogoz, L. David, C. Rochas, A. Domard, T. Delair, Polyelectrolyte complexes from polysaccharides: formation and stoichiometry monitoring, Langmuir, 23 (2007) 10950-10958. https://doi.org/10.1021/la7008545.

[11] R. Gernandt, L. Wågberg, L. Gärdlund, H. Dautzenberg, Polyelectrolyte complexes for surface modification of wood fibres: I. Preparation and characterisation of complexes for dry and wet strength improvement of paper, Colloids Surf., A, 213 (2003) 15-25. https://doi.org/10.1016/S0927-7757(02)00335-7.

[12] C. Tan, G.B. Celli, M.J. Selig, A. Abbaspourrad, Catechin modulates the copigmentation and encapsulation of anthocyanins in polyelectrolyte complexes (PECs) for natural colorant stabilization, Food Chem., 264 (2018) 342-349. https://doi.org/10.1016/j.foodchem.2018.05.018.

[13] M. Ishihara, S. Kishimoto, S. Nakamura, Y. Sato, H. Hattori, Polyelectrolyte complexes of natural polymers and their biomedical applications, Polymers, 11 (2019) 672. https://doi.org/10.3390/polym11040672.

[14] J.M. Horn, R.A. Kapelner, A.C. Obermeyer, Macro-and microphase separated protein-polyelectrolyte complexes: Design parameters and current progress, Polymers, 11 (2019) 578. https://doi.org/10.3390/polym11040578.

[15] Y. Luo, Q. Wang, Recent development of chitosan-based polyelectrolyte complexes with natural polysaccharides for drug delivery, Int. J. Biol. Macromol., 64 (2014) 353-367. https://doi.org/10.1016/j.ijbiomac.2013.12.017.

[16] J. Necas, L. Bartosikova, P. Brauner, J. Kolar, Hyaluronic acid (hyaluronan): a review, Vet. Med. (Prague, Czech Repub.), 53 (2008) 397-411. https://doi.org/10.17221/1930-VETMED.

[17] G. Mattheolabakis, L. Milane, A. Singh, M.M. Amiji, Hyaluronic acid targeting of CD44 for cancer therapy: from receptor biology to nanomedicine, J. Drug Targeting, 23 (2015) 605-618. https://doi.org/10.3109/1061186X.2015.1052072.

[18] B. Luppi, F. Bigucci, L. Mercolini, A. Musenga, M. Sorrenti, L. Catenacci, V. Zecchi, Novel mucoadhesive nasal inserts based on chitosan/hyaluronate polyelectrolyte complexes for peptide and protein delivery, J. Pharm. Pharmacol., 61 (2009) 151-157. https://doi.org/10.1211/jpp.61.02.0003.

[19] F. Vecchies, P. Sacco, E. Decleva, R. Menegazzi, D. Porrelli, I. Donati, G. Turco, S. Paoletti, E. Marsich, Complex coacervates between a lactose-modified chitosan and hyaluronic acid as radical-scavenging drug carriers, Biomacromolecules, 19 (2018) 3936-3944. https://doi.org/10.1021/acs.biomac.8b00863.

[20] L. Yang, S. Gao, S. Asghar, G. Liu, J. Song, X. Wang, Q. Ping, C. Zhang, Y. Xiao, Hyaluronic acid/chitosan nanoparticles for delivery of curcuminoid and its in vitro

evaluation in glioma cells, Int. J. Biol. Macromol., 72 (2015) 1391-1401. https://doi.org/10.1016/j.ijbiomac.2014.10.039.

[21] A. Manosroi, J. Manosroi, Micro encapsulation of human insulin DEAE-dextran complex and the complex in liposomes by the emulsion non-solvent addition method, J. Microencapsulation, 14 (1997) 761-768. https://doi.org/10.3109/02652049709006826.

[22] T. Gulick, Transfection using DEAE-dextran, Curr. Protoc. mol. Biol., 40 (1997) 9.2. 1-9.2. 10. https://doi.org/10.1002/0471142727.mb0902s40.

[23] M. Huguet, R. Neufeld, E. Dellacherie, Calcium-alginate beads coated with polycationic polymers: comparison of chitosan and DEAE-dextran, Process Biochem. (Oxford, U. K.), 31 (1996) 347-353. https://doi.org/10.1016/0032-9592(95)00076-3.

[24] P. Menon, T.Y. Yin, M. Misran, Preparation and characterization of liposomes coated with DEAE-Dextran, Colloids Surf., A, 481 (2015) 345-350. https://doi.org/10.1016/j.colsurfa.2015.05.036.

[25] B. Larsen, K. Olsen, Inhibitory effect of polycations on the transplantability of mouse leukaemia reversed by heparin, Eur. J. Cancer (1965-1981), 4 (1968) 157-162. https://doi.org/10.1016/0014-2964(68)90013-3.

[26] E. Thorling, B. Larsen, H. Nielsen, Inhibitory effect of DEAE-dextran on tumour growth: 3. Effect of Charge Density and Molecular Size, Acta Pathol. Microbiol. Scand., Sect. A, 79 (1971) 81-90. https://doi.org/10.1111/j.1699-0463.1971.tb03316.x.

[27] A. Kayitmazer, A. Koksal, E.K. Iyilik, Complex coacervation of hyaluronic acid and chitosan: effects of pH, ionic strength, charge density, chain length and the charge ratio, Soft Matter, 11 (2015) 8605-8612. https://doi.org/10.1039/C5SM01829C.

[28] D. Le Cerf, A.S. Pepin, P.M. Niang, M. Cristea, C. Karakasyan-Dia, L. Picton, Formation of polyelectrolyte complexes with diethylaminoethyl dextran: Charge ratio and molar mass effect, Carbohydr. Polym., 113 (2014) 217-224. https://doi.org/10.1016/j.carbpol.2014.07.015.

[29] B. Aricha, I. Fishov, Z. Cohen, N. Sikron, S. Pesakhov, I. Khozin-Goldberg, R. Dagan, N. Porat, Differences in membrane fluidity and fatty acid composition between phenotypic variants of Streptococcus pneumoniae, J. Bacteriol., 186 (2004) 4638-4644. http://doi.org/10.1128/JB.186.14.4638-4644.2004.

[30] J. Burdíková, F. Mravec, M. Pekař, The formation of mixed micelles of sugar surfactants and phospholipids and their interactions with hyaluronan, Colloid Polym. Sci., 294 (2016) 823-831. https://doi.org/10.1007/s00396-016-3840-8.

[31] H. Morikawa, Y. Morishima, S. Motokucho, H. Morinaga, H. Nishida, T. Endo, Synthesis and association behavior of cationic amphiphilic copolymers consisting of quaternary ammonium and nonionic surfactant moieties, J. Polym. Sci., Part A: Polym. Chem., 45 (2007) 5022-5030. https://doi.org/10.1002/pola.22322.

[32] T. Akagi, P. Piyapakorn, M. Akashi, Formation of unimer nanoparticles by controlling the self-association of hydrophobically modified poly(amino acid)s, Langmuir, 28 (2012) 5249-5256. https://doi.org/10.1021/la205093j.

[33] V. Kabanov, A. Zezin, A new class of complex water-soluble polyelectrolytes, Makromol. Chem., 6 (1984) 259-276. https://doi.org/10.1070/RC1982v051n09ABEH002921.

[34] Z. Souguir, S. Roudesli, E. About-Jaudet, L. Picton, D. Le Cerf, Novel cationic and amphiphilic pullulan derivatives II: pH dependant physicochemical properties, Carbohydr. Polym., 80 (2010) 123-129. https://doi.org/10.1016/j.carbpol.2009.11.003.

[35] E. Tsuchida, Formation of polyelectrolyte complexes and their structures, J. Macromol. Sci., Part A: Pure Appl.Chem., 31 (1994) 1-15. https://doi.org/10.1080/10601329409349713.

[36] M. Müller, B. Keßler, J. Fröhlich, S. Poeschla, B. Torger, Polyelectrolyte complex nanoparticles of poly(ethyleneimine) and poly(acrylic acid): preparation and applications, Polymers, 3 (2011) 762-778. https://doi.org/10.3390/polym3020762.

[37] S.V. Raik, E.R. Gasilova, N.V. Dubashynskaya, A.V. Dobrodumov, Y.A. Skorik, Diethylaminoethyl chitosan–hyaluronic acid polyelectrolyte complexes, Int. J. Biol. Macromol., 146 (2020) 1161-1168. https://doi.org/10.1016/j.ijbiomac.2019.10.054.

[38] R. Zhang, B. Shklovskii, Phase diagram of solution of oppositely charged polyelectrolytes, Phys. A (Amsterdam, Neth.), 352 (2005) 216-238. https://doi.org/10.1016/j.physa.2004.12.037.

[39] Malvern Panalytical, Understanding the colloidal stability of protein therapeutics using dynamic light scattering, 2020.

[40] S. Bhattacharjee, DLS and zeta potential–what they are and what they are not?, J. Controlled Release, 235 (2016) 337-351. https://doi.org/10.1016/j.jconrel.2016.06.017.

[41] R.B. Best, G.E. Jackson, K.J. Naidoo, Molecular dynamics and NMR study of the α (1→ 4) and α (1→ 6) glycosidic linkages: maltose and isomaltose, J. Phys. Chem. B, 105 (2001) 4742-4751. https://doi.org/10.1021/jp0040704.

[42] P.A. Williams, G.O. Phillips, Introduction to food hydrocolloids, in: G.O. Phillips, P.A. Williams (Eds.), Handbook of Hydrocolloids, Woodhead Publishing, Cambridge, 2009, pp. 1-22. https://doi.org/10.1533/9781845695873.1.

[43] L. Li, A.M. Rumyantsev, S. Srivastava, S. Meng, J.J. de Pablo, M.V. Tirrell, Effect of Solvent Quality on the Phase Behavior of Polyelectrolyte Complexes, Macromolecules, 54 (2020) 105-114. https://doi.org/10.1021/acs.macromol.0c01000.

[44] L. Li, S. Srivastava, S. Meng, J.M. Ting, M.V. Tirrell, Effects of non-electrostatic intermolecular interactions on the phase behavior of pH-sensitive polyelectrolyte complexes, Macromolecules, 53 (2020) 7835-7844. https://doi.org/10.1021/acs.macromol.0c00999.

[45] H. Dautzenberg, Polyelectrolyte complex formation in highly aggregating systems. 1. Effect of salt: polyelectrolyte complex formation in the presence of NaCl, Macromolecules, 30 (1997) 7810-7815. https://doi.org/10.1021/ma970803f.

[46] E. Hergli, A. Aschi, Polycation-globular protein complex: Ionic strength and chain length effects on the structure and properties, e-Polymers, 19 (2019) 120-128. https://doi.org/10.1515/epoly-2019-0014.

[47] B.H. Zimm, The scattering of light and the radial distribution function of high polymer solutions, J. Chem. Phys., 16 (1948) 1093-1099. https://doi.org/10.1063/1.1746738.

[48] F. Tranchepain, B. Deschrevel, M.-N. Courel, N. Levasseur, D. Le Cerf, C. Loutelier-Bourhis, J.-C. Vincent, A complete set of hyaluronan fragments obtained from hydrolysis catalyzed by hyaluronidase: Application to studies of hyaluronan mass distribution by simple HPLC devices, Anal. Biochem., 348 (2006) 232-242. https://doi.org/10.1016/j.ab.2005.09.042.

II.3. Etude complémentaire : Impact du pH sur les PECs

Comme présenté dans l'étude bibliographique, le pH peut également exercer une influence importante sur la stabilité des PECs. Dans ce contexte, nous avons voulu vérifier les impacts de ce paramètre sur les PECs de HA/DEAE-D. Pour cela, nous avons ajouté du HCl ou du NaOH à une concentration de 0,1 ou 0,01 mol.L^{-1} dans les suspensions de PECs de HA/DEAE-D de n-/n+ = 0,8 ou 1,25 préparés à C_P = 0,5 g.L^{-1} pour fait varier le pH du milieu. Le comportement des phases ainsi que la taille et le potentiel zêta des PECs ont ensuite été évalués en fonction du pH (**Figure II-1**).

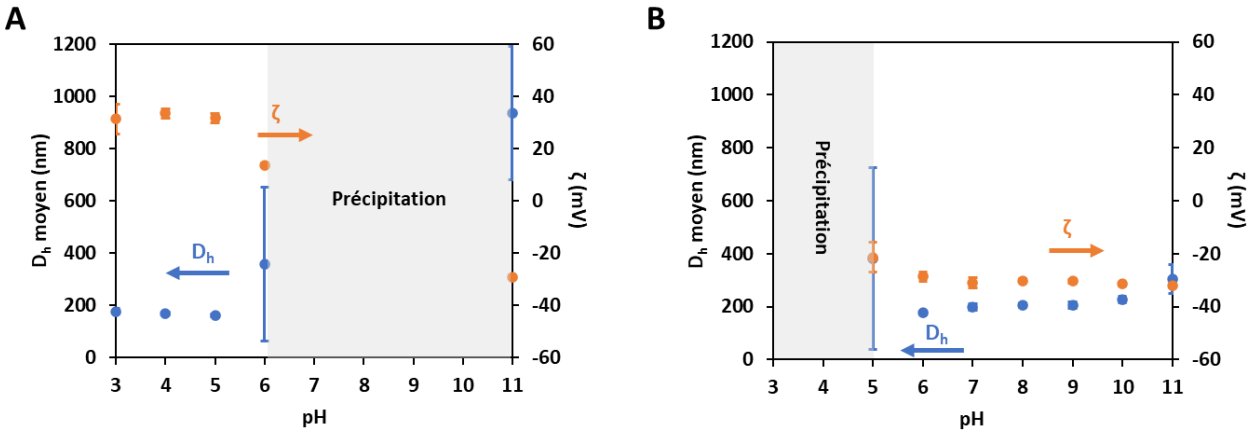

Figure II-1. D_h moyen (●) et potentiel zêta (●) en fonction de pH des PECs de HA/DEAE-D préparé à C_P = 0,5 g.L^{-1} et à n-/n+ de 0,8 (**A**) ou 1,25 (**B**) dans l'eau Milli-Q (n ≥ 3).

Dans la gamme de pH étudiée (pH = 3-11), les PECs à n-/n+ = 0,8 augmentent de taille avec une diminution de leur potentiel zêta quand le pH approche de 6 puis précipitent quand le pH se trouve entre 6 et 11 (**Figure II-1**), alors que cette séparation de phases a été observée quand le pH est inférieur à 5 pour les PECs ayant n-/n+ = 1,25. Ces comportements des phases peuvent être expliqués par le changement du taux d'ionisation des polymères et ainsi du n-/n+ apparent lors de la modification du pH. Plus précisément, dans le cas des PECs préparés à n-/n+ = 0,8 (pH initial

de 5,3 ± 0,2), l'augmentation du pH au-delà de 6 diminue le taux d'ionisation du DEAE-D alors que celui du HA reste inchangé (**Figure 2** dans **Section II.2**), conduisant alors à une augmentation du n-/n+ des PECs vers 1 qui favorise l'agrégation à cause d'un affaiblissement de la stabilisation électrostatique (diminution du potentiel zêta). Quand le pH est encore augmenté, le n-/n+ peut dépasser 1 et la stabilisation électrostatique peut se rétablir, ce qui peut faciliter une désintégration partielle des agrégats et donc la disparition des précipités comme observé à pH 11, bien que la taille des PECs reste encore importante (700-1300 nm). Il faut noter que le résultat obtenu à un pH si extrême peut être également affecté par la force ionique très élevée en raison de la quantité importante de NaOH ajoutée à ce point, qui peut soit favoriser soit empêcher la désagrégation par deux effets contradictoires de l'écrantage électrostatique au niveau macromoléculaire ou particulaire comme discuté dans la **Section II.2**. En revanche, une diminution de pH vers 3 peut conduire à un n-/n+ inférieure à 0,8 et ainsi à des PEC-NGs globalement plus chargés et donc légèrement plus gonflés comme constaté dans la **Section II.2**, alors que l'augmentation du potentiel zêta n'est pas évidente (**Figure II-1**A), probablement à cause de l'augmentation de la force ionique. Logiquement, le même mécanisme peut être appliqué pour les PECs à n-/n+ = 1,25 (pH initial de 6,1 ± 0,2), où la diminution du pH peut conduire à un potentiel zêta moins négatif et peut ainsi favoriser la précipitation, alors que la taille des PECs montre une augmentation quand le pH devient plus élevé (**Figure II-1**B). Ces résultats ont donc montré que les PECs de HA/DEAE-D sont très sensibles au pH, comme pour les autres systèmes de PECs à base de HA dans la littérature [1-3].

Références

[1] N. Nazeri, M.R. Avadi, M.A. Faramarzi, S. Safarian, G. Tavoosidana, M.R. Khoshayand, A. Amani, Effect of preparation parameters on ultra low molecular weight

chitosan/hyaluronic acid nanoparticles, International Journal of Biological Macromolecules, 62 (2013) 642-646. https://doi.org/10.1016/j.ijbiomac.2013.09.041.

[2] W. Zhong, C. Li, M. Diao, M. Yan, C. Wang, T. Zhang, Characterization of interactions between whey protein isolate and hyaluronic acid in aqueous solution: Effects of pH and mixing ratio, Colloids and Surfaces B: Biointerfaces, 203 (2021) 111758. https://doi.org/10.1016/j.colsurfb.2021.111758.

[3] R. Liu, X. Yan, Z. Liu, D.J. McClements, F. Liu, X. Liu, Fabrication and characterization of functional protein–polysaccharide–polyphenol complexes assembled from lactoferrin, hyaluronic acid and (−)-epigallocatechin gallate, Food & Function, 10 (2019) 1098-1108. https://doi.org/10.1039/c8fo02146e.

II.4. Conclusion et perspectives

Dans ce chapitre, nous avons trouvé les conditions extrinsèques et intrinsèques les plus favorables pour former des PECs colloïdaux à partir de HA et de DEAE-D, avec des tailles submicroniques dont la moyenne varie entre 150-350 nm avec un PDI entre 0,1-0,4. Des macroséparations de phases ont été constatées dans les conditions défavorables que sont (i) une MW ou une concentration importante des polymères, (ii) un ratio de n-/n+ très proche de 1, (iii) une force ionique élevée, (iv) un changement inapproprié du pH et (v) un ajout lent du polymère en excès pendant la préparation. Toutefois, dans le cadre de notre projet, il est apparu que les PECs colloïdaux obtenus dans ce chapitre peuvent également être désignés comme nanogels de PECs (PEC-NGs) mais ne sont pas encore satisfaisants pour le piégeage et la délivrance des SAs peu hydrosolubles à cause de leur faible stabilité en milieu salin physiologique (i.e. concentration en NaCl d'environ 0,15 $mol.L^{-1}$) et de leur faible hydrophobicité. Pour surmonter ces limitations, dans le chapitre suivant, nous allons reconceptualiser ces PEC-NGs avec des greffons amphiphiles à

nature thermosensible (i.e. Jeffamine® M-2005) sur le HA et le remplacement du DEAE-D par un polycation potentiellement moins hydrophile (i.e. poly-L-lysine), en gardant la méthode de préparation qui paraît la plus favorable pour obtenir des PECs colloïdaux, i.e. ajout *one-shot* du HA de MW intermédiaire ($M_W = 2,7 \times 10^5$ g.mol^{-1}) dans la solution de polycation dans l'eau Milli-Q à $C_P = 0,5$ g.L^{-1}.

Chapitre III

Préparation et caractérisation des nanogels de l'acide hyaluronique greffé Jeffamine® M-2005 en complexe avec le diéthylaminoéthyl dextrane ou la poly-L-lysine

III.1. Introduction

Ce chapitre présente les PEC-NGs préparés avec du HA greffé Jeffamine® M-2005 (HA-M2005) en complexe avec deux polycations de structures chimiques bien différentes : le DEAE-D ou la poly-L-lysine (PLL). La Jeffamine® M-2005 (M2005) est un copolymère thermosensible de type LCST à structure de poly(oxyde d'éthylène)-*co*-poly(oxyde de propylène) à terminaison amine (**Section III.2**). La méthode de synthèse du HA-M2005 a été développée dans le cadre de la thèse de Mathieu MADAU [1] et la caractérisation rhéologique a montré une gélation favorisée par interactions hydrophobes entre les greffons M2005 quand la température est augmentée [2]. La PLL, quant à elle, a été utilisée comme polycation pour la complexation avec le HA dans certains travaux [3, 4]. Elle peut avoir une hydrophobicité plus élevée à l'état neutralisé [3, 5] et peut présenter aussi des interactions biologiques favorables pour l'internalisation cellulaire des nanovéhicules [6]. Nous avons ainsi voulu exploiter ces deux polymères pour développer des PEC-NGs qui présenteraient probablement des caractéristiques intéressantes, notamment une hydrophobicité plus élevée, une meilleure résistance à la salinité et une thermosensibilité. Ces aspects ont été vérifiés à travers plusieurs caractérisations comme l'évaluation de la taille des PEC-NGs par diffusion dynamique de la lumière (DLS) et de leur hydrophobicité relative par fluorescence du pyrène incorporé dans leur structure, ainsi que leur stabilité dans des conditions variées (i.e. salinité et température). De plus, l'amélioration de l'hydrophobicité et l'apparition de la thermosensibilité ont été également évaluées avec des études d'encapsulation de la curcumine en tant que SA hydrophobe dans les PEC-NGs. La curcumine a été choisie puisqu'elle est souvent utilisée comme une SA modèle classique dans plusieurs travaux de la littérature sur la nanoencapsulation [7-9], où ses propriétés et les méthodes pour sa quantification ont été décrites. De plus, sa couleur jaune très vive facilite l'évaluation de l'aspect visuel des échantillons. Outre

la thermosensibilité, nous avons également vérifié la sensibilité des PEC-NGs à la hyaluronidase (HAase), qui est souvent surexprimée dans les tumeurs et peut probablement alors servir comme un facteur qui favorise la dégradation des PECs pour activer la libérations des SAs [10]. L'ensemble de ces travaux a été publié dans ***Carbohydrate Polymers*** *(2022), Vol. 292, p. 119711* dont le contenu est présenté ci-dessous. Seront ensuite présentés des résultats complémentaires concernant l'étalonnage de la quantification de la curcumine, l'évolution de la taille des PEC-NGs thermosensibles en fonction de température, ainsi que la libération *in vitro* de la curcumine à partir de ces PEC-NGs et la possibilité de moduler cette libération par contrôle de la température. De ce fait, nous allons montrer la sensibilité simultanée des PEC-NGs à deux stimuli (température et HAase), qui pourrait être prometteuse pour la délivrance ciblée des SAs, notamment avec le déclenchement de la libération des agents anticancéreux en appliquant une hyperthermie locale au niveau des tumeurs et en profitant de la surexpression de la HAase au sein de ces cellules.

Références

[1] M. Madau, Hydrogels adaptatifs stimuli-sensibles (temperature et lumière) à base d'acide hyaluronique (HA), Thèse de doctorat, Normandie Université (2021).

[2] M. Madau, D. Le Cerf, V. Dulong, L. Picton, Hyaluronic Acid Functionalization with Jeffamine® M2005: A Comparison of the Thermo-Responsiveness Properties of the Hydrogel Obtained through Two Different Synthesis Routes, Gels, 7 (2021) 88. https://doi.org/10.3390/gels7030088.

[3] W. Pan, D.-X. Yin, H.-R. Jing, H.-J. Chang, H. Wen, D.-H. Liang, Core-corona structure formed by hyaluronic acid and poly (L-lysine) via kinetic path, Chinese Journal of Polymer Science, 37 (2019) 36-42. https://doi.org/10.1007/s10118-018-2166-z.

[4] E. Tračuma, D. Loca, Hyaluronic Acid/Polylysine Composites for Local Drug Delivery: A Review, Key Engineering Materials, Trans Tech Publ, 2020, pp. 213-218.

[5] H.J. Dyson, P.E. Wright, H.A. Scheraga, The role of hydrophobic interactions in initiation and propagation of protein folding, Proceedings of the National Academy of Sciences, 103 (2006) 13057-13061. https://doi.org/10.1073/pnas.0605504103.

[6] W.X. Siow, Y.-T. Chang, M. Babič, Y.-C. Lu, D. Horák, Y.-H. Ma, Interaction of poly-L-lysine coating and heparan sulfate proteoglycan on magnetic nanoparticle uptake by tumor cells, International Journal of Nanomedicine, 13 (2018) 1693. https://doi.org/10.2147/IJN.S156029.

[7] L. Yang, S. Gao, S. Asghar, G. Liu, J. Song, X. Wang, Q. Ping, C. Zhang, Y. Xiao, Hyaluronic acid/chitosan nanoparticles for delivery of curcuminoid and its in vitro evaluation in glioma cells, International Journal of Biological Macromolecules, 72 (2015) 1391-1401. https://doi.org/10.1016/j.ijbiomac.2014.10.039.

[8] P. Sarika, N.R. James, Polyelectrolyte complex nanoparticles from cationised gelatin and sodium alginate for curcumin delivery, Carbohydrate Polymers, 148 (2016) 354-361. https://doi.org/10.1016/j.carbpol.2016.04.073.

[9] Y. Xu, S. Asghar, L. Yang, Z. Chen, H. Li, W. Shi, Y. Li, Q. Shi, Q. Ping, Y. Xiao, Nanoparticles based on chitosan hydrochloride/hyaluronic acid/PEG containing curcumin: In vitro evaluation and pharmacokinetics in rats, International Journal of Biological Macromolecules, 102 (2017) 1083-1091. https://doi.org/10.1016/j.ijbiomac.2017.04.105.

[10] W. Li, X. Zhang, Y. Nan, L. Jia, J. Sun, L. Zhang, Y. Wang, Hyaluronidase and pH Dual-Responsive Nanoparticles for Targeted Breast Cancer Stem Cells, Frontiers in Oncology, 11 (2021). https://doi.org/10.3389/fonc.2021.760423.

III.2. Publication : Thermoresponsive nanogels based on polyelectrolyte complexes between polycations and functionalized hyaluronic acid

Le, H. V., Dulong, V., Picton, L., & Le Cerf, D. (2022). Carbohydrate Polymers, Volume 292, 119711.

Thermoresponsive nanogels based on polyelectrolyte complexes between polycations and functionalized hyaluronic acid

Huu Van LE, Virginie DULONG, Luc PICTON, Didier LE CERF *

Normandie Univ, UNIROUEN, INSA Rouen, CNRS, PBS UMR 6270, 76000 Rouen, France

*Corresponding author: E-mail address: didier.lecerf@univ-rouen.fr

Tel: 00 33 02 35 14 65 43; Fax: 00 33 02 35 14 67 04

Abstract: A novel kind of thermoresponsive polyelectrolyte complex-based nanogels (PEC-NGs) was elaborated by mixing hyaluronic acid (HA) functionalized with Jeffamine® M-2005 (M2005, a thermoresponsive amine-terminated polyether) and diethylaminoethyl dextran (DEAE-D) or poly-L-lysine (PLL) in water. The presence of M2005 grafts led to PEC-NGs with larger particle size, lower net surface charge and thermoresponsiveness, namely shrinkage with increasing hydrophobicity at higher temperature. Both M2005 grafts and replacing DEAE-D with PLL as polycation allowed PEC-NGs to have higher stability against salinity and better encapsulation of curcumin, most probably through intraparticle hydrophobic interactions, whereas interparticle hydrophobic interactions may facilitate particle aggregation over time. Curcumin encapsulation can be optimized by applying higher temperature during the complexation. Enzymatic degradability of PEC-NGs was also verified through particle size evolution in the presence of hyaluronidase. These results provide new insights into the physicochemical aspect of such systems as promising nanocarriers for drug delivery.

Keywords: nanogels; polyelectrolyte complexes; thermoresponsive; hyaluronic acid; Jeffamine® M-2005

Graphical abstract:

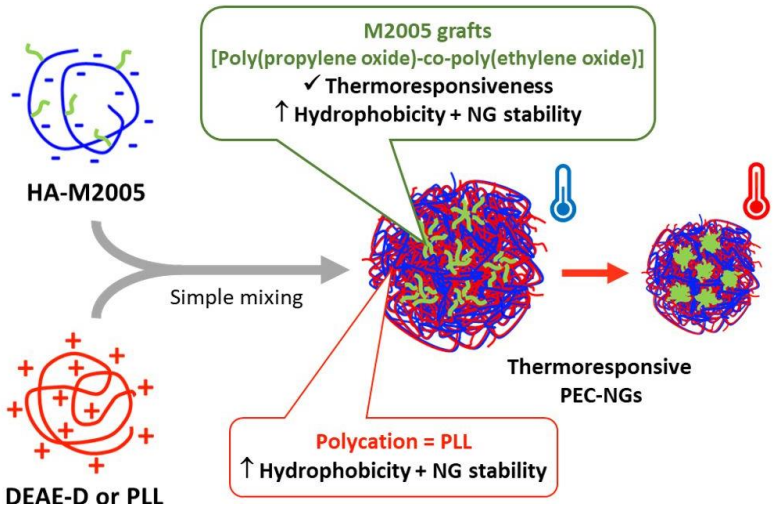

1. Introduction

Nanogels (NGs) based on polyelectrolyte complexes (PECs) can be formed spontaneously through ion pairing between polyanions and polycations upon simple mixing in aqueous media (Bonaccorso et al., 2021). Particularly, PEC-based NGs (PEC-NGs) from polysaccharides have attracted a great deal of interest as drug delivery systems (DDS) due to their biocompatibility and simple preparation requiring neither high energy nor organic solvents (Debele, Mekuria, & Tsai, 2016).

Thermoresponsive nanocarriers have received increasing attention as robust DDS (Bordat, Boissenot, Nicolas, & Tsapis, 2019). They can be elaborated from thermoresponsive copolymers, which display a temperature-dependent hydrophilic-hydrophobic balance due to the difference in solvation status between component monomers at different temperatures (Bordat et al., 2019; Gandhi, Paul, Sen, & Sen, 2015). Among them, polymers disposing lower critical solution temperature (LCST), which are water-soluble below a critical temperature but become insoluble at a higher temperature due to higher hydrophobicity, have been extensively studied and employed in DDS (Karimi et al., 2016). Nanoparticles from these polymers can show shrinkage along with higher hydrophobicity at higher temperature, leading to applications in either triggered-release or sustained-release of drugs (Karimi et al., 2016; Kim et al., 2019). Accordingly, employing thermoresponsive derivatives of polysaccharides (i.e. polysaccharides grafted with suitable LCST groups) in DDS has also become an emerging topic of research since they can improve the encapsulation and release of hydrophobic drugs while conserving the advantages of precursor biopolymers (Graham, Marina, & Blencowe, 2019).

From such perspectives, systems combining both the abovementioned aspects, i.e. PEC-NGs from thermoresponsive polysaccharide derivatives, would be of high interest as DDS,

yet have not been reported in the literature to the best of our knowledge. In this context, our work aimed to elaborate and characterize such a novel kind of DDS from readily available materials, namely HA-M2005 which is hyaluronic acid (HA) functionalized with Jeffamine® M-2005 (M2005) and diethylaminoethyl dextran (DEAE-D) or poly-L-lysine (PLL) (**Figure 1**).

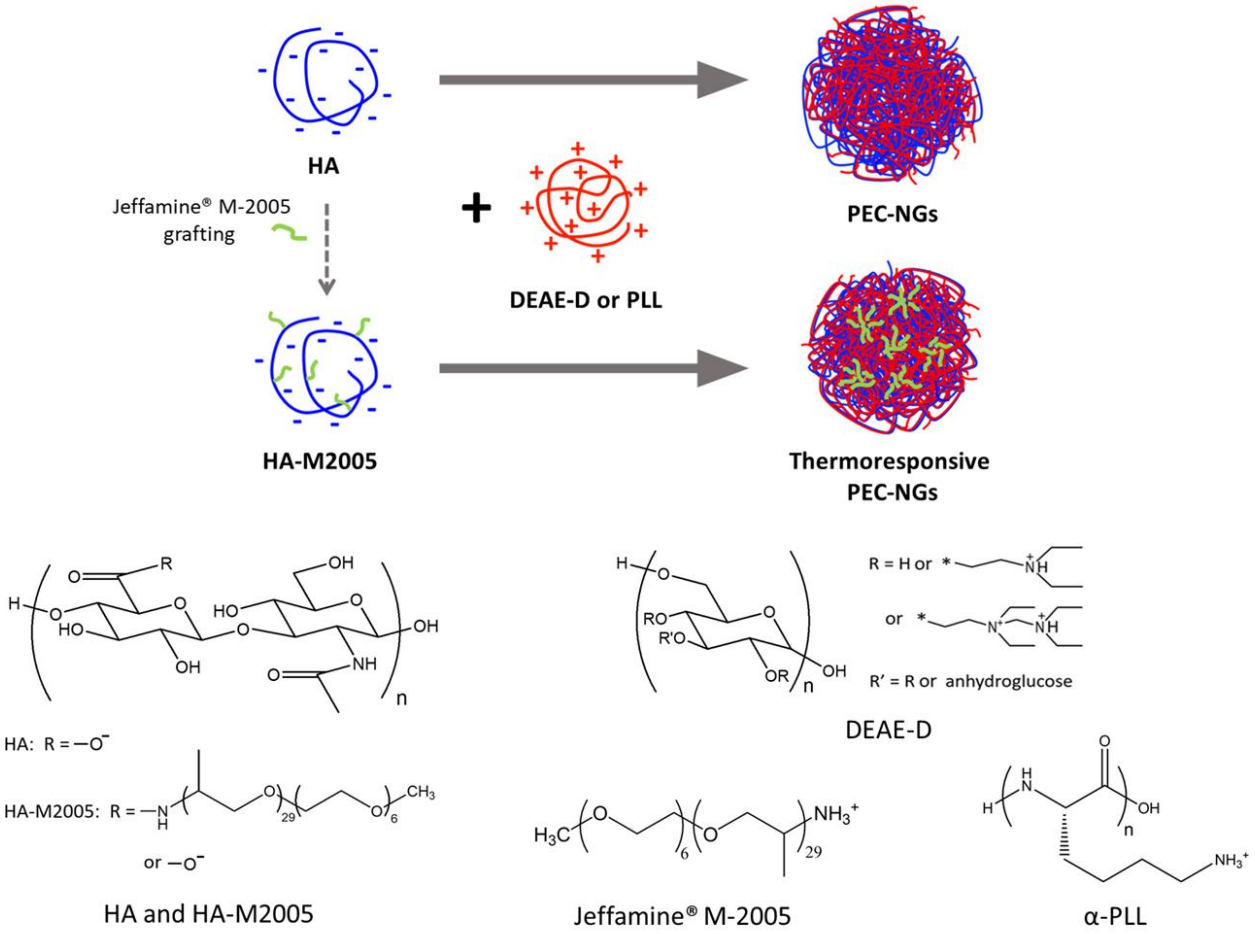

Figure 1. Scheme of PEC-NG formation from polyanions (blue) (HA: hyaluronic acid or HA-M2005: hyaluronic acid functionalized with Jeffamine® M-2005 (green)) electrostatically complexed with polycations (red) (DEAE-D: diethylaminoethyl dextran or PLL: poly-L-lysine) and their chemical structures.

HA is an anionic polysaccharide extensively employed in DDS development due to its excellent biocompatibility and biodegradability (Necas, Bartosikova, Brauner, & Kolar, 2008). CD44 receptors, which are natural receptors of HA, and hyaluronidase (HAase), which is a family of enzymes catalyzing HA degradation, are both overexpressed in many cancer cells, e.g. in breast and brain tumors (Stern, 2008; Xu, Niu, Yuan, Wu, & Liu, 2020). This renders HA-based nano-DDS particularly interesting for drug targeting since they can be specifically uptaken and degraded to release drugs inside these cells (Yang, Zhang, Chen, Chen, & Liu, 2016). M2005 is a commercial diblock copolyether monoamine made up of amine-terminated poly(propylene oxide) (PPO) and poly(ethylene oxide) (PEO), constituting a thermoresponsive copolymer with LCST temperature of 14-30 °C (Agut, Brûlet, Taton, & Lecommandoux, 2007; Dulong, Mocanu, Picton, & Le Cerf, 2012; Niang et al., 2016). In our previous work, M2005 was successfully grafted on HA to obtain HA-M2005 as a thermoresponsive HA derivative with a sol-gel transition depending on temperature (Madau, Le Cerf, Dulong, & Picton, 2021). DEAE-D is a polycation with cationic DEAE groups grafted on dextran, a natural polysaccharide extracted from plants or microbial fermentations (Díaz-Montes, 2021; Gulick, 1997). It is mainly used as a means for nucleic acids transfection or proteins delivery with good biocompatibility and high solubility (Gulick, 1997; Huguet, Neufeld, & Dellacherie, 1996; Manosroi & Manosroi, 1997). PLL is a biocompatible and biodegradable cationic polyaminoacid, which is largely used as a coating agent for cell adhesion promotion (Huguet et al., 1996). PLL coating can also increase cell uptake of nanoparticles, which would improve therapeutic efficacy in targeted nanomedicine (Siow et al., 2018).

Previously, our work has shown that mixing of HA and DEAE-D solutions can lead to the formation of HA/DEAE-D PEC-NGs having mean size of 150-350 nm with relatively hydrophobic cores surrounded by hydrophilic corona shells from polar uncomplexed

polyelectrolyte segments (Le, Dulong, Picton, & Le Cerf, 2021). They can have good shelf stability in water but generally poor stability against salt and slight hydrophobicity (Le et al., 2021). Our hypothesis is that PEC-NGs prepared with HA-M2005 should present more interesting properties, such as dual-responsiveness (thermoresponsiveness beside enzymatic-induced degradation), than with non-modified HA. In this work, the effects of M2005 grafts and polycation structure on HA-based PEC-NGs were elucidated after their preparation and characterization in terms of morphology, particle size, zeta potential (ζ) and hydrophobicity with varying parameters, including constituent polymers (**Figure 1**), temperature, salinity and storage time. Encapsulation of curcumin as a model drug was realized to evaluate the potential of these systems as nanocarriers for delivering poorly water-soluble drugs. Enzymatic degradation of such PEC-NGs was also investigated and confirmed by observing particle size in the presence of HAase.

2. Materials and methods

2.1. Materials

HA and Jeffamine® M-2005 were kindly provided by Givaudan (France) and Huntsman (USA) respectively. DEAE-D hydrochloride and α-PLL hydrobromide were purchased from Sigma-Aldrich (USA). HA-M2005 was obtained by grafting Jeffamine® M-2005 to HA (degree of substitution of 3.6 %) through EDC/NHS coupling reaction (Supplementary Information **SI-1**) as reported in our earlier study (Madau et al., 2021). **Table 1** summarizes macromolecular characteristics of the polyelectrolytes (Supplementary Information **SI-2**), with those of HA and DEAE-D retrieved from our previous work (Le et al., 2021). Pyrene was purchased from Acros Organics (USA). Curcumin, phosphate-buffered saline (PBS) tablets and HAase from sheep testes (400 $IU.mg^{-1}$) were purchased from Sigma-Aldrich (USA). Water purified by Milli-Q system (Millipore, USA) was used for all experiments.

Table 1. Characteristics of polyelectrolytes

Polyelectrolyte	M_n (g.mol^{-1})	M_w (g.mol^{-1})	Đ
HA	210,000	270,000	1.3
DEAE-D	270,000	700,000	2.6
PLL	200,000	490,000	2.5
HA-M2005	180,000	240,000	1.3

M_n: number average molecular weight; M_w: weight average molecular weight; Đ: dispersity

2.2. Preparation of PEC-NGs

PEC-NGs were prepared following the same method as our previous work (Le et al., 2021). Polyelectrolyte solutions at defined total polymer concentrations (C_p, excluding counterions) were prepared beforehand by dissolving polyelectrolytes in Milli-Q water under stirring overnight at room temperature and afterwards filtered through regenerated cellulose 0.45 μm membrane filter units (Sartorius, Germany). Each PEC-NG suspension at a definite C_P and n-/n+ (molar ratio of negative to positive charges on component polyelectrolytes) was obtained by one-shot addition of polyanion to polycation solutions of the same C_P with the volume ratio deduced from n-/n+ (Supplementary Information **SI-3**), followed by 30 min of stirring at room temperature. At least three batches were prepared for each formulation.

For preparing curcumin-loaded NGs, before polycation addition, there was an additional step of dropping an amount of curcumin 5 g.L^{-1} stock solution in acetone to the polyanion solution. The ratio of curcumin to polyelectrolytes was fixed at 2/5 m/m. After 30 min of stirring at studied temperatures (25 °C, 50 °C or 70 °C), all samples were left at room temperature over 12 h for acetone evaporation. The precipitated non-encapsulated curcumin was then removed by centrifugation at 3,000×g for 15 min and the supernatant was filtered through polyvinylidene difluoride (PVDF) 0.45 μm membrane filter units (Millipore, Germany) to obtain the filtrate as

PEC-NG suspensions. Samples without polymers were also prepared as reference. All samples were protected from light to avoid curcumin degradation.

2.3. Particle size, zeta potential and morphology analyses

Particle size and zeta potential (ζ) were characterized only for visually homogeneous NG suspensions without further dilution using Zetasizer Ultra (Malvern Panalytical, UK). Mean hydrodynamic diameter (D_h) and polydispersity index (PDI) were determined by dynamic light scattering (DLS) with back-scatter mode. ζ was measured by electrophoretic light scattering. Every sample was measured at least in triplicate after stabilization for 120 s at 25 °C or 300 s at 37 °C or 50 °C.

The morphologies of PEC-NGs were examined using a transmission electron microscope (TEM) FEI Tecnai 12 BioTwin (Philips, The Netherlands) operating at 80 kV. For specimen preparation, 10 µL of a PEC-NG suspension was placed on a formvar and carbon coated copper grid for 15 min for adhesion of PEC-NGs on the grid and the excess suspension was then removed by filter paper. 10 µL of phosphotungstic acid 1 % solution was thereafter deposited on the grid for contrast enhancement and wicked away after 30 s, followed by air-drying of the grid before observation.

2.4. Pyrene fluorescence

Samples for pyrene fluorescence analyses were prepared as previously described (Le et al., 2021). 1 mL of pyrene 8×10^{-7} mol.L^{-1} aqueous solution was mixed with an equal volume of PEC-NG suspensions (C_P = 0.5 g.L^{-1}) under stirring overnight. Fluorescence emission spectra of samples upon excitation at 335 nm wavelength were recorded at certain temperatures (25 °C, 37 °C or 50 °C) using a Fluoromax-4 spectrofluorometer (Horiba Jobin Yvon, France). The ratio

I_I/I_{III} was calculated as intensity ratio of the first to the third vibronic bands recorded respectively at 373 and 383 nm. All measurements were done at least in triplicate.

2.5. Stability studies

Stability of PEC-NGs in Milli-Q water and physiological salines (NaCl 0.9% eq. 0.154 mol.L^{-1} and PBS) was evaluated (Dioury et al., 2021). To reach NG suspensions having final salinity of NaCl 0.9% or PBS 1X, 80 µL NaCl 4 mol.L^{-1} or 52 µL PBS 40X was added to 2 mL PEC-NG suspension (C_P variation assumed to be inconsiderable). All samples were then vortexed and left for 30 min before DLS analysis at 25 °C, then stored at 4 or 25 °C for revaluation by DLS after 1, 3, 7 and 30 days. pH measurements for certain samples were done using a pH meter (Mettler Toledo, Switzerland).

2.6. Enzymatic degradation studies

NG degradation was studied through particle size evolution in the presence of HAase (Yang et al., 2016). Firstly, HAase 30 and 3 mg.mL^{-1} solutions were prepared by dissolving HAase in Milli-Q water. 10 µL of these solutions was then vortexed with 1 mL of PEC-NG suspensions of interest to reach final HAase concentrations of 0.3 or 0.03 mg.mL^{-1}. All samples, including samples without HAase as reference, were then analyzed by DLS at predetermined time points during their incubation at 37 °C.

2.7. Curcumin quantification

Curcumin quantification method was adapted from other studies with some modifications (Gómez-Mascaraque, Sipoli, de La Torre, & López-Rubio, 2017; Sarika & James, 2016). Briefly, 200 mL of PEC-NG suspension was vortexed with 20 mL of HCl 1 N to protonate HA and facilitate PEC disintegration (Kayitmazer, Koksal, & Iyilik, 2015). The mixture was then vortexed with 1.1 mL (880 mg) of ethanol for curcumin solubilization. The precipitated polymer was then

separated by centrifugation at 3,000×*g* for 15 min. The curcumin concentration C in the supernatants (μg.mL^{-1}) was determined by UV–visible spectrophotometer Cary 100 (Agilent Technology, USA) with a standard curve of absorbance at 420 nm (A_{420}) as a function of curcumin concentration between 0.05-10 μg.mL^{-1} in water/HCl 1N/EtOH 10/1/55 v/v (A_{420} = 0.1407×C – 0.0022 with R^2 = 0.9999). Curcumin concentrations in the starting PEC-NG suspensions ($C_{CUR/SUS}$) were accordingly deduced, with densities of PEC-NG suspensions and the supernatant (EtOH/aqueous phase 5/1 v/v or 4/1 m/m) at room temperature being 1 and 0.84 g.mL^{-1} respectively (Rumble, 2021). The loading capacity (LC) and encapsulation efficiency (EE) were calculated as followed:

$$LC = (C_{CUR/SUS} - C_{CUR/WATER})/C_P \times 100\ (\%) \qquad \text{(Equation 1)}$$

$$EE = (C_{CUR/SUS} - C_{CUR/WATER})/C_{CUR0} \times 100\ (\%) \qquad \text{(Equation 2)}$$

with $C_{CUR/WATER}$ as curcumin concentration of reference sample, which contained solely water saturated in curcumin, C_P as polymer concentration and C_{CUR0} as the concentration of added curcumin with respect to the aqueous phase during the preparation.

3. Results and discussion

3.1. PEC-NG initial characterization

PEC-NGs were generated by simply mixing polyanion with polycation solutions, which was spontaneous *via* electrostatic interactions since no chemical reaction was observed from their FT-IR spectra (**Figure S3**). Such preparation process is thus simple and rapid, requiring no organic solvent, chemical agent or high energy. For clarifying the effect of M2005 grafting, **Figure 2** shows particle properties of HA-M2005/DEAE-D PEC-NGs at C_P = 0.5 g.L^{-1} after 30 min of

complexation, compared to those of HA/DEAE-D PEC-NGs from our previous study (Le et al., 2021).

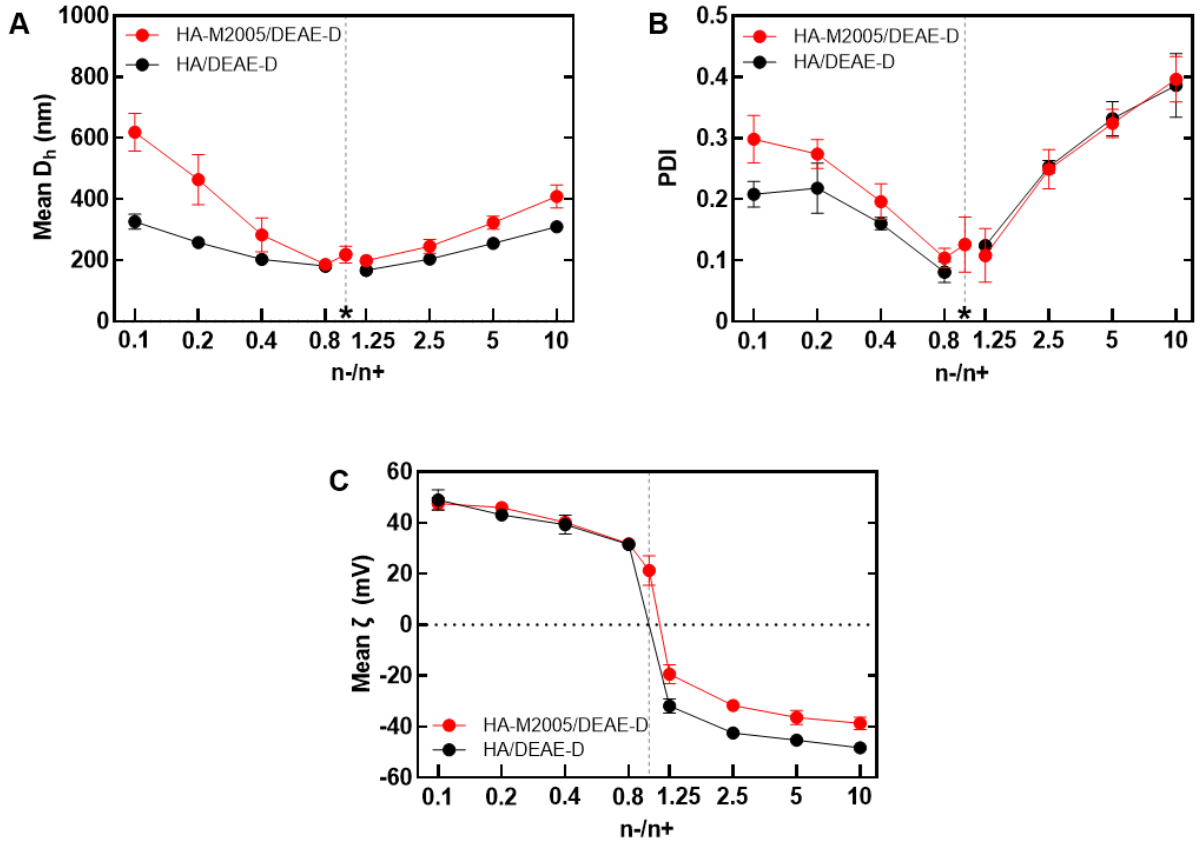

Figure 2. Mean D_h (**A**), PDI (**B**) and mean ζ (**C**) measured at 25 °C of HA/DEAE-D and HA-M2005/DEAE-D PEC-NGs (C_P = 0.5 g.L^{-1} in Milli-Q water) after 30 min of complexation. Asterisk represents n-/n+ = 1, at which precipitation was observed for HA/DEAE-D PEC-NGs. Data are presented as mean ± standard deviation (n ≥ 3).

As seen from **Figure 2**A-B, homogeneous HA-M2005/DEAE-D PEC-NGs samples have mean D_h of 200-600 nm and PDI of 0.1-0.4. However, such D_h is always larger than that of HA/DEAE-D PEC-NGs at the same n-/n+ (**Figure 2**A). This may stem from steric effects of the bulky M2005 grafts inside PEC-NGs. It should also be noticed that for the same n-/n+, the mass

ratio of polyanion to polycation in HA-M2005/DEAE-D PECs was higher than in HA/DEAE-D PECs to compensate the loss of negative charges after M2005 grafting, which may also contribute to the difference in their particle sizes. Furthermore, the difference in D_h and PDI between the two kinds of PEC-NGs is more obvious at $n-/n+ < 0.8$, where DEAE-D exceeds HA (**Figure 2**A-B). As discussed in our previous work, at $n-/n+ < 0.8$, PECs from intermediate molecular weight HA and high molecular weight DEAE-D showed rapid aggregation continuing after 30 min of complexation, being ascribed to hydrophobic segregation of unstable short double-stranded PEC segments (Le et al., 2021). With M2005 grafts, this effect may be enhanced due to higher hydrophobicity of such segments and hence generate much larger secondary PECs. Regarding net surface charge, HA-M2005/DEAE-D and HA/DEAE-D PEC-NGs show quite a similar curve of mean ζ as a function of n-/n+ (**Figure 2**C), except the less negative ζ observed at $n-/n+ \geq 1$ for PECs possessing M2005 grafts. This could be attributed to shrinkage of HA backbone towards particle interior due to hydrophobic interactions of M2005 on HA and therefore its negative charges are less accessible on NG surface. Mean ζ of PECs of $n-/n+ = 1$ is hence deviated away from zero when HA-M2005 replaces HA (**Figure 2**C), rendering precipitation absent at the stoichiometric n-/n+ as observed but assumedly present between n-/n+ of 1 and 1.25.

For preparing HA/PLL PEC-NGs, we also used intermediate molecular weight HA with PLL of higher molecular weight. Such PEC-NGs also present physicochemical parameters (**Figure 3**A-C) following the same trends as a function of n-/n+ as HA/DEAE-D PEC-NGs (**Figure 2**A-C).

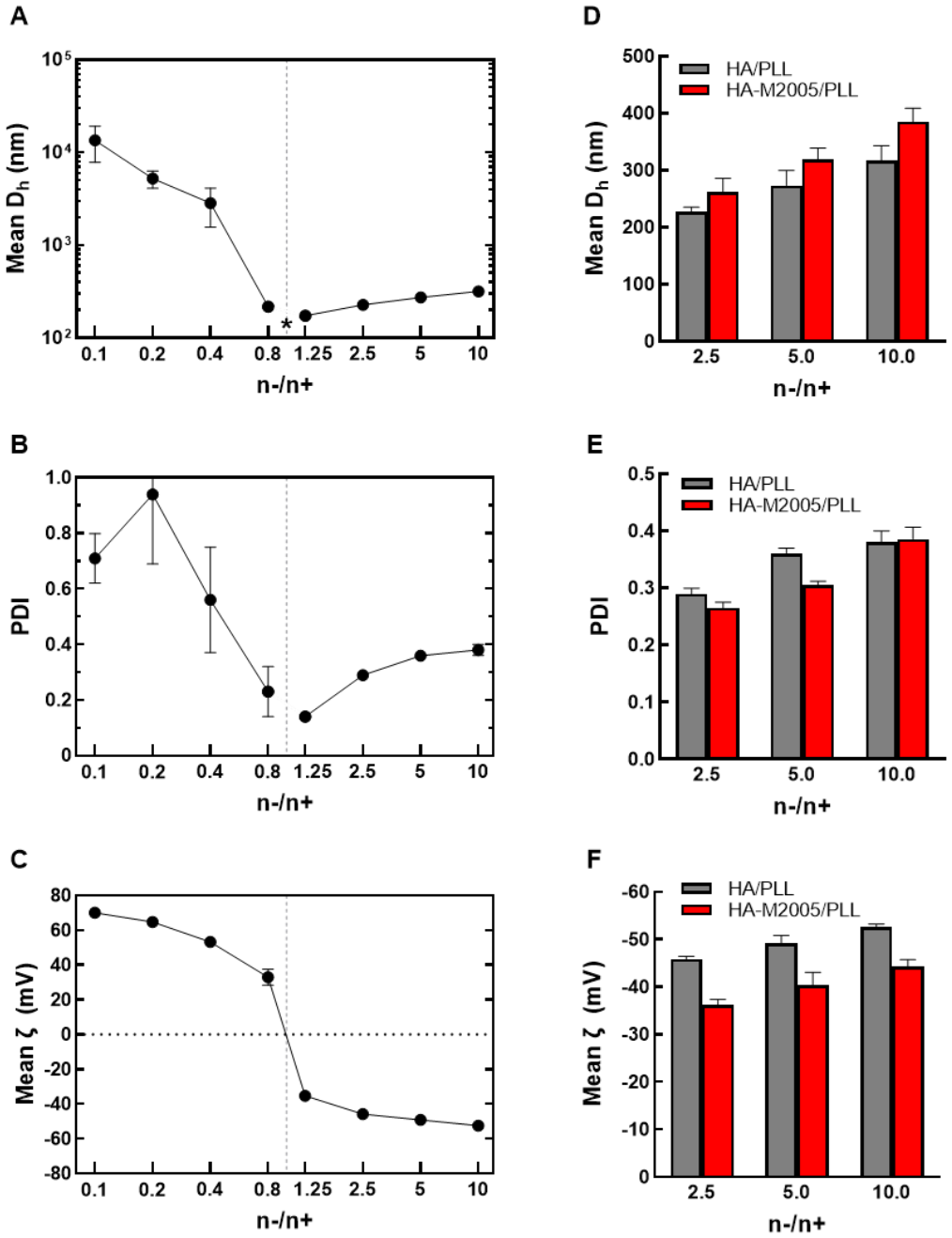

Figure 3. Mean D_h, PDI and mean ζ of HA/PLL PEC-NGs (**A**, **B**, **C** respectively) and of HA-M2005/PLL PEC-NGs in comparison with HA/PLL PEC-NGs (**D**, **E**, **F** respectively) at C_P = 0.5 g.L^{-1} in Milli-Q water after 30 min of complexation. Asterisk represents precipitation at n-/n+ = 1 (DLS not performed). Data are presented as mean ± standard deviation (n ≥ 3).

HA/PLL PEC-NGs at n-/n+ > 1 exhibited consistent characteristics with mean D_h between 100-300 nm and PDI < 0.4. In contrast, at n-/n+ < 0.8, unusually large D_h (1000-10,000 nm) and PDI higher than 0.5 were remarked (**Figure 3**A-B). These results approach the upper limit of reliability for DLS and should not be considered as accurate characteristics but rather a relative indication of large aggregates uncontrolled in size. PEC-NGs at n-/n+ of 0.8, despite their more relevant D_h (around 200 nm), still showed low batch-to-batch consistency in PDI (**Figure 3**B). Large aggregates were also reported for HA/PLL PECs of n-/n+ < 1 with increasing particle size over time, from 400 to 800-1000 nm after 8 h (Pan et al., 2019). Such aggregation is probably caused by stronger intercomplex hydrophobic interactions between PECs containing mainly PLL, which has been known to be considerably hydrophobic upon charge neutralization due to the four succeeding methylene groups in lysine units (Dyson, Wright, & Scheraga, 2006; Pan et al., 2019).

Considering the results of HA/PLL PEC-NGs, for HA-M2005/PLL PEC-NGs, we focused only on n-/n+ > 1 due to their more consistent and measurable properties. However, for n-/n+ of 1.25, precipitation was observed and DLS characterization was not performed. For the other n-/n+, M2005 grafts seem to display the same impact as in HA/DEAE-D PECs (**Figure 3**D-F *vs.* **Figure 2**A-C), i.e. increasing D_h and reducing ζ. Accordingly, this may explain the observed precipitation at n-/n+ of 1.25 since the readily low net surface charge at such n-/n+ can be further reduced and thus facilitate aggregation.

For further characterization of PEC-NGs, the morphologies of all the four types of PEC-NGs at n-/n+ = 2.5 and $C_P = 0.5\ g.L^{-1}$ were also examined by TEM (**Figure 4**), which verified the formation of PEC-NGs as particles having generally spherical shape and particle size in coherence with DLS results. Particle morphologies seem to be distinct depending on the constituent polycation, while M2005 grafts led to no visible difference in this aspect. At higher

magnification, some particles can clearly show their structure comprising a dense core surrounded by a corona shell (**Figure 4**E), which confirms the suggested core-shell structure of PEC-NGs.

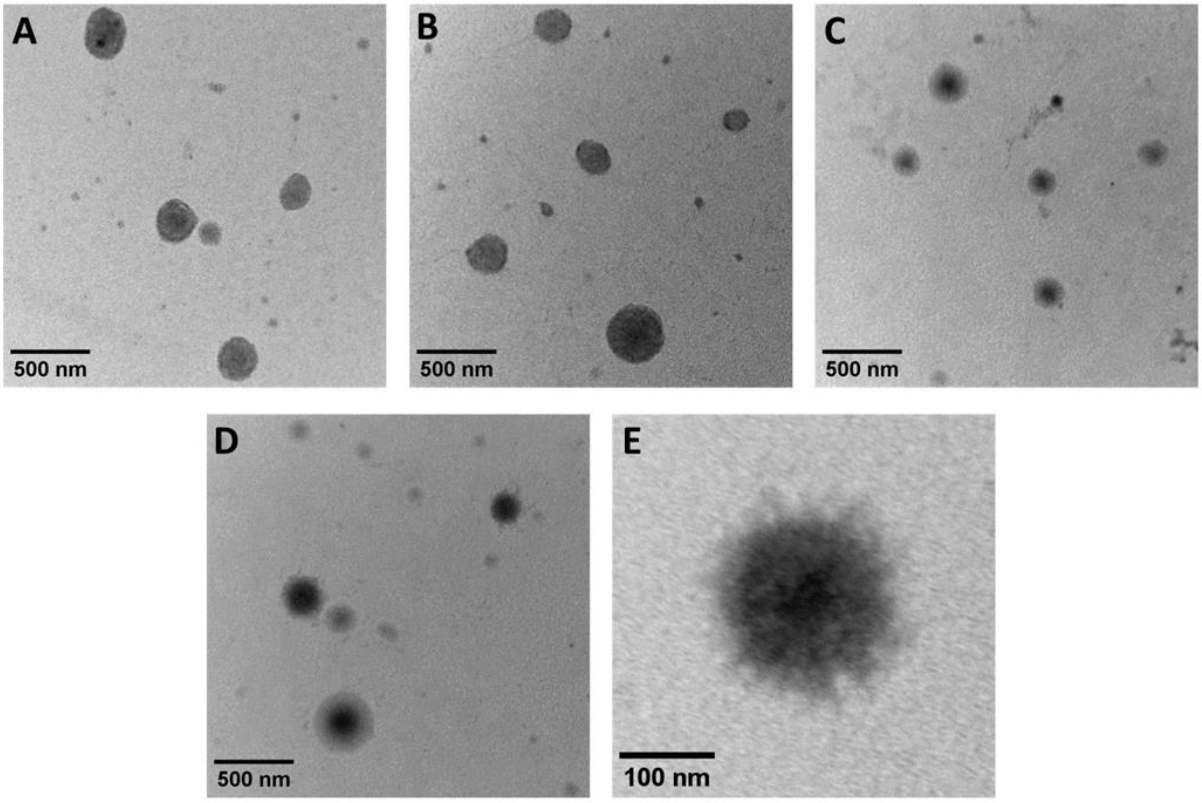

Figure 4. TEM images of PEC-NGs from HA/DEAE-D (**A**), HA-M2005/DEAE-D (**B**), HA/PLL (**C** and **E**) and HA-M2005/PLL (**D**) at n-/n+ = 2.5 and C_P = 0.5 g.L^{-1}.

3.2. Stability studies

Particle sizes of different PEC-NGs at C_P = 0.5 g.L^{-1} were monitored during one month in different conditions (i.e. storage temperature, saline and buffered media) to evaluate the influence of M2005 grafts and polycation nature on their stability. The stability of mean D_h is shown in **Figure 5** and their PDIs with the same trend can be consulted from **Figure S4**.

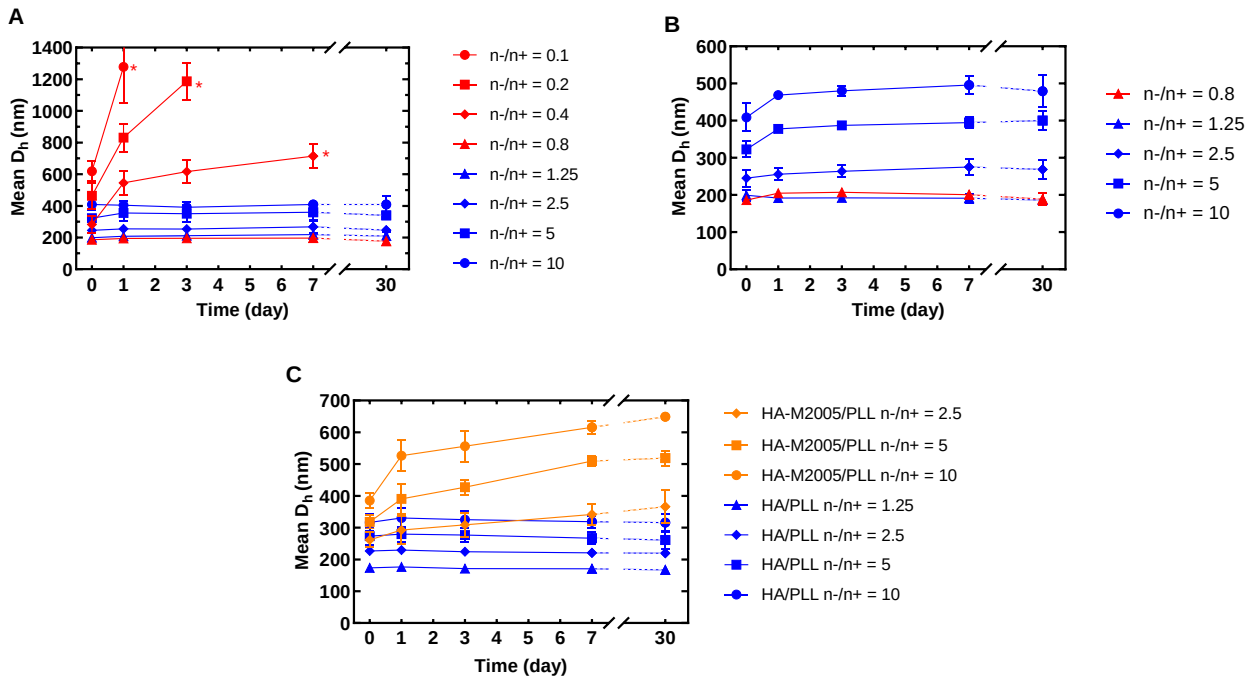

Figure 5. Mean D_h of PEC-NGs (C_P = 0.5 g.L^{-1} in Milli-Q water) as a function of time: (**A**) HA-M2005/DEAE-D PEC-NGs stored at 4 °C, (**B**) HA-M2005/DEAE-D PEC-NGs stored at 25 °C, (**C**) HA-M2005/PLL and HA/PLL PEC-NGs stored at 4 °C. Data are presented as mean ± standard deviation ($n \geq 3$). Asterisks represent samples having large particle sizes (mean D_h > 700 nm) with inconsistently large distribution.

As shown in **Figure 5**A, when stored at 4 °C, HA-M2005/DEAE-D PEC-NGs of n-/n+ ≥ 0.8 were stable but those of n-/n+ < 0.8 showed particle size increased after one day. Stability evaluations were ceased when their mean particle sizes became too high (over 700 nm) with largely varying PDIs. This is similar to HA/DEAE-D PEC-NGs in our previous work and could be explained by the same hypothetical mechanism, that neutral double-stranded segments in these PECs would be very short and hence unstable, favoring their segregation over time to reach a more stable state (Le et al., 2021).

In a second time, HA-M2005/DEAE-D PEC-NGs having good stability at 4 °C were subjected to stability evaluation at 25 °C. Interestingly, higher storage temperature seems to render such PEC-NGs less stable, evidenced by increasing D_h at n-/n+ ≥ 2.5 (**Figure 5**B). This was not observed with PEC-NGs without M2005 (Le et al., 2021) and therefore can be interpreted as particle aggregation due to enhanced hydrophobic interactions between M2005 grafts on PEC-NG surfaces at higher temperature. Meanwhile, HA-M2005/PLL PEC-NGs at the same n-/n+ showed D_h increasing over time despite being stored at low temperature (4 °C), in contrast to HA/PLL PEC-NGs which were stable (**Figure 5**C). This suggests that replacing DEAE-D with PLL renders PEC-NGs containing M2005 more susceptible to agglomeration, probably because of stronger interparticle hydrophobic interactions contributed by PLL as mentioned in **Section 3.1** beside that of M2005.

In order to study the stability of PEC-NGs against physiological saline conditions, different PEC-NG formulations were subjected to saline solutions (NaCl 0.9 % and PBS) and stored at 4 °C for stability monitoring. However, the suspensions of HA/DEAE and HA-M2005/DEAE-D PEC-NGs (C_P = 0.5 g.L^{-1}) showed precipitation after 30 min in NaCl 0.9 % or PBS (results not shown) and were thus not suitable for DLS analysis. This is in accordance with the low stability of HA/DEAE-D PECs upon increasing ionic strength in our previous work (Le et al., 2021) and confirms that such PECs are still highly sensitive to ionic strength even with M20005 grafts. Interestingly, replacing DEAE-D with PLL led to very different behaviors of PECs, which displayed no precipitation and were therefore satisfactory for DLS characterization (**Figure 6**).

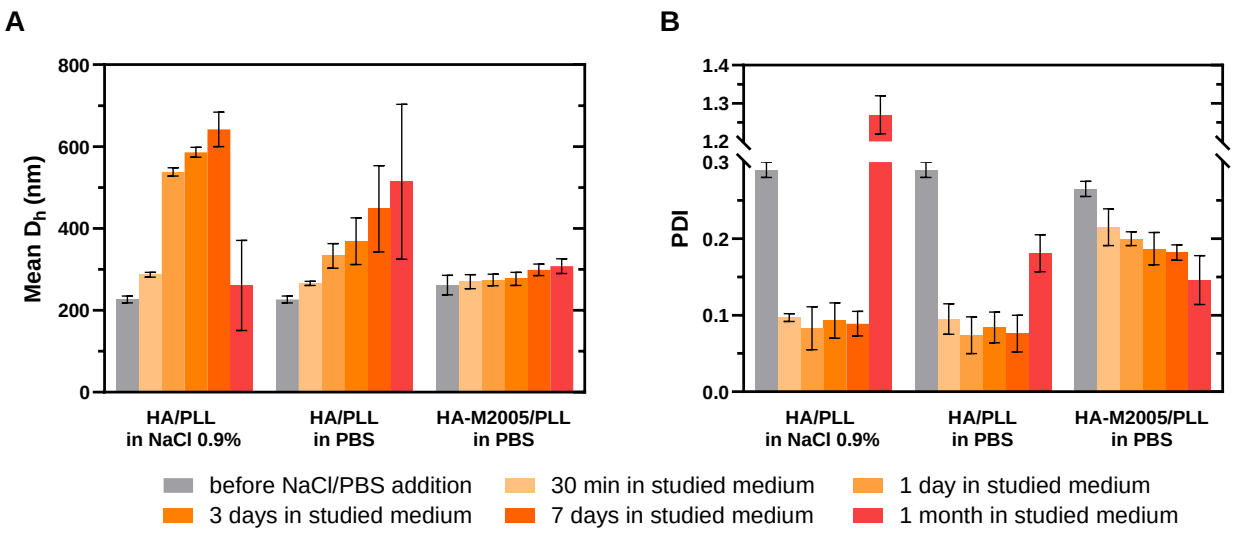

Figure 6. (**A**) Mean D_h and (**B**) PDI of different PEC-NGs (C_P = 0.5 g.L^{-1}) stored at 4 °C in different media. Data are presented as mean ± standard deviation (n ≥ 3).

Following NaCl or PBS addition, HA/PLL PEC-NGs showed significantly increased D_h with an abrupt fall in PDI. This is most probably due to particle aggregation when electrostatic repulsion between particles is weakened by counterions through charge screening. As PDI represents the relation between the absolute distribution width and the mean value of particle size, the fall of PDI during the aggregation can be interpreted as the absolute distribution width remaining the same or changing to a lesser extent than the increase of the mean particle size.

Nevertheless, in NaCl 0.9 %, the D_h continued to increase after seven days but decreased after one month, coinciding with a significant increase in PDI to more than 1. This can be explained by the appearance of another particle population having a smaller size, which was around 10-100 nm (**Figure S5**). As discussed in our previous work (Le et al., 2021), charge screening by salt ions can take place not only at particle level to cause particle aggregation but also at macromolecular level, which may cause PEC decomplexation into smaller fragments. In the current case, the latter effect seems to take place much later than the former. This could be

explained by a longer time required for infiltration of salt ions into the interior of PEC-NGs to interfere with ion pairing. This was also the case in PBS, as shown by the increase in PDI after one month, but seemingly to a lesser extent than in NaCl 0.9 % since the mean particle size did not obviously decrease. Such difference could hardly be explained by the difference between their initial pH, which were measured as 6.28 ± 0.18 and 7.40 ± 0.04 in NaCl 0.9 % and PBS respectively and thus cause no considerable difference in ionization rate and actual n-/n+ of PECs (Supplementary Information **SI-3**). Such a better stability of PEC-NGs in PBS may be due to the long-term pH stability in this buffer. More interestingly, HA-M2005/PLL PEC-NGs showed relatively stable particle size after PBS addition (**Figure 6**A). However, a minor increase in particle size over one month was still observed but to a smaller extent than in Milli-Q water at the same condition (**Figure 5**C) and their PDI was gradually decreased over time. Such results evidence that the presence of salt does not deteriorate but indeed improve the stability of PEC-NGs having M2005 grafts. This finding is especially interesting since PECs from polyelectrolytes disposing weak charges are generally known to be highly unstable under physiological ionic strength (Wu & Delair, 2015). The exact mechanism of such stabilizing effect remains unclear but may be related to salting-out effect of salt, which can reinforce intraparticle hydrophobic interactions between PPO blocks of M2005 grafts (Dulong et al., 2012; Gupta et al., 2015; Niang et al., 2016) and therefore stabilize PEC structure.

Collectively, such results prove that PEC-NGs with PLL as polycation are more resistant against ionic strength than with DEAE-D. As an explanation, regular charge distribution on both PLL and HA (**Figure 1**) may contribute to more close-knit ion pairing and hence their stronger association. On the contrary, arbitrary distribution of positive charges on DEAE-D may lead to nonoptimal charge compensation with HA and thus more loosely and unstable structures of PECs.

3.3. Thermoresponsiveness studies

Thermoresponsive properties of nanocarriers possessing LCST pendant groups, i.e. shrinkage and increase in hydrophobicity at higher temperature, have been known to be the mechanism and hence the prerequisite for their interesting drug delivery applications, namely triggering and/or controlling the drug release spatiotemporally *in vivo* by applying local hyperthermia (Molina et al., 2015). To verify the thermoresponsiveness of PEC-NGs from HA-M2005, we evaluated at different temperatures their hydrophobicity by fluorescence spectroscopy with pyrene probe and their particle sizes by DLS. The principle of the former technique is that a decrease in intensity ratio of the first to the third peaks (I_I/I_{III}) in the emission spectra upon excitation at 335 nm of pyrene incorporated in the systems indicates the presence of more hydrophobic nanodomains (Burdíková, Mravec, & Pekař, 2016). Compared to the previous I_I/I_{III} results of HA/DEAE-D PEC-NGs incorporating pyrene (HA/DEAE-D/Py) at 25 °C (Le et al., 2021), those of HA-M2005/DEAE-D/Py PEC-NGs were not significantly different and suggest that M2005 grafts do not significantly enhance the hydrophobicity of PEC-NGs at 25 °C (**Figure S6**A). However, whereas the former system showed unchanged I_I/I_{III} upon heating (**Figure S6**B), HA-M2005/DEAE-D/Py PEC-NGs exhibited lower I_I/I_{III} when the temperature was increased from 25 °C to 37 °C and 50 °C, more significantly at n-/n+ > 1 than at n-/n+ < 1 (**Figure 7**A). These results prove an increase in hydrophobicity upon heating, probably due to stronger hydrophobic association of the thermosensitive M2005 grafts. This tendency was the same for HA-M2005/PLL/Py PEC-NGs (**Figure 7**C). Furthermore, this effect seems to be more important when n-/n+ is nearer to 1 regardless of component polycation (**Figure 7**A and C). This may be attributed to PEC structure being readily more compact at such n-/n+ (Le et al., 2021),

rendering M2005 chains already located in close proximity and hence favoring their approximation to form more hydrophobic clusters.

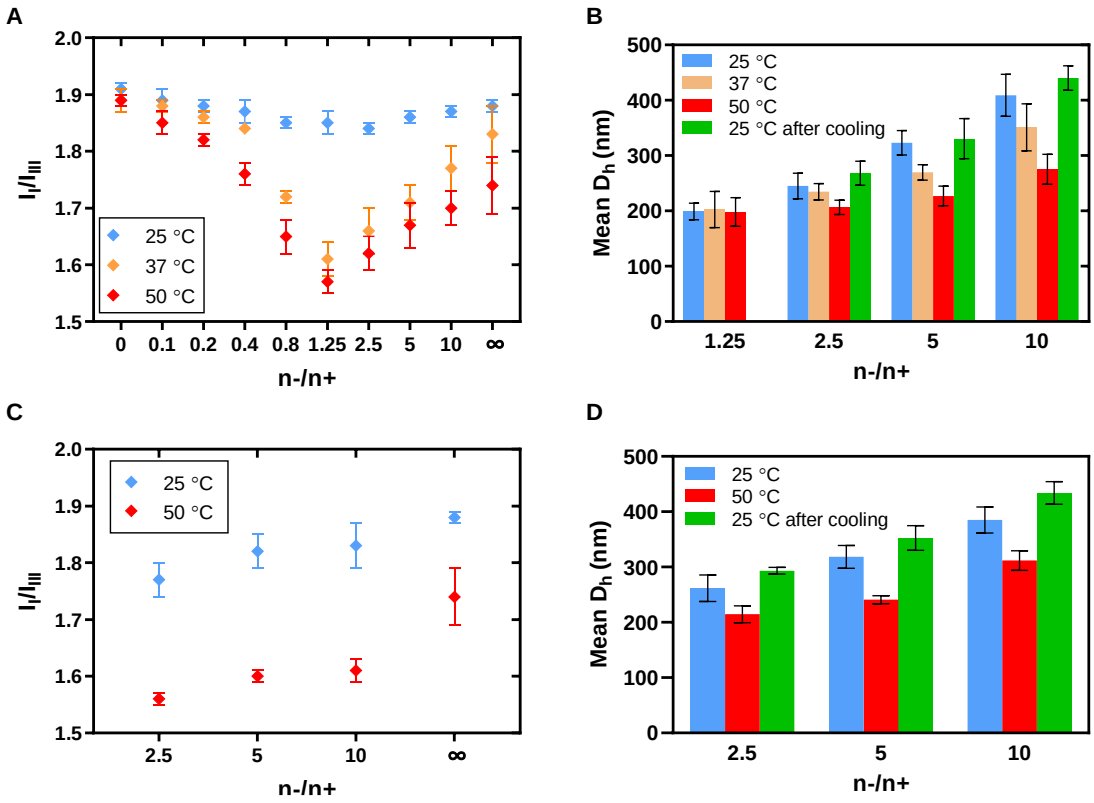

Figure 7. I_I/I_{III} in pyrene fluorescence and particle sizes at different temperatures of HA-M2005/DEAE-D PEC-NGs (**A-B** respectively) and HA-M2005/PLL PEC-NGs (**C-D** respectively) in Milli-Q water. C_P = 0.5 g.L^{-1} for particle size analyses and 0.25 g.L^{-1} for pyrene fluorescence studies due to dilution. The values 0 and ∞ represent solutions containing solely polycations and polyanions respectively. Data are presented as mean ± standard deviation (n ≥ 3).

For characterizing the thermal dependence of particle size, we also focused on PEC-NGs with n-/n+ > 1 since these systems showed more consistent results of initial particle size (**Section 3.1**). Upon heating, HA-M2005/DEAE-D PEC-NGs showed a decrease in D_h (**Figure 7**B) and the same for their PDI (**Figure S7**A). For HA-M2005/PLL PEC-NGs, except for those at n-/n+ = 1.25 which could not be characterized by DLS because of

precipitation (**Section 3.1**), PEC-NGs at n-/n+ ≥ 2.5 also displayed lower D_h (**Figure 7**D) and PDI (**Figure S7**B) at higher temperature. Such decrease in particle size takes place within only 200-300 s of heating before reaching an equilibrium (**Figure S7**D). In contrast, PECs without M2005 grafts did not show such change upon heating (**Figure S7**C). Together with the earlier results on hydrophobicity, these results suggest that the LCST property of M2005 grafts on HA contributes to a quasi-instantaneous series of thermoresponsive behaviors of our PEC-NGs, namely compaction of intraparticle hydrophobic clusters which leads to rapid particle shrinkage. However, different from the increase in hydrophobicity, the shrinkage is less obvious when n-/n+ is nearer to 1 and even unobservable at n-/n+ = 1.25 for HA-M2005/DEAE-D PEC-NGs, presumably because the readily compact structure of PEC-NGs at n-/n+ nearer to 1 is less susceptible to shrinkage than the highly porous structure at other n-/n+. Furthermore, after one hour of cooling at room temperature, their D_h resurged but slightly surpassed the initial values (**Figure 7**B and D) and less clearly for PDI (**Figure S7**A-B). This suggests a completely reversible thermoresponsive behavior but which may accompany a slight rearrangement within the PEC-NG structure. This experiment was repeated up to three cycles of heating-cooling and such reversibility was still conserved during the whole process (**Figure S7**E).

3.4. Curcumin encapsulation

Curcumin was used as a model compound to verify the potential of our system in encapsulating poorly water-soluble drugs. Our previous study reported that pyrene is encapsulated more efficiently in PECs if it is added before the complexation (Le et al., 2021). Thus, the preparation of PEC-NGs encapsulating curcumin in the current work was performed by adding polycation to polyanion solutions readily mixed with curcumin. From the pyrene fluorescence studies (**Figure 7**), PEC-NGs having n-/n+ of 1.25-2.5 seem to be the most potential for

encapsulating hydrophobic molecules. However, our preliminary curcumin encapsulation trials with PEC-NGs of n-/n+ = 1.25 showed inconsistent results, namely large batch-to-batch variation in visual aspect and curcumin concentration of the samples (results not shown). This possibly stems from the weak net surface charge of PEC-NGs at this n-/n+, which facilitate their precipitation and sedimentation along with the insoluble curcumin in excess. PEC-NGs having n-/n+ of 2.5, displaying more consistent results (**Table 2**), were thus chosen as the main subjects for these studies. As shown in **Table 2**, curcumin concentration in HA/DEAE-D/Cur PEC-NGs is higher than in curcumin-saturated water, proving the encapsulation of curcumin inside such PEC-NGs. Furthermore, the encapsulation was improved with PEC-NGs having M2005 grafts, most probably due to M2005 hydrophobic clusters in the NGs.

Table 2. Curcumin quantification results in different formulations

Formulation parameters		Curcumin quantification results [c]		
System	T_{prep}	C_{CUR} (μg.mL^{-1})	LC (%)	EE (%)
Milli-Q/Cur [a]	25 °C	0.30 ± 0.05	-	-
HA/DEAE-D/Cur [b]	25 °C	1.11 ± 0.05	0.16 ± 0.01	0.40 ± 0.03
HA-M2005/DEAE-D/Cur [b]	25 °C	1.70 ± 0.13	0.28 ± 0.03	0.70 ± 0.06
HA/DEAE-D/Cur [b]	50 °C	1.15 ± 0.13	0.17 ± 0.03	0.43 ± 0.06
HA-M2005/DEAE-D/Cur [b]	50 °C	3.55 ± 0.41	0.65 ± 0.08	1.63 ± 0.20
HA-M2005/DEAE-D/Cur [b]	70 °C	3.61 ± 0.18	0.66 ± 0.04	1.65 ± 0.09
HA-M2005/PLL/Cur [b]	50 °C	5.06 ± 0.25	0.94 ± 0.05	2.38 ± 0.12

T_{prep}: preparation temperature, C_{CUR}: curcumin concentration, LC: loading capacity, EE: encapsulation efficiency
[a] Milli-Q water saturated in curcumin, [b] C_P = 0.5 g.L^{-1} and n-/n+ = 2.5, [c] mean ± standard deviation (n ≥ 3)

To optimize the encapsulation, we carried out the complexation at a higher temperature (50 °C or 70 °C), hypothesizing that this approach would lead to more hydrophobic clusters of M2005 and incorporate more curcumin, which is then protected from leakage upon cooling by the

hydrophilic shell of PEC-NGs. As expected, HA-M2005/DEAE-D/Cur PEC-NGs prepared at 50 °C displayed remarkably higher curcumin content than those prepared at 25 °C, which was not observed for PEC-NGs without M2005 grafts (**Table 2**). This is in coherence with pyrene fluorescence studies and confirms the role of the temperature-dependent hydrophobic interactions of M2005 grafts in encapsulating hydrophobic molecules. However, increasing the complexation temperature from 50 °C to 70 °C did not further improve the encapsulation rate (**Table 2**), suggesting that the hydrophobic interactions of M2005 grafts are already optimal at 50 °C. In addition, replacing DEAE-D with PLL also significantly improved the encapsulation (**Table 2**), confirming the more hydrophobic nature of PLL compared with DEAE-D as suggested in **Section 3.1**. Furthermore, PEC-NGs encapsulating curcumin prepared at 50 °C presented comparable mean D_h and ζ (**Table S1**) to those of PEC-NGs without curcumin prepared at room temperature (**Section 3.1**), suggesting that the encapsulated curcumin and the preparation temperature have no considerable effect on the ultimate state of PEC-NGs. The modest EE (**Table 2**) may be ascribed to the excessively large amount of starting curcumin during the preparation and the highly hydrophobic nature of this compound with respect to our PEC-NGs which are still globally hydrophilic. Formulation and process optimization is thus still in need before further characterizations like drug release studies or bioassays. Anyway, these results evidence that such PEC-NGs can increase the aqueous solubility of curcumin with the possibility of encapsulation tuning and optimization through temperature control, showing therefore the potential for encapsulating other hydrophobic drugs.

3.5. Enzymatic degradation

The current PEC-NGs, as other HA-based nanocarriers, are potential for target drug delivery towards cancer cells since they are supposed to be degraded by HAase overexpressed

specifically inside these cells and exhibit therefore more efficient intracellular drug release than in normal cells (Yang et al., 2016). From this perspective, it is of high interest to verify and understand HAase-induced degradation of our PEC-NGs. To this aim, we investigated the evolution of their particle size in the presence of HAase 0.03 g.L^{-1} (12 IU.mL^{-1}) during 24 h at 37 °C. Such evolution of D_h is reported in **Figure 8**A, with PDI following relatively similar trends in **Figure S8**.

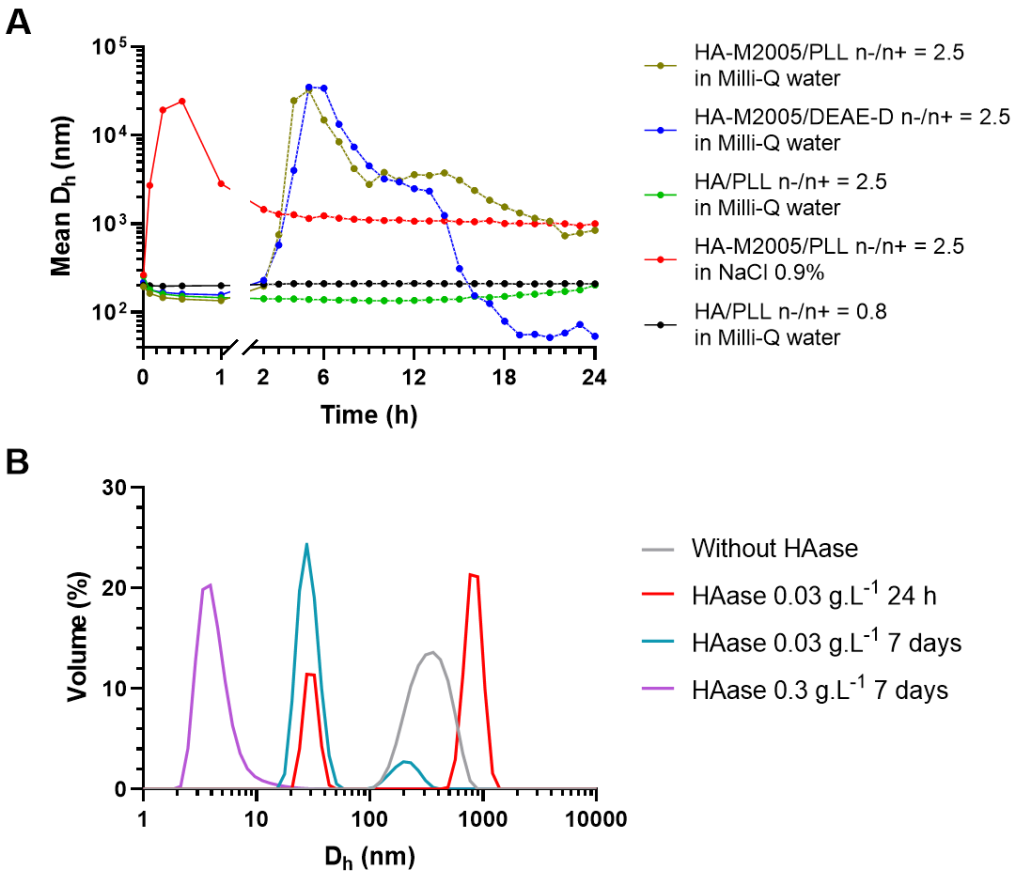

Figure 8. (**A**) Temporal evolution of mean D_h of different PEC-NGs in the presence of HAase 0.03 g.L^{-1} (12 IU.mL^{-1}) during 24 h at 37 °C. (**B**) Volume-weighted particle size distribution of HA-M2005/PLL PEC-NGs (n-/n+ = 2.5, C_P = 0.5 g.L^{-1}) in NaCl 0.9% before and after being treated with HAase at different enzyme concentrations and time points. Data were obtained from one experiment, results of replicated experiments showed similar trends.

Whereas PEC-NGs displayed no significant change in D_h over time in the absence of HAase (results not shown), HA-M2005/PLL and HA-M2005/DEAE-D PEC-NGs of n-/n+ = 2.5 in Milli-Q water showed D_h changed after HAase addition, including a decrease in the first one hour followed by a sudden increase to reach a maximum after 5-6 h. For HA/PLL PEC-NGs of the same n-/n+, such phenomenon evolved much more slowly as their D_h only started to gradually increase after 12 h of slight diminution since HAase addition (**Figure 8**A) and then showed a mean D_h of nearly 2000 nm with PDI of 0.88 after 3 days (results not shown). Such change in particle size may be because HAase preferentially degrades uncomplexed HA on the corona shell of PEC-NGs, leading to reduction of particle size at the beginning but also loss of surface charge and steric effect, which would in turn reduce interparticle electrostatic repulsion and cause hydrophobic aggregation. The speediness of such evolution for PEC-NGs containing M2005 probably stems from their weaker net surface charge and more hydrophobic structure brought about by M2005 grafts (see **Section 3.1**). Meanwhile, HA-M2005/PLL PEC-NGs in NaCl 0.9 % showed an immediate increase in particle size after HAase addition, probably because of two synergistic effects of salt: (i) charge screening to restrict non-specific complexation between HA and HAase, thus enhancing enzyme activity (Astériou, Vincent, Tranchepain, & Deschrevel, 2006) and (ii) reducing electrostatic repulsion between PEC-NGs while reinforcing hydrophobic interactions of M2005 to enhance particle aggregation (see **Section 3.2**). However, after reaching the maxima, the particle sizes started to decrease (**Figure 8**A), which can be interpreted by PEC deterioration following HA degradation. This was more considerable with DEAE-D than with PLL as polycation, presumably due to the more fragile PEC structure between HA and DEAE-D as described in **Section 3.2**. Meanwhile, HA/PLL PEC-NGs at n-/n+ = 0.8 presented no change in D_h

in the presence of HAase (**Figure 8**A), suggesting a protective effect of PLL shell on HA inside PEC-NGs against the enzyme.

Regarding D_h distribution (**Figure 8**B), HA-M2005/PLL PEC-NGs of n-/n+ = 2.5 treated with HAase 0.03 $g.L^{-1}$ in NaCl 0.9 % over 24 h had a population of low D_h (20-50 nm) beside few large aggregates (500-1000 nm). The former population was further accentuated with disappearance of the aggregates after 7 days, confirming the degradation of PEC-NGs by HAase. For the same treatment time, a higher enzyme concentration of 0.3 $g.L^{-1}$ led to PEC-NGs being broken down into much smaller fragments (2-20 nm). These results further confirm that PEC-NG degradation by HAase is dependent on treatment time and enzyme concentration.

4. Conclusion

In this work, mixing the solutions of HA or HA-M2005 with DEAE-D or PLL allowed the spontaneous formation of PEC-NGs through electrostatic interactions, which is a rapid and simple elaboration process. The M2005 grafts on HA can prompt inter- and intraparticle hydrophobic interactions while also rendering PEC-NGs thermoresponsive, which is applicable in optimizing drug encapsulation. Compared with DEAE-D, PLL can offer additional hydrophobicity and better stabilization of PEC-NGs. A synergistic combination between HA-M2005 and PLL can therefore generate PEC-NGs showing good stability under physiological ionic strength and the highest encapsulation capacity. With HA-M2005 as the main component, these PEC-NGs are not only thermosensitive but also degradable in the presence of HAase, thus promising as a dual-responsive system for targeted delivery of poorly water-soluble drugs. This should be especially advantageous for targeting tumors, where the overexpression of CD44 receptors and HAase should lead to enhanced cellular uptake and degradation of our NGs for drug release, while the thermoresponsiveness of the system may allow controlling not only encapsulation of anticancer

drugs, which usually have low aqueous solubility, but also their spatiotemporal delivery *in vivo* by applying local hyperthermia. However, further studies, namely formulation and conservation optimization by freeze-drying and drug release studies, remain to be done before biological *in vitro* and *in vivo* evaluations.

Acknowledgments

We thank the Normandy region and the European Union for their financial support. We also thank Dr Sophie BERNARD and PRIMACEN (the Cell Imaging Platform of Normandy, IRIB, Faculty of Sciences, University of Rouen Normandy; http://www.primacen.crihan.fr) for the TEM training session.

This paper is dedicated to the memory of our dear colleague Dr Georgeta MOCANU ("Petru Poni" Institute of Macromolecular Chemistry, Iasi, Romania).

Supplementary information

SI-1. Synthesis of HA-M2005

M2005 was grafted on HA through amidation reaction by N-(3-Dimethylaminopropyl)-N′-ethylcarbodiimide (EDC) and N-hydroxysuccinimide (NHS) as coupling reagents (**Figure S1**A), following to the protocol reported by Madau *et al.* (Madau, Le Cerf, Dulong, & Picton, 2021). Briefly, HA (500 mg, eq. 1.25 mol of HA unit) and M2005 (2.47 g, eq. 1.25 mol) were respectively dissolved in 85 mL and 10 mL Milli-Q water by stirring overnight at 4 °C. The pH of M2005 solution was then adjusted to 4.7 with HCl and NaOH 1 N or 0.1 N. The resulting solution was added to the HA solution (2 mL Milli-Q water used for rinsing). After 30 min of stirring at 4 °C, the pH of the resulting mixture was again adjusted to 4.7 with HCl and NaOH 1 N or 0.1 N. 239 mg of EDC (1.25 mol) and 5.7 mg of NHS (0.05 mol) were dissolved together in 2 mL of Milli-Q water and the obtained EDC/NHS solution was all added to the earlier mixture of HA and M2005 (with 1 mL Milli-Q water for rinsing). The reaction was left under stirring for 24 h at 4°C. The mixture was then subjected to dialysis in different media following this order: NaOH 0.1 N (1 h), Milli-Q water (1 day), HCl 0.1 N (1 h), Milli-Q water (1 day), NaOH 0.1 N (1 h), Milli-Q water (1 day), EtOH/water 1/2 v/v (2 days) and Milli-Q water (2 days). HA-M2005 was then recuperated by freeze-drying, followed by washing in acetone and vacuum drying. The degree of substitution (DS) was determined by ^{1}H NMR spectroscopy, which gave a result of DS = 3.6 % (**Figure S1**B). For further details on the synthesis and characterization of HA-M2005, readers are invited to consult the work of Madau *et al.* (Madau et al., 2021).

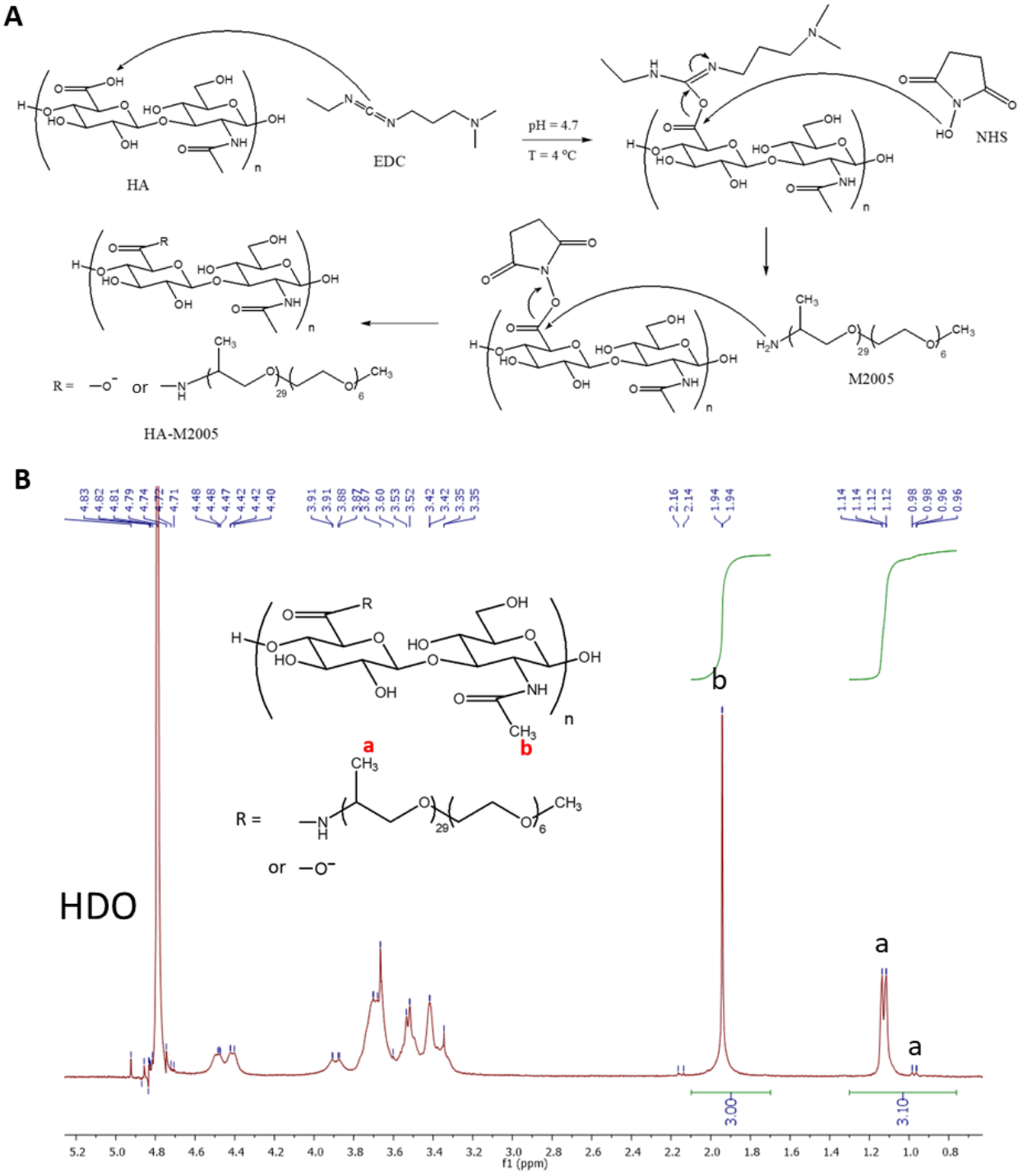

Figure S1. (**A**) Reaction scheme of grafting M2005 on HA, adapted from the reference (Madau et al., 2021). (**B**) ^{1}H NMR spectrum of HA-M2005 (C_P = 5 g.L^{-1} in D_2O containing NaOD 0.1 N), DS was calculated from integrations of peaks a and b.

SI-2. Macromolecular characterization

As for HA and DEAE-D characterizations reported in our previous work (Le, Dulong, Picton, & Le Cerf, 2021), average molecular weights and molecular weight distributions of HA-M2005 and PLL in the present work were also determined at 25 °C by size exclusion chromatography (SEC) coupled on-line with a DAWN Heleos-II multi-angle light scattering systems (MALS) (Wyatt Technology, USA), a ViscoStar II viscometer (Wyatt Technology, USA) and a RID-10A differential refractive index (DRI) detector (Shimadzu, Japan). The MALS system consisted of a 50 µL K5 cell, a Ga-As laser (wavelength of 690 nm) and 18 photodiodes, which were relatively normalized to the 90° detector with bovine serum albumin. The SEC line included a DGU-20A3 degasser (Shimadzu, Japan), a LC10Ai pump (Shimadzu, Japan) and a SIL-20A automatic injector (Shimadzu, Japan) with analytical size-exclusion columns: CATSEC 100 and 1000 columns (Eprogen, USA) for PLL or OHpak SB 804-806 HQ columns (Shodex Showa Denko K.K., Japan) for HA-M2005. The eluents were $LiNO_3$ 0.1 $mol.L^{-1}$ and acetate buffer 0.1 $mol.L^{-1}$ (pH = 5) for HA-M2005 and PLL respectively. For SEC analysis, solutions of HA-M2005 or PLL of C_P = 1 $g.L^{-1}$ were prepared in the corresponding eluents and filtered through regenerated cellulose membrane 0.45 µm filter units (Sartorius, Germany). 100 µL of sample was injected for each analysis and the flow rate was 0.5 $mL.min^{-1}$. The refractive index increment (dn/dC) of 0.15 $mL.g^{-1}$ was applied for both HA-M2005 and PLL (Lai & Van Zanten, 2001; Madau et al., 2021). The data were analyzed with Astra 6.1.7.16 ® software using Zimm order 1. The elution profiles of HA-M2005 and PLL are shown in **Figure S2**.

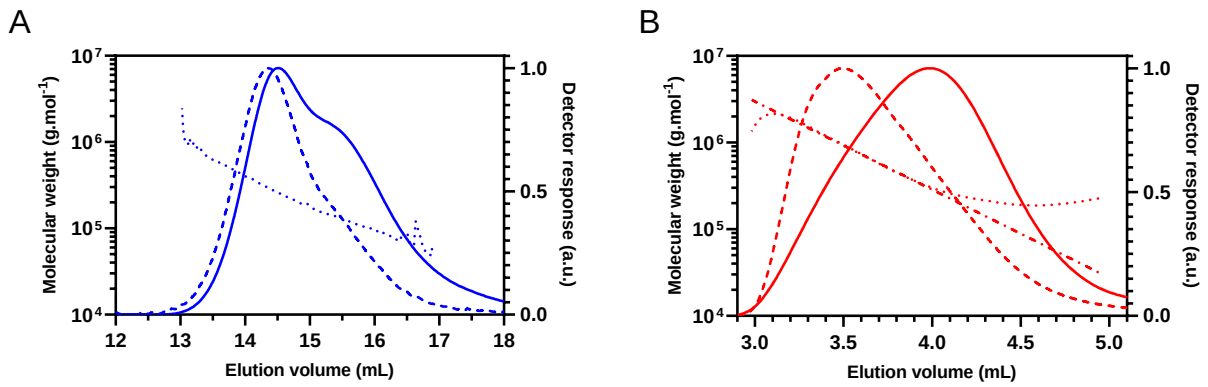

Figure S2. SEC elution profiles at 25 °C of HA-M2005 (**A**) and PLL (**B**). The full and dashed lines represent the responses of DRI and 90° light scattering detectors respectively. The dotted and dashdotted lines represent respectively unfitted and 1st order exponentially fitted molecular weight distributions.

SI-3. Calculation of volume ratio for complexation

Firstly, the ionization rate α in function of pH of the studied polymers were determined. Those of HA and DEAE-D were readily obtained in our previous work (Le et al., 2021). For HA-M2005, α is the number of deprotonated carboxylic groups per D-glucuronic-N-acetylglucosamine unit (either non-modified or grafted with M2005) and can be estimated in function of pH by using the modified Henderson-Hasselbalch equation for acids:

$$pH = pKa + \log[k\alpha/(1 - k\alpha)] \qquad \text{(Equation S1)}$$

with pKa of HA equal to 2.9 (Kayitmazer, Koksal, & Iyilik, 2015) and k is the ratio of total units to the units having carboxylic groups, which is equal to 1/0.964 for M2005 grafting with DS = 3.6 %. For PLL, α as the number of protonated amine per lysine unit can be calculated from the modified Henderson-Hasselbalch equation for bases (Equation S2) with pKa of PLL being 10.5 (Schwaighofer, Alcaráz, Araman, Goicoechea, & Lendl, 2016):

$$pH = pKa + \log[(1 - \alpha)/\alpha] \qquad \text{(Equation S2)}$$

The volume ratios between two reacting polymer solutions were calculated from targeted n-/n+ by using Equation S3:

$$n-/n+ = (\alpha^- \times V^- \times C^- \times M_o^+)/(\alpha^+ \times V^+ \times C^+ \times M_o^-) \qquad \text{(Equation S3)}$$

where α, V, C and M_o are respectively ionization rate, solution volume, solution concentration (m/v) and unit average molecular weight of the polyanions (-) and polycations (+). M_o of HA (D-glucuronic-N-acetylglucosamine units), DEAE-D (anhydroglucose units) and PLL (lysine units) are respectively 378, 217 and 128 $g.mol^{-1}$. M_o of HA-M2005 is 449 $g.mol^{-1}$ taking account of DS = 3.6 % and M2005 molecular weight being 1979 $g.mol^{-1}$. According to Equations S1 and S2, α values of the polymers in Milli-Q water (pH = 5–7) were at their maxima (1, 0.964, 0.55 and 1 for HA, HA-M2005, DEAE-D and PLL respectively).

SI-4. PEC-NG initial characterization

The IR spectra (**Figure S3**) were obtained using a Nicolet IS50 FT-IR spectrometer (Thermo Scientific, USA). There were no different peaks between the spectra of PEC-NGs and their corresponding polymer mixtures, proving the absence of significant chemical reactions between component polymers in PEC-NGs.

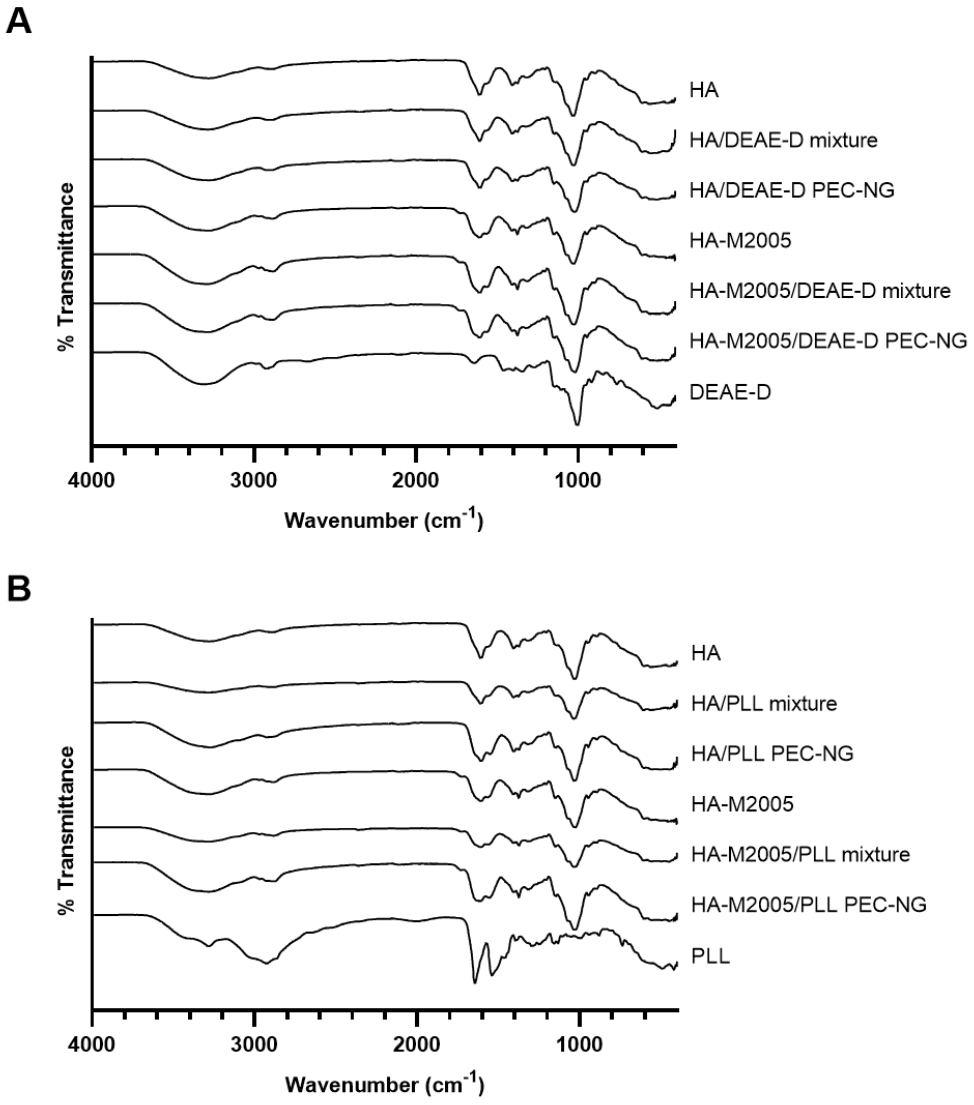

Figure S3. FT-IR spectra of material polymers, freeze-dried PEC-NGs (n-/n+ = 2.5) and polymer physical mixtures in the same mass ratio for systems comprising (**A**) HA or HA-M2005 and DEAE-D or (**B**) HA or HA-M2005 and PLL.

SI-5. Storage stability of PEC-NGs

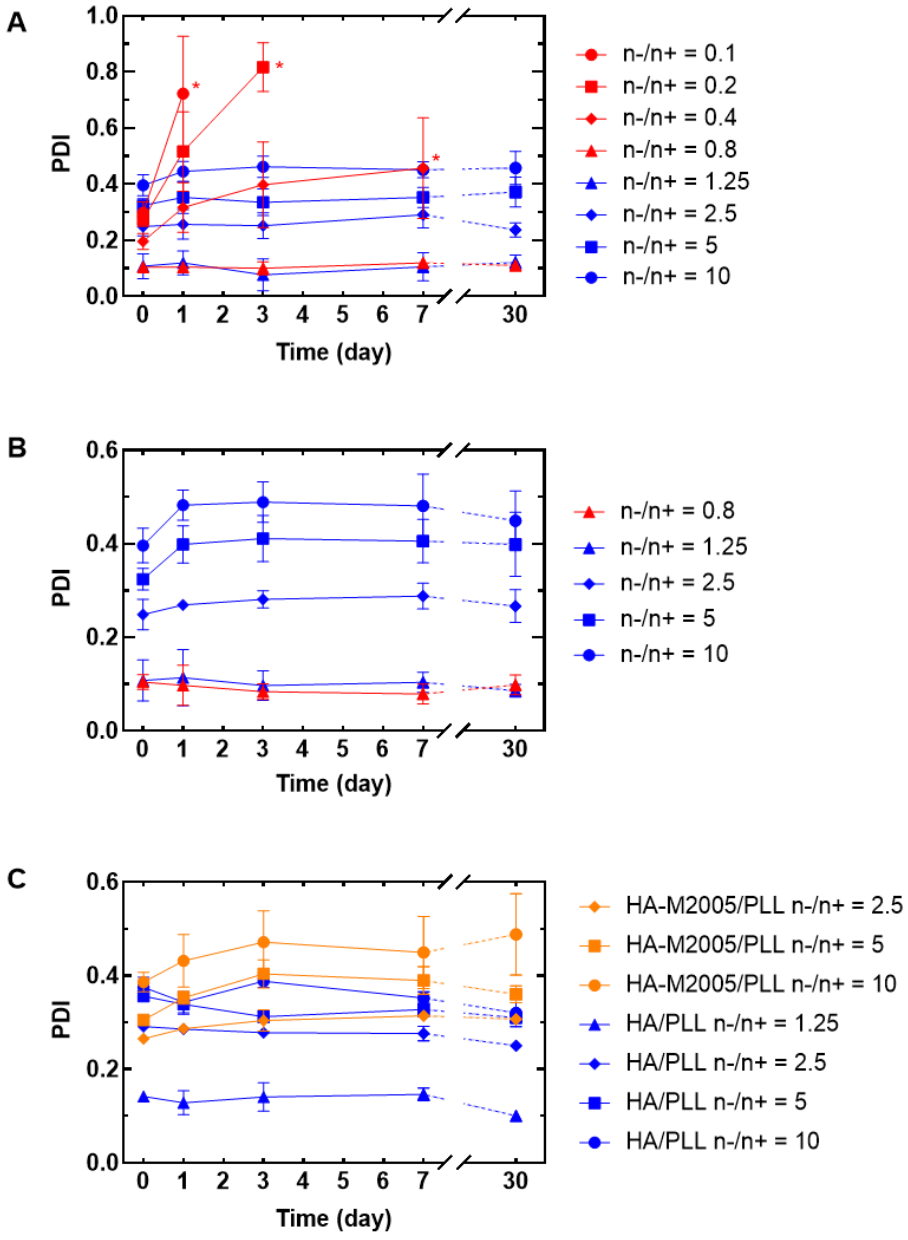

Figure S4. PDI of PEC-NGs (C_P = 0.5 g.L^{-1} in Milli-Q water) as a function of time: (**A**) HA-M2005/DEAE-D PEC-NGs stored at 4 °C, (**B**) HA-M2005/DEAE-D PEC-NGs stored at 25 °C and (**C**) HA-M2005/PLL and HA/PLL PEC-NGs stored at 4 °C. Asterisks represent samples having high particle sizes (mean D_h > 700 nm) with inconsistently large and heterogeneous distributions. Data are presented as mean ± standard deviation (n ≥ 3).

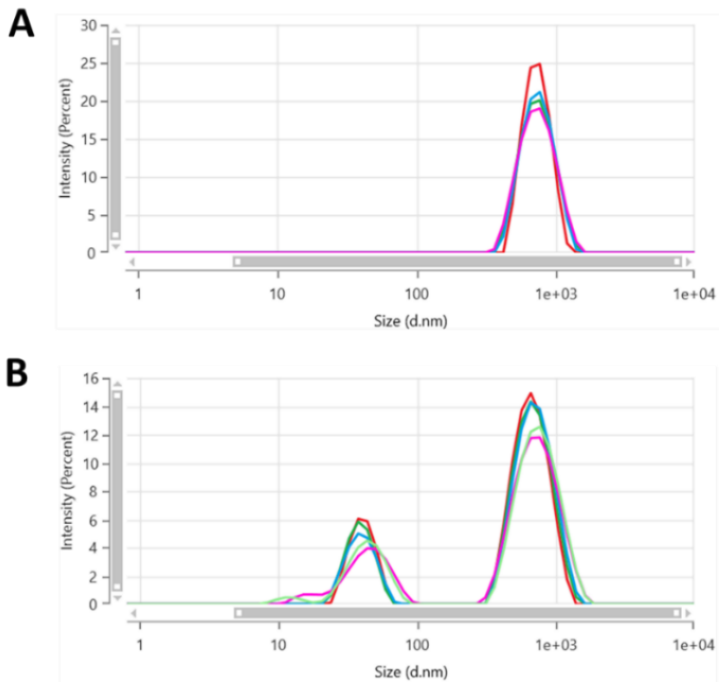

Figure S5. Intensity-weighted particle size distribution of HA/PLL PEC-NGs (n-/n+ = 2.5 and C_P = 0.5 g.L^{-1}) after seven days (A) and one month (B) in NaCl 0.9 % (analysis on one batch).

SI-6. Thermoresponsiveness of PEC-NGs

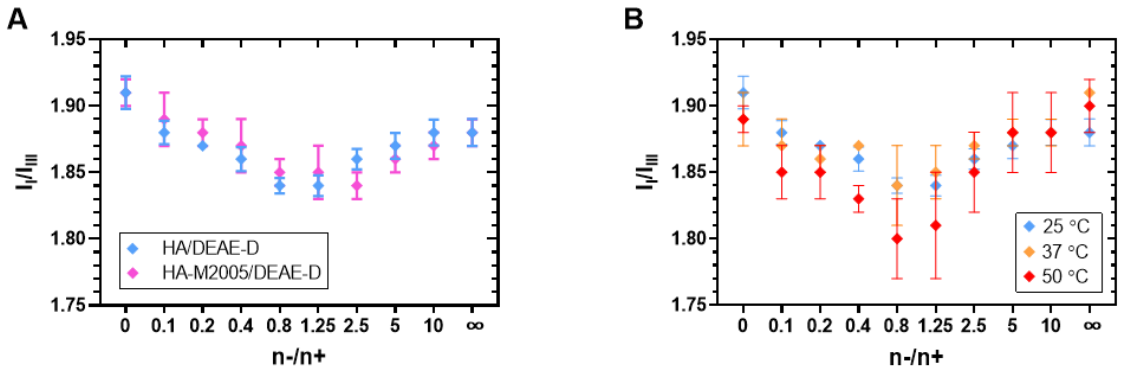

Figure S6. I_I/I_{III} in pyrene fluorescence of (**A**) HA-M2005/DEAE-D at 25 °C in comparison with HA/DEAE-D PEC-NGs in the previous work (Le et al., 2021) and (**B**) HA/DEAE-D PEC-NGs at different temperatures. The values 0 and ∞ represent solutions containing solely polycations and polyanions respectively. All results were obtained at C_P = 0.25 g.L^{-1}. Data are presented as mean ± standard deviation (n ≥ 3).

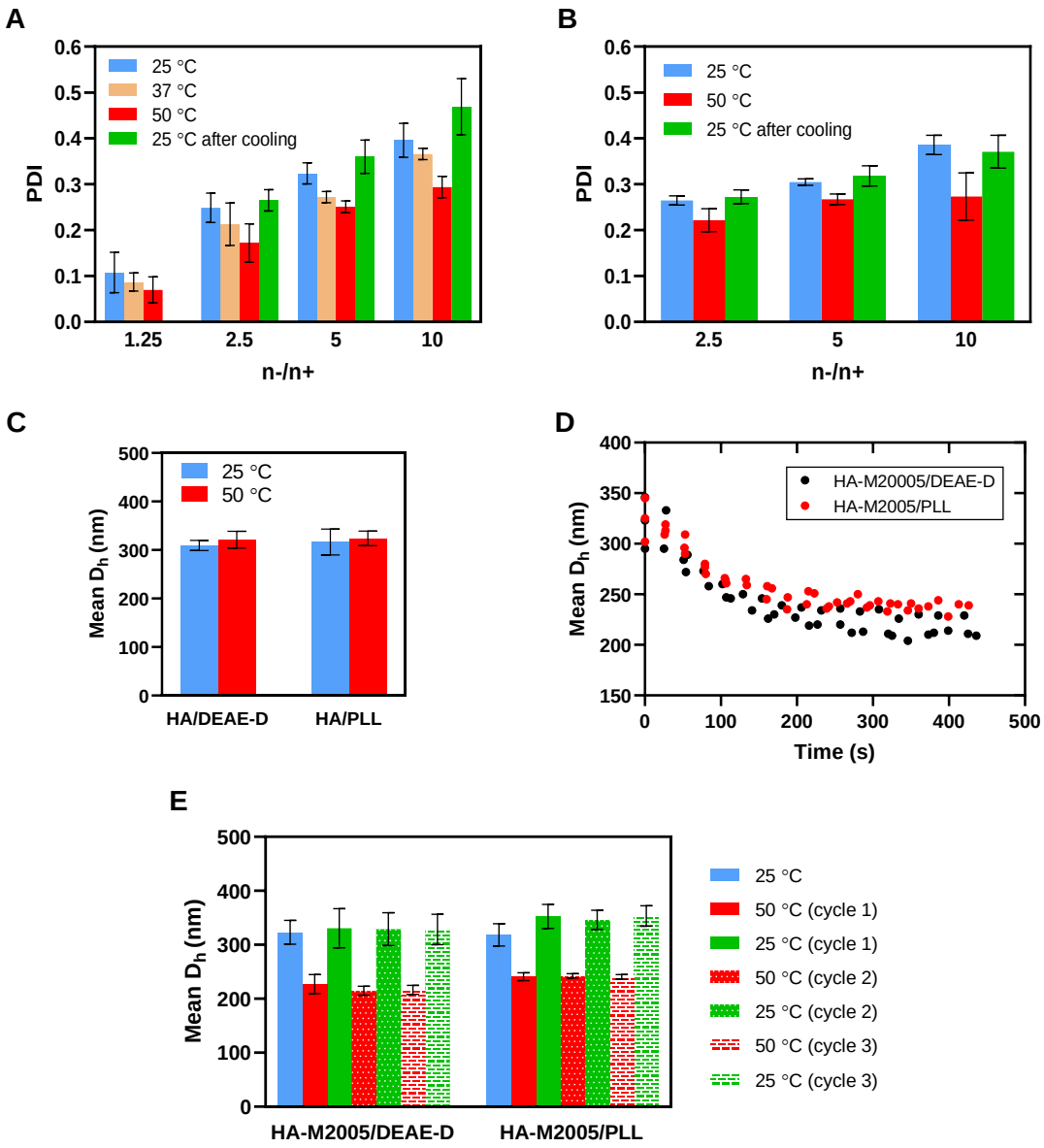

Figure S7. A-B: PDI of HA-M2005/DEAE-D and HA-M2005/PLL PEC-NGs respectively (C_P = 0.5 g.L^{-1}) at different temperatures. **C**: Mean D_h of HA/DEAE-D and HA/PLL PEC-NGs (n-/n+ = 10 and C_P = 0.5 g.L^{-1}) at 25 and 50 °C. **D**: Mean D_h of HA-M2005/DEAE-D and HA-M2005/PLL PEC-NGs (n-/n+ = 5 and C_P = 0.5 g.L^{-1}) as a function of time after temperature elevation to 50 °C. **E**: Mean D_h of HA-M2005/DEAE-D and HA-M2005/PLL PEC-NGs (n-/n+ = 5 and C_P = 0.5 g.L^{-1}) during three cycles of heating-cooling. Data in subfigures **A**, **B**, **C** and **E** are presented as mean ± standard deviation (n ≥ 3).

SI-7. Curcumin encapsulation

Table S1. Physico-chemical characteristics of PEC-NGs encapsulating curcumin

Sample*	Physicochemical characteristics **		
	Mean D_h (nm)	**PDI**	**Mean ζ (mV)**
HA-M2005/DEAE-D/Cur	266 ± 18	0.281 ± 0.075	-33.3 ± 3.8
HA-M2005/PLL/Cur	287 ± 26	0.276 ± 0.043	-42.7 ± 1.4

* C_P = 0.5 g.L^{-1}, n-/n+ = 2.5, complexation at 50 °C

** Data presented as mean ± standard deviation (n ≥ 3)

SI-8. Enzymatic degradation

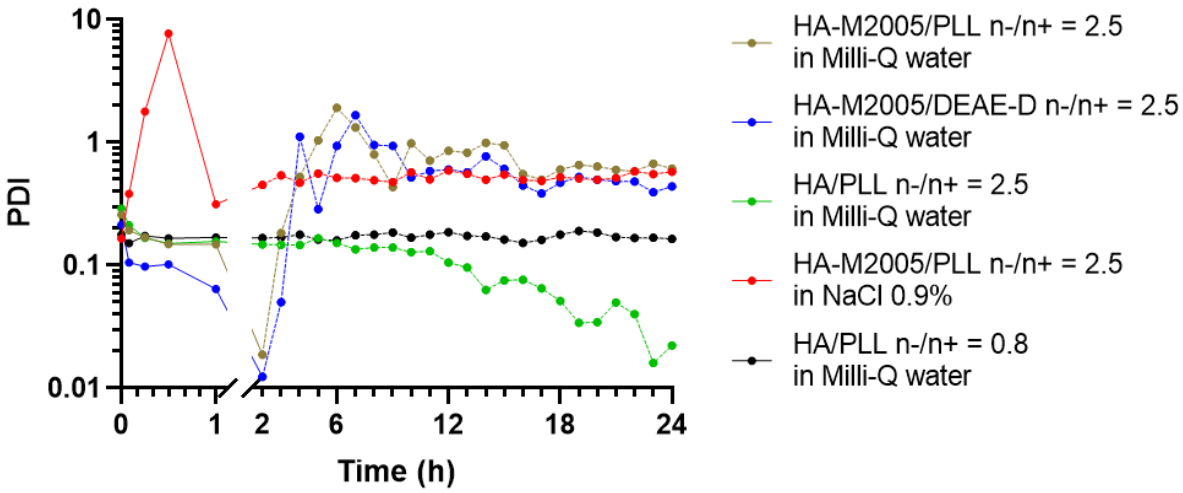

Figure S8. Temporal evolution of PDI of different PEC-NGs in the presence of HAase 0.03 g.L^{-1} (12 IU.mL^{-1}) during 24 h at 37 °C. Data were obtained from one experiment, results of replicated experiments showed similar trends.

References

Agut, W., Brûlet, A., Taton, D., & Lecommandoux, S. (2007). Thermoresponsive micelles from Jeffamine-b-poly (L-glutamic acid) double hydrophilic block copolymers. *Langmuir*, 23(23), 11526-11533. https://doi.org/10.1021/la701482w.

Astériou, T., Vincent, J.-C., Tranchepain, F., & Deschrevel, B. (2006). Inhibition of hyaluronan hydrolysis catalysed by hyaluronidase at high substrate concentration and low ionic strength. *Matrix Biology*, 25(3), 166-174. https://doi.org/10.1016/j.matbio.2005.11.005.

Bonaccorso, A., Carbone, C., Tomasello, B., Italiani, P., Musumeci, T., Puglisi, g., et al. (2021). Optimization of dextran sulfate/poly-l-lysine based nanogels polyelectrolyte complex for intranasal ovalbumin delivery. *Journal of Drug Delivery Science and Technology*, 65, 102678. https://doi.org/10.1016/j.jddst.2021.102678.

Bordat, A., Boissenot, T., Nicolas, J., & Tsapis, N. (2019). Thermoresponsive polymer nanocarriers for biomedical applications. *Advanced Drug Delivery Reviews*, 138, 167-192. https://doi.org/10.1016/j.addr.2018.10.005.

Burdíková, J., Mravec, F., & Pekař, M. (2016). The formation of mixed micelles of sugar surfactants and phospholipids and their interactions with hyaluronan. *Colloid and Polymer Science*, 294(5), 823-831. https://doi.org/10.1007/s00396-016-3840-8.

Debele, T. A., Mekuria, S. L., & Tsai, H.-C. (2016). Polysaccharide based nanogels in the drug delivery system: Application as the carrier of pharmaceutical agents. *Materials Science and Engineering: C*, 68, 964-981. https://doi.org/10.1016/j.msec.2016.05.121.

Díaz-Montes, E. (2021). Dextran: Sources, Structures, and Properties. *Polysaccharides*, 2(3), 554-565. https://doi.org/10.3390/polysaccharides2030033.

Dioury, F., Callewaert, M., Cadiou, C., Henoumont, C., Molinari, M., Laurent, S., et al. (2021). Pyclen-based Gd complex with ionisable side-chain as a contrastophore for the design of hypersensitive MRI nanoprobes: Synthesis and relaxation studies. *Results in Chemistry*, 3, 100237. https://doi.org/10.1016/j.rechem.2021.100237.

Dulong, V., Mocanu, g., Picton, L., & Le Cerf, D. (2012). Amphiphilic and thermosensitive copolymers based on pullulan and Jeffamine®: Synthesis, characterization and physicochemical properties. *Carbohydrate Polymers,* 87(2), 1522-1531. https://doi.org/10.1016/j.carbpol.2011.09.049.

Dyson, H. J., Wright, P. E., & Scheraga, H. A. (2006). The role of hydrophobic interactions in initiation and propagation of protein folding. *Proceedings of the National Academy of Sciences,* 103(35), 13057-13061. https://doi.org/10.1073/pnas.0605504103.

Gandhi, A., Paul, A., Sen, S. O., & Sen, K. K. (2015). Studies on thermoresponsive polymers: Phase behaviour, drug delivery and biomedical applications. *Asian Journal of Pharmaceutical Sciences,* 10(2), 99-107. https://doi.org/10.1016/j.ajps.2014.08.010.

Gómez-Mascaraque, L. g., Sipoli, C. C., de La Torre, L. g., & López-Rubio, A. (2017). Microencapsulation structures based on protein-coated liposomes obtained through electrospraying for the stabilization and improved bioaccessibility of curcumin. *Food Chemistry,* 233, 343-350. https://doi.org/10.1016/j.foodchem.2017.04.133.

Graham, S., Marina, P. F., & Blencowe, A. (2019). Thermoresponsive polysaccharides and their thermoreversible physical hydrogel networks. *Carbohydrate Polymers,* 207, 143-159. https://doi.org/10.1016/j.carbpol.2018.11.053.

Gulick, T. (1997). Transfection using DEAE‐dextran. *Current Protocols in Molecular Biology,* 40(1), 9.2. 1-9.2. 10. https://doi.org/10.1002/0471142727.mb0902s40.

Gupta, N. R., Wadgaonkar, P. P., Rajamohanan, P., Ducouret, g., Hourdet, D., Creton, C., et al. (2015). Synthesis and characterization of PEPO grafted carboxymethyl guar and carboxymethyl tamarind as new thermo-associating polymers. *Carbohydrate Polymers,* 117, 331-338. https://doi.org/10.1016/j.carbpol.2014.09.073.

Huguet, M., Neufeld, R., & Dellacherie, E. (1996). Calcium-alginate beads coated with polycationic polymers: comparison of chitosan and DEAE-dextran. *Process Biochemistry,* 31(4), 347-353. https://doi.org/10.1016/0032-9592(95)00076-3.

Karimi, M., Sahandi Zangabad, P., Ghasemi, A., Amiri, M., Bahrami, M., Malekzad, H., et al. (2016). Temperature-responsive smart nanocarriers for delivery of therapeutic agents: applications and recent advances. *ACS Applied Materials & Interfaces,* 8(33), 21107-21133. https://doi.org/10.1021/acsami.6b00371.

Kayitmazer, A., Koksal, A., & Iyilik, E. K. (2015). Complex coacervation of hyaluronic acid and chitosan: effects of pH, ionic strength, charge density, chain length and the charge ratio. *Soft Matter,* 11(44), 8605-8612. https://doi.org/10.1039/C5SM01829C.

Kim, Y. K., Kim, E.-J., Lim, J. H., Cho, H. K., Hong, W. J., Jeon, H. H., et al. (2019). Dual stimuli-triggered nanogels in response to temperature and pH changes for controlled drug release. *Nanoscale Research Letters,* 14(1), 1-9. https://doi.org/10.1186/s11671-019-2909-y.

Lai, E., & Van Zanten, J. H. (2001). Monitoring DNA/poly-L-lysine polyplex formation with time-resolved multiangle laser light scattering. *Biophysical Journal,* 80(2), 864-873. https://doi.org/10.1016/S0006-3495(01)76065-1.

Le, H. V., Dulong, V., Picton, L., & Le Cerf, D. (2021). Polyelectrolyte complexes of hyaluronic acid and diethylaminoethyl dextran: Formation, stability and hydrophobicity. *Colloids and Surfaces A: Physicochemical and Engineering Aspects,* 629, 127485. https://doi.org/10.1016/j.colsurfa.2021.127485.

Madau, M., Le Cerf, D., Dulong, V., & Picton, L. (2021). Hyaluronic Acid Functionalization with Jeffamine® M2005: A Comparison of the Thermo-Responsiveness Properties of the Hydrogel Obtained through Two Different Synthesis Routes. *Gels,* 7(3), 88. https://doi.org/10.3390/gels7030088.

Manosroi, A., & Manosroi, J. (1997). Micro encapsulation of human insulin DEAE-dextran complex and the complex in liposomes by the emulsion non-solvent addition method. *Journal of Microencapsulation,* 14(6), 761-768. https://doi.org/10.3109/02652049709006826.

Molina, M., Asadian-Birjand, M., Balach, J., Bergueiro, J., Miceli, E., & Calderón, M. (2015). Stimuli-responsive nanogel composites and their application in nanomedicine. *Chemical Society Reviews,* 44(17), 6161-6186. https://doi.org/10.1039/C5CS00199D.

Necas, J., Bartosikova, L., Brauner, P., & Kolar, J. (2008). Hyaluronic acid (hyaluronan): a review. *Veterinární Medicína,* 53(8), 397-411. https://doi.org/10.17221/1930-VETMED.

Niang, P. M., Huang, Z., Dulong, V., Souguir, Z., Le Cerf, D., & Picton, L. (2016). Thermo-controlled rheology of electro-assembled polyanionic polysaccharide (alginate) and polycationic thermo-sensitive polymers. *Carbohydrate Polymers,* 139, 67-74. https://doi.org/10.1016/j.carbpol.2015.12.022.

Pan, W., Yin, D.-X., Jing, H.-R., Chang, H.-J., Wen, H., & Liang, D.-H. (2019). Core-Corona structure formed by hyaluronic acid and poly (L-lysine) via kinetic path. *Chinese Journal of Polymer Science,* 37(1), 36-42. https://doi.org/10.1007/s10118-018-2166-z.

Rumble, J. (2021). CRC Handbook of Chemistry and Physics, 102nd Edition (Internet Version 2021). CRC Press: Boca Raton, FL, USA. https://hbcp.chemnetbase.com.

Sarika, P., & James, N. R. (2016). Polyelectrolyte complex nanoparticles from cationised gelatin and sodium alginate for curcumin delivery. *Carbohydrate Polymers,* 148, 354-361. https://doi.org/10.1016/j.carbpol.2016.04.073.

Schwaighofer, A., Alcaráz, M. R., Araman, C., Goicoechea, H., & Lendl, B. (2016). External cavity-quantum cascade laser infrared spectroscopy for secondary structure analysis of proteins at low concentrations. *Scientific Reports,* 6(1), 1-10. https://doi.org/10.1038/srep33556.

Siow, W. X., Chang, Y.-T., Babič, M., Lu, Y.-C., Horák, D., & Ma, Y.-H. (2018). Interaction of poly-L-lysine coating and heparan sulfate proteoglycan on magnetic nanoparticle uptake by tumor cells. *International Journal of Nanomedicine,* 13, 1693. https://doi.org/10.2147/IJN.S156029.

Stern, R. (2008). *Hyaluronidases in Cancer Biology*. In R. Stern (Ed.), *Hyaluronan in Cancer Biology* (pp. 207-220). San Diego: Academic Press. https://doi.org/10.1016/B978-012374178-3.10012-2.

Wu, D., & Delair, T. (2015). Stabilization of chitosan/hyaluronan colloidal polyelectrolyte complexes in physiological conditions. *Carbohydrate Polymers,* 119, 149-158. https://doi.org/10.1016/j.carbpol.2014.11.042.

Xu, H., Niu, M., Yuan, X., Wu, K., & Liu, A. (2020). CD44 as a tumor biomarker and therapeutic target. *Experimental Hematology & Oncology*, 9(1), 1-14. https://doi.org/10.1186/s40164-020-00192-0.

Yang, Y., Zhang, Y.-M., Chen, Y., Chen, J.-T., & Liu, Y. (2016). Polysaccharide-based noncovalent assembly for targeted delivery of taxol. *Scientific Reports*, 6(1), 1-10. https://doi.org/10.1038/srep19212.

III.3. Etudes complémentaires

III.3.1. Etalonnage de la quantification de la curcumine

Pour préparer la gamme étalon de curcumine à 0,05-10 µg.mL^{-1} dans eau/HCl 1M/EtOH 10/1/55 v/v (**Section III.2**), 100 µL de solution mère de curcumine à 5 mg.mL^{-1} dans l'acétone sont d'abord ajoutés dans une fiole jaugée de 50 mL et laissés au repos pendant 30 min pour l'évaporation de l'acétone. La fiole est ensuite remplie avec de l'eau/HCl 1M/EtOH 10/1/55 v/v et la solution est agitée pendant 1 h pour obtenir la solution étalon à 10 µg.mL^{-1} en curcumine. Elle est ensuite diluée pour obtenir les solutions étalons aux concentrations de 5, 1, 0,5, 0,1 et 0,05 µg.mL^{-1} en curcumine. L'absorbance à λ = 420 nm (A_{420}) de ces solutions est ensuite mesurée et la courbe d'étalonnage est ainsi obtenue (**Figure III-1**).

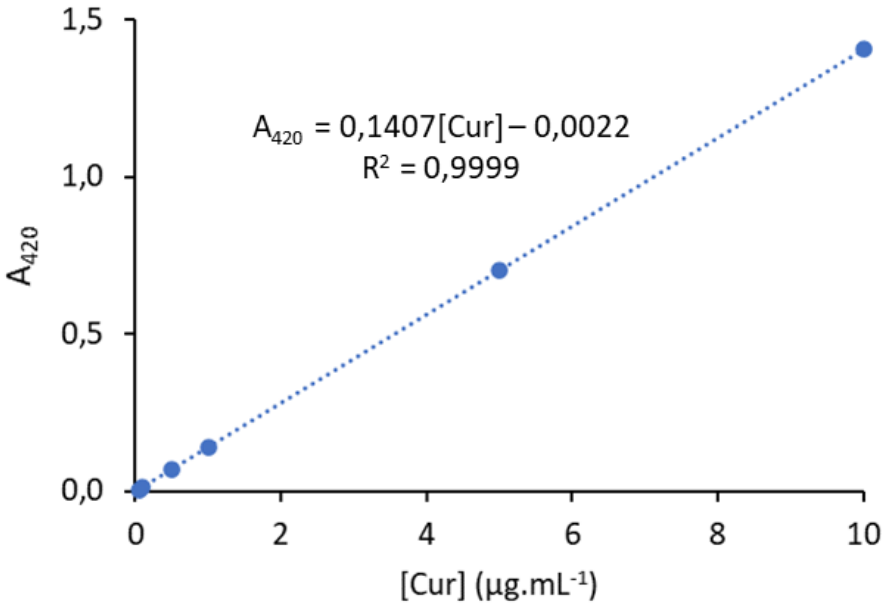

Figure III-1. Absorbance à λ = 420 nm (A_{420}) en fonction de concentration de curcumine [Cur] dans eau/HCl 1M/EtOH 10/1/55 v/v (n = 1)

III.3.2. Evolution de la taille des PEC-NGs thermosensibles en fonction de température

Nous avons examiné l'évolution de la taille des PEC-NGs de HA-M2005/PLL (C_P = 0,5 g.L^{-1}, n-/n+ = 2,5) lors d'une augmentation de température de 25 à 60 °C pour déterminer la température à laquelle la contraction des PEC-NGs est maximale. Comme présenté dans la **Figure III-2**, il apparait que la taille moyenne de ces PEC-NGs ne diminue plus quand la température dépasse 45 °C mais atteint un plateau. Par conséquent, les tailles des PEC-NGs à 50 °C présentées dans la **Section III.2** peuvent être considérées comme leur état le plus contracté lors de l'augmentation de la température dans les conditions normales (i.e. à pression atmosphérique).

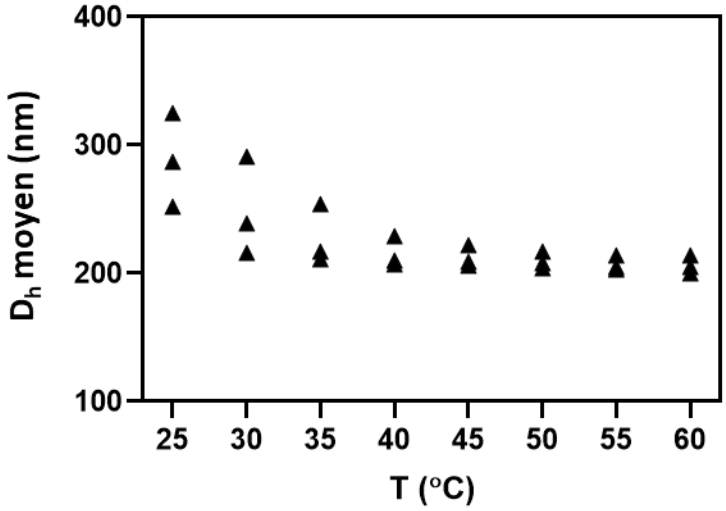

Figure III-2. D_h moyen des PEC-NGs de HA-M2005/PLL (C_P = 0,5 g.L^{-1}, n-/n+ = 2,5) en fonction de température (n = 3)

III.3.3. Libération in vitro de la curcumine

Pour vérifier la capacité de libérer des substances actives (SAs) de manière contrôlée des PEC-NGs, nous avons réalisé une étude de libération de la curcumine par la méthode de dialyse pour les PEC-NGs avec le taux d'encapsulation le plus élevée parmi les systèmes précédemment étudiés, soit les PEC-NGs de HA-M2005/PLL/Cur à n-/n+ = 2,5 et C_P = 0,5 g.L^{-1} préparés à la température de complexation de 50 °C. En principe, pour ce type d'étude, les formulations d'intérêt sont souvent mises en dialyse contre un volume important de solvant aqueux correspondant à la condition *sink* (e.g. au moins 3 à 10 fois le volume de saturation pour la quantité totale de la SA dans la formulation d'intérêt [1]) pour simuler le milieu physiologique, avant la quantification de la fraction libérée des molécules d'intérêt dans le milieu de dialyse au cours du temps. Cependant, dans notre cas, la concentration peu élevée en curcumine encapsulée dans les PEC-NGs pourrait entrainer des difficultés en termes d'exactitude pour sa quantification pendant la libération. Pour contourner ce problème, deux stratégies sont envisageables : (i) augmentation de la concentration en curcumine dans les formulations d'intérêt par lyophilisation et reconstitution de manière à atteindre un volume moins élevé que celui de départ, ou (ii) utilisation de moins de solvant de dialyse en ajoutant un tensioactif pour augmenter la capacité de solubilisation pour maintenir la condition *sink*. La première approche nécessite tout un travail en amont afin de pouvoir redisperser les PEC-NGs à l'état colloïdal après lyophilisation. Ce travail sera présenté dans le dernier chapitre. Nous avons ici privilégié la deuxième approche en utilisant le monolaurate de polyoxyéthylène sorbitane (i.e. Tween 20) comme tensioactif [2]. Le protocole a été adapté des méthodes décrites dans la littérature [2, 3]. Plus précisément, 3 mL de suspension de PEC-NGs et 75 µL de PBS 40X sont introduits dans un tube de dialyse à seuil de coupure de 12-14 kDa (Millipore, Allemagne) et dialysés contre 21 mL de tampon PBS 1X (pH 7,4) avec une

concentration globale de 0,5 % (w/v) en Tween 20 (Sigma-Aldrich, Allemagne) et de 0,5 mmol.L^{-1} en acide ascorbique (Acros Organics, États-Unis), qui permet d'éviter l'oxydation et donc la dégradation de la curcumine [3]. La dialyse est effectuée sous agitation (100 rpm) à 37 °C. Pour quantifier la fraction cumulative de la curcumine libérée, 700 µL de milieu de dialyse sont prélevés à des moments prédéterminés pour réaliser les mesures d'absorbance à 420 nm (A_{420}) (Agilent Technology, États-Unis) et sont remplacés par un même volume de solvant de dialyse pour maintenir la condition *sink*. La courbe d'étalonnage de A_{420} du solvant de dialyse pour une gamme de concentration en curcumine [Cur] de 0,01-1 µg.L^{-1} est présentée dans la **Figure III-3**. Afin d'étudier l'impact de la température sur la cinétique de libération, les mêmes expériences sont également réalisées à 42 °C, soit la température maximale applicable pour une hyperthermie locale en clinique [4, 5]. Les expériences sont répétées sur trois lots de PEC-NGs.

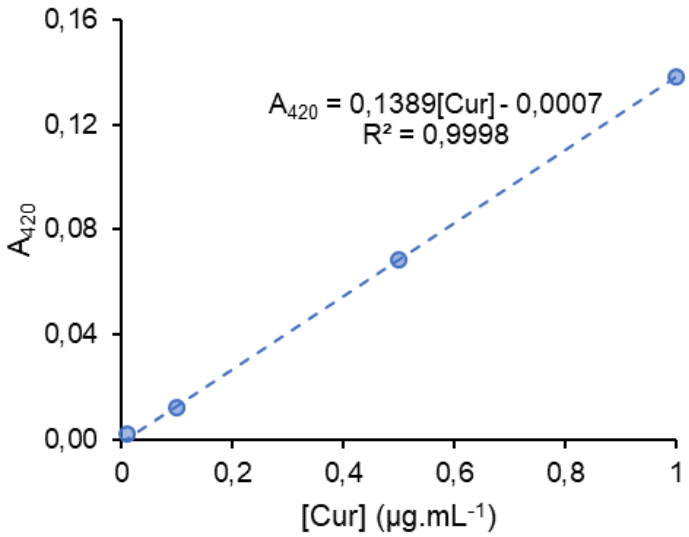

Figure III-3. Courbe d'étalonnage pour la quantification de la curcumine dans le tampon PBS à pH = 7,4 avec 0,5 % (m/v) en Tween 20 et 0,5 mmol.L^{-1} en acide ascorbique par mesure d'absorbance à 420 nm.

Les résultats de cinétique de libération sont illustrés dans la **Figure III-4**. Selon la **Figure III-4**A, la cinétique de libération à 37 °C commence avec une libération rapide dans les premières heures et s'avère progressivement plus lente par la suite pour atteindre une fraction cumulative de curcumine libérée d'environ 90 % après 96 h.

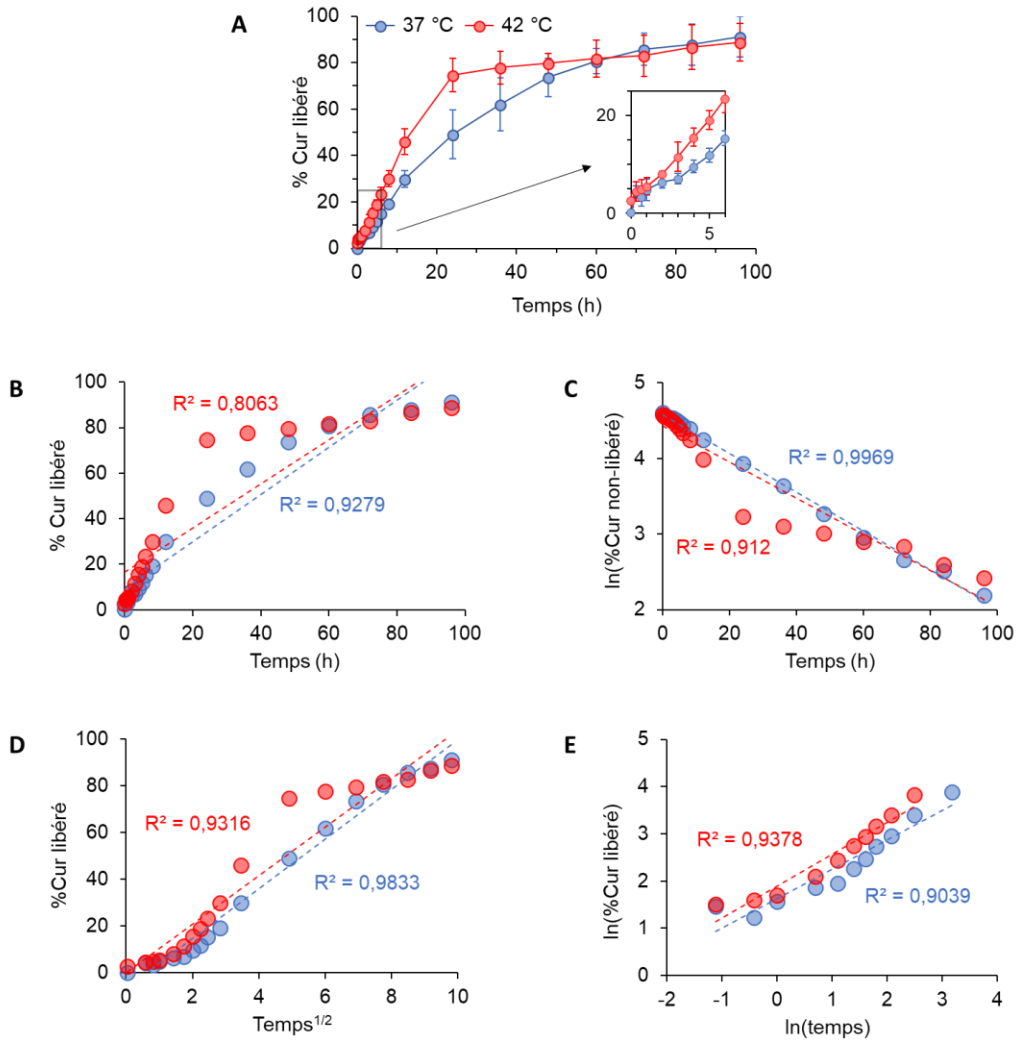

Figure III-4. (**A**) Libération cumulative *in vitro* de la curcumine encapsulée dans les PEC-NGs de HA-M2005/PLL (n-/n+ = 2,5, C_P = 0,5 g.L^{-1}) par dialyse dans du tampon PBS 10 mM à pH 7,4 avec 0,5 % (m/v) en Tween 20 et 0,5 mmol.L^{-1} en acide ascorbique à 37 °C (bleu) et à 42 °C (rouge). (**B**), (**C**), (**D**), (**E**) : Données de libération cumulative ajustées selon quatre modèles respectivement : ordre zéro, premier ordre, Higuchi et Korsmeyer-Peppas.

La libération rapide du début est souvent appelée effet *burst* dans la littérature. Elle est due à la libération des molécules de curcumine situées au voisinage de la couche externe très hydrophile des PEC-NGs, alors que la libération lente par la suite est probablement liée à la sortie de la curcumine séquestrée dans le cœur des particules, qui a une hydrophobicité importante avec une forte affinité avec la curcumine et ralentit ainsi sa libération. Par rapport à la libération à 37 °C, celle à 42 °C présente plus clairement les deux phases avec une libération significativement plus rapide que celle à 37 °C dans la première phase, en accord avec les résultats précédents qui montraient la contraction des NGs avec l'augmentation de la température. Logiquement, ce dernier phénomène peut conduire à l'expulsion de l'eau et de la curcumine et donc une libération plus rapide [4]. Des résultats similaires ont également été observés dans plusieurs études précédentes sur des systèmes thermosensibles de type LCST, e.g. la libération du méthotrexate des micelles polymères de poly(N-isopropylacrylamide-*co*-acrylamide)-*b*-poly(n-butylmethacrylate) (P(NIPAAm-*co*-AAm)-*b*-PBMA) [5] ou de la curcumine et de la doxorubicine des nanoparticules de Fe_3O_4 enduites du poly(N-isopropylacrylamide) (PNIPAM) [6]. Dans leur ensemble, ces résultats ont une fois encore confirmé l'application potentielle de nos NGs pour une libération contrôlée des SAs activable par hyperthermie locale.

Concernant le mécanisme de libération, celle-ci peut être contrôlée par une complexité de différents facteurs, comme la diffusion simple ou/et le gonflement et la dégradation/désintégration des NGs, ou même par les stimuli externes comme le changement de température dans le cas des NGs thermosensibles [7]. Afin de mieux comprendre les mécanismes principaux de la libération de manière prédictive, les données de la cinétiques de libération peuvent être tracées selon les modèles mathématiques, dont les plus classiques sont ceux d'ordre zéro (régression linéaire entre la quantité de SA libéré et le temps), de premier ordre (régression linéaire entre le logarithme de

la quantité de SA restant dans la formulation et le temps), de Higuchi (régression linéaire entre la quantité de SA libéré et la racine carrée du temps) et de Korsmeyer-Peppas (régression linéaire entre le logarithme de la quantité de SA libéré et celui du temps pour le premier 60 % de SA libérée). Les équations de ces différents modèles sont largement utilisées dans la littérature [7, 8]. En appliquant ces démarches sur la libération de la curcumine de nos PEC-NGs (**Figure III-4**B-E) et en comparant les coefficients de régression (R^2) obtenus, il semble que le modèle de premier ordre montre le meilleur ajustement à la libération à 37 °C (R^2 = 0,9969), ce qui démontre que la vitesse de libération de la curcumine n'est pas constante mais dépend de sa concentration au sein des NGs au cours du temps [8]. Par contre, l'ajustement du profil de libération à 42 °C avec ce même modèle n'est pas aussi bon (R^2 = 0,9120) car les points expérimentaux sur les temps longs semblent s'écarter de la première linéarité. En général, en présentant deux phases strictement distinctes, la libération à 42 °C semble impliquer des mécanismes différents selon les phases et ainsi plus compliqués que ceux de la libération à 37 °C. En regardant les valeurs R^2 du l'ajustement des modèles pour la libération à 42 °C, il semble qu'aucun modèle parmi les modèles classiques examinés n'est capable d'expliquer parfaitement les mécanismes de libération dans ce cas. En conséquence, des études plus approfondies, notamment au niveau de la modélisation, seraient nécessaires pour une compréhension précise des propres mécanismes de libération des SAs à partir des PEC-NGs de HA-M2005/PLL à cette température.

Références

[1] D.D. Sun, H. Wen, L.S. Taylor, Non-sink dissolution conditions for predicting product quality and in vivo performance of supersaturating drug delivery systems, Journal of Pharmaceutical Sciences, 105 (2016) 2477-2488. https://doi.org/10.1016/j.xphs.2016.03.024.

[2] A. Puiggalí-Jou, P. Micheletti, F. Estrany, L.J. Del Valle, C. Alemán, Electrostimulated release of neutral drugs from Polythiophene nanoparticles: smart regulation of drug–polymer interactions, Advanced Healthcare Materials, 6 (2017) 1700453. https://doi.org/10.1002/adhm.201700453.

[3] J.-M. Rabanel, J. Faivre, G.D. Paka, C. Ramassamy, P. Hildgen, X. Banquy, Effect of polymer architecture on curcumin encapsulation and release from PEGylated polymer nanoparticles: Toward a drug delivery nano-platform to the CNS, European Journal of Pharmaceutics and Biopharmaceutics, 96 (2015) 409-420. https://doi.org/10.1016/j.ejpb.2015.09.004.

[4] A. Bordat, T. Boissenot, J. Nicolas, N. Tsapis, Thermoresponsive polymer nanocarriers for biomedical applications, Advanced Drug Delivery Reviews, 138 (2019) 167-192. https://doi.org/10.1016/j.addr.2018.10.005.

[5] F. Sun, Y. Wang, Y. Wei, G. Cheng, G. Ma, Thermo-triggered drug delivery from polymeric micelles of poly (N-isopropylacrylamide-co-acrylamide)-b-poly (n-butyl methacrylate) for tumor targeting, Journal of Bioactive and Compatible Polymers, 29 (2014) 301-317. https://doi.org/10.1177/0883911514535288.

[6] K. Asghar, M. Qasim, G. Dharmapuri, D. Das, Investigation on a smart nanocarrier with a mesoporous magnetic core and thermo-responsive shell for co-delivery of doxorubicin and curcumin: a new approach towards combination therapy of cancer, RSC Advances, 7 (2017) 28802-28818. https://doi.org/10.1039/c7ra03735j.

[7] J.H. Lee, Y. Yeo, Controlled drug release from pharmaceutical nanocarriers, Chemical Engineering Science, 125 (2015) 75-84. https://doi.org/10.1016/j.ces.2014.08.046.

[8] M.L. Bruschi, 5 - Mathematical models of drug release, in: M.L. Bruschi (Ed.), Strategies to Modify the Drug Release from Pharmaceutical Systems, Woodhead Publishing, 2015, pp. 63-86. https://doi.org/10.1016/B978-0-08-100092-2.00005-9.

III.4. Conclusion et perspectives

A travers les résultats de ce chapitre, nous avons vu que l'incorporation des greffons M2005 sur le HA et le remplacement du DEAE-D par la PLL permettent d'élaborer des PEC-NGs plus hydrophobes pour encapsuler la curcumine et plus stables vis-à-vis de la salinité physiologique par rapport aux PECs de HA/DEAE-D discutés dans le chapitre précédent. De plus, la thermosensibilité apportée aux PEC-NGs par les greffons M2005 peut permettre d'améliorer le taux d'encapsulation des SAs et d'accélérer leur libération par augmentation de la température. La dégradation de ces PEC-NGs peut également être provoquée par la HAase, qui pourra probablement faciliter la libération des SAs. L'ensemble de ces aspects constituera un système prometteur pour l'administration des SAs hydrophobes dans les tumeurs, où la HAase est présente en grande quantité, et l'application d'une hyperthermie locale est possible pour synergétiquement susciter la libération des SAs. Toutefois, vue l'augmentation lente de la taille des PEC-NGs conservés en milieu aqueux, il est probable qu'une conservation à long terme conduira à des changements plus significatifs. De plus, comme discuté ci-dessus, la concentration en SAs encapsulées peut être trop faible pour certaines applications. Par conséquent, il est nécessaire d'optimiser davantage les formulations en matière de stabilité et de teneur en SAs, ce qui sera abordé dans le chapitre suivant avec l'utilisation de la lyophilisation et de l'autoclave.

Chapitre IV

Lyophilisation et traitement autoclave des nanogels

IV.1. Introduction

Ce chapitre porte sur l'application de la lyophilisation et de l'autoclave sur nos formulations de PEC-NGs, avec un intérêt plus particulier pour ceux à nature thermosensible. En effet, il s'agit deux procédés assez classiques couramment utilisés pour les produits pharmaceutiques et biomédicaux, soit pour la suppression d'eau (lyophilisation) afin d'une conservation à long terme soit pour leur stérilisation (autoclave). Malgré ces intérêts classiques, peu de travail dans la littérature porte sur l'application de ces deux procédés pour optimiser la formulation des PEC-NGs. Dans ces perspectives, nous avons étudié le traitement de nos PEC-NGs par ces techniques en vue de vérifier leur applicabilité pour optimiser la formulation, la conservation et la stabilité de nos formulations. Dans chacune des sections suivantes, le contexte scientifique ainsi que les objectifs pour les études sur chaque procédé seront abordés en détail avant la présentation des résultats obtenus.

IV.2. Lyophilisation des PEC-NGs

IV.2.1. Intérêts de la lyophilisation des PEC-NGs

La lyophilisation est un procédé de déshydratation par sublimation de l'eau congelée sous vide [1]. Elle est largement appliquée pour la conservation à sec et l'amélioration de la stabilité à long terme des produits pharmaceutiques et biopharmaceutiques, notamment les vaccins, les protéines, les probiotiques ou les nanovéhicules comme les liposomes ou les nanoparticules polymères [2]. Dans le cadre de notre travail sur les PEC-NGs, la lyophilisation présente deux intérêts principaux concernant les aspects de conservation et de formulation. Premièrement, la conservation des PEC-NGs à l'état sec pourrait maintenir leur stabilité physico-chimique à plus long terme par rapport à l'état de dispersion en milieu aqueux [3]. Comme présenté dans le chapitre précédent, la taille des PEC-NGs à base de HA-M2005 à l'état de suspension augmente après un mois de conservation. Bien que cette augmentation reste peu importante à moyen terme, une conservation à plus long terme en suspension peut probablement conduire à une augmentation plus considérable de la taille des PEC-NGs. De plus, la présence d'eau pourrait augmenter le risque de contamination microbiologique, qui peut entrainer la dégradation du HA par des enzymes bactériennes [4]. La thermosensibilité des PEC-NGs en milieu aqueux peut également les rendre sensible à la variation de la température de l'environnement lors de leur conservation et de leur transport [1]. Comme pour toutes les autres formes pharmaceutiques, la lyophilisation peut également permettre de réduire le volume et la masse des formulations pour faciliter leur stockage et leur manipulation [1, 2]. L'état sec peut également éviter la dégradation et la fuite précoce des SAs encapsulées dans les nanoformulations [5]. A côté de l'aspect de stabilité, la formulation peut être modifiée et optimisée à la suite de sa lyophilisation. Comme proposé dans le chapitre précédent, après lyophilisation, les PEC-NGs pourraient être redispersés dans un volume approprié

de milieu aqueux pour atteindre la concentration souhaitée en polymère ainsi qu'en SA [6]. Outre la possibilité d'ajuster le volume, le type de milieu dispersant, cette fois-ci, peut être modifié, e.g. avec des tampons à différentes valeurs de pH pour s'adapter aux études ou aux applications visées. Malgré ces avantages, le procédé de lyophilisation puis de réhydratation des nanoformulations peut s'accompagner de modifications de microstructures, notamment l'augmentation de la taille des particules par l'agrégation à cause des stress présents lors de la congélation comme la formation des cristaux de glace, la cryoconcentration et la déshydratation [7, 8]. Pour arriver à une lyophilisation optimale de ces nanoobjets, il est souvent incontournable d'utiliser des cryoprotecteurs qui sont des agents à ajouter pour stabiliser et protéger la microstructure des produits pendant la congélation [2]. Malgré ces aspects complexes à côté des avantages énormes de la lyophilisation, il existe jusqu'à ce jour peu de travail de recherche décrivant en détail l'optimisation de la lyophilisation des PEC-NGs, surtout pour ceux à base de HA. Le travail le plus complet de ce type est vraisemblablement celui d'Umerska *et al.* [9], qui ont étudié les effets de la composition des PECs et du choix de cryoprotecteur sur des nano-PECs à base de chitosane (CTS) ou de protamine (PROT) en complexe avec du HA ou du sulfate de chondroïtine, pour lesquels le PEG et le tréhalose ont été utilisés comme cryoprotecteurs. Egalement, Gheran *et al.* ont lyophilisé des NGs à base de HA en complexe avec le CTS en utilisant du glucose pour la cryoprotection de ceux-ci [10]. En effet, il n'existe pas de type ni de concentration universelle de cryoprotecteur pour toutes les nanoformulations, exigeant alors des études préalables pour adapter la méthode de lyophilisation à des systèmes de structures différentes [8]. Dans ce contexte, il est nécessaire de réaliser des études exploratoires sur l'influence des différents paramètres de formulation et des cryoprotecteurs en vue de trouver la bonne stratégie pour la lyophilisation des différents PEC-NGs étudiés.

IV.2.2. Méthode d'étude

Dans le cadre de ce travail, nous avons évalué les propriétés des PEC-NGs après la lyophilisation et la réhydratation pour estimer l'efficacité de la préservation de leur structure colloïdale lors de ce procédé. Nous avons commencé l'étude sur des PEC-NGs de HA/DEAE-D pour mettre en évidence les principales tendances. Ensuite, nous reproduirons les conditions optimales sur des PEC-NGs avec de la PLL et/ou avec les greffons M2005, car les PEC-NGs de HA-M2005/PLL constituent le système le plus satisfaisant selon le chapitre précédent. Cela nous permettra également de voir les effets du choix du polycation et des greffons sur le changement de la structure des NGs après lyophilisation. En outre, les effets des autres paramètres sur l'aspect de formulation seront aussi étudiés, notamment le choix et la concentration du cryoprotecteur et les paramètres de préparation qui reflètent la structure des PEC-NGs comme le ratio de charge (qui reflète la charge de surface des PEC-NGs et la concentration initiale en polymères (qui gouverne la taille initiale des PEC-NGs).

Concernant le protocole de lyophilisation et de reconstitution, une quantité déterminée en cryoprotecteurs est ajoutée et dissoute par agitation au vortex pendant 30 s dans les suspensions de PEC-NGs d'intérêt. Un volume défini de suspensions obtenues, sans ou avec des cryoprotecteurs (concentration variable), est congelé à -20 °C dans un congélateur pendant une nuit. Les échantillons congelés sont ensuite lyophilisés à l'aide d'un lyophilisateur à paillasse Alpha 1-2 LD plus (Martin Christ, Allemagne) en mode de dessication primaire pendant 24 h avec une pression inférieure à 0,1 mbar et la température du condenseur de -60 °C. Pour la reconstitution des suspensions de PEC-NGs, à moins d'indications contraires, les PEC-NGs lyophilisés sont dispersés dans le même volume d'eau Milli-Q comme avant la lyophilisation et ensuite agités au vortex pendant 60 s avant leur caractérisation. Nous avons réalisé une évaluation de l'homogénéité

visuelle après redispersion et, pour les suspensions homogènes, des mesures de la taille (diamètre hydrodynamique – D_h), de la distribution de la taille (indice de polydispersité – PDI) et du potentiel zêta (ζ) des PEC-NGs. L'ensemble des techniques utilisées ont déjà fait l'objet d'un descriptif dans les publications dans les **Chapitres II** et **III**. Pour certaines expériences, un autre volume ou un autre type de solvant (i.e. tampon PBS) peut être appliqué lors de la réhydratation selon l'objectif de l'étude. En présence de curcumine, nous avons réutilisé les mêmes méthodes de la **Section III.2** du chapitre précédent pour son encapsulation et sa quantification.

IV.2.3. Impact du ratio de charge

Dans un premier temps, pour comprendre l'impact de la charge de surface des PEC-NGs sur l'efficacité de la préservation de leur taille lors de la lyophilisation, nous avons effectué la lyophilisation et la reconstitution sur 1 mL de suspension des PEC-NGs de HA/DEAE-D à n-/n+ de trois valeurs différentes (1,25, 2,5 et 5) à une C_P fixée à 0,5 $g.L^{-1}$ sans cryoprotecteur. En effet, nous nous sommes focalisés sur les PEC-NGs à n-/n+ > 1 car ceux sont les systèmes les plus satisfaisants et les plus prometteurs selon les études présentées dans le chapitre précédent. Toutefois, après leur lyophilisation, seulement les PEC-NGs à n-/n+ = 5 ont pu être redispersés de manière homogène pour reconstituer une suspension translucide, alors que les lyophilisats des PEC-NGs à n-/n+ = 1,25 et 2,5 ont formé des macro-agrégats visibles dans l'eau. Ainsi, nous avons réalisé à nouveau les expériences sur ces deux derniers systèmes avec du tréhalose comme cryoprotecteur à différentes concentrations, croissantes à des intervalles de 1 % jusqu'à l'obtention d'une redispersibilité satisfaisante après lyophilisation. Le tréhalose est préalablement choisi car il s'avère le plus utilisé parmi les cryoprotecteurs selon la littérature [9, 11, 12], alors que l'étude plus précise sur le choix du cryoprotecteur sera détaillée dans la section suivante. Les concentrations les plus faibles en tréhalose permettant la dispersion homogène des lyophilisats, les

tailles moyennes des PEC-NGs et leurs PDIs dans les suspensions reconstituées, aussi bien que les rapports R entre ces valeurs et celles avant lyophilisation, sont présentés dans le **Tableau IV-1**.

Tableau IV-1. Caractéristiques des suspensions de PEC-NGs reconstituées aux concentrations les plus faibles en tréhalose permettant la dispersion homogène ($n \geq 3$)

n-/n+	Caractéristiques des suspensions reconstituées				
	C^*_{TRE} (% m/v)	**D_h moyen (nm)**	**R-D_h**	**PDI**	**R-PDI**
1,25	8	182 ± 6	1,07 ± 0,02	0,09 ± 0,01	0,84 ± 0,12
2,5	1	315 ± 15	1,39 ± 0,06	0,21 ± 0,01	0,85 ± 0,03
5	0	264 ± 37	1,04 ± 0,11	0,30 ± 0,01	0,94 ± 0,06

C^*_{TRE} : concentration la plus faible en tréhalose pour la dispersion homogène après lyophilisation et reconstitution
R-D_h : rapport entre le D_h moyen après reconstitution et le D_h initial
R-PDI : rapport entre le PDI après reconstitution et le PDI initial

Comme présenté dans le **Tableau IV-1**, plus le n-/n+ est éloigné de l'unité, moins de tréhalose est nécessaire lors de lyophilisation pour garantir une reconstitution homogène, qui se traduit par des tailles de PEC-NGs restant dans la gamme sous-micrométrique et des distributions monodisperses de celles-ci. Ces résultats montrent que les caractéristiques colloïdales des PEC-NGs sont mieux préservées pour des PEC-NGs à charge nette de surface plus élevée. Effectivement, la réduction en volume de la phase liquide lors de formation de glace pendant la congélation peut conduire à l'augmentation de la densité locale des PEC-NGs et de la concentration des contre-ions [8]. Par conséquent, cela présente un stress qui favorise respectivement le rapprochement des particules et la réduction de la stabilisation électrostatique suite à l'abaissement du potentiel zêta, qui peut ainsi favoriser leur agrégation [8, 13]. Lors de la réhydratation, ces interactions ne peuvent être retrouvées que partiellement et donc des particules de taille plus importante sont observées [14]. Logiquement, une répulsion plus importante entre les PEC-NGs en raison d'un potentiel zêta plus élevé peut limiter cet effet aussi bien que favoriser

leur désassemblement à partir des agglomérats lors de redispersion dans l'eau, comme constaté dans les travaux d' Umerska *et al.* [9] et d'Eliyahu *et al.* [15]. Pourtant, bien que presque toutes les caractéristiques granulométriques des PEC-NGs soient bien préservées par rapport aux valeurs initiales lors de lyophilisation en utilisant du tréhalose, la taille des PEC-NGs à n-/n+ = 2,5 démontre une augmentation visible de presque 40 % (**Tableau IV-1**). Comme le système à ce ratio de charge est le plus intéressant en matière d'encapsulation des SAs hydrophobes comme indiqué dans le chapitre précédent, nous allons chercher à optimiser leur lyophilisation en étudiant les effets du type et de la concentration des cryoprotecteurs dans la section suivante.

IV.2.4. Impact de la nature et de la concentration du cryoprotecteur

Pour étudier l'efficacité de différents types de cryoprotecteur en matière de préservation de la structure des PEC-NGs lors de la lyophilisation et de la reconstitution, nous avons évalué les propriétés des PEC-NGs de HA/DEAE-D à C_P = 0,5 g.L^{-1} et à n-/n+ = 2,5 après leur lyophilisation et reconstitution à 1 % (m/v) en cryoprotecteur de quatre types différents, i.e. le tréhalose, le sucrose, le glucose et les PEGs à masse molaire (MW) moyenne de 2, 10 ou 20 kDa. Ces différents agents se retrouvent comme cryoprotecteurs largement étudiés pour les nanoformulations dans la littérature [16, 17]. Dans notre cas, l'ajout des PEGs dans les suspensions de PEC-NGs a entrainé des agrégats largement visibles après la reconstitution (PEG à MW de 20 kDa) ou même avant la lyophilisation (PEGs à MW de 2 ou 10 kDa). Au contraire, l'ajout de tréhalose, de sucrose ou de glucose comme cryoprotecteur n'a pas conduit à ces problèmes ni au changement de la taille des PEC-NGs (**Tableau IV-2**) et les suspensions obtenues peuvent être lyophilisées et reconstituées de manière homogène, permettant leurs caractérisations par DLS. L'aspect visuel des lyophilisats et les rapports R sur ces échantillons sont présentés dans la **Figure IV-1**.

Tableau IV-2. Rapport (R_i) entre la valeur après l'ajout du cryoprotecteur (1% m/v) et la valeur initiale du D_h et du PDI des PEC-NGs de HA/DEAE-D (C_P = 0,5 g.L^{-1} et n-/n+ = 2,5) (n ≥ 3)

Cryoprotecteur	R_i-D_h	R_i-PDI
Tréhalose	1,01 ± 0,02	0,97 ± 0,04
Sucrose	0,98 ± 0,02	1,02 ± 0,02
Glucose	1,00 ± 0,02	0,99 ± 0,04

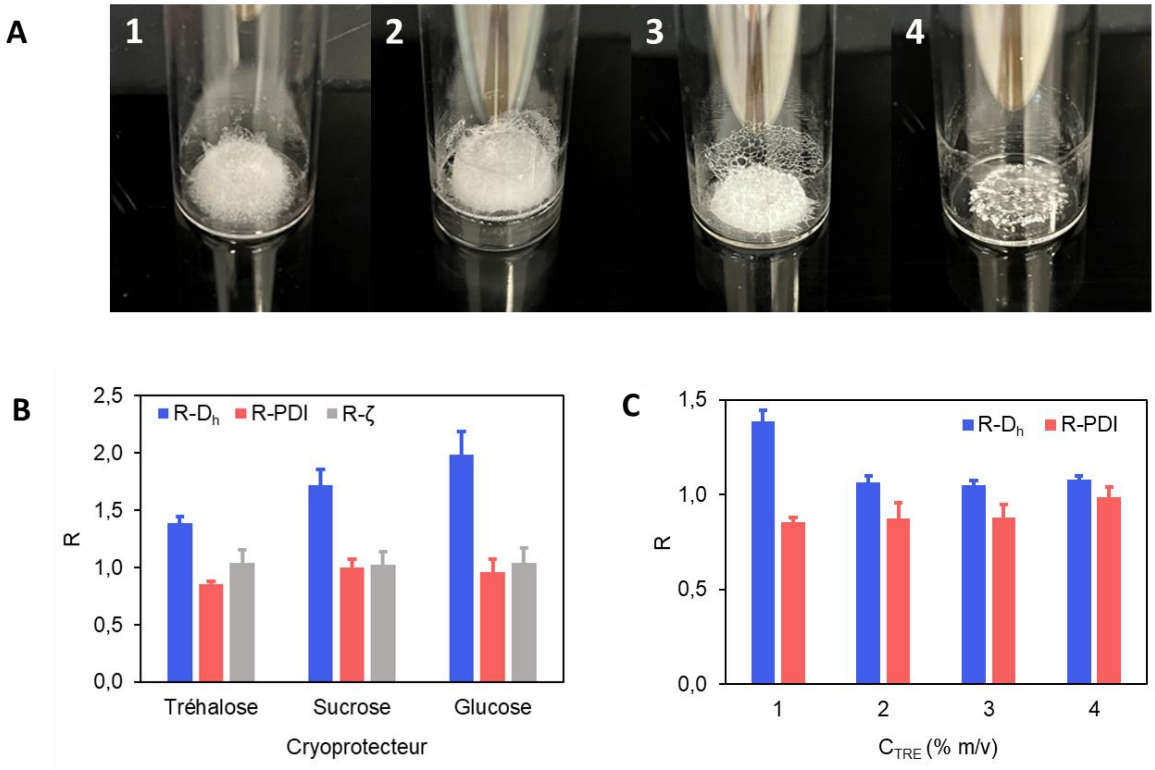

Figure IV-1. Lyophilisation des PEC-NGs de HA/DEAE-D (C_P = 0,5 g.L^{-1} et n-/n+ = 2,5) : (**A**) Aspects visuels des lyophilisats des PEC-NGs sans cryoprotecteur (1) ou avec 1% (m/v) en tréhalose (2), en sucrose (3) ou en glucose (4) ; (**B-C**) Rapports (R) des valeurs caractéristiques des PEC-NGs après reconstitution par rapport aux valeurs avant lyophilisation avec différents cryoprotecteurs à une concentration de 1 % (m/v) (**B**) ou avec du tréhalose à différentes concentrations C_{TRE} (**C**) (n ≥ 3).

Concernant l'aspect visuel, les cryoprotecteurs de type disaccharide permettent de former des lyophilisats bien poreux comme celui sans cryoprotecteurs, alors que l'utilisation du glucose conduit à un effondrement macroscopique du lyophilisat. Par conséquent, à une concentration fixée de 1 % (m/v), le glucose s'avère le moins efficace alors que le tréhalose semble le plus efficace pour préserver la taille des PEC-NGs, bien qu'une augmentation de la taille des PEC-NGs est toujours constatée avec les trois sucres à cette même concentration de 1 %. En augmentant la concentration en tréhalose à partir de 2 % (m/v), la taille des PEC-NGs est parfaitement préservée. Cependant, le PDI et le ζ ne présentent pas de changement significatif lors de la lyophilisation et de la reconstitution en présence de cryoprotecteurs. Effectivement, l'effet protecteur des cryoprotecteurs sur les NGs peut s'expliquer par trois théories de mécanisme selon la littérature : la vitrification, le remplacement d'eau et la séquestration d'eau (**Figure IV-2**).

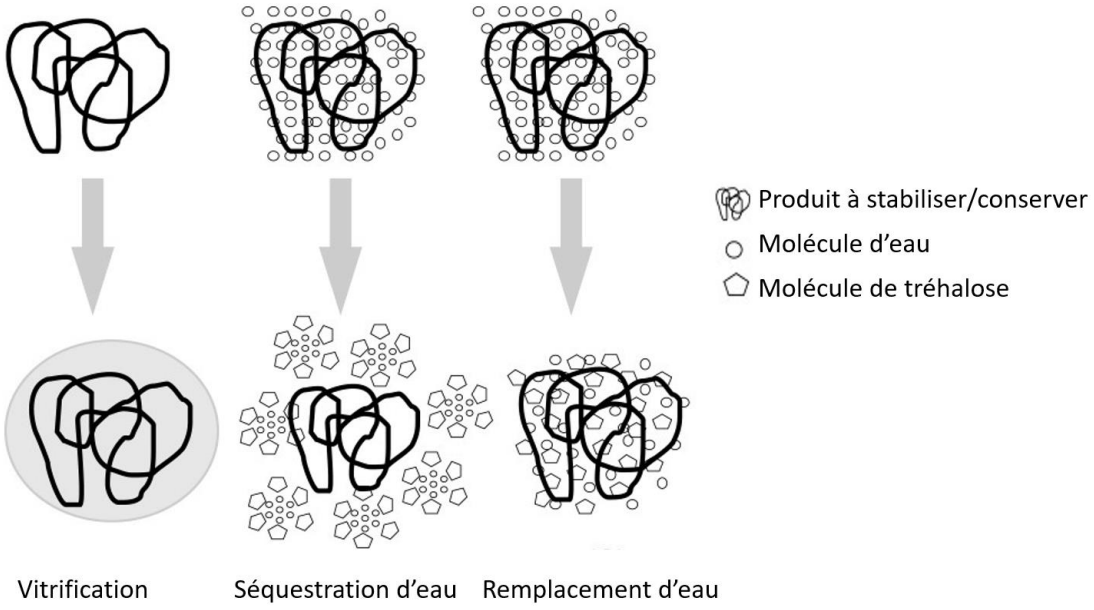

Figure IV-2. Mécanismes de cryoprotection par tréhalose (modifiée de [18])

Concernant la vitrification, lors de la séparation entre la phase solide de l'eau congelée et la phase liquide hautement concentrée en soluté et en NGs, la concentration élevée en cryoprotecteur peut rendre cette dernière phase très visqueuse et éventuellement vitreuse quand l'eau est presque totalement éliminée du système. Ce fait peut rendre les NGs peu mobiles et empêcher leur rapprochement pour éviter leur fusion ou leur agrégation, et finalement constitue une matrice solide vitreuse assez stable pour maintenir tout le système à sec [2]. Dans cet aspect, la température de transition vitreuse (T_g) des cryoprotecteurs est un paramètre permettant d'envisager leur effet protecteur car une T_g plus élevée devrait constituer une matrice plus stable [8]. Par conséquent, les disaccharides sont souvent préférés aux monosaccharides comme cryoprotecteur car les premiers présentent souvent des T_g plus élevées [8]. Pour les trois sucres étudiés dans ce travail, les résultats obtenus concernant leur efficacité dans le maintien des tailles des PEC-NGs s'accordent bien avec l'ordre de leurs T_g trouvées dans la littérature : T_g du glucose < T_g du sucrose < T_g du tréhalose (30 °C, 58 °C et 108 °C, respectivement) [19]. La faible T_g du glucose conduit également à une faible T_g' (T_g de la solution cryo-concentrée au maximum en soluté) par rapport aux disaccharides et explique ainsi l'effondrement du lyophilisat obtenu [8]. Bien que ce phénomène n'affecte pas forcément la stabilité des produits à conserver, il représente un défaut esthétique pour ceux-ci et exige souvent un temps plus long pour la lyophilisation et pour la reconstitution à cause de l'insuffisance de porosité [20, 21]. Cependant, dans le mécanisme de remplacement d'eau, quand les molécules d'eau sont séparées de la phase liquide lors de formation des cristaux de glace et ensuite enlevées par sublimation, les cryoprotecteurs peuvent remplacer ces molécules pour former des liaisons hydrogène avec les NGs et constituer ainsi un état « pseudo-hydraté » pour éviter des perturbations dans leurs microstructures [22, 23]. A côté de ces deux mécanismes de cryoprotection largement abordés, il

existe également un troisième mécanisme moins rencontré concernant le phénomène d'exclusion préférentielle et parfois appelé « séquestration d'eau », qui est proposé le plus souvent pour la cryoprotection des protéines [24]. Selon cette hypothèse, les molécules de tréhalose peuvent structurer et séquestrer les molécules d'eau pour que ces dernières s'écartent des protéines. De cette façon, il y a moins d'eau présente autour des protéines alors que celles-ci sont plus compactées, ce qui peut stabiliser les protéines et limiter les dégâts de la formation de glace sur leurs structures [25]. Bien que le sucrose et le tréhalose sont des disaccharides d'une même structure chimique, ils présentent des structures géométriques différentes à partir desquelles certaines recherches suggèrent que le sucrose peut présenter des liaisons hydrogène intramoléculaires, réduisant ainsi sa capacité de former les liaisons hydrogène avec l'eau ou avec les produits à conserver par rapport au tréhalose et conduisant à un effet cryoprotecteur moins efficace [26, 27].

Quant aux PEGs, malgré leurs effets cryoprotecteurs bien décrits pour certains systèmes, leur ajout peut alors, dans certains cas, faciliter l'agglomération ou l'agrégation [17]. En particulier, le PEG est bien connu pour être incompatible avec le dextrane et le mélange de ces deux polymères peut présenter une séparation de phases (*aqueous two-phase system*) [8, 28], ce qui peut probablement expliquer les macro-agrégats formés après l'ajout des PEGs dans les suspensions de PEG-NGs de HA/DEAE-D. De plus, il est constaté que la présence du PEG comme agent d'encombrement dans la phase continue peut renforcer la complexation entre le HA et la ε-PLL et peut ainsi faciliter la séparation de phases [29]. En outre, dans les nanoformulations, les polymères comme le PEG peuvent parfois se présenter comme des polymères de collage qui favorisent le rapprochement des particules et peuvent ainsi provoquer leur agglomération (*polymer bridging flocculation*) [2, 30]. Dans le cas particulier du PEG à MW de 20 kDa, la viscosité très

élevée obtenue peut être également un facteur qui empêche la dispersion homogène des PEC-NGs pendant la réhydratation.

En général, concernant le choix du cryoprotecteur pour les PEC-NGs dans ce travail, les PEGs semblent beaucoup moins efficaces que les trois sucres étudiés, alors que le tréhalose s'avère comme le cryoprotecteur le plus pertinent. Cette efficacité marquée de la cryoprotection par le tréhalose est en accord avec les résultats obtenus pour d'autres systèmes comme des NPs à base de CTS et de HA [17], des NPs de HA conjugué au cisplatine [31] et des nanocomposites sous forme de NGs micellaires à base de HA [32]. Concernant la concentration en cryoprotecteur, selon les mécanismes de cryoprotection susmentionnés, une amélioration de l'effet cryoprotecteur peut être réalisée quand la concentration en cryoprotecteur est augmentée pour atteindre une concentration suffisamment élevée où cet effet est optimal, comme 2 % en tréhalose dans la **Figure IV-1**. A la vue de ces résultats, le tréhalose a été retenu comme cryoprotecteur avec une gamme de concentration d'intérêt de 0 à 2 % pour les études ultérieures.

IV.2.5. Impact du greffage de la M2005 et de la nature du polycation

Dans cette étude, pour évaluer la préservation de la taille des PEC-NGs ayant des greffons de M2005 en fonction du polycation utilisé lors de lyophilisation et de reconstitution, nous avons effectué ce procédé sur les PEC-NGs de HA-M2005/DEAE-D et de HA-M2005/PLL à C_P = 0,5 g.L^{-1} et à n-/n+ = 2,5 sans ou avec du tréhalose à C_{TRE} de 1 ou 2 % (m/v). Comme avec les PEC-NGs de HA/DEAE-D aux mêmes conditions, les PEC-NGs de HA-M2005/DEAE-D et de HA-M2005/PLL n'ont pas pu être complètement redispersés dans l'eau après lyophilisation en absence de tréhalose, alors qu'une concentration en tréhalose d'au moins 1 % permet une redispersion homogène et ainsi l'évaluation des tailles des PEC-NGs réhydratés (**Figure IV-3**).

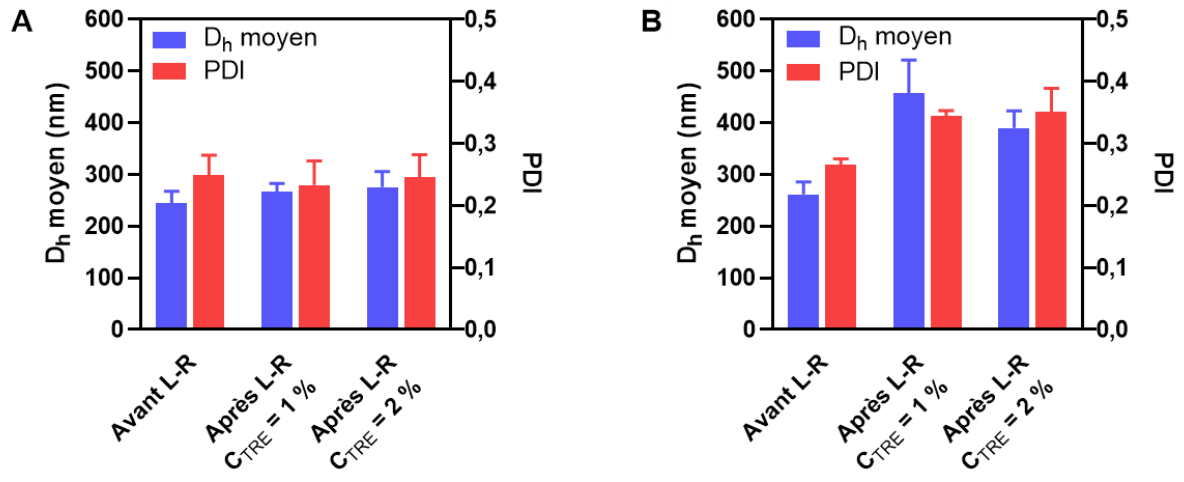

Figure IV-3. Caractéristiques avant et après lyophilisation et reconstitution (L-R) des PEC-NGs de HA-M2005/DEAE-D (**A**) et de HA-M2005/PLL (**B**) à C_P = 0,5 g.L^{-1} et n-/n+ = 2,5 à différentes concentrations en tréhalose (C_{TRE}, m/v) comme cryoprotecteur ($n \geq 3$).

En particulier, pour les PEC-NGs de HA-M2005/DEAE-D, une concentration de 1 % en tréhalose est suffisante pour bien préserver leur taille (**Figure IV-3**A), démontrant une préservation plus efficace que celle des PEC-NGs de HA/DEAE-D, pour lesquels une concentration d'au moins 2 % en tréhalose est nécessaire (**Section IV.2.4**). Cette amélioration peut être due à l'effet stabilisant des greffons M2005 comme proposé dans le chapitre précédent. Les résultats sont moins encourageants pour les PEC-NGs de HA-M2005/PLL car, même à 2 % en tréhalose, il n'est pas possible d'éviter une augmentation importante de taille (facteur d'environ 1,5) après la redispersion du lyophilisat. Cela conduit à un D_h moyen de presque 400 nm (**Figure IV-3**B). Ce fait peut s'expliquer par la nature plus hydrophobe des PEC-NGs de HA-M2005/PLL qui facilite leur agrégation sous les stress de congélation. Nous avons également essayé d'augmenter la C_{TRE} à 4 % mais cette concentration élevée en tréhalose semble déstabiliser les PEC-NGs à base de HA-M2005, car elle a entrainé la formation d'aggrégats visibles pour les

PEC-NGs de HA-M2005/DEAE-D et une augmentation significative de la taille des PEC-NGs de HA-M2005/PLL (de 262 ± 24 nm à 377 ± 29 nm) dans les conditions étudiées (C_P = 0,5 g.L^{-1} et n-/n+ = 2,5 dans l'eau Milli-Q). Effectivement, il est important de noter que le dépassement de la concentration optimale en cryoprotecteur peut parfois entrainer la déstabilisation des systèmes à conserver à travers un ensemble complexe d'interactions sans que leurs mécanismes précis soient toujours clairement expliqués [2, 3, 33, 34]. Dans le cas de ces PEC-NGs plus ou moins hydrophobes en présence des greffons M2005, le phénomène d'exclusion préférentielle, autrement dit la séquestration d'eau par le tréhalose comme discuté dans la section précédente, peut être la cause de leur agrégation avec un effet très similaire à celui de type « salting-out » des sels. De toute manière, la C_{TRE} de 2 % s'avère la plus optimale dans la condition expérimentale de ce travail pour la lyophilisation des PEC-NGs de HA-M2005/PLL à C_P = 0,5 g.L^{-1} et à n-/n+ = 2,5, soit le système le plus intéressant parmi ceux étudiés selon le chapitre précédent, bien que l'efficacité en matière de préservation de leur taille reste insatisfaisante.

IV.2.6. Impact de la concentration initiale en polymère

Dans l'objectif d'obtenir des PEC-NGs de HA-M2005/PLL à n-/n+ = 2,5 après lyophilisation et reconstitution avec une taille granulométrique pas trop élevée (i.e. D_h moyen aux alentours de 250-350 nm avec un PDI inférieur à 0,3), nous avons appliqué une nouvelle stratégie en partant de suspensions peu concentrées en polymère avant lyophilisation, soit à une C_P = 0,2 g.L^{-1}, qui peuvent ensuite être réhydratées dans un plus petit volume afin d'atteindre la concentration souhaitée. Cette stratégie part de notre hypothèse selon qu'une taille plus faible des PEC-NGs au départ permettrait une taille finale moins élevée après reconstitution. Cette fois-ci, nous avons également essayé d'utiliser le tampon PBS comme milieu de réhydratation pour des applications éventuelles de ces suspensions, notamment pour des études biologiques *in vitro* et

in vivo. Dans un premier temps, nous avons utilisé un volume de reconstitution de 40 % du volume initial pour avoir une C_P finale de 0,5 $g.L^{-1}$. Il est constaté que les PEC-NGs reconstitués dans ce cas peuvent être bien redispersés même sans tréhalose mais montrent une taille assez élevée (i.e. environ 400 nm), traduisant une augmentation par un facteur de 2,6 à partir de la taille initiale d'environ 150 nm à C_P = 0,2 $g.L^{-1}$ (**Figure IV-4**). Par contre, nous avons pu obtenir des PEC-NGs de taille satisfaisante, i.e. d'environ 250 nm, en reprenant ces études avec du tréhalose à une concentration de 1 ou 2 % avant lyophilisation (i.e. C_{TRE} de 2,5 ou 5 % après réhydratation), sans différence significative entre ces deux C_{TRE} en matière d'efficacité de la préservation de la taille des PEC-NGs (**Figure IV-4**). Par conséquent, pour une même C_P finale, le fait de partir avec des suspensions moins concentrées avant la lyophilisation s'avère efficace pour obtenir une taille finale des PEC-NGs qui se trouve dans la gamme souhaitée.

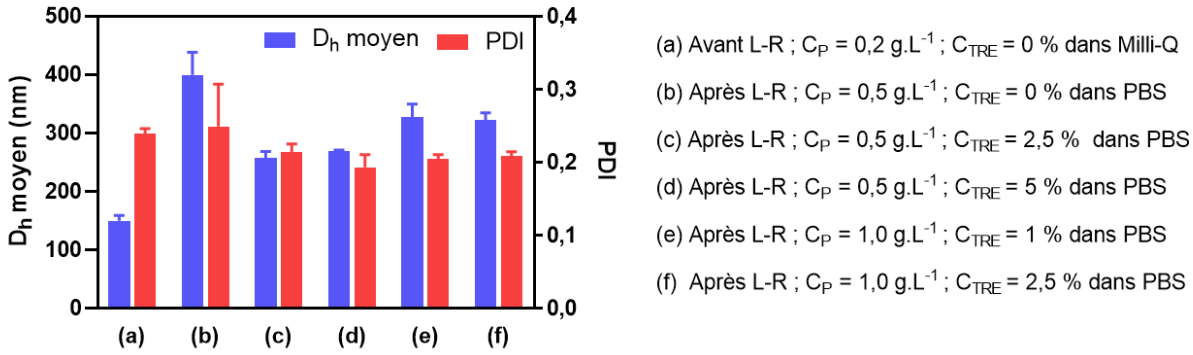

Figure IV-4. Caratéristiques des PEC-NGs de HA-M2005/PLL à n-/n+ = 2,5 avant et après lyophilisation et reconstitution (L-R) à différentes concentrations en tréhalose (C_{TRE}) à partir des PEC-NGs fabriqués à C_P = 0,2 $g.L^{-1}$ ($n \geq 3$).

Après ces observations, nous avons essayé d'obtenir des suspensions encore plus concentrées en réduisant le volume de PBS pour la réhydratation, i.e. un volume de 20 % par rapport à celui au départ pour obtenir une C_P finale de 1 $g.L^{-1}$, avec une C_{TRE} initiale de 0,2 ou

0,5 %. Une telle réduction en volume de réhydration semble augmenter légèrement la taille finale des PEC-NGs par rapport aux précédentes expériences mais cette taille reste acceptable comme elle est toujours proche de 300 nm et un PDI faible autour de 0,2 est toujours préservé (**Figure IV-4**). En conséquence, il serait possible d'appliquer cette méthode de lyophilisation pour préparer les suspensions concentrées en SA encapsulée.

A la suite de ces résultats, nous avons également essayé de diminuer la concentration initiale à C_P = 0,1 g.L^{-1} en vue de réduire encore la taille des PEC-NGs après reconstitution. Cette-fois ci, il semble que cette approche ne conduit pas à une amélioration considérable en matière de taille finale des PEC-NGs puisqu'elle reste toujours un peu près de 300 nm avec un PDI autour de 0,2, sans différence significative entre les C_{TRE} initiales de 0,1 et 0,2 % (i.e. C_{TRE} après reconstitution de 1 et 2 % respectivement) (**Figure IV-5**).

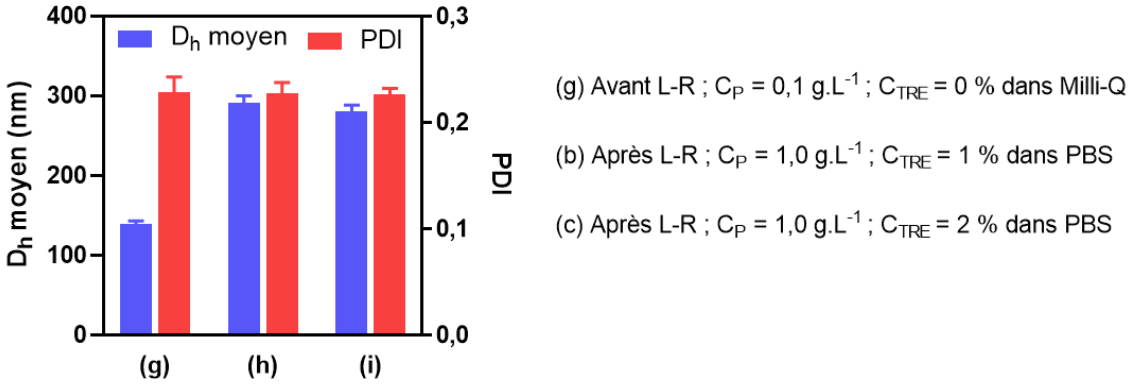

Figure IV-5. Caratéristiques des PEC-NGs de HA-M2005/PLL à n-/n+ = 2,5 avant et après lyophilisation et reconstitution (L-R) à différentes concentrations en tréhalose (C_{TRE}) à partir des PEC-NGs fabriqués à C_P = 0,1 g.L^{-1} (n ≥ 3).

Pour vérifier l'application potentielle comme système de séquestration de SAs hydrophobes, nous avons repris les PEC-NGs de HA-M2005/PLL (n-/n+ = 2,5) chargés en

curcumine et évalué la concentration en curcumine dans les suspensions à C_P = 1 g.L^{-1} reconstituées après la lyophilisation des suspensions à C_P = 0,1 ou 0,2 g.L^{-1} avec du tréhalose comme cryoprotecteur. Pour rappel, nous avons repris le protocole décrit dans le chapitre précédent avec une température de complexation de 50 °C pour préparer les PEC-NGs chargés en curcumine à C_P = 0,1 ou 0,2 g.L^{-1}. Comme présenté dans **Figure IV-6**A, en se référant à la suspension de même type fraîchement préparée à C_P = 0,5 g.L^{-1}, la suspension reconstituée à C_P = 1 g.L^{-1} en partant de la lyophilisation à C_P initiale de 0,2 g.L^{-1} présente un aspect homogène avec une couleur jaune plus soutenue sans précipitation de la curcumine, qui indique *à priori* une augmentation effective de sa concentration. Après quantification, les teneurs en curcumine dans les suspensions avant lyophilisation et après reconstitution sont toutes en accord avec celle de la suspension référente à C_P = 0,5 g.L^{-1}, traduisant le même taux d'encapsulation des PEC-NGs préparés dans cette gamme de C_P (**Figure IV-6**B). Toutefois, les PEC-NGs préparés à C_P de 0,1 g.L^{-1} montrent un taux d'encapsulation plus faible qu'à C_P de 0,2 g.L^{-1}, conduisant ainsi à des suspensions moins concentrées en curcumine après la constitution malgré la même C_P finale de 1 g.L^{-1} (**Figure IV-6**B). En effet, la faible capacité d'encapsulation des PEC-NGs à C_P de 0,1 g.L^{-1} est vraisemblablement due à leur structure plus poreuse et lâche, comme les tailles des PEC-NGs élaborés à C_P de 0,1 et de 0,2 g.L^{-1} sont comparables (**Figure IV-5** *vs.* **Figure IV-4**) malgré la masse beaucoup plus faible en polymères pour les premiers. Il est ainsi possible de conclure que la lyophilisation des suspensions à la C_P de 0,2 g.L^{-1} avec C_{TRE} = 0,2 % est la méthode la plus pertinente pour la lyophilisation des PEC-NGs de HA-M2005/PLL à n-/n+ = 2,5 en raison de la possibilité de concentrer efficacement des SAs encapsulées à l'étape de reconstitution sans entrainer des tailles trop élevées des NGs.

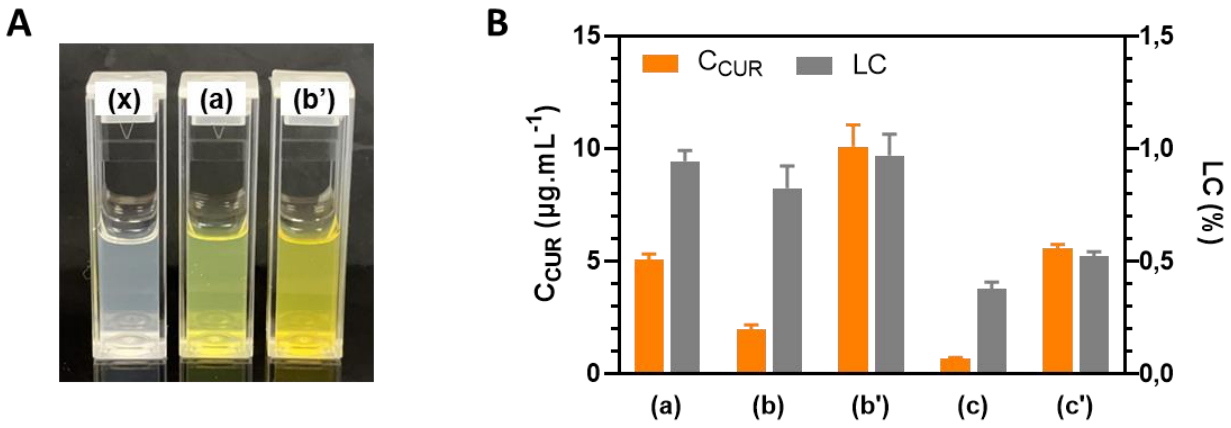

(x) : HA-M2005/PLL à C_P = 0,5 g.L^{-1} fraîchement préparés
(a) : HA-M2005/PLL/Cur à C_P = 0,5 g.L^{-1} fraîchement préparés
(b) : HA-M2005/PLL/Cur à C_P = 0,2 g.L^{-1} fraîchement préparés
(b') : HA-M2005/PLL/Cur à C_P = 1,0 g.L^{-1} après L-R de (b)
(c) : HA-M2005/PLL/Cur à C_P = 0,1 g.L^{-1} fraîchement préparés
(c') : HA-M2005/PLL/Cur à C_P = 1,0 g.L^{-1} après L-R de (c)

Figure IV-6. (**A**) Aspect visuel et (**B**) concentration en curcumine (C_{CUR}) et taux d'encapsulation de curcumine (LC) des suspensions de PEC-NGs (n-/n+ = 2,5) fraîchement préparées ou après lyophilisation et reconstitution (L-R) à C_{TRE} initiale à 0,2 % (m/v) ($n \geq 3$). Les échantillons (x) et (a) obtenus dans les études précédentes sont présentés comme référence.

IV.3. Renforcement des interactions hydrophobes par traitement autoclave

IV.3.1. Intérêts du traitement autoclave pour les nanoformulations

Le traitement autoclave, par définition, est le traitement des matériels sous température et pression élevées en utilisant la vapeur d'eau saturée dans un récipient hermétique (autoclave). Ce procédé est couramment utilisé comme une méthode très classique pour la stérilisation.

Récemment, l'équipe de Matricardi *et al.* a montré qu'un traitement autoclave peut permettre de fabriquer des NGs à partir de dérivés amphiphiles de polysaccharides [35-39]. En particulier, le traitement d'une solution de HA greffé par du cholestérol (HA-CH) de MW moyenne d'environ 1,5 × 10^5 g.mol^{-1} à C_P de 1 g.L^{-1} par un cycle d'autoclave classique (121 °C, 20 min) a

permis la formation des NGs de taille aux alentours de 350 nm, stables pendant au moins un mois avec une conservation à 4 °C [38]. Des NGs stables ont également été préparés de la même manière à partir de Gellane greffé par du cholestérol [38] ou de HA fonctionnalisé par du tétrabutyrate de riboflavine [40]. Le mécanisme proposé pour cette élaboration sous traitement autoclave est le déclenchement et le renforcement des interactions hydrophobes entre les greffons hydrophobes, qui favorise ainsi l'autoassemblage stable des chaines de polymère sous forme de NGs [38]. Ce traitement peut s'accompagner d'un abaissement de MW des polymères par rupture de lien glycosidique pendant le traitement autoclave. De plus, des SAs thermostables de nature hydrophile (e.g. tobramycine) aussi bien qu'hydrophobe (e.g. dexaméthasone et piroxicam) peuvent être encapsulées dans les NGs pendant ce traitement, alors que les principes actifs thermosensibles (e.g. enzymes, antioxydants comme la curcumine, l'astaxanthine, le resvératrol ou des composés thérapeutiques comme le diclofénac) peuvent être incorporées au sein des NGs à température ambiante après leur formation [35, 37, 39]. Evidemment, cette méthode permet non seulement de fabriquer des NGs chargés en SAs de manière assez simple et rapide sans agents chimiques, tensioactifs ni solvants organiques mais également de les stériliser dans un même procédé. Cela présente un aspect assez utile et pratique car la stérilisation des nanoformulations à base de polysaccharides avec les méthodes classiques est souvent compliquée et parfois infaisable à grande échelle à cause de plusieurs obstacles, notamment la perte de matières à cause de l'obstruction de filtre (stérilisation par filtration) ou la dégradation des matières polymères à cause de la température extrême (stérilisation par autoclave) ou des rayonnements (stérilisation par rayonnement) [41]. A la vue des applications intéressantes susmentionnées de l'autoclave, nous avons essayé ce traitement sur des PEC-NGs à base de HA-M2005 en posant l'hypothèse que la température et la pression élevées pendant ce traitement pourraient accentuer les interactions

hydrophobes intraparticulaires pour stabiliser les PEC-NGs. Pour cela, nous avons appliqué la même méthode de traitement autoclave décrite par Montanari *et al.*, i.e. un cycle d'autoclave standard à 121 °C pendant 20 min avec une pression d'environ 1,1 bar [38], sur 2 mL de suspension de PEC-NGs à C_P = 0,5 g.L^{-1} mis dans un flacon en verre. Après ce traitement, les échantillons sont laissés au repos à température ambiante pendant 1 h avant les mesures de taille en DLS avec toujours le même protocole de détermination. Ces échantillons sont ensuite conservés à 4 °C pour l'évaluation de leur stabilité à long terme par des mesures en DLS au cours des 12 mois suivants.

IV.3.2. Résultats et discussion

Après le traitement par autoclave des suspensions de PEC-NGs à base de HA non-modifié, leurs caractéristiques ne présentent aucun changement important (**Figure IV-7**). Par contre, les PEC-NGs de HA-M2005/DEAE-D ou de HA-M2005/PLL à n-/n+ de 2,5 ou 10 présentent une diminution importante (i.e. de 40-50 %) de la taille avec un abaissement aussi significatif (i.e. de 50-60 %) de leur PDI (**Figure IV-8**).

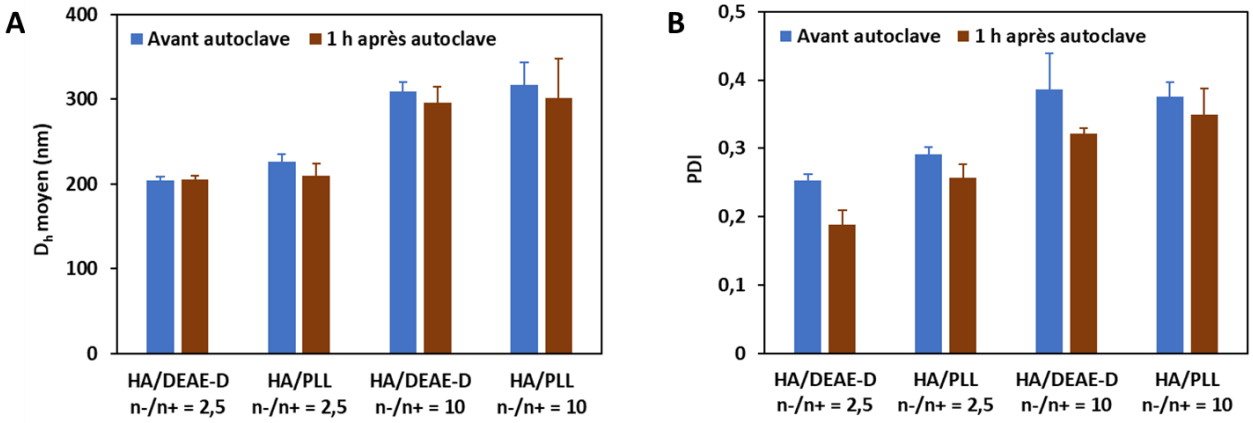

Figure IV-7. D_h moyen (**A**) et PDI (**B**) des PEC-NGs à base de HA non-modifié à C_P = 0,5 g.L^{-1} avant et après traitement autoclave (n ≥ 3).

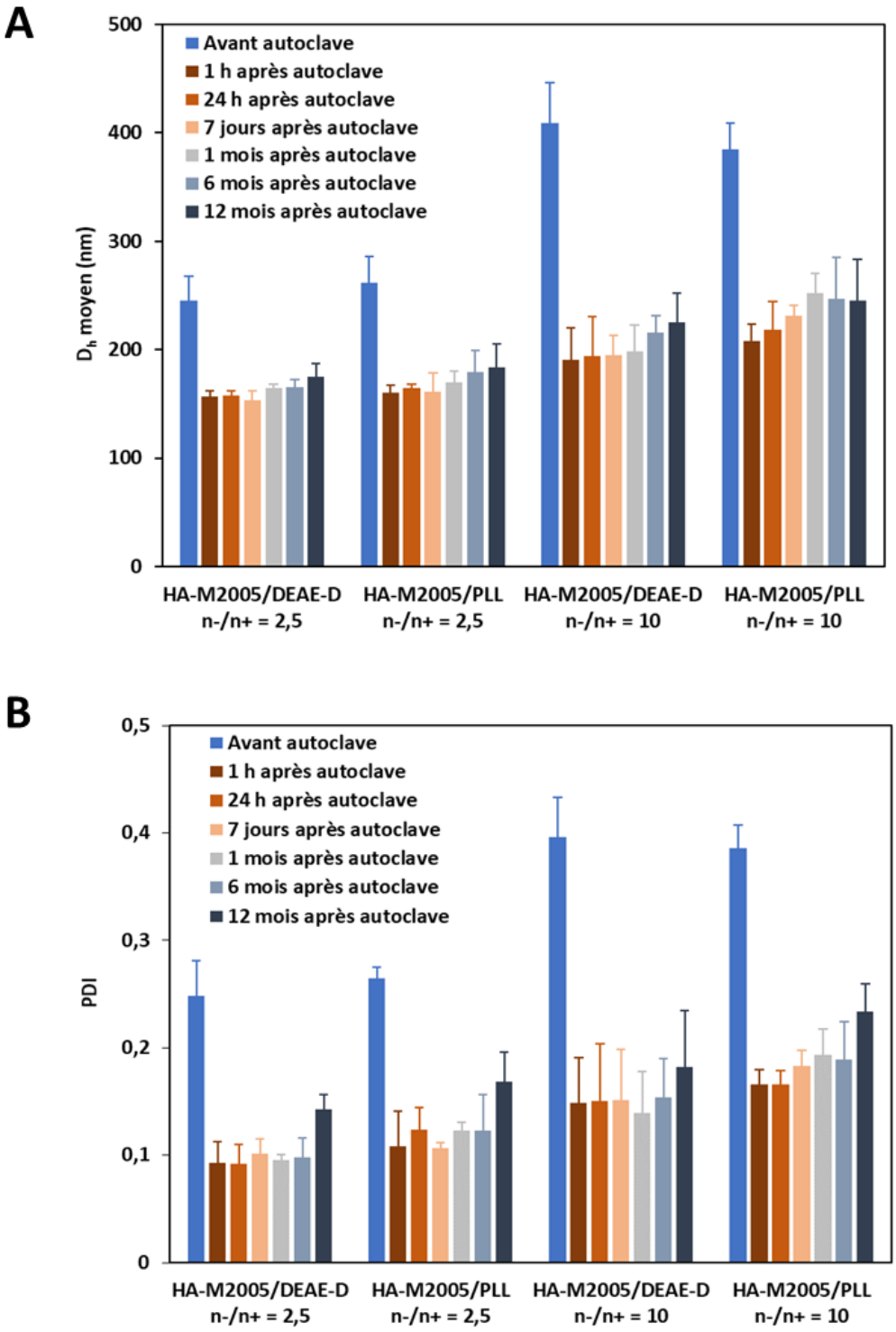

Figure IV-8. D_h moyen (**A**) et PDI (**B**) des PEC-NGs à base de HA-M2005 à C_P = 0,5 g.L^{-1} avant et après traitement autoclave ($n \geq 3$).

La diminution importante de la taille des PEC-NGs à base de HA-M2005 après le traitement autoclave est probablement la conséquence d'une forte contraction de leur structure quand les interactions hydrophobes entre les greffons de M2005 sont fortement accentuées sous les conditions critiques dans l'autoclave. La taille de ces NGs obtenus par autoclave ne présente qu'une très faible augmentation de manière progressive au cours des 12 mois de conservation à 4 °C, prouvant que la contraction des PEC-NGs à cause du traitement autoclave est assez forte et stable pour avoir un effet stabilisant à long terme. Cependant, en contrepartie de cette stabilisation, il est logique que ces PEC-NGs nouvellement obtenus à l'état très compact perdent leur capacité de contraction puis regonflement en fonction de température, comme le montrent les très faibles changements de taille lors de variation de température (**Figure IV-9**).

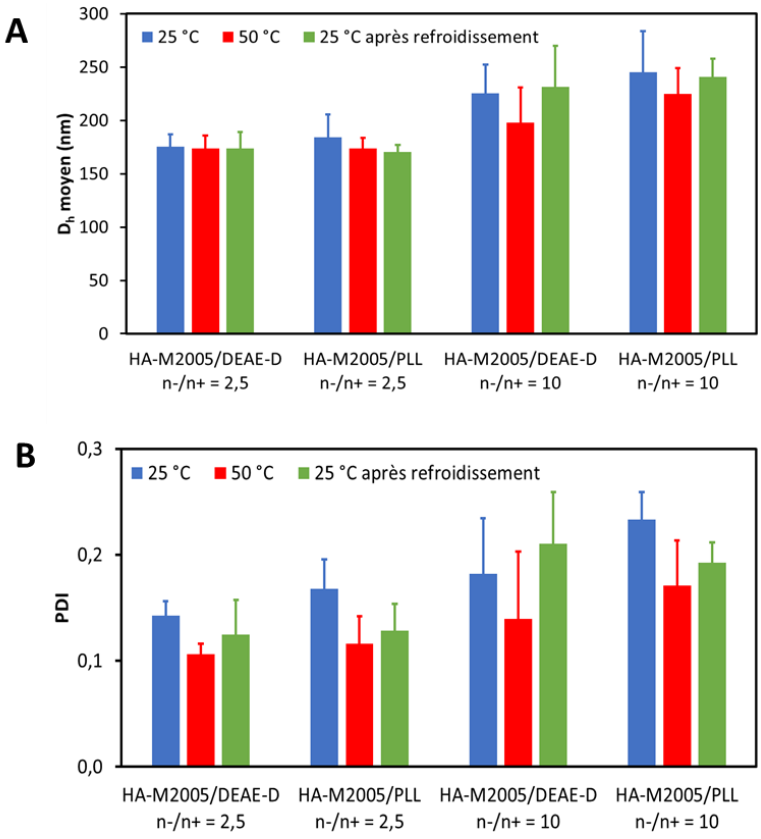

Figure IV-9. D_h moyen (**A**) et PDI (**B**) à différentes températures des PEC-NGs (C_P = 0,5 g.L^{-1}) 12 mois après l'autoclave ($n \geq 3$).

Nous avons également effectué une analyse par SEC/MALS sur les solutions de HA avant et après traitement par autoclave, qui montre un changement négligeable de la MW du HA pendant ce traitement (**Figure IV-10**). Ces résultats montrent que le HA n'est pas significativement dégradé dans les conditions étudiées du traitement autoclave.

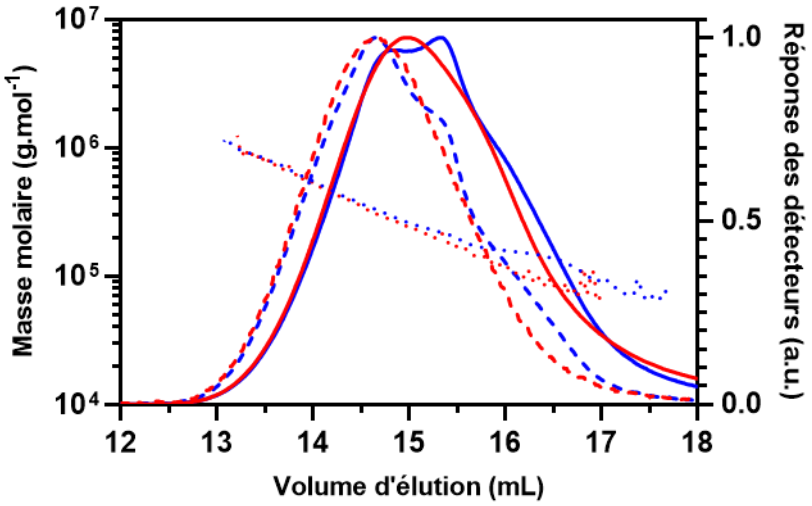

Figure IV-10. Profil d'élution dans $LiNO_3$ (0,1 mol.L^{-1}) à 25 °C du HA (C_P = 1 g.L^{-1}) avant (bleu) et après (rouge) traitement autoclave : réponses des détecteurs (trait plein pour indice de réfraction et trait discontinu pour diffusion de la lumière à 90°) avec la distribution des masses molaires (trait pointillé).

En général, tous ces résultats préliminaires ont révélé une application très prometteuse de l'autoclave comme une méthode assez simple pour obtenir les nanoparticules polymères hautement stables et stérilisés à base de PECs thermosensibles. La poursuite de ces études pourra être envisagée avec d'autres études plus approfondies, notamment la possibilité d'encapsulation des SAs dans les PEC-NGs pendant ou après traitement autoclave ainsi que la réévaluation de leur cinétique de libération.

IV.4. Conclusion et perspectives

Ce chapitre a montré la possibilité d'optimiser et/ou de reformuler les PEC-NGs à base de HA-M2005 en utilisant la lyophilisation ou le traitement autoclave. Pour ces PEC-NGs, les avantages présentés par les procédés susmentionnés vont au-delà de leurs utilités classiques, i.e. la conservation à sec (lyophilisation) et la stérilisation (autoclave).

Concernant la lyophilisation, avec la méthode la plus optimale que nous avons obtenue, soit la lyophilisation des PEC-NGs préparés à C_P = 0,2 $g.L^{-1}$ et C_{TRE} = 0,2 %, associée à la conservation à long terme, l'augmentation de la concentration des PEC-NGs est aussi possible sans entrainer des tailles trop élevées de ceux-ci lors de redispersion. De cette manière, des suspensions à des concentrations élevées en SAs peuvent être préparées pour les études qui les exigent, notamment les études de libération ou les études sur l'effet thérapeutique *in vitro* ou *in vivo*. Cependant, préalablement aux applications *in vivo*, il serait nécessaire de vérifier l'osmolalité des formulations après la reconstitution, car la présence des cryoprotecteurs peut probablement augmenter l'osmolalité et rendre ces formulations hypertoniques et ainsi peu compatibles avec le milieu physiologique *in vivo*, notamment le plasma dont l'osmolalité est d'environ 285-290 $mOsmol.kg^{-1}$ [42].

L'autoclave, quant à lui, peut être utilisé pour non seulement stériliser mais également stabiliser les PEC-NGs à base de HA-M2005 en profitant de leur amphiphilicité et thermosensibilité, en leur conférant des structures plus compactes et très stables mais en perdant leurs comportements thermosensibles. Dans les cas où cette thermosensibilité n'est pas souhaitée dans l'application, le traitement autoclave est ainsi une technique prometteuse pour fabriquer des nanoparticules stables à base de PECs. Dans cette perspective, il serait intéressant d'étudier la capacité de ces nanoparticules d'encapsuler les SAs pendant ou après leur formation par autoclave.

Références

[1] H. Zhang, Introduction to freeze-drying and ice templating, in: A. Jungbauer (Ed.), Ice Templating and Freeze-Drying for Porous Materials and Their Applications, Wiley-VCH, Weinheim, 2018, pp. 1-27. https://doi.org/10.1002/9783527807390.ch1.

[2] W. Abdelwahed, G. Degobert, S. Stainmesse, H. Fessi, Freeze-drying of nanoparticles: formulation, process and storage considerations, Advanced Drug Delivery Reviews, 58 (2006) 1688-1713. https://doi.org/10.1016/j.addr.2006.09.017.

[3] M. Mohammady, G. Yousefi, Freeze-drying of pharmaceutical and nutraceutical nanoparticles: The effects of formulation and technique parameters on nanoparticles characteristics, Journal of Pharmaceutical Sciences, 109 (2020) 3235-3247. https://doi.org/10.1016/j.xphs.2020.07.015.

[4] V. Simulescu, M. Kalina, J. Mondek, M. Pekař, Long-term degradation study of hyaluronic acid in aqueous solutions without protection against microorganisms, Carbohydrate Polymers, 137 (2016) 664-668. https://doi.org/10.1016/j.carbpol.2015.10.101.

[5] K. Park, Prevention of nanoparticle aggregation during freeze-drying, Journal of Controlled Release, 248 (2017) 153. https://doi.org/10.1016/j.jconrel.2017.01.038.

[6] K. Freimann, P. Arukuusk, K. Kurrikoff, L. Pärnaste, R. Raid, A. Piirsoo, M. Pooga, Ü. Langel, Formulation of stable and homogeneous cell-penetrating peptide NF55 nanoparticles for efficient gene delivery in vivo, Molecular Therapy-Nucleic Acids, 10 (2018) 28-35. https://doi.org/10.1016/j.omtn.2017.10.011.

[7] B.S. Bhatnagar, R.H. Bogner, M.J. Pikal, Protein stability during freezing: separation of stresses and mechanisms of protein stabilization, Pharmaceutical Development and Technology, 12 (2007) 505-523. https://doi.org/10.1080/10837450701481157.

[8] E. Trenkenschuh, W. Friess, Freeze-drying of nanoparticles: How to overcome colloidal instability by formulation and process optimization, European Journal of Pharmaceutics and Biopharmaceutics, 165 (2021) 345-360. https://doi.org/10.1016/j.ejpb.2021.05.024.

[9] A. Umerska, K.J. Paluch, M.J. Santos-Martinez, O.I. Corrigan, C. Medina, L. Tajber, Freeze drying of polyelectrolyte complex nanoparticles: Effect of nanoparticle composition and cryoprotectant selection, International Journal of Pharmaceutics, 552 (2018) 27-38. https://doi.org/10.1016/j.ijpharm.2018.09.035.

[10] C.V. Gheran, S.N. Voicu, B. Galateanu, M. Callewaert, J. Moreau, C. Cadiou, F. Chuburu, A. Dinischiotu, In Vitro Studies Regarding the Safety of Chitosan and Hyaluronic Acid-Based Nanohydrogels Containing Contrast Agents for Magnetic Resonance Imaging, International Journal of Molecular Sciences, 23 (2022) 3258. https://doi.org/10.3390/ijms23063258.

[11] J. Mudassir, Y. Darwis, S. Muhamad, A.A. Khan, Self-assembled insulin and nanogels polyelectrolyte complex (Ins/NGs-PEC) for oral insulin delivery: Characterization, lyophilization and in-vivo evaluation, International Journal of Nanomedicine, 14 (2019) 4895. https://doi.org/10.2147/ijn.s199507.

[12] A. Merivaara, J. Zini, E. Koivunotko, S. Valkonen, O. Korhonen, F.M. Fernandes, M. Yliperttula, Preservation of biomaterials and cells by freeze-drying: Change of paradigm, Journal of Controlled Release, 336 (2021) 480-498. https://doi.org/10.1016/j.jconrel.2021.06.042.

[13] A.S. Picco, L.F. Ferreira, M.S. Liberato, G.B. Mondo, M.B. Cardoso, Freeze-drying of silica nanoparticles: redispersibility toward nanomedicine applications, Nanomedicine, 13 (2018) 179-190. https://doi.org/10.2217/nnm-2017-0280.

[14] S.D. Allison, A. Dong, J.F. Carpenter, Counteracting effects of thiocyanate and sucrose on chymotrypsinogen secondary structure and aggregation during freezing, drying, and rehydration, Biophysical Journal, 71 (1996) 2022-2032. https://doi.org/10.1016/s0006-3495(96)79400-6.

[15] S. Eliyahu, A. Almeida, M.H. Macedo, J. das Neves, B. Sarmento, H. Bianco-Peled, The effect of freeze-drying on mucoadhesion and transport of acrylated chitosan nanoparticles, International Journal of Pharmaceutics, 573 (2020) 118739. https://doi.org/10.1016/j.ijpharm.2019.118739.

[16] W.-C. Luo, A.O.R. Beringhs, R. Kim, W. Zhang, S.M. Patel, R.H. Bogner, X. Lu, Impact of formulation on the quality and stability of freeze-dried nanoparticles, European Journal of Pharmaceutics and Biopharmaceutics, 169 (2021) 256-267. https://doi.org/10.1016/j.ejpb.2021.10.014.

[17] A. Almalik, I. Alradwan, M.A. Kalam, A. Alshamsan, Effect of cryoprotection on particle size stability and preservation of chitosan nanoparticles with and without hyaluronate or alginate coating, Saudi Pharmaceutical Journal, 25 (2017) 861-867. https://doi.org/10.1016/j.jsps.2016.12.008.

[18] N.K. Jain, I. Roy, Effect of trehalose on protein structure, Protein Science, 18 (2009) 24-36. https://doi.org/10.1002/pro.3.

[19] M. Zhang, H. Oldenhof, B. Sydykov, J. Bigalk, H. Sieme, W.F. Wolkers, Freeze-drying of mammalian cells using trehalose: preservation of DNA integrity, Scientific Reports, 7 (2017) 1-10. https://doi.org/10.1038/s41598-017-06542-z.

[20] M.B. Tejedor, J. Fransson, A. Millqvist-Fureby, Freeze-dried cake structural and physical heterogeneity in relation to freeze-drying cycle parameters, International Journal of Pharmaceutics, 590 (2020) 119891. https://doi.org/10.1016/j.ijpharm.2020.119891.

[21] K. Schersch, O. Betz, P. Garidel, S. Muehlau, S. Bassarab, G. Winter, Systematic investigation of the effect of lyophilizate collapse on pharmaceutically relevant proteins III: collapse during storage at elevated temperatures, European Journal of Pharmaceutics and Biopharmaceutics, 85 (2013) 240-252. https://doi.org/10.1016/j.ejpb.2013.05.009.

[22] A. Rampino, M. Borgogna, P. Blasi, B. Bellich, A. Cesàro, Chitosan nanoparticles: Preparation, size evolution and stability, International Journal of Pharmaceutics, 455 (2013) 219-228. https://doi.org/10.1016/j.ijpharm.2013.07.034.

[23] J.H. Crowe, J.S. Clegg, L.M. Crowe, Anhydrobiosis: the water replacement hypothesis, in: D. Reid (Ed.), The properties of water in foods ISOPOW 6, Springer New York, New York, 1998, pp. 440-455. https://doi.org/10.1007/978-1-4613-0311-4_20.

[24] D. Vinciguerra, M.B. Gelb, H.D. Maynard, Synthesis and Application of Trehalose Materials, JACS Au, (2022). https://doi.org/10.1021/jacsau.2c00309.

[25] P.-L. Chiu, D.F. Kelly, T. Walz, The use of trehalose in the preparation of specimens for molecular electron microscopy, Micron, 42 (2011) 762-772. https://doi.org/10.1016/j.micron.2011.06.005.

[26] M. Mathlouthi, X-ray diffraction study of the molecular association in aqueous solutions of d-fructose, d-glucose, and sucrose, Carbohydrate Research, 91 (1981) 113-123. https://doi.org/10.1016/s0008-6215(00)86024-3.

[27] A. Lerbret, P. Bordat, F. Affouard, M. Descamps, F. Migliardo, How homogeneous are the trehalose, maltose, and sucrose water solutions? An insight from molecular dynamics

simulations, The Journal of Physical Chemistry B, 109 (2005) 11046-11057. https://doi.org/10.1021/jp0468657.

[28] A. Diamond, J. Hsu, Phase diagrams for dextran-PEG aqueous two-phase systems at 22°C, Biotechnology Techniques, 3 (1989) 119-124. https://doi.org/10.1007/bf01875564.

[29] S. Park, R. Barnes, Y. Lin, B.-j. Jeon, S. Najafi, K.T. Delaney, G.H. Fredrickson, J.-E. Shea, D.S. Hwang, S. Han, Dehydration entropy drives liquid-liquid phase separation by molecular crowding, Communications Chemistry, 3 (2020) 1-12. https://doi.org/10.1038/s42004-020-0328-8.

[30] M. Smalley, H. Hatharasinghe, I. Osborne, J. Swenson, S. King, Bridging Flocculation in Vermiculite−PEO Mixtures, Langmuir, 17 (2001) 3800-3812. https://doi.org/10.1021/la0008232.

[31] S. Ishiguro, S. Cai, D. Uppalapati, K. Turner, T. Zhang, W.C. Forrest, M.L. Forrest, M. Tamura, Intratracheal administration of hyaluronan-cisplatin conjugate nanoparticles significantly attenuates lung cancer growth in mice, Pharmaceutical Research, 33 (2016) 2517-2529. https://doi.org/10.1007/s11095-016-1976-3.

[32] M.A. Grimaudo, G. Amato, C. Carbone, P. Diaz-Rodriguez, T. Musumeci, A. Concheiro, C. Alvarez-Lorenzo, G. Puglisi, Micelle-nanogel platform for ferulic acid ocular delivery, International Journal of Pharmaceutics, 576 (2020) 118986. https://doi.org/10.1016/j.ijpharm.2019.118986.

[33] M.K. Lee, M.Y. Kim, S. Kim, J. Lee, Cryoprotectants for freeze drying of drug nano-suspensions: effect of freezing rate, Journal of Pharmaceutical Sciences, 98 (2009) 4808-4817. https://doi.org/10.1002/jps.21786.

[34] T. Furst, G.R. Dakwar, E. Zagato, A. Lechanteur, K. Remaut, B. Evrard, K. Braeckmans, G. Piel, Freeze-dried mucoadhesive polymeric system containing pegylated lipoplexes: Towards a vaginal sustained released system for siRNA, Journal of Controlled Release, 236 (2016) 68-78. https://doi.org/10.1016/j.jconrel.2016.06.028.

[35] N. Zoratto, L. Forcina, R. Matassa, L. Mosca, G. Familiari, A. Musarò, M. Mattei, T. Coviello, C. Di Meo, P. Matricardi, Hyaluronan-Cholesterol Nanogels for the Enhancement of the Ocular Delivery of Therapeutics, Pharmaceutics, 13 (2021) 1781. https://doi.org/10.3390/pharmaceutics13111781.

[36] N.P. Akentieva, Đ. Gizatullin, N.A. Sanina, N.N. Dremova, V.I. Torbov, N.I. Shkondina, N. Zhelev, S.M. Aldoshin, Fabrication of chitosan-hyaluronic acid nanoparticles and encapsulation into nanoparticles of dinitrosyl iron complexes as potential cardiological drugs, Nanomedicine Journal, 7 (2020) 199-210. https://doi.org/10.22038/NMJ.2020.07.0004.

[37] E. Montanari, C. Di Meo, S. Sennato, A. Francioso, A.L. Marinelli, F. Ranzo, S. Schippa, T. Coviello, F. Bordi, P. Matricardi, Hyaluronan-cholesterol nanohydrogels: Characterisation and effectiveness in carrying alginate lyase, New Biotechnology, 37 (2017) 80-89. https://doi.org/10.1016/j.nbt.2016.08.004.

[38] E. Montanari, M.C. De Rugeriis, C. Di Meo, R. Censi, T. Coviello, F. Alhaique, P. Matricardi, One-step formation and sterilization of gellan and hyaluronan nanohydrogels using autoclave, Journal of Materials Science: Materials in Medicine, 26 (2015) 1-6. https://doi.org/10.1007/s10856-014-5362-6.

[39] E. Montanari, C. Di Meo, T. Coviello, V. Gueguen, G. Pavon-Djavid, P. Matricardi, Intracellular delivery of natural antioxidants via hyaluronan nanohydrogels, Pharmaceutics, 11 (2019) 532. https://doi.org/10.3390/pharmaceutics11100532.

[40] C. Di Meo, E. Montanari, L. Manzi, C. Villani, T. Coviello, P. Matricardi, Highly versatile nanohydrogel platform based on riboflavin-polysaccharide derivatives useful in the development of intrinsically fluorescent and cytocompatible drug carriers, Carbohydrate Polymers, 115 (2015) 502-509. https://doi.org/10.1016/j.carbpol.2014.08.107.

[41] S.A. Bernal-Chávez, M.L. Del Prado-Audelo, I.H. Caballero-Florán, D.M. Giraldo-Gomez, G. Figueroa-Gonzalez, O.D. Reyes-Hernandez, M. González-Del Carmen, M. González-Torres, H. Cortés, G. Leyva-Gómez, Insights into terminal sterilization processes of nanoparticles for biomedical applications, Molecules, 26 (2021) 2068. https://doi.org/10.3390/molecules26072068.

[42] R. Lord, Osmosis, osmometry, and osmoregulation, Postgraduate Medical Journal, 75 (1999) 67-73. http://dx.doi.org/10.1136/pgmj.75.880.67.

Conclusion générale et perspectives

Dans un contexte de recherche sur des matériaux innovants pour les applications biomédicales, notamment la délivrance ciblée et contrôlable de médicaments, les nanogels de complexes polyélectrolytes (PEC-NGs) à base de HA font l'objet d'une attention accrue ces dernières années. Ces systèmes sont très prometteurs avec des avantages indéniables. Dans notre étude bibliographique (**Chapitre I**), le mérite des PEC-NGs à base de HA provient d'une combinaison de plusieurs aspects : la nanomédecine, la chimie verte et les propriétés remarquables du HA, notamment la biodégradabilité, le ciblage biologique et une structure chimiquement modifiable. Nous avons ainsi sélectionné de nombreux articles scientifiques pour discuter de la formation des PEC-NGs en s'attardant sur les différents facteurs intrinsèques et extrinsèques pouvant gouverner les structures obtenues, puis nous avons présenté de nombreuses applications, notamment l'administration contrôlée et ciblée des agents thérapeutiques à petites molécules ou macromoléculaires ainsi que les agents de contraste pour le diagnostic ou la théranostique, ou la construction des matériaux multifonctionnels en vue des finalités biomédicales très diverses.

Dans ce contexte-là, l'objectif de notre projet est l'élaboration de nouveaux PEC-NGs à base de HA pour des applications en encapsulation et en libération contrôlée de SAs peu hydrosolubles, avec une attention particulière pour les systèmes thermosensibles impliquant du HA fonctionnalisé par de la Jeffamine® M-2005 (HA-M2005), qui a été récemment développé par notre équipe. Pour atteindre ces objectifs, notre travail s'articule autour de trois axes principaux :

(i) L'élaboration et la caractérisation de PEC-NGs à base de HA natif et de diéthylaminoéthyl dextrane (DEAE-D) et l'évaluation des impacts des différents facteurs sur leurs caractéristiques ;

(ii) L'élaboration et la caractérisation de PEC-NGs à base de HA-M2005 en complexe avec la poly-L-lysine (PLL) au lieu du DEAE-D, avec l'encapsulation et la libération contrôlée de la curcumine comme SA hydrophobe modèle ;

(iii) L'optimisation de la formulation, de la conservation et de la stabilité des PEC-NGs par lyophilisation et par autoclave.

Dans le premier axe, qui a fait l'objet du **Chapitre II**, nous avons élaboré des PECs de HA/DEAE-D et évalué leurs caractéristiques physico-chimiques comme leur taille et la distribution de celle-ci, leur potentiel zêta et leur hydrophobicité dans des conditions différentes. Nous avons pu comprendre les propriétés et les comportements de ces systèmes, à partir desquels nous avons proposé une structure de type cœur-coquille (*core-shell*) pour les PECs obtenus sous forme colloïdale. De plus, nous avons également vérifié les rôles des paramètres intrinsèques et extrinsèques lors de la préparation et de la conservation de ces PECs. Ces paramètres concernent les aspects du polymère de départ (i.e. la masse molaire du HA), de la formulation (i.e. le ratio de charge n-/n+, la concentration totale en polymère C_P, la force ionique et le pH) et de la technique de préparation (i.e. l'ordre et la vitesse d'ajout). Il a été constaté que ces PECs ne peuvent se former sous forme colloïdale (D_h moyen de 150-350 nm et PDI entre 0,1-0,4) que sous certaines conditions. En effet, une déstabilisation et/ou une macro-agrégation des PECs peuvent apparaitre quand un des facteurs ci-dessus devient défavorable, notamment une masse molaire importante du HA, un ratio n-/n+ proche de 1, une concentration élevée en polymère ou en contre-ions, un pH faible ou élevé, ou un ajout lent du polymère en excès. Nous avons ainsi établi une méthode de préparation pour obtenir des PECs sous forme colloïdale qui consiste à un ajout rapide (*one-shot*) de la solution de HA à masse molaire intermédiaire à celle du polycation pour une C_P de 0,5 $g.L^{-1}$ dans l'eau Milli-Q. Toutefois, bien que ces PECs colloïdaux, également appelés PEC-NGs, puissent être préparés en contrôlant les paramètres susmentionnés, ils présentent encore deux limitations pour les applications visées : (i) une hydrophobicité insuffisamment élevée qui peut empêcher l'encapsulation effective des SAs hydrophobes et (ii) une structure possiblement

déstabilisée par les conditions physiologiques, notamment une concentration en NaCl d'environ 0,15 mol.L^{-1} en cas d'application *in vivo*.

Nous avons ensuite continué nos recherches avec le deuxième axe (**Chapitre III**), où nous avons fonctionnalisé le HA avec des greffons thermosensibles de M2005 et ensuite remplacé le DEAE-D par la PLL comme polycation pour obtenir des PEC-NGs ayant des propriétés progressivement plus pertinentes, notamment une hydrophobicité plus élevée, une meilleure stabilité vis-à-vis la salinité physiologique et la thermosensibilité. Les améliorations apportées sur l'hydrophobicité et sur la stabilité sont la conséquence des interactions hydrophobes intraparticulaires exercées par les greffons de M2005 et la PLL à l'état neutralisé. Les effets synergiques de ces deux éléments ont pu permettre aux PEC-NGs de HA-M2005/PLL d'avoir la stabilité requise et la capacité d'encapsulation de la curcumine la plus satisfaisante parmi les systèmes étudiés. De plus, la thermosensibilité, apportée par les greffons de M2005, peut conférer aux PEC-NGs une capacité d'encapsulation et de libération de la curcumine de manière contrôlable par un effet de température. Plus précisément, il est vraisemblable que l'augmentation de la température lors de la complexation des polymères conduit à des assemblages avec des interactions hydrophobes renforcées par les greffons M2005 pour encapsuler une quantité plus importante de curcumine à l'intérieur des PEC-NGs. La présence de la couche externe hydrophile de la structure à noyau/enveloppe des PEC-NGs, visible par de la microscopie électronique à transmission, sert probablement comme une barrière hydrophile pour séquestrer la curcumine et empêcher sa fuite quand le système retrouve la température ambiante. Cependant, quand le système est soumis à une dilution importante pour la libération de la SA en condition *sink*, un chauffage peut entrainer la contraction des PEC-NGs et ainsi l'expulsion de l'eau pour accélérer la sortie de la SA. En possédant ces caractéristiques très spécifiques avec une structure dégradable par la HAase associée

à un ciblage possible du HA vis-à-vis des récepteurs CD44, ces PEC-NGs seront probablement utiles pour l'administration des SAs hydrophobes de manière ciblée et efficace au niveau des tumeurs avec une hyperthermie locale qui est réalisable en clinique. Il sera ainsi intéressant d'effectuer des études plus approfondies pour confirmer cette applicabilité, *i.e.* avec des études biologiques *in vitro* sur des cellules cancéreuses et *in vivo* sur un modèle animal. Cependant, il nous reste encore des limitations à régler dans les propriétés de ces systèmes avant de poursuivre ces études complémentaires : (i) la stabilité des PEC-NGs probablement réduite lors de la conservation en milieu aqueux à long terme et (ii) la concentration en SA possiblement insuffisante pour les études *in vitro* ou *in vivo*.

Dans le troisième axe (**Chapitre IV**), pour résoudre les limitations précédemment évoquées, nous avons cherché à optimiser la formulation, la conservation et la stabilité des différents PEC-NGs élaborés en appliquant une étape de lyophilisation/reconstitution ou un traitement autoclave, avec une priorité sur ceux à base de HA-M2005. Concernant la lyophilisation, à travers des études portant sur les effets de différents paramètres de formulation, nous avons pu trouver une approche pertinente pour redisperser facilement à l'état colloïdal les PEC-NGs après lyophilisation. Celle-ci consiste à la lyophilisation en présence de tréhalose (0,2 % m/v) sur des suspensions de PEC-NGs préparés à une faible concentration en polymère (*i.e.* C_P = 0,2 $g.L^{-1}$), que l'on reconstitue ensuite à un volume plus faible pour obtenir des suspensions plus concentrées en SAs avec des tailles des PEC-NGs pas trop élevées, notamment au-dessous de 350 nm. Quant au traitement par autoclave, nos études préliminaires montrent des PEC-NGs à base de HA-M2005 plus compactes et stables à long terme en milieu aqueux. Bien que ce traitement conduit à une perte significative du comportement thermosensible des PEC-NGs, il est une

méthode intéressante et qui mérite d'être exploré de façon plus importante pour la préparation des nanoparticules stables et stériles à partir des PECs.

Dans la continuité de ce travail, de nombreuses perspectives s'ouvrent pour la poursuite de nos recherches :

(i) Perspectives à court terme : Pour les PEC-NGs à base de HA-M2005 obtenus après traitement par autoclave, il sera intéressant de vérifier la possibilité d'encapsuler des SAs dans ces PEC-NGs pendant ou après ce traitement. La lyophilisation de ces PEC-NGs sera également étudiée. Ces études sont envisageables dans le cadre d'un contrat ATER pour les neuf prochains mois.

(ii) Perspectives à moyen terme : La biocompatibilité des PEC-NGs peut être vérifiée par les études *in vitro* sur les cellules normales, alors que les études sur des cellules cancéreuses pour l'évaluation des effets thérapeutiques sont envisageables pour les PEC-NGs chargés en SAs, soit la curcumine soit un autre agent cytotoxique. Avec les PEC-NGs chargés en curcumine, il sera également possible de vérifier le ciblage des cellules cancéreuses par microscopie confocale en exploitant la fluorescence de la curcumine. Dans le cas de résultats positifs, les études *in vivo* sur un modèle animal seront également nécessaires pour confirmer les effets antitumoraux. Avec ces études, il serait aussi possible de vérifier l'amélioration des effets antitumoraux par l'accélération de la libération des SAs par des PEC-NGs thermosensibles en appliquant une hyperthermie locale, notamment à l'aide des rayonnements électromagnétiques [1] ou d'ultrasons [2].

(iii) Perspectives à long terme : avec les résultats positifs obtenus avec le HA-M2005 lors de cette thèse, il serait intéressant d'essayer d'élaborer des PEC-NGs avec un autre dérivé thermosensible du HA, notamment du HA fonctionnalisé avec des copolymères de poly(2-isopropyl-2-oxazoline)-*co*-poly(2-n-butyl-2-oxazoline), qui a été élaboré dans la thèse de Mathieu MADAU au sein de

notre équipe [3-5]. Avec ces greffons, dont la LCST peut être contrôlée à travers la proportion des monomères, l'hydrophobicité et la thermosensibilité des PEC-NGs seraient ainsi plus modulables pour une gamme plus vaste d'applications.

Références

[1] M. Paulides, H.D. Trefna, S. Curto, D. Rodrigues, Recent technological advancements in radiofrequency- and microwave-mediated hyperthermia for enhancing drug delivery, Advanced Drug Delivery Reviews, 163 (2020) 3-18. https://doi.org/10.1016/j.addr.2020.03.004.

[2] C.-H. Wu, M.-K. Sun, Y. Kung, Y.-C. Wang, S.-L. Chen, H.-H. Shen, W.-S. Chen, T.-H. Young, One injection for one-week controlled release: In vitro and in vivo assessment of ultrasound-triggered drug release from injectable thermoresponsive biocompatible hydrogels, Ultrasonics Sonochemistry, 62 (2020) 104875. https://doi.org/10.1016/j.ultsonch.2019.104875.

[3] M. Madau, Hydrogels adaptatifs stimuli-sensibles (temperature et lumière) à base d'acide hyaluronique (HA), Thèse de doctorat, Normandie Université (2021).

[4] M. Madau, G. Morandi, V. Lapinte, D. Le Cerf, V. Dulong, L. Picton, Thermo-responsive hydrogels from hyaluronic acid functionalized with poly (2-alkyl-2-oxazoline) copolymers with tuneable transition temperature, Polymer, 244 (2022) 124643. https://doi.org/10.1016/j.polymer.2022.124643.

[5] M. Madau, G. Morandi, C. Rihouey, V. Lapinte, H. Oulyadi, D.L. Cerf, V. Dulong, L. Picton, A mild and straightforward one-pot hyaluronic acid functionalization through termination of poly-(2-alkyl-2-oxazoline), Polymer, 230 (2021) 124059. https://doi.org/10.1016/j.polymer.2021.124059.

PRODUCTION SCIENTIFIQUE

Communications orales

Le, H. V., Dulong, V., Picton, L., & Le Cerf, D. Preparation and characterization of polyelectrolyte complexes from hyaluronic acid and diethylaminoethyl dextran. *Journée de l'Ecole Doctorale Normande de Chimie* (visioconférence, 24-25 juin 2021).

Le, H. V., Dulong, V., Picton, L., & Le Cerf, D. Complexes polyélectrolytiques entre l'acide hyaluronique et le diéthylaminoéthyl dextrane : taille des particules et encapsulation de molécules hydrophobes. *41èmes journées de la Section Grand Ouest du GFP* (visioconférence, 8-9 juillet 2021).

Le, H. V., Dulong, V., Picton, L., & Le Cerf, D. Elaboration and physicochemical characterization of nanogels from polyelectrolyte complexes of hyaluronic acid and diethylaminoethyl dextran. *7th International Congress of the European Polysaccharide Network of Excellence (EPNOE)* (11-15 octobre 2021, Nantes, France).

Communications en poster

Le, H. V., Dulong, V., Picton, L., & Le Cerf, D. Elaboration of polyelectrolyte complex-based nanoparticles from hyaluronic acid and diethylaminoethyl dextran for drug delivery applications. *SFNano 7th Annual Meeting* (6-8 décembre 2021, Angers, France)

Publications

Le, H. V., Dulong, V., Picton, L., & Le Cerf, D. (2021). Polyelectrolyte complexes of hyaluronic acid and diethylaminoethyl dextran: Formation, stability and hydrophobicity. *Colloids and Surfaces A: Physicochemical and Engineering Aspects*, 629, 127485.

Le, H. V., Dulong, V., Picton, L., & Le Cerf, D. (2022). Thermoresponsive nanogels based on polyelectrolyte complexes between polycations and functionalized hyaluronic acid. *Carbohydrate Polymers*, 292, 119711

Le, H. V. & Le Cerf, D. (2022). Colloidal Polyelectrolyte Complexes from Hyaluronic Acid: Preparation and Biomedical Applications. *Small*, 2204283.

Nanogels à base d'acide hyaluronique fonctionnalisé, application à la séquestration et la libération contrôlée de composés hydrophobes

Résumé : Les nanogels à base de complexes polyélectrolytes (PEC-NGs) d'acide hyaluronique (HA) reçoivent actuellement une attention croissante dans le domaine biomédical, surtout pour la délivrance d'agents anticancéreux avec les avantages de la nanomédecine, de la chimie verte et les propriétés spécifiques du HA. Dans ce contexte, cette étude cherche à élaborer des PEC-NGs innovants à base de HA pour l'encapsulation et la libération contrôlée des substances actives (SAs) peu hydrosolubles, avec une attention particulière pour les PEC-NGs thermosensibles à partir de HA fonctionnalisé par de la Jeffamine® M-2005 (HA-M2005). Les études exploratoires sur les PECs entre le HA natif et le diéthylaminoéthyl dextrane (DEAE-D) ont permis une compréhension fondamentale des PECs et ainsi la détermination des conditions les plus appropriées pour leur préparation sous forme colloïdale. Le remplacement du HA par le HA-M2005 ou/et du DEAE-D par la poly-L-lysine (PLL) peut améliorer la stabilité des PEC-NGs en milieu salin ainsi que leur hydrophobicité pour une meilleure encapsulation de la curcumine comme SA modèle. Avec la thermosensibilité des PEC-NGs, une température élevée peut être appliquée pour optimiser l'encapsulation et stimuler la libération de la curcumine. La dégradation des PEC-NGs par la hyaluronidase a été confirmée, phénomène avantageux pour la délivrance ciblée des SAs aux sites spécifiques *in vivo*. Pour une conservation à long terme, la lyophilisation des PEC-NGs à une concentration faible en polymère (i.e. 0,2 $g.L^{-1}$) avec du tréhalose comme cryoprotecteur peut être appliquée donnant la possibilité de concentrer ces suspensions sans entrainer des tailles trop élevées des PEC-NGs. Egalement, l'autoclave s'avère prometteur comme moyen pour fabriquer des nanoparticules stériles et stables à long terme à partir des PEC-NGs thermosensibles. L'ensemble de ces études a montré que les PEC-NGs thermosensibles à base de HA étaient un prototype de matériau à fort potentiel avec une utilisation flexible pour les applications de délivrance de SAs.

Mots clés : Nanogel, nanomédecine, complexe polyélectrolyte, acide hyaluronique, thermosensibilité, délivrance contrôlée de médicaments

Abstract: Polyelectrolyte complex-based nanogels (PEC-NGs) from hyaluronic acid (HA) have received increasing interest in biomedical fields, especially for cancer drug delivery, by combining the advantages of nanomedicine, green chemistry and the inherent merit of HA. In this context, the aim of this work is to elaborate a novel kind of PEC-NGs from HA for encapsulation and controlled release of poorly water-soluble drugs, with a focus on thermoresponsive PEC-NGs prepared from HA functionalized with Jeffamine® M-2005 (HA-M2005). The exploratory studies on PECs from HA and diethylaminoethyl dextran (DEAE-D) allowed a basic understanding of PECs and therefore to determine the appropriate condition to prepare them in colloidal form, i.e. PEC-NGs. Replacing HA with HA-M2005 or/and DEAE-D with poly-L-lysine (PLL) can improve the stability of PEC-NGs in saline media as well as their hydrophobicity for better encapsulation of curcumin as a model drug. With the thermoresponsiveness of PEC-NGs, temperature elevation can be applied in order to optimize curcumin encapsulation and stimulate curcumin release. PEC-NG degradation by hyaluronidase was also confirmed, which may be beneficial for targeting drug delivery at specific sites *in vivo*. For long-term storage, lyophilization of PEC-NGs at a low polymer concentration (i.e. 0.2 $g.L^{-1}$) with trehalose as a cryoprotectant can be applied, which also allows to concentrate PEC-NGs afterwards without causing too large particle sizes. Additionally, autoclave can be promising as a means to fabricate sterilized and long-term stable nanoparticles from thermoresponsive PEC-NGs. All of these studies have shown thermoresponsive PEC-NGs based on HA as a potential kind of material with flexible utility for drug delivery applications.

Keywords: Nanogel, nanomedicine, polyelectrolyte complex, hyaluronic acid, thermoresponsiveness, controlled drug delivery